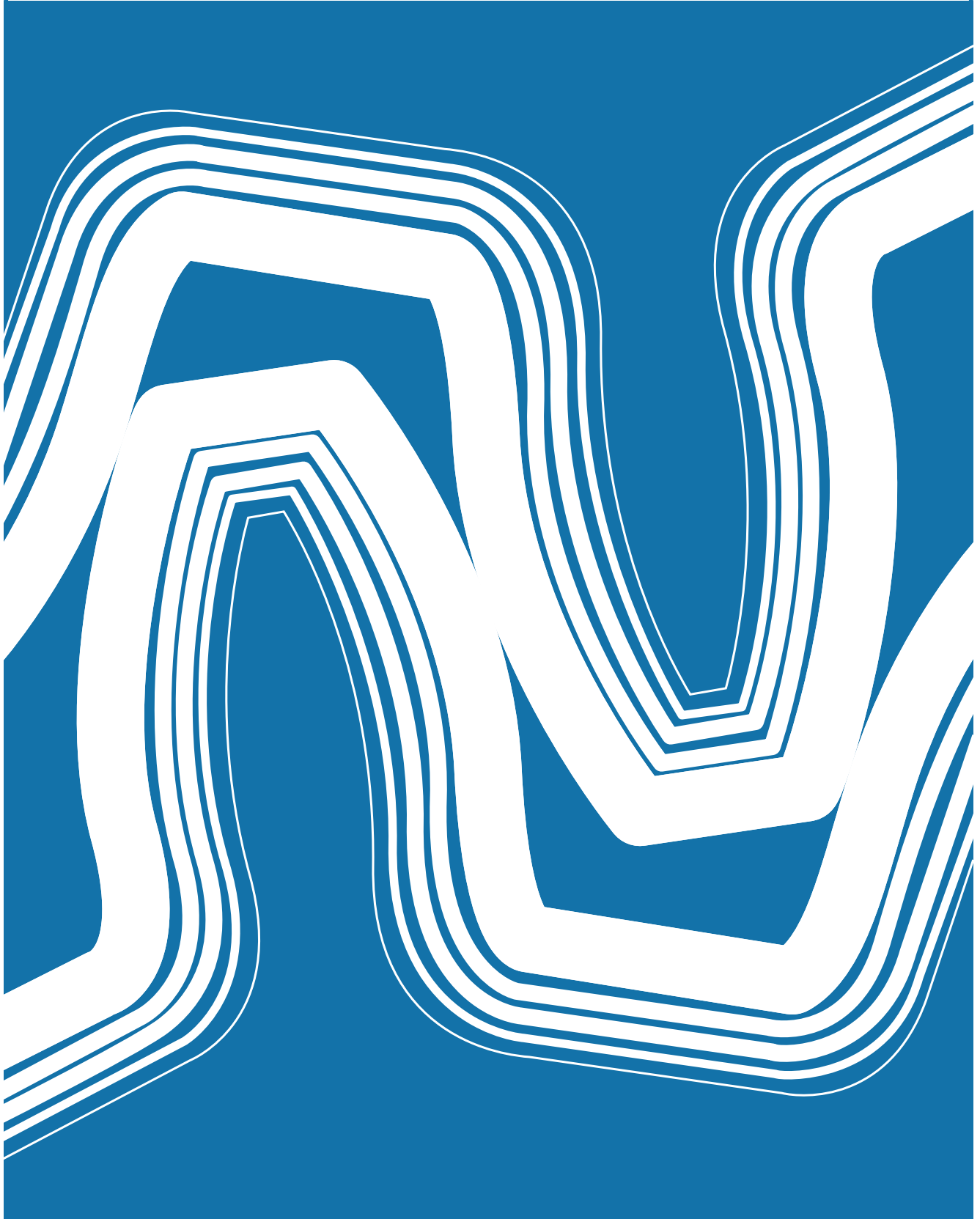


# **2** **FUNDAMENTALS OF MACHINE DESIGN**

MIR PUBLISHERS MOSCOW

**P. ORLOV**



**П. ОРЛОВ**

---

**ОСНОВЫ  
КОНСТРУИРОВАНИЯ**

ИЗДАТЕЛЬСТВО  
«МАШИНОСТРОЕНИЕ»  
МОСКВА

# **2** **FUNDAMENTALS OF MACHINE DESIGN**

---

**P. ORLOV**

TRANSLATED FROM THE RUSSIAN  
by YU. TRAVNICHEV

MIR PUBLISHERS · MOSCOW

### The Russian Alphabet and Transliteration

А а	а	К к	к	Х х	kh
Б б	b	Л л	l	Ц ц	ts
В в	v	М м	m	Ч ч	ch
Г г	g	Н н	n	Ш ш	sh
Д д	d	О о	o	Щ щ	shch
Е е	e	П п	p	Ъ ъ	''
Ё ё	e	Р р	r	Ы ы	y
Ж ж	zh	С с	s	Ь ь	'
З з	z	Т т	t	Э э	e
И и	i	У у	u	Ю ю	yu
Й й	y	Ф ф	f	Я я	ya

### The Greek Alphabet

Α α	Alpha	Ι ι	Iota	Ρ ρ	Rho
Β β	Beta	Κ κ	Kappa	Σ σ	Sigma
Γ γ	Gamma	Λ λ	Lambda	Τ τ	Tau
Δ δ	Delta	Μ μ	Mu	Υ υ	Upsilon
Ε ε	Epsilon	Ν ν	Nu	Φ φ	Phi
Ζ ζ	Zeta	Ξ ξ	Xi	Χ χ	Chi
Η η	Eta	Ο ο	Omicron	Ψ ψ	Psi
Θ θ	Theta	Π π	Pi	Ω ω	Omega

*На английском языке*

# Contents

<b>Chapter 1.</b>	<b>Tightened Connections</b>	<b>7</b>
1.1.	Unloaded Connections	7
1.2.	Loaded Connections	12
<b>Chapter 2.</b>	<b>Press-Fitted Connections</b>	<b>37</b>
2.1.	Press (Drive) Fits	37
2.2.	Strength of Press-Fitted Connections	38
2.3.	Selection of Fits	46
2.4.	Calculation Diagrams	47
2.5.	Probability Calculations for Press-Fitted Connections	59
2.6.	Press-Fitting with Heating or Cooling of Parts	64
2.7.	Pressed Connections with Electrodeposited Coatings	65
2.8.	Design of Pressed Connections	67
2.9.	Conical Fits	75
2.10.	Serrated Connections	77
2.11.	Glued Connections	78
<b>Chapter 3.</b>	<b>Centring Connections</b>	<b>79</b>
3.1.	Design Rules	80
<b>Chapter 4.</b>	<b>Screwed Connections</b>	<b>88</b>
4.1.	Longitudinal and Transverse Location of Parts in Screwed Connections	90
4.2.	Centring in Screwed Connections	92
4.3.	Design Rules	94
4.4.	Reinforcement of Fastening Joints	98
<b>Chapter 5.</b>	<b>Flanged Connections</b>	<b>102</b>
5.1.	Alignment of Flanges	105
5.2.	Machining the End Faces of Fastening Holes	107
5.3.	Diameter and Spacing of Bolts	110
5.4.	Three-Flange Joints	111
5.5.	Conical Flange Joints	113
<b>Chapter 6.</b>	<b>General Principles which Should Be Followed when Designing Units and Parts</b>	<b>96</b>
6.1.	Unification of Design Elements	96
6.2.	Unification of Parts	119
6.3.	Principle of Unitization	121
6.4.	Elimination of Adjustments	124
6.5.	Rationalization of Power Schemes	126
6.6.	Compensators	129
6.7.	Torsion Bars	133
6.8.	Floating Cross-Sliding Couplings	136

---

6.9. Elimination and Reduction of Bending . . . . .	137
6.10. Elimination of Deformation Due to Tightening . . . . .	143
6.11. Design Compactness . . . . .	146
6.12. Combining Design Functions . . . . .	150
6.13. Equistrength . . . . .	152
6.14. Uniform Loading of Supports . . . . .	156
6.15. Self-Alignment Principle . . . . .	157
6.16. Cambering . . . . .	162
6.17. Effect of Elasticity upon Load Distribution . . . . .	164
6.18. Fitting to Several Surfaces . . . . .	170
6.19. Tightening Up on Two Surfaces . . . . .	171
6.20. Axial Fixing of Parts . . . . .	172
6.21. Control of Direction . . . . .	174
6.22. Mounting Surfaces . . . . .	175
6.23. Butt-Jointing on Intersecting Surfaces . . . . .	177
6.24. Interchangeability of Rapidly Wearing Parts . . . . .	178
6.25. Accuracy of the Alignment of Parts . . . . .	179
6.26. Relief of Precision Mechanisms . . . . .	181
6.27. Coupling Parts Made from Hard and Soft Materials . . . . .	183
6.28. Elimination of Local Weak Spots . . . . .	186
6.29. Strengthening of Deformable Areas . . . . .	188
6.30. Composite Constructions . . . . .	189
6.31. Shoulders . . . . .	194
6.32. Chamfers and Fillets . . . . .	196

# Tightened Connections

Depending on their operating conditions tightened connections can be divided into unloaded and loaded ones.

## 1.1. Unloaded Connections

These include joints of non-bearing covers, non-bearing housing components, etc. In this case the necessary bolt (or stud) tightening force is determined proceeding from the condition that the joint should remain tight and unparted with all possible deformations in the system and with possible slacking of the screwed connections as a result of the threads or the supporting surfaces of the nut and bolt being crushed in the course of time. If the loads arising in the system during operation are not considered, then the bolt load is only the force of preliminary tightening (preload).

Such connections in the majority of cases are not calculated. The material, diameter and thread pitch of bolts are selected on the basis of existing practice, and the tightening force is set so that the stresses developing in the bolt correspond to a 3- 5-fold safety margin (in terms of the yield strength) as usual.

In non-critical connections the tightening force is not specified, but left to the fitter to decide upon by his experience. In mechanized assembly shops such joints are tightened mechanically with the aid of electric or pneumatic torque-control bolt drivers and nut runners.

The tightening torque  $M_{tight}$ , which is equal to the product of the force applied to the wrench end and the wrench arm, produces axial force  $P_{ax}$  (Fig. 1) stretching the bolt and overcomes the moment of friction in the threads and on the nut bearing surface

$$M_{tight} = 10^{-3} \left( \frac{P_{ax} \tan \varphi d_0}{2} + f_1 \frac{P_{ax} d_0}{2} + f_2 \frac{P_{ax} D}{2} \right) \text{ kgf} \cdot \text{m} \quad (1.1)$$

where  $P_{ax}$  = axial force arising as a result of the bolt tightening, kgf

$d_0$  = pitch diameter of the thread, mm

$D$  = mean diameter of nut bearing surface, mm

$f_1$  and  $f_2$  = coefficient of friction in the threads and on the nut bearing surface, respectively

$\varphi$  = thread helix angle

Introducing  $\tan \varphi = \frac{s}{\pi d_0}$  (where  $s$  is the thread pitch) gives

$$M_{tight} = 10^{-3} \frac{P_{ax} d}{2} \left( \frac{1}{\pi} \cdot \frac{s}{d} + f_1 \frac{d_0}{d} + f_2 \frac{D}{d} \right) \text{ kgf} \cdot \text{m} \quad (1.2)$$

where  $d$  is the nominal diameter of the thread, mm.

For the current diameter ranges of fastening bolts it is usual to take on the average  $s/d = 0.15$ ;  $d_0/d = 0.9$ ; and  $D/d = 1.3$ .

Substituting these values into Eq. (1.2), we get

$$M_{tight} = 10^{-3} P_{ax} d (0.024 + 0.45f_1 + 0.65f_2) \text{ kgf} \cdot \text{m}$$

whence

$$P_{ax} = 10^3 \frac{M_{tight}}{d (0.024 + 0.45f_1 + 0.65f_2)} \quad (1.3)$$

Let  $f_1 = 0.22$  and  $f_2 = 0.11$ . Then

$$P_{ax} \approx 10^3 \frac{5M_{tight}}{d} \quad (1.4)$$

Force  $P_{ax}$  induces tensile stresses in the bolt

$$\sigma_{tens} = \frac{P_{ax}}{0.785d_1^2}$$

where  $d_1$  is the minor diameter of the thread (for light bolts — the diameter of the bolt stem), mm.

The moment of friction in the threads  $\frac{P_{ax} d_0}{2} f_1$  causes torsional stresses in the bolt

$$\tau = \frac{P_{ax} d_0 f_1}{2W_{tors}}$$

where  $W_{tors} \approx 0.2d_1^3$  is the torsion resisting moment of the bolt cross-section.

Consequently

$$\tau = \frac{P_{ax} d_0 f_1}{0.4d_1^3}$$

The total stress, according to the third theory of strength, is

$$\sigma = \sqrt{\sigma_{tens}^2 + 4\tau^2} \approx \frac{P_{ax}}{d_1^2} \sqrt{1.6 + 25f_1^2 \left( \frac{d_0}{d_1} \right)^2} \quad (1.5)$$

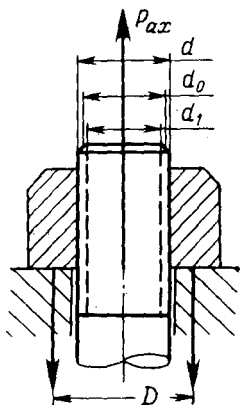


Fig. 1. Determination of bolt tightening torque



Assuming (on the average) that  $d_1 = 0.8d$ , and substituting the values  $f_1 = 0.22$  and  $d_0/d = 0.9$ , we obtain

$$\sigma \approx 2.6 \frac{P_{ax}}{d^2} \quad (1.6)$$

Substituting into this expression the value of  $P_{ax}$  from Eq. (1.4), we have

$$\sigma \approx 10^3 \frac{13M_{tight}}{d^3} \text{ kgf/mm}^2 \quad (1.7)$$

where  $M_{tight}$  = tightening torque, kgf·m

$d$  = nominal diameter of the thread, mm

The values of  $\sigma$  versus  $M_{tight}$ , shown in Fig. 2, are estimated from Eq. (1.7) for bolts of different diameters. The diagram can be used

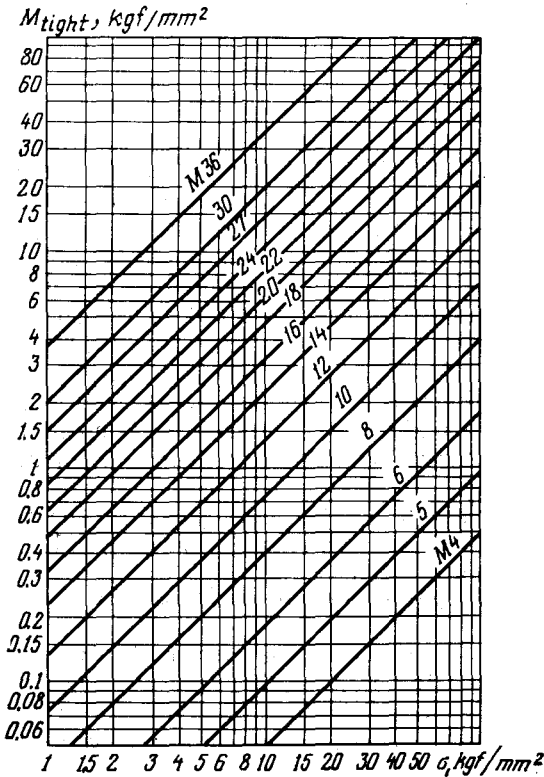


Fig. 2. Tightening torque  $M_{tight}$  and stresses  $\sigma$  for bolts of different diameters

for approximate determination of stresses developing in a bolt tightened with various torques. From the permissible stress it is possible to find the ultimate tightening torque.

The inverse-cube relationship between the stresses due to tightening and bolt diameter [see Eq. (1.7)] accounts for the abrupt rise of the stresses, occurring when the bolt diameter is reduced. When manually tightening small-diameter bolts, one may overstress the bolts, thus stretching and even breaking them.

Approximate values of forces and torques when tightening bolts by hand are given in Table 1.

Table 1

Forces and Torques when Tightening Bolts Manually

Bolts	Wrench arm, m	Tightening force, kgf	Tightening torque, kgf·m
Small (M4-M8)	0.1-0.15	≈ 10	1-1.5
Medium (M10-M14)	0.15-0.2	≈ 15	2-3
Large (M16-M24)	0.2-0.25	≈ 20	4-5

Assume, for example, that the tightening torque is 1.5 kgf·m. Drawing in Fig. 2 a horizontal line  $M_{tight} = 1.5 \text{ kgf}\cdot\text{m}$ , we read the stress values on the abscissa axis: for bolts M8—37 kgf/mm<sup>2</sup>; for bolts M6—80 kgf/mm<sup>2</sup>. The latter figure is well above the yield limit of commercial carbon steels. Consequently, bolts smaller than M6 may easily be broken when tightened by hand, and with the application of excessive forces bolts M8 may also be broken.

The magnitude of stresses due to tightening, in accordance with Eq. (1.3), strongly depends on the coefficient of friction in the threads and on the nut bearing surface. Friction blocks, as it were, the tightening force, so that a major part of the latter is spent in overcoming friction, only an insignificant portion being taken up by the bolt stem.

For example, when  $f_1 = 0.22$  and  $f_2 = 0.11$  the portion of the torque utilized for the bolt tightening, according to Eq. (1.3), will be

$$\frac{0.024}{0.024 + 0.1 + 0.72} \cdot 100\% \approx 12\%$$

The remaining 88% of the torque is spent in overcoming friction.

Equation (1.7) and the diagram in Fig. 2 are based on rather high values of the friction coefficients ( $f_1 = 0.22$ ;  $f_2 = 0.11$ ) corresponding to non-lubricated surfaces. If some lubricant gets onto the friction surfaces, then, with the same torque, the bolt stresses will rise.

Table 2 gives the values of stresses, calculated from Eq. (1.7), which arise in bolts tightened by means of standard wrenches with the application of 15-kgf tightening force. From the Table it is clear that with low friction values it is possible to break even M10 bolts when tightening them manually. The possibility of overstres-

Table 2

**Stresses in Bolts when Tightening with Standard Wrenches**

Bolt dia.	Stresses in kgf/mm <sup>2</sup> when	
	$f_1 = 0.22$ $f_2 = 0.11$	$f_1 = 0.11$ $f_2 = 0.055$
M6	100	180
M8	50	90
M10	30	54
M12	17	30
M14	12	22
M16	9	16

Note. The heavy line delimits stresses exceeding the yield limit of commercial carbon steels.

sing bolts with threads larger than M12 when tightening them with standard wrenches is practically excluded.

If, however, small-sized bolts must be used for some design reasons, then appropriate measures must be taken to limit the tightening

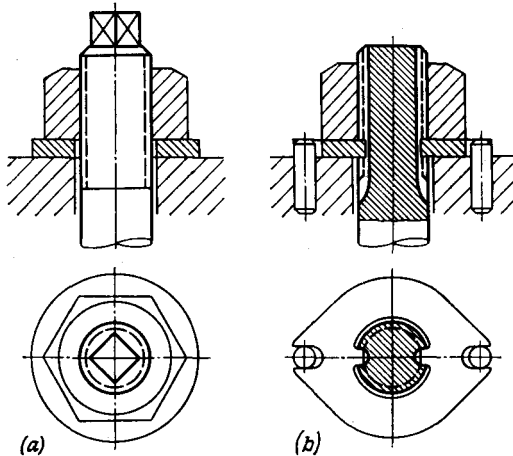


Fig. 3. Methods of eliminating bolt twist when tightening

torque or the bolts must be made from a high-grade heat-treated steel.

The simplest way to limit the tightening torque is to shorten the wrench arm correspondingly with the decrease of the bolt diameter. This practice is, in effect, stipulated by current standards covering wrenches and spanners.

The twisting-off of a bolt can be avoided if during tightening it is held by a special element (Fig. 3a) or if the bolt end is locked to the housing (Fig. 3b). In these cases only tensile stresses occur in the bolt.

Assume that in Eq. (1.5)  $\tau = 0$ , and  $d_1 = 0.8d$  (as before), then

$$\sigma = 1.56 \frac{P_{ax}}{d^2}$$

Comparing this expression with Eq. (1.6), we see that the stresses amount only to  $\frac{1.56}{2.6} = 0.65$  of the stresses when tightening a bolt with its being twisted.

Torsional stresses arise only during tightening and subsequently vanish due to the bolt elasticity. Therefore, when designing tightened connections for long-term strength the torsional stresses are usually neglected, the bolt calculations being limited to the axial force  $P_{ax}$  only [see Eq. (1.3)].

## 1.2. Loaded Connections

These include connections subjected to the action of a force which stretches the joint and imposes an additional load upon the fastening bolts. This force can be constant (e.g., the static pressure of gases and liquids in vessels) or variable (the pressure of gases in internal combustion engines and piston compressors, inertia forces of moving masses in connecting rods and bearings of crank mechanisms).

Here the bolt preload is selected so that, regardless of possible working force fluctuations, a constant tension at the joint is maintained, averting its opening which could break the joint seal and, in the case of variable forces, cause the crushing and work hardening of the metal surfaces.

The connection may be additionally loaded by thermal forces arising as the system gets heated.

Figure 4 shows a bolted connection subjected to the action of internal working pressure  $P_{work}$ . To assure normal functioning of the joint the bolts must be pretightened by a force  $P_{tight}$  sufficient to keep the joint tight under the action of working force  $P_{work}$ .

Now let us clarify what deformations occur in the system when force  $P_{tight}$  is applied to it. For the sake of simplicity we neglect changes

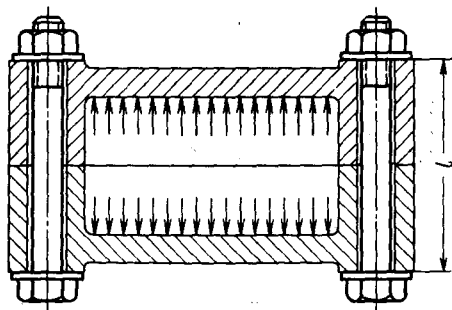


Fig. 4. Tightened connection

in the length of the threaded bolt ends and consider that the working length  $l$  of the bolts is equal to the thickness of the joined parts.

Under the action of force  $P_{tight}$  the bolts will lengthen by the value

$$\lambda_1 = \frac{P_{tight}l}{E_1F_1}$$

while the joined flanges will shrink by the value

$$\lambda_2 = \frac{P_{tight}l}{E_2F_2}$$

where  $E_1$ ,  $E_2$  and  $F_1$ ,  $F_2$  are the elasticity moduli of the materials and cross-sectional areas of the bolts and housing, respectively.

The force with which the housing members are compressed is equal to the tightening force, i.e.,

$$P_{comp} = P_{tight} \quad (1.8)$$

After the application of the working force  $P_{work}$  the bolts will additionally extend by the value  $\Delta\lambda$ , and, accordingly, the housing compressive deformation will decrease by the same value. As a result, the pressure exerted by the housing upon the bolts is reduced by the amount  $\Delta P$ .

The force tensioning the bolts becomes

$$P_{tens} = P_{work} + P_{tight} - \Delta P \quad (1.9)$$

and the force of the housing compression

$$P_{comp} = P_{tight} - \Delta P \quad (1.10)$$

Force  $\Delta P$  can be deduced from the following relationships.

In accord with Hooke's law, the value of the housing deformation decrease is

$$\Delta\lambda = \frac{\Delta Pl}{E_2F_2} \quad (1.11)$$

In bolts the same amount of deformation is produced by the difference of forces prior to and after the application of force  $P_{work}$ , i.e.,

$$P_{tens} - P_{tight} = P_{work} + P_{tight} - \Delta P - P_{tight} = P_{work} - \Delta P$$

Consequently, in respect to the bolts

$$\Delta\lambda = \frac{(P_{work} - \Delta P)l}{E_1F_1} \quad (1.12)$$

Equating Eqs. (1.11) and (1.12), gives

$$\Delta P = \frac{P_{work}}{1 + \frac{E_1F_1}{E_2F_2}} \quad (1.13)$$

Substituting this expression into Eqs. (1.9) and (1.10) gives the bolt tension force

$$P_{tens} = P_{work} + P_{tight} - \frac{P_{work}}{1 + \frac{E_1 F_1}{E_2 F_2}} = P_{tight} + \frac{P_{work}}{1 + \frac{E_2 F_2}{E_1 F_1}} \quad (1.14)$$

and the joint compression force

$$P_{comp} = P_{tight} - \frac{P_{work}}{1 + \frac{E_1 F_1}{E_2 F_2}} \quad (1.15)$$

If the working force varies from zero up to  $P_{work}$ , then the bolt tension force will pulsate with an amplitude

$$\Delta_{tens} = P_{tens} - P_{tight} = \frac{P_{work}}{1 + \frac{E_2 F_2}{E_1 F_1}} \quad (1.16)$$

while the housing compression force will pulsate with an amplitude

$$\Delta_{comp} = P_{tight} - P_{comp} = \frac{P_{work}}{1 + \frac{E_1 F_1}{E_2 F_2}} \quad (1.17)$$

Length does not enter into Eqs. (1.14)-(1.17). This means that the forces acting at the joint are theoretically equal when tightening low flanges and high housing components by bolts.

Actually the forces under consideration are affected by the elastic and plastic deformations of the threads and bearing surfaces of the nuts and bolt heads, etc., which may appreciably reduce the forces that tension the bolts and compress the connection.

The relative significance of terminal conditions is much greater for shorter bolts than for longer ones. That is why the joints fastened with short bolts weaken more quickly in use, particularly when subjected to pulsating loads. As a general rule, it is better to use long bolts (high flanges) or introduce elastic elements compensating for local plastic deformations of the system.

On the basis of Eqs. (1.14) and (1.15) it is often concluded that smaller ratios  $E_1 F_1 / E_2 F_2$  are more beneficial, in other words, the best combination is elastic bolts and rigid housings.

From Eq. (1.14) it is evident that the bolt tension force is minimum ( $P_{tens} = P_{tight}$ ) when  $\frac{E_1 F_1}{E_2 F_2} = 0$  (perfectly elastic bolts or perfectly rigid housings) and increases with an increase in  $\frac{E_1 F_1}{E_2 F_2}$ , reaching its maximum ( $P_{tens} = P_{tight} + P_{work}$ ) when  $\frac{E_1 F_1}{E_2 F_2} = \infty$  (perfectly elastic housings or perfectly rigid bolts). The amplitude of the pulsating tension force [Eq. (1.16)] also falls down with a decrease in  $\frac{E_1 F_1}{E_2 F_2}$ . In the limiting case ( $\frac{E_1 F_1}{E_2 F_2} = 0$ ) the bolt tension force

remains constant and is  $P_{tens} = P_{tight}$ , i.e., the load on the bolts becomes static despite the pulsating working force. With an increase in  $\frac{E_1 F_1}{E_2 F_2}$  the load on the bolts becomes cyclic. When  $\frac{E_1 F_1}{E_2 F_2} = \infty$  the pulsation amplitude is  $\Delta_{tens} = P_{work}$ .

With a decrease in  $\frac{E_1 F_1}{E_2 F_2}$  the joint compression force  $P_{comp}$  [Eq. (1.15)] is also reduced. This is beneficial for the housing strength, but is disadvantageous for the joint sealing, since the force sealing the split connection is equal to  $P_{comp}$ . At the same time, with the decrease of  $\frac{E_1 F_1}{E_2 F_2}$  the pulsation of force  $P_{comp}$  [Eq. (1.17)] is increased, but since the housing strength is usually much greater than the bolt strength and the compression force fluctuations are not so dangerous as the bolt tension force fluctuations, then it is recommended to employ low  $\frac{E_1 F_1}{E_2 F_2}$  values, as it is considered that this lowers the bolt load. From this stems the time-honoured design rule for split connections: *elastic bolts—rigid flanges*.

To this rule certain essential corrections are necessary.

To fully reveal the essence of this phenomenon, it is necessary to ascribe definiteness to the member  $P_{tight}$  entering into Eqs. (1.14) and (1.15), i.e., to agree upon how to select the tightening force. There are two methods of such a selection. In accord with the first method, widely applied until recently, the tightening force was taken in proportion to the working force  $P_{work}$

$$P_{tight} = \gamma P_{work} \quad (1.18)$$

where  $\gamma$  is the tightening factor (usually  $\gamma = 1-2$ ).

According to the second method, the tightening force is found on condition that the joint compression force  $P_{comp}$  is proportional to the working force, i.e.,

$$P_{comp} = \theta P_{work} \quad (1.19)$$

where  $\theta$  is the proportionality factor (generally  $\theta = 0.25-1$ ).

Let us consider both of these cases.

**The case when  $P_{tight} = \gamma P_{work}$ .** Substituting into Eqs (1.14 and 1.15)  $P_{tight} = \gamma P_{work}$ , gives

$$P_{tens} = P_{work} \left( \gamma + \frac{1}{1 + \frac{E_2 F_2}{E_1 F_1}} \right) \quad (1.20)$$

$$P_{comp} = P_{work} \left( \gamma - \frac{1}{1 + \frac{E_1 F_1}{E_2 F_2}} \right) \quad (1.21)$$

From Eq. (1.20) it is clear that variations of the ratio  $\frac{E_1 F_1}{E_2 F_2}$  even within the widest limits affects the magnitude of the force  $P_{tens}$

comparatively little. In the limiting cases  $P_{tens} = P_{work}\gamma$  (when  $\frac{E_1F_1}{E_2F_2} = 0$ ) and  $P_{tens} = P_{work}(1 + \gamma)$  (when  $\frac{E_1F_1}{E_2F_2} = \infty$ ). Hence, the entire range of force  $P_{tens}$  is confined within the limits  $\frac{1 + \gamma}{\gamma}$ .

It should be noted that in the expression  $\frac{E_1F_1}{E_2F_2}$  the number of possible values of the ratio  $E_1/E_2$  is limited. Bolts are made almost

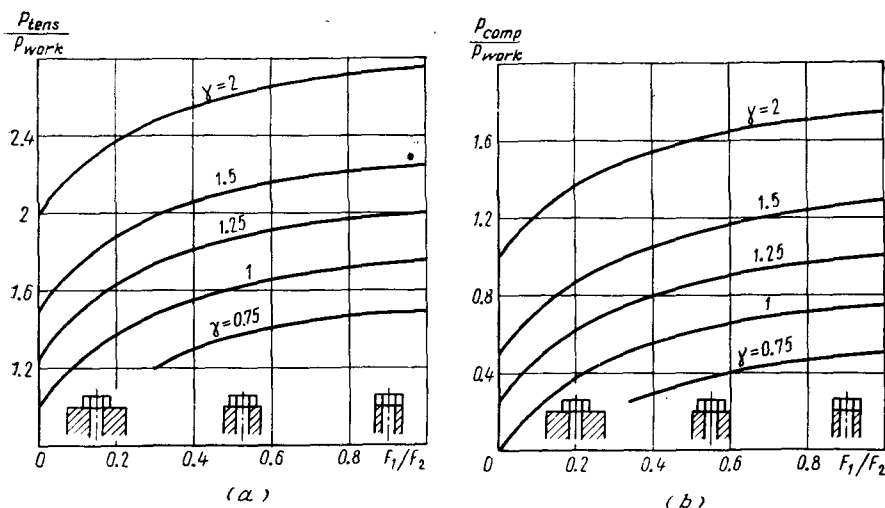


Fig. 5. Ratios  $P_{tens}/P_{work}$  and  $P_{comp}/P_{work}$  as a function of  $F_1/F_2$  for different values of tightening factor  $\gamma$

exclusively of steels ( $E = 20 \cdot 10^3 - 22 \cdot 10^3$  kgf/mm<sup>2</sup>) and in very rare cases (in special constructions) — of titanium alloys ( $E = 11.5 \cdot 10^3 - 12.5 \cdot 10^3$  kgf/mm<sup>2</sup>).

Joined members are made of steels, cast irons, light and titanium alloys (Table 3).

There are three values of the ratio  $E_1/E_2$  having practical importance:  $E_1/E_2 = 1$  (steel-steel; titanium alloy-titanium alloy);  $E_1/E_2 \approx 2.5$  (steel-cast iron);  $E_1/E_2 \approx 3$  (steel-aluminium alloys).

With specified materials the  $\frac{E_1F_1}{E_2F_2}$  value can be influenced only by changing the ratio  $F_1/F_2$ , which entails changes in the strength of the bolts and housings.

When clamping a split aluminium housing with steel bolts ( $E_1/E_2 \approx 3$ ) the ratio  $P_{tens}/P_{work}$ , for different values of  $\gamma$  taken in a wide range of  $F_1/F_2$  values (from zero to unity), will vary inappreciably, only by 1.5-2 times on the average, as evident from Fig. 5a.



Table 3

## Material Combinations for Bolts and Joined Components

Bolt material	Joined components		$E_1/E_2$
	material	$E_2$ , kgf/mm <sup>2</sup>	
Steel $E_1 = 21\,000$ kgf/mm <sup>2</sup>	Steel	21 000	1
	Cast iron	8 000	2.6
	Aluminium alloys	7 200	2.9
	Magnesium alloys	4 500	4.7
	Titanium alloys	12 000	1.75
Titanium alloy $E_1 = 12\,000$ kgf/mm <sup>2</sup>	Titanium alloys	12 000	1

Thus, the gain from decreasing  $F_1/F_2$  is not very great. The picture is similar for other  $E_1/E_2$  ratios.

Decreasing the force  $P_{tens}$  still does not mean an improvement in the bolt strength which is determined by the stress  $\sigma = \frac{P_{tens}}{F_1}$ . Such an improvement will only be reached if the ratio  $F_1/F_2$  is reduced by increasing the housing cross-section and not by reducing the bolt cross-sections. It can easily be proved that reducing the bolt cross-sections decreases relatively little the force  $P_{tens}$ , and, at the same time, sharply increases the bolt stresses.

On the other hand, increasing the ratio  $F_1/F_2$  by enlarging the bolt cross-sections provides a definite gain in the bolt strength.

In relation to joints for which good sealing is imperative it is extremely important to find how the compression force  $P_{comp}$  changes with  $F_1/F_2$ , for this force determines the tightening of the joint seal.

The values of the ratio  $P_{comp}/P_{work}$  (for  $E_1/E_2 = 3$ ), estimated from Eq. (1.24), are plotted in Fig. 5b. The compression force decreases with the reduction of the ratio  $F_1/F_2$  (rigid housings), the decrease being the sharper the less the value of  $\gamma$ . For example, with  $\gamma = 1.25$  force  $P_{comp}$  within the range of  $F_1/F_2$  of from 0 to 1 is reduced four times. Hence, the decrease of the ratio  $F_1/F_2$  adversely affects the reliability of the joint.

To assure reliable sealing in the case of rigid housings it is necessary to increase the tightening force, i.e., to increase the bolt tension, which makes the gain from lowering  $F_1/F_2$  fictive.

Conversely, making the housing more pliable lowers the necessary tightening force. With compliant housings it is possible to tighten

the joint with  $\gamma < 1$  without running the risk of the joint loosening ( $P_{comp}/P_{work} > 0$ ) and without impairing its reliability.

Let us now examine the effect of the ratio  $F_1/F_2$  upon the pulsation amplitude of forces  $P_{tens}$  and  $P_{comp}$  (Fig. 6). It is evident from the graph that decreasing the ratio  $F_1/F_2$  (rigid housings) lowers the pulsation amplitude of force  $P_{tens}$ , which is advantageous for the bolt strength. However, the pulsation of force  $P_{comp}$  increases as the ratio  $F_1/F_2$  is reduced, this adversely affecting the reliability of the joint.

Thus, we may conclude that with  $P_{tight} = \gamma P_{work}$ , low ratios  $F_1/F_2$  (rigid housings) are advantageous for the bolt strength when

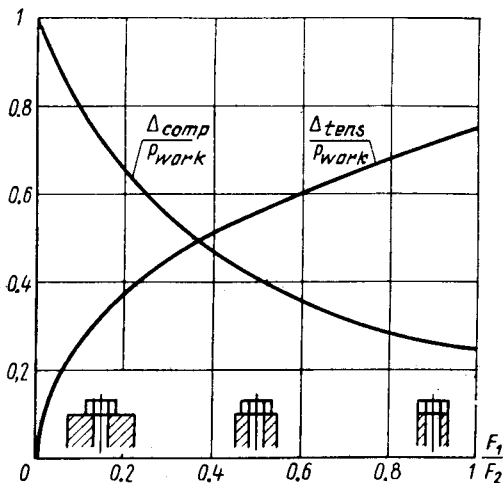


Fig. 6. Ratios  $\Delta_{tens}/P_{work}$  and  $\Delta_{comp}/P_{work}$  as a function of  $F_1/F_2$  for different values of tightening factor  $\gamma$

the loads on the joint are pulsating. For static (in particular thermal) loads, and also when the reliability of the joint is of prime importance, higher ratios  $F_1/F_2$  (compliant housings) are preferable.

The foregoing conclusions are of special significance for connections in which the rigidity of the joined parts is commensurable with that of the clamping bolts. Such a situation is encountered, for instance, when clamping hydraulic and air power cylinders (Fig. 7a) and cylinders of internal combustion engines and piston compressors of half-block (Fig. 7b) or full-block (Fig. 7c) designs. Here the designer can vary within broad limits the ratio  $F_1/F_2$  by changing the cross-sections of the clamped components and thus make it most suitable for the given operating conditions.

With conventional flange connections manoeuvring possibilities are less. As shown by experiments, actually in operation is the cylin-

drical flange volume of external diameter  $D \approx 2d_0$  and internal diameter  $d \approx d_0$  (Fig. 8a). The ratio of the bolt cross-sectional

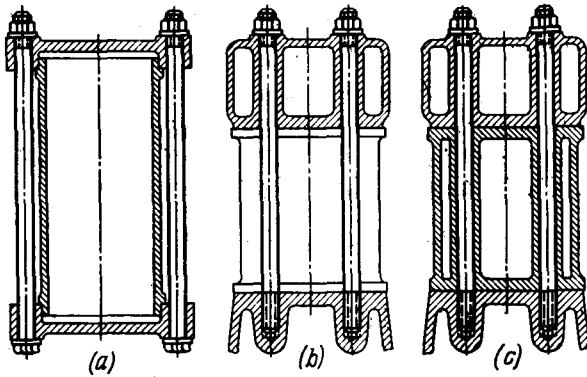


Fig. 7. Tightened connections

area to the design area of the clamped parts is

$$\frac{F_1}{F_2} \approx \frac{d_0^2}{D^2 - d_0^2} = 0.33$$

This ratio can be increased by placing an elastic gasket between the parts being connected, or reduced by placing under the bolt some massive washers of increased diameter, and also by decreasing the bolt stem diameter (Fig. 8b).

Assuming that  $D_1 = 3d_0$  and  $d_1 = 0.8d_0$ , we have

$$\frac{F_1}{F_2} \approx \frac{(0.8d_0)^2}{D_1^2 - d_0^2} = 0.08$$

The ratio  $F_1/F_2$  can also be reduced by placing elastic elements between the flange and bolt faces.

The case when  $P_{comp} = \theta P_{work}$ . The relationships become different when the tightening force is chosen so that  $P_{comp}$  of the joint is proportional to  $P_{work}$ . This condition is quite logical: the higher

the working pressure, the greater must be the compression to ensure the required reliability of the joint. Selecting the tightening force in such a way establishes a direct relation between the joint com-

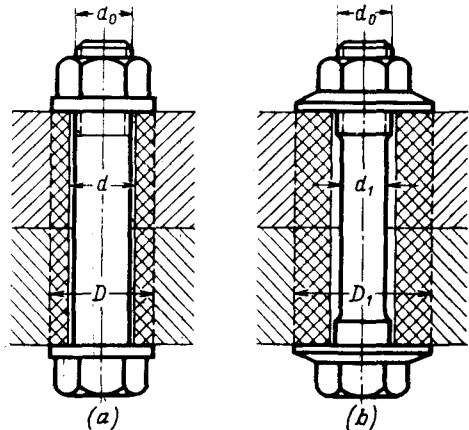


Fig. 8. Tightened flanges

pression force and the working force, whereas in the previous case this relation is a derivative of the preliminarily chosen tightening factor  $\gamma$  and of elasticity characteristics of the system.

The bolt tension force is always equal to the sum of the working and compression forces. Hence,

$$P_{tens} = P_{work} + P_{comp} = (1 + \theta) P_{work} \quad (1.22)$$

Thus, the forces  $P_{tens}$  and  $P_{comp}$  (for a given force  $P_{work}$ ) in this case are constant and independent of the ratio  $E_1 F_1 / E_2 F_2$ .

From Eq. (1.15) the required tightening force

$$P_{tight} = P_{comp} + \frac{P_{work}}{1 + \frac{E_1 F_1}{E_2 F_2}} \quad (1.23)$$

Substituting into this relation the value  $P_{comp} = \theta P_{work}$ , we get

$$P_{tight} = P_{work} \left( \theta + \frac{1}{1 + \frac{E_1 F_1}{E_2 F_2}} \right) \quad (1.24)$$

The ratio  $P_{tight}/P_{work}$  as a function of  $F_1/F_2$  (when  $E_1/E_2 = 3$ ) is plotted for various values of  $\theta$  in Fig. 9. The graph shows that increasing the ratio  $F_1/F_2$  (compliant housings) reduces the required tightening force.

The determination of the tightening force on condition that  $P_{comp} = \theta P_{work}$  is undoubtedly more rational than on condition that  $P_{tight} = \gamma P_{work}$ . The latter method must be rejected as being wrong in principle. In this connection the problem of the influence of the  $E_1 F_1 / E_2 F_2$  factor on the operation of the joint should be reconsidered.

As is obvious from the foregoing, when  $P_{comp} = \theta P_{work}$  the ratio  $E_1 F_1 / E_2 F_2$  has no influence on the forces  $P_{tens}$  and  $P_{comp}$  which are defined

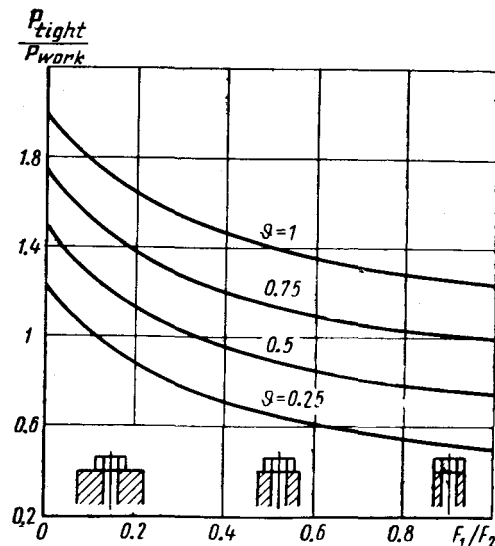


Fig. 9. Ratio  $P_{tight}/P_{work}$  as a function of  $F_1/F_2$  for different values of factor  $\theta$

exclusively by the magnitude of factor  $\theta$ .

The ratio  $E_1 F_1 / E_2 F_2$  affects the tightening force only. Higher values of  $E_1 F_1 / E_2 F_2$  (compliant housings) are more advantageous as they enable the required tightening force to be decreased.

In connections loaded by a pulsating force the ratio  $E_1F_1/E_2F_2$  also affects the pulsation amplitude of forces  $P_{tens}$  and  $P_{comp}$ . According to Eqs. (1.16) and (1.17), as  $E_1F_1/E_2F_2$  decreases (rigid housings), the pulsation amplitude of  $P_{tens}$  is reduced, while that of  $P_{comp}$ , increased. Conversely, increasing  $E_1F_1/E_2F_2$  (compliant housings) augments the pulsation amplitude of  $P_{tens}$  and diminishes that of  $P_{comp}$ . Consequently, we may conclude that under pulsating loads rigid housings are more advantageous for the bolt strength and compliant housings, for reliable sealing.

In joints loaded by a constant force the magnitude of  $E_1F_1/E_2F_2$  seems indifferent both for the bolt strength and for the quality of sealing. All the above considerations on the relative advantages of rigid and compliant housings under a static load are valid only when  $P_{tight} = \gamma P_{work}$  and lose their value when  $P_{comp} = \theta P_{work}$ .

The magnitude of factor  $\theta$ , which in the given case is of decisive importance for the joint parameters, is chosen to suit the reliability requirements for the seal: for non-critical joints  $\theta = 0.25$  to  $0.3$  and for critical joints,  $0.5$  to  $1$ .

The calculation on condition that  $P_{comp} = \theta P_{work}$  is simpler. There is no need for the cut-and-try procedure of finding  $P_{tight}$  and checking the resulting  $P_{comp}$ , and the calculation comes to the application of the simplest formulae (1.22), (1.23) and (1.24) which at once yield all the values determining the strength and reliability of the joint.

### (a) Temperature Factors

If a joint operates at elevated temperatures, and the temperatures of the clamping bolts and joined parts differ, or if the parts are made of materials possessing different coefficients of linear expansion, a thermal stress  $P_t$  then develops in the joint. In accord with Eq. (7.1) [see *Fundamentals of Machine Design*, Vol. 1, Chapter 7], this stress is

$$P_t = (\alpha_2 t_2 - \alpha_1 t_1) \frac{E_1 F_1}{1 + \frac{E_1 F_1}{E_2 F_2}} \quad (1.25)$$

where  $\alpha_1, \alpha_2$  = coefficients of linear expansion of the materials of the bolts and housing, respectively

$t_1, t_2$  = working temperatures of the bolts and housing

The total bolt tension force is equal to the sum of forces  $P_{tens}$  and  $P_t$

$$P'_{tens} = P_{tens} + P_t = P_{tight} + \frac{P_{work}}{1 + \frac{E_1 F_1}{E_2 F_2}} + \frac{(\alpha_2 t_2 - \alpha_1 t_1) E_1 F_1}{1 + \frac{E_1 F_1}{E_2 F_2}} \quad (1.26)$$

The total joint compression force is equal to the sum of forces  $P_{comp}$  and  $P_t$

$$P'_{comp} = P_{comp} + P_t = P_{tight} - \frac{P_{work}}{1 + \frac{E_1 F_1}{E_2 F_2}} + \frac{(\alpha_2 t_2 - \alpha_1 t_1) E_1 F_1}{1 + \frac{E_1 F_1}{E_2 F_2}} \quad (1.27)$$

(b) *Housings with Changing Sections*

Often met in practice are cases when the parts being clamped have changing (variable) sections (Fig. 10a) or are made of materials with different moduli of elasticity.

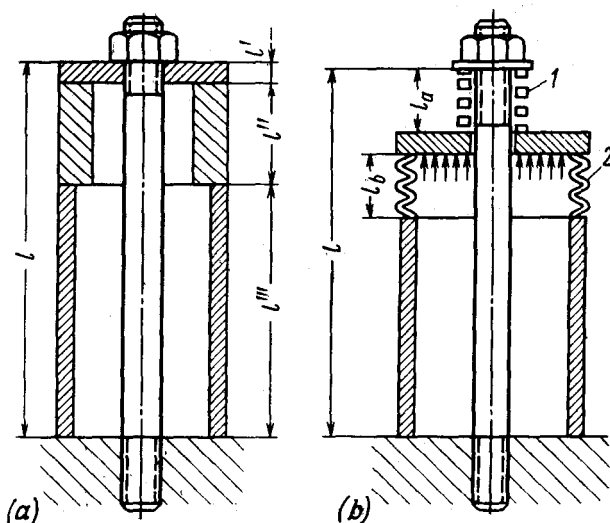


Fig. 10. Complex systems  
(a) with elements of changing section; (b) with elastic elements

Let  $l'$ ,  $l''$ ,  $l'''$ , ... be the lengths of the dissimilar sections ( $l' + l'' + l''' + \dots = l$ ) and let each have its corresponding rigidity factor  $E'F'$ ,  $E''F''$ ,  $E'''F'''$ , ...

Then the rigidity factor  $E_2 F_2$  in the previous expressions should be changed to a corrected factor whose magnitude is determined from the following considerations.

Let a complex system be acted upon by a force  $P$ . The total deformation  $\lambda$  of the system, produced by the force, will be the sum of the deformations of its individual elements

$$\lambda = \lambda' + \lambda'' + \dots = \frac{Pl'}{E'F'} + \frac{Pl''}{E''F''} + \dots$$

The relative deformation of the system

$$e = \frac{\lambda}{l} = \frac{P}{l} \left( \frac{l'}{E'F'} + \frac{l''}{E''F''} + \dots \right)$$

The corrected rigidity factor of the system

$$\mathfrak{E}\mathfrak{F} = \frac{P}{e} = \frac{1}{\frac{l'}{E'F'l} + \frac{l''}{E''F''l} + \dots} \quad (1.28)$$

Introducing this factor into the previous equations in place of  $E_2F_2$ , the calculation can be carried out as previously.

In this case the temperature deformation is

$$\Delta e = l'\alpha_1't_2 + l''\alpha_2''t_2 + \dots - l\alpha_1 t_1$$

where  $\alpha_1$  = coefficient of linear expansion of the bolt material  
 $t_1$  = bolt temperature

In relative units

$$\Delta e = \frac{l'}{l} \alpha_1't_2 + \frac{l''}{l} \alpha_2''t_2 + \dots - \alpha_1 t_1 \quad (1.29)$$

The sum of the deformations of the individual elements in the system may be expressed as a function of the thermal stress in the following way:

$$\Delta e = \frac{P'l'}{E'F'l} + \frac{P'l''}{E''F''l} + \dots + \frac{P_t}{E_1F_1} = P_t \left( \frac{1}{\mathfrak{E}\mathfrak{F}} + \frac{1}{E_1F_1} \right) \quad (1.30)$$

Equating Eqs. (1.29) and (1.30), one will obtain

$$P_t = \frac{(\alpha_1't_2 \frac{l'}{l} + \alpha_2''t_2 \frac{l''}{l} + \dots - \alpha_1 t_1) E_1 F_1}{1 + \frac{E_1 F_1}{\mathfrak{E}\mathfrak{F}}} \quad (1.31)$$

### (c) Elastic Elements

The elasticity of a bolt-housing system can be varied without changing the sections of the system components by introducing elastic elements (Fig. 10b). This is widely employed in practice.

Depending on their arrangement, such elastic elements increase the elasticity of either the bolts or housings. In order to evaluate the effect of the elastic elements it is necessary first to find out which elements belong to the bolt system and which to the housing one. If the application of the working force  $P_{work}$  increases the load on an element, the latter then belongs to the bolt system, regardless of whether the load is tensile or compressive. If the working force lessens the load on the element, this element then belongs to the housing system.

For instance, the load on element 1 (Fig. 10b) is increased when the working force  $P_{work}$  is applied. Therefore, this element belongs to the bolt system; its elasticity should be included into that of the fastening bolts. Element 2, on the contrary, is unloaded when the working force is applied and, hence, must be regarded as belonging to the housing system.

The deformation of an elastic element under the effect of the applied load is

$$\lambda' = Pfl_e$$

where  $l_e$  = length of the element

$f$  = elastic ratio of the element (relative deformation produced by 1-kgf force)

The deformation related to the total length  $l$  of the joint is

$$e' = Pf \frac{l_e}{l}$$

The total relative deformation of a bolt with an elastic element having length  $l_a$  and elasticity  $f_a$  is the sum of the deformations of the bolt and element

$$e = e_1 + e' = P \left( \frac{1}{E_1 F_1} + f_a \frac{l_a}{l} \right) = \frac{P}{\mathfrak{C}_a \mathfrak{F}_a} \quad (1.32)$$

The quantity

$$\mathfrak{C}_a \mathfrak{F}_a = \frac{1}{\frac{1}{E_1 F_1} + f_a \frac{l_a}{l}}$$

is the corrected rigidity factor of the system.

The corrected rigidity factor of a housing with an elastic element of length  $l_b$  and elasticity  $f_b$  is

$$\mathfrak{C}_b \mathfrak{F}_b = \frac{1}{\frac{1}{E_2 F_2} + f_b \frac{l_b}{l}} \quad (1.33)$$

These quantities can be introduced into the previous equations in place of  $E_1 F_1$  and  $E_2 F_2$  and the calculations carried out as previously.

With the help of elastic elements the operating parameters of a connection can be beneficially influenced. For example, introducing elastic elements into the housing system can improve the reliability of sealing of the connection and reduce the necessary bolt tightening force. The pulsation of the bolt tension force can also be reduced by introducing elastic elements.

Elastic elements are an efficient means for preventing the gradual weakening of the tightening force due to relaxation.



## (d) Relaxation

Tightened joints (particularly those operating under elevated temperatures) in the course of time weaken due to a slowly developing plastic deformation of the bolts (and, occasionally, of the clamped parts as well) under the influence of loads acting for a long time. The plastic deformation phenomenon occurring under stresses well below those corresponding to the yield point of the material is called *relaxation*. The property of metals to flow when being acted upon by a continuous load can be ascertained only in special tests, during which specimens are held under load for 3000 to 10 000 hours.

Relaxation is often defined as a spontaneous change with time of stresses with unchanging deformation. This definition cannot be accepted. The fall in stresses during relaxation is inevitably accompanied by plastic deformation. Moreover, plastic deformation is the first reason for relaxation. It is more legitimate to speak about a room-temperature creep of materials, which is akin to high-temperature creep, the difference being that the room-temperature creep deformation develops slower and has a smaller magnitude.

The process of relaxation can be followed schematically on an example of housing-type components clamped with bolts. For the sake of simplicity we assume at first that the housing under consideration is perfectly rigid and the only deformable element is the bolt. At first glance it seems that the system operates under the conditions of constant deformation. Actually this is not true. Eventually the bolt elongates plastically. The original relative elastic deformation  $\Delta e$  of the bolt, due to the bolt preload, now decreases by the amount of relative residual deformation  $\Delta_{res}$  so that the resultant elastic deformation becomes  $\Delta e' = \Delta e - \Delta_{res}$ .

If the initial tightening force equalled  $P_{tight} = \Delta e E_1 F_1$  ( $E_1 =$  = elasticity modulus of the bolt material,  $F_1 =$  bolt cross-section), then after elongation the force becomes  $P'_{tight} = (\Delta e - \Delta_{res}) E_1 F_1$ , i.e., it decreases in comparison to the original tightening force by  $\left(1 - \frac{\Delta e}{\Delta_{res}}\right)$  times. Upon removing the bolt and measuring its length, it is found that the bolt has lengthened by the value  $l\Delta_{res}$  ( $l =$  = original bolt length).

With the decrease of the tightening force the stresses in the bolt fall down. When they reach the level at which the bolt elongation discontinues or becomes negligible, the process of relaxation ceases and the stresses in the system become stable.

In real systems of clamped elastic parts the course of this process is somewhat different. As the bolt elongation proceeds, the clamped parts, while expanding elastically continue to exert pressure on the bolt, although somewhat lower in comparison with the initial

pressure. Under such circumstances the relaxation process stops and the system becomes stable with a relatively greater bolt elongation than in the previous case.

We have analysed a non-loaded connection. In systems subjected to a constantly acting static or cyclic load relaxation progresses continuously. The state of practical stabilization sets in only as a result of the slowing down of the elongation process, which is observed in most materials in the course of time, provided the connection has not failed before this due to the separation of the joint

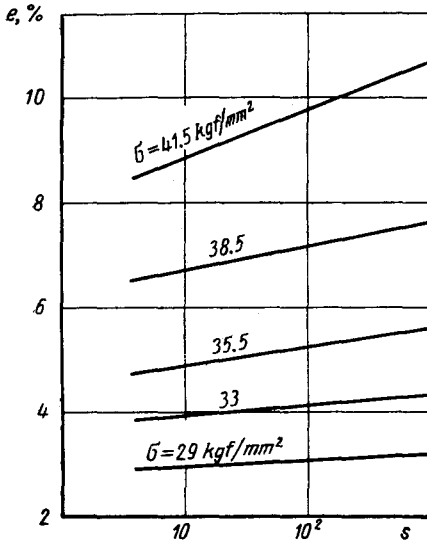


Fig. 11a. Total deformation  $e$  of a carbon-steel specimen (0.1%C) after being held under tensile stress  $\sigma$ . Test temperature 20°C (after Rogan Alexander)

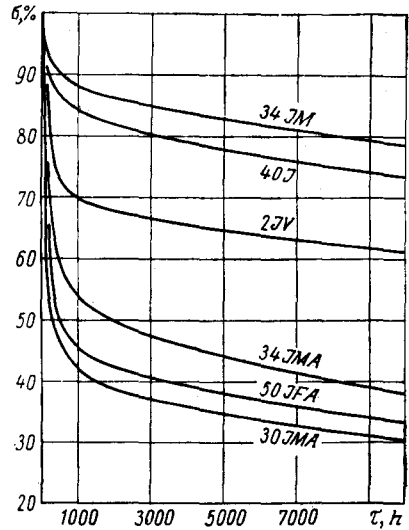


Fig. 11b. Residual stresses in per cent of original stress ( $\sigma_0 = 25 \text{ kgf/mm}^2$ ) as a function of holding time. Test temperature 400-450°C

faces. The higher the stress, the greater the creep of materials (Fig. 11a), and it sharply increases with the rise in temperature. The creep is greater under cyclic loads than under static ones. It varies with different metals and alloys and depends on the type of heat treatment.

This requires the introduction of a concept of relaxation resistance understood as the ability of a material to resist plastic deformation under continuous loads.

The method of determining relaxation resistance is not as yet fully established. The majority of the methods applied at present are based on inducing in specimens a certain, rather high stress; the specimens are held at this particular stress and at an elevated tem-

perature for a long period of time (up to 10 000 hours). Generally, the chosen stress amounts to 0.5-0.6 of the yield limit of the material at the given temperature.

A split-ring method is the one most often employed. The specimen is a ring with a wedge-shaped cut. The required stress is produced by forcing a wedge into the cut, which causes bending stresses to develop in the opposite ring section shaped so as to have the same bending resistance throughout its entire length. In this state the specimen is kept at the given temperature for the given period of time.

At definite time intervals the load is removed and the residual deformation measured. This is used for calculating the stress remaining in the specimen at the end of each interval.

The diagram shown in Fig. 11 is a result of such tests. The remaining stresses are shown in Fig. 11b as a function of time and characterize the relaxation resistance of the material. The higher the stress remaining in the specimen (i.e., the lower the residual deformation of the specimen), the greater the relaxation resistance of the material.

The remaining stresses sharply drop during the first 1000 hours of tests and then lower at a slower pace. This shows that as the holding period grows longer the yielding of the material decreases (seemingly as a result of strain hardening).

The relaxation resistances of various materials are different. Thus, for example, a specimen made from steel grade 40X, after being held at 400°C for 3000 hours, retains 80% of its initial stresses, while one made from steel grade 50XΦA retains only 40%. If we convert the results obtained for bending loads to the case of tensile loads, then a bolt made from steel 50XΦA will, after 3000 hours' work, extend to a length equal to 60% of its initial elastic deformation due to tightening, in which case the tightening force will be reduced by 60%. Naturally, account should also be taken of the above-described effects of the elasticity of the clamped parts and of the working forces which add to the bolt elongation.

Estimating the relaxation resistance by the magnitude of the residual stresses is controversial. To reflect the physical essence of the phenomenon and make calculations more convenient it is advisable to characterize the resistance to relaxation by the magnitude of the deformations remaining in the specimen after its being held under a load corresponding to the actual loading conditions (for fastening bolts, under a tensile load).

Methods to prevent the weakening of tightened connections as a result of relaxation consist in making bolts from relaxation-resistant materials and subjecting them to appropriate heat treatment. Silicon steels possess a high relaxation resistance. Normalizing followed by high tempering is an optimum heat treatment from the standpoint of relaxation resistance. It seems possible to obtain

a significant effect by strengthening the bolts through their preliminary elongation (ageing) which acceleratively simulates the greatest yield stage of the material.

All measures should be taken to reduce stresses in bolts and the pulsation amplitude of the tension force in cyclically loaded connections. It is also advisable to introduce elastic elements of relaxation-resistant materials so as to compensate for residual deformations as they develop.

### (e) Graphical Calculations of Tightened Connections

The totality of the phenomena occurring in tightened connections is easily amenable to graphical interpretation with the help of *P-e* (force vs. relative deformation) diagrams.

Let us take the simplest case, namely, the tightening of a split connection with force  $P_{tight}$  (Fig. 12a). In solving the problem the forces will be plotted on the ordinate axis, and relative deformations — on the abscissa axis, assuming tension to be a positive, and compression, a negative deformation. Line  $Oa$  shows the bolt elongation and its slope relative to the abscissa axis is

$$\tan \alpha = \frac{\eta}{\mu} E_1 F_1$$

where  $\eta$  = scale of forces

$\mu$  = scale of relative deformations

The compression of the parts being tightened is presented by the straight line  $Ob$  whose slope relative to the abscissa axis is

$$\tan \beta = \frac{\eta}{\mu} E_2 F_2$$

If we draw on the diagram a horizontal line  $ba$  at a distance corresponding to the tightening force  $P_{tight}$  from the abscissa axis, it will intersect the tension-compression lines at points  $a$  and  $b$ , the abscissae of which are equal to the relative deformations  $e_1$  of the bolts and  $e_2$  of the housing when tightened.

It is more convenient to plot the diagram as shown in Fig. 12b, i.e., by drawing the compression line through point  $a$  on the tension line, which corresponds to  $P = P_{tight}$ .

Now assume that a force  $P_{work}$  develops in the joint and that this force imposes an additional load on the bolts while unloading the joint (Fig. 12c).

When determining the bolt tension force, we assume, as previously, that the relative deformations of the bolts and clamped components are the same.

At a distance  $P_{work}$  (along the vertical) from the bolt tension line  $Oa$  draw a straight line (dashed) parallel to it. Through point  $k$ ,

where this line intersects the clamped parts' compression line, draw a vertical line until the latter intersects the tension line (point *c*). This vertical line will cut off a line-segment of length  $\Delta e$  on the

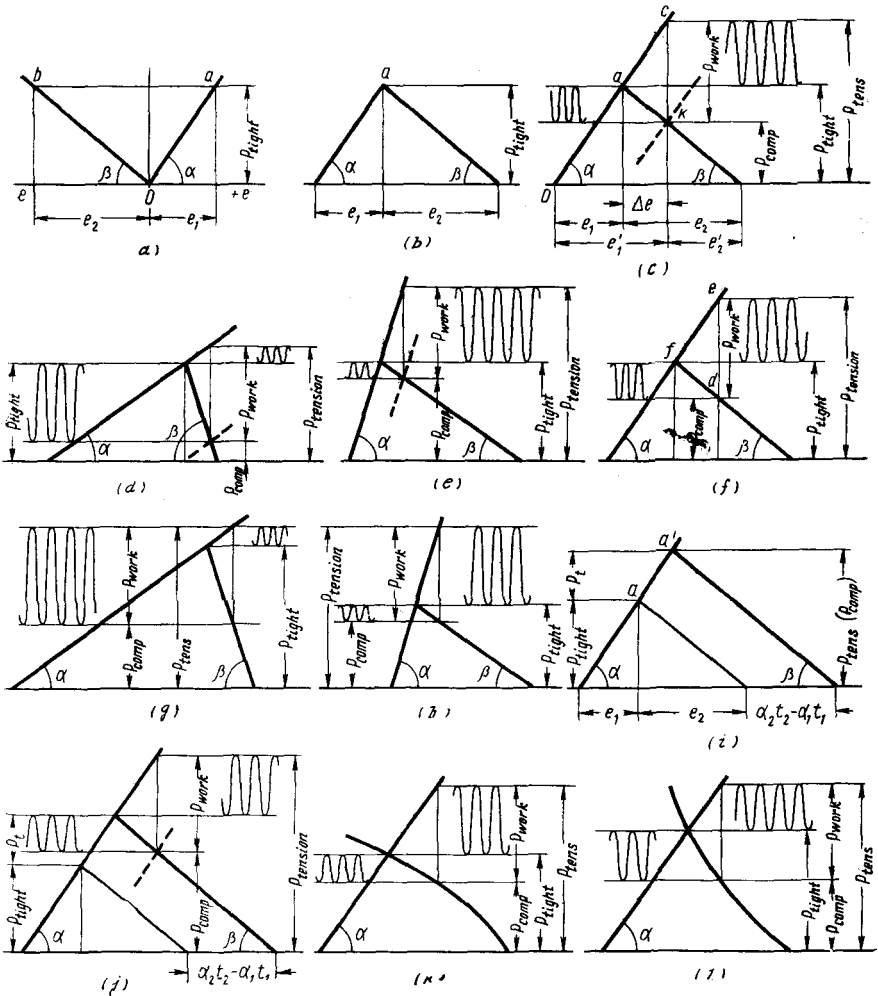


Fig. 12. Graphical calculations of tightened connections

abscissa axis. Clearly, this scheme reproduces the condition of equal  $\Delta e$  for the bolts and clamped components.

This construction gives all the necessary data. The ordinate of point *c* shows to scale the bolt tension force  $P_{tens}$ ; the ordinate of point *k*, the joint compression force  $P_{comp}$ ; line-segments  $e'_1$  and  $e'_2$

relative deformations of the bolts and clamped components after application of working force  $P_{work}$ .

If the working force pulsates from zero to  $P_{work}$ , the pulsation amplitude of force  $P_{tens}$  will then equal  $P_{tens} - P_{tight}$  (the right-hand wavy curve) and that of force  $P_{comp}$ ,  $P_{tight} - P_{comp}$  (the left-hand wavy curve).

Now let us consider how the system's behaviour is influenced by the variation of the rigidity of bolts and clamped parts (i.e., by changes in the slope angles  $\alpha$  and  $\beta$  of the tension and compression lines, respectively).

Figure 12*d* illustrates the case of a rigid housing and elastic bolts, while Fig. 12*e*, that of rigid bolts and an elastic housing. The tightening force  $P_{tight}$  is assumed to be the same in both cases. Figures 12*d* and 12*e* clearly illustrate the above-described regularities. The increase of the bolt elasticity with a simultaneous increase in the housing rigidity (reduction of the ratio  $E_1F_1/E_2F_2$ ) lowers the bolt tension force and the pulsation amplitude of this force (see Fig. 12*d*). At the same time this decreases the joint compression force and increases its pulsation amplitude.

Increasing the ratio  $E_1F_1/E_2F_2$  (elastic housing and rigid bolts) acts in the opposite direction (see Fig. 12*e*): force  $P_{tens}$  and the amplitude of its pulsation increase,  $P_{comp}$  rises too, but the amplitude of its pulsation decreases.

As stated earlier, when determining connection parameters it is more proper to proceed from the condition of proportionality between the compression force and working pressure ( $P_{comp} = \theta P_{work}$ ).

In this case the graph is plotted in the following order (Fig. 12*f*). First, draw horizontals at distances  $P_{comp} = \theta P_{work}$  and  $P_{tens} = (1 + \theta) P_{work}$  from the abscissa axis (in Fig. 12*f* it is assumed that  $\theta = 0.6$ ). Then from any arbitrary point draw at an angle  $\beta$  an inclined line representing the housing compression. From point *d* at which this line intersects the horizontal line  $P_{comp}$  draw a vertical until it meets the horizontal line  $P_{tens}$  and through point *e* of their intersection draw at an angle  $\alpha$  an inclined line representing the bolt tension. The ordinate of point *f*, where the two inclined lines intersect, gives the value of the tightening force  $P_{tight}$ .

The difference  $P_{tens} - P_{tight}$  shows, as before, pulsation amplitude of force  $P_{tens}$ , and the difference  $P_{tight} - P_{comp}$ , the pulsation amplitude of force  $P_{comp}$ .

Figures 12*g* and 12*h* show how the rigidity of the housing and bolts influences the operation of the joint (with  $P_{work}$  and  $\theta$  values being the same as above). In the case of elastic bolts and a rigid housing (Fig. 12*g*) force  $P_{tight}$  increases, the pulsation amplitude of force  $P_{tens}$  decreases and the pulsation amplitude of force  $P_{comp}$  increases.

In the case of rigid bolts and an elastic housing (Fig. 12h) the force  $P_{tight}$  decreases, the pulsation amplitude of force  $P_{tens}$  increases and the pulsation amplitude of force  $P_{comp}$  decreases.

For an unloaded connection ( $P_{work} = 0$ ) subjected to heating, which causes a thermal stress  $P_t$  to develop in the joint (Fig. 12i), one should draw a line parallel to and spaced from the compression line at a distance of  $\alpha_2 t_2 - \alpha_1 t_1$  (along the horizontal), equal to the relative deformation due to the heating. The ordinate of point  $a'$ , at which this line intersects the tension line, is equal to  $P_{tens}$  (identical to force  $P_{comp}$  compressing the housing) after the heating; the difference between the ordinates of points  $a$  and  $a'$  represents the thermal stress  $P_t$ .

For connections which are simultaneously subjected to heating and to the action of force  $P_{work}$  the plotting differs in that the inclined tension and compression lines are set apart (horizontally) at a distance of  $\alpha_2 t_2 - \alpha_1 t_1$  (Fig. 12j). The rest of the construction is as before.

The elasticity characteristic of the clamped parts does not always follow the linear relation  $P = eE_2 F_2$ . Such is, for instance, the case with thin-walled intricately shaped components whose walls in certain areas are either inclined or perpendicular to the direction of the compressive force. Here the compressive deformations of the walls are complemented with the elastic bending deformations of their inclined and horizontal portions. Furthermore, the walls may be subject to buckling. If so, the rigidity of the clamped parts sharply drops and the characteristic curve assumes a gently sloping shape.

Occasionally the elasticity characteristic becomes curvilinear because the individual elements of a construction come into operation not at the same time, but one after another as the load increases. The elasticity characteristic of such complex constructions can only be determined experimentally. To this end a fully finished construction is subjected to compression on a test rig and its elasticity characteristic is plotted point by point on the basis of the test data.

In this instance the graphical method of calculation is the only way possible. The curve obtained from the test is plotted on the graph in place of the inclined line  $P = eE_2 F_2$  (Fig. 12k, l). Further construction is as described above.

When calculating for a known force  $P_{comp} = \theta P_{work}$ , the curvilinear nature of the characteristic has an effect on the magnitude of the tightening force and of the pulsation amplitude of forces  $P_{tens}$  and  $P_{comp}$ . With a convex characteristic (Fig. 12k) the required force  $P_{tight}$  diminishes, the pulsation amplitude of force  $P_{tens}$  increases and that of force  $P_{comp}$  decreases. If the characteristic is concave (Fig. 12l) the picture is reversed.

(f) *Methods of Controlling the Tightening Force (Preload)*

Because the preload has a great effect on the bolt tension and joint compression forces, it is very important during assembly to strictly keep to the calculated magnitude of the tightening force. This is achieved by tightening nuts with torque wrenches, by turning them through calculated angles or by measuring the elongation of bolts.

The application of torque measuring wrenches does not provide for adequate accuracy, since the force needed to tighten nuts depends to a large extent on the thread condition, coefficient of friction in the threads and on the bearing surfaces, etc. For this reason, bolts tightened with the same torque may, in fact, be loaded differently.

To lessen the friction effect critical connections are sometimes tightened on a vibration table. The rather sharp decrease in the friction forces because of vibration must be considered when choosing the design tightening torque.

When tightening nuts by rotating them through a calculated angle they are first brought into close contact with the bearing surfaces, i.e., up to the point when bolts begin to extend. After this the nuts are turned with a wrench through the required angle  $\nu$ .

This angle is determined from the given tightening force  $P_{tight}$ , proceeding from the following considerations.

When tightening a nut, it is necessary to choose the bolt elongation  $\lambda_1 = \frac{P_{tight} l}{E_1 F_1}$  and clamped parts contraction  $\lambda_2 = \frac{P_{tight} l}{E_2 F_2}$ .

The axial displacement of the nut relative to the bolt is

$$\lambda = \lambda_1 + \lambda_2 = P_{tight} l \left( \frac{1}{E_1 F_1} + \frac{1}{E_2 F_2} \right) \quad (1.34)$$

The tangent of the thread helix angle

$$\tan \varphi = \frac{s}{\pi d_0} \quad (1.35)$$

where  $s$  = thread pitch

$d_0$  = thread pitch diameter

The displacement of the nut by value  $\lambda$  corresponds to its rotation over arc  $C$  of the circumference of radius  $d_0/2$

$$C = \frac{\lambda}{\tan \varphi} \quad (1.36)$$

On the other hand, the value of  $C$  is

$$C = \frac{d_0}{2} \nu = \frac{d_0}{2} \cdot \frac{2\pi}{360^\circ} \nu^0 \quad (1.37)$$

where  $\nu$  is the nut rotation angle in radians, and  $\nu^0$ , the same in degrees.



Equating Eqs. (1.36) and (1.37), we have

$$\nu^\circ = \frac{\lambda}{\tan \varphi} \cdot \frac{360^\circ}{\pi d_0}$$

Substituting into this equation  $\lambda$  and  $\tan \varphi$  from Eqs. (1.34) and (1.35), we have

$$\nu^\circ = 360^\circ P_{tight} \frac{l}{s} \left( \frac{1}{E_1 F_1} + \frac{1}{E_2 F_2} \right) \quad (1.38)$$

Clearly, the tightening angle is independent of the bolt diameter.

Nuts are practically tightened by the following method. First all the clearances in the system are taken up (by tightening all the nuts home in a certain succession). This done, the nuts are slackened off and again tightened by hand or by means of a light torque-control wrench until the nuts are in close contact with the bearing surfaces. Thereafter all the nuts are tightened in a definite sequence (staggered, cross-like, serpentine-like) depending on the configuration of the joint faces and assuring a uniform tightening of the connection by turning them first through an angle of  $\nu/2$  and then, in the same succession, through the full angle  $\nu$ .

To measure the nut rotation angle the wrench is provided with pointer and the tightened component, a graduated disk.

This method is more accurate than the first one, although it also contains sources of errors due to the difficulty of determining the right moment to start the tightening. It is only by fitting experience that this error can be reduced to minimum.

In respect to slender bolts and studs the accuracy of measurement is influenced by their twisting during tightening, which is due to friction in the threads. To eliminate the twisting, the bolt end is held with a spanner when tightening (see Fig. 3a). However, this method is not convenient in actual fitting. Figure 13 depicts a wrench design which excludes any effect of the bolt twisting upon the accuracy of the tightening angle measurement.

Inserted into the wrench stem is a spring-loaded locking device 1 having a tapered end with a tapered shank of cross-like section,

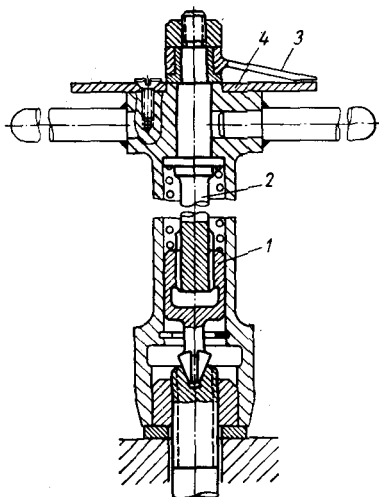


Fig. 13. Wrench design enabling accurate measurement of nut turning angle relative to bolt

which fits into a corresponding socket in the bolt end. The locking device is spline-connected with rod 2 whose projecting end holds a friction-mounted pointer 3 positioned over graduated dial 4 attached to the wrench end face.

As the wrench is applied to the nut, the locking device enters the bolt socket, thus providing a direct connection between the bolt and pointer. Prior to tightening, the pointer is set to the dial zero position. During the tightening the pointer indicates the rotation angle of the nut relative to the bolt, i.e., the nut tightening angle.

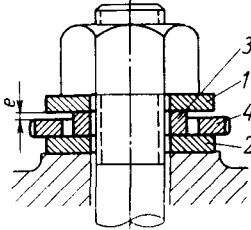


Fig. 14. Control of tightening force by means of deformable ring

The elongation of short bolts is measured by means of a micrometer calliper gauge. The technique is applicable whenever the calliper jaws can be directly applied to the bolt ends. In this way, for example, is measured the elongation of connecting rod bolts, pinch bolts in clamp connections, fastening bolts of hydraulic cylinders, etc. For greater measuring convenience the bolt head and stem end are made spherical.

The elongation of studs can be measured with the aid of an indicator, if its foot is set up on an independent support. When installed on the component being tightened the indicator will read the total of the elongation of the stud and the contraction of the tightened parts.

Sometimes the tightening force is controlled by means of a system of deformable washers (Fig. 14). Rigid washers 1 and 2 and measuring ring 3 of a plastic metal (e.g., annealed copper) are placed under the nut. Reference washer 4 is placed concentrically around the measuring ring. The thickness of ring 3 is selected so that after the preliminary, light tightening of the nut a design clearance  $e$  (equal to the sum of elastic deformations in the tightened system) remains between the ring and reference washer. As the nut is finally tightened the measuring ring is flattened out. The tightening is stopped when the clearance  $e$  is taken up completely (this being indicated by the reference washer losing its mobility).

The measuring ring must be changed whenever the nut has to be retightened.

### (g) Calculation Example

An engine cylinder block having a cross-section as shown in Fig. 15 is fastened to the crankcase by means of studs 400 mm long; the stud stem diameter is 18 mm, thread M24 (pitch  $s = 1.5$  mm).

Assume that the ignition force  $P_{work} = 10\,000$  kgf is taken up by the four studs nearest to the cylinder and that the studs' tightening force spreads over

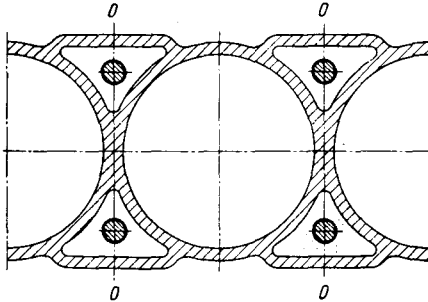


Fig. 15. Cross-sectional view of cylinder block

the block portion adjacent to the cylinder (delimited by lines  $O-O$  in the Figure) with a cross-sectional area of  $7000\text{ mm}^2$ .

The block is made from aluminium alloy grade AJ15 ( $E_2 = 7500\text{ kgf/mm}^2$ ,  $\alpha_2 = 22 \cdot 10^{-6}$ ); the studs are of steel grade 30XTC ( $E_1 = 21\,000\text{ kgf/mm}^2$ ;  $\alpha_1 = 11 \cdot 10^{-6}$ ). The temperature of the block and studs in the running engine is  $80^\circ\text{C}$ .

Find the maximum stresses in the studs and crankcase in both the cold (dead) and hot (running) engine.

Assume that  $\theta = 0.5$ .

Joint compression force

$$P_{comp} = 0.5P_{work} = 5000\text{ kgf}$$

Total stud tension force [Eq. (1.22)]

$$P_{tens} = (1 + 0.5)P_{work} = 15\,000\text{ kgf}$$

Tension force per stud

$$P_{tens.1} = \frac{15\,000}{4} = 3750\text{ kgf}$$

Tensile stress in studs

$$\sigma_{tens} = \frac{3750}{0.785 \cdot 18^2} = 15\text{ kgf/mm}^2$$

Compressive stress in cylinder block

$$\sigma_{comp} = \frac{P_{comp}}{F_2} = \frac{5000}{7000} = 0.7\text{ kgf/mm}^2$$

Total tightening force  $P_{tight}$  [Eq. (1.24)] required

$$P_{tight} = P_{work} \left( \theta + \frac{1}{1 + \frac{E_1 F_1}{E_2 F_2}} \right)$$

Factor  $E_1 F_1$

$$E_1 F_1 = 21\,000 \cdot 4 \cdot 0.785 \cdot 18^2 = 2.1 \cdot 10^7\text{ kgf}$$

Factor  $E_2 F_2$

$$E_2 F_2 = 7500 \cdot 7000 = 5.3 \cdot 10^7\text{ kgf}$$

Hence,

$$P_{tight} = 10\,000 \left( 0.5 + \frac{1}{1 + \frac{2.1}{5.3}} \right) = 12\,000\text{ kgf}$$

Angle through which nuts must be turned when tightening [Eq. (1.38)]

$$\begin{aligned} \nu &= 360^\circ P_{tight} \frac{l}{s} \left( \frac{1}{0.25E_1F_1} + \frac{1}{E_2F_2} \right) = \\ &= 360^\circ \cdot 3000 \frac{400}{1.5} \left( \frac{1}{5.2 \cdot 10^6} + \frac{1}{5.3 \cdot 10^7} \right) = 60^\circ \end{aligned}$$

Thermal stress in the joint when heated [Eq. (1.25)]

$$P_t = (\alpha_2 t_2 - \alpha_1 t_1) \frac{E_1 F_1}{1 + \frac{E_1 F_1}{E_2 F_2}}$$

By hypothesis,  $t_2 = t_1 = 80^\circ\text{C}$ . Substituting numerical values, we have

$$P_t = 80 (22 - 11) \cdot 10^{-6} \cdot \frac{2.1 \cdot 10^7}{1 + \frac{2.1}{5.3}} = 13\,000 \text{ kgf}$$

After heating:

stud tension force

$$P'_{tens} = P_{tens} + P_t = 15\,000 + 13\,000 = 28\,000 \text{ kgf}$$

joint compression force

$$P'_{comp} = P_{comp} + P_t = 5000 + 13\,000 = 18\,000 \text{ kgf}$$

tensile stress in studs

$$\sigma'_{tens} = \frac{P'_{tens}}{4 \cdot 0.785 d^2} = \frac{28\,000}{4 \cdot 0.785 \cdot 18^2} = 28 \text{ kgf/mm}^2$$

compressive stress in cylinder block

$$\sigma'_{comp} = \frac{18\,000}{7000} = 2.6 \text{ kgf/mm}^2$$

tension force pulsation amplitude

$$\Delta_{tens} = P'_{tens} - (P_{tight} + P_t) = 28\,000 - (12\,000 + 13\,000) = 3000 \text{ kgf}$$

coefficient of cycle skewness

$$r = \frac{P'_{tens} - \Delta_{tens}}{P'_{tens}} = 1 - \frac{3000}{28\,000} \approx 0.9$$

compression force pulsation amplitude

$$\Delta_{comp} = P_{tight} + P_t - P'_{comp} = 12\,000 + 13\,000 - 18\,000 = 7000 \text{ kgf}$$

coefficient of cycle skewness

$$r = \frac{P'_{comp}}{P_{tight} + P_t} = \frac{18\,000}{12\,000 + 13\,000} = 0.7.$$

The fatigue limit of steel grade 30XTC under a pulsating cycle with a coefficient of skewness of 0.9 equals  $75 \text{ kgf/mm}^2$ . The fatigue limit of aluminium alloy grade AL5 under a pulsating cycle with a coefficient of skewness of 0.7 equals  $8 \text{ kgf/mm}^2$ . Consequently, the safety factor for the studs is  $\frac{75}{28} = 2.7$  and that

for the cylinder blocks,  $\frac{8}{2.6} = 3$ .

# Press-Fitted Connections

Press (drive) fits are extensively applied in general engineering to make permanent joints or those seldom dismantled. The relative displacement of press-fitted parts is prevented by the forces due to elastic compressive deformation (in the male part) and tensile deformation (in the female part), which are proportional to the amount of interference in the joint.

## 2.1. Press (drive) Fits

The USSR State Standard ГOCT 7713-62 stipulates the following press fits for the basic hole system.

<i>1st grade of accuracy</i>		<i>2nd grade of accuracy</i>	
1st heavy drive fit ( $Dh1_1$ ) ... $\Pi p1_1$		Light drive fit ( $Dl$ ) . . . . . $\Pi A$	
2nd heavy drive fit ( $Dh2_1$ ) ... $\Pi p2_1$		Heavy drive fit ( $Dh$ ) . . . . . $\Pi p$	
		Shrink fit ( $Sh$ ) . . . . . $\Gamma p$	
<i>2a grade of accuracy</i>		<i>3rd grade of accuracy</i>	
1st heavy drive fit ( $Dh1_{2a}$ ) ... $\Pi p1_{2a}$		1st heavy drive fit ( $Dh1_3$ ) ... $\Pi p1_3$	
2nd heavy drive fit ( $Dh2_{2a}$ ) ... $\Pi p2_{2a}$		2nd heavy drive fit ( $Dh2_3$ ) ... $\Pi p2_3$	
		3rd heavy drive fit ( $Dh3_3$ ) ... $\Pi p3_3$	

Figure 16a gives mean interferences  $\Delta_{mean}$   $\mu\text{m}$  as a function of the shaft diameter  $d$  mm for different press fits; Fig. 16b—mean relative interferences  $\frac{\Delta_{mean}}{d}$   $\mu\text{m}/\text{mm}$  and  $\frac{\Delta_{mean}}{d}$ .

From Fig. 16b it is seen that the relative interferences sharply increase in the small diameter range. For this reason one must be especially careful when designing small diameter joints since the strength of press-fitted parts depends first of all on the amount of their relative interference.

Light drive fits ( $Dl$ ) are obtained with the least interferences. Fits  $Dh1_1$  are close to the latter in terms of the mean interferences. Fits  $Dh2_1$ ,  $Dh$ ,  $Dh1_{2a}$  and  $Dh1_3$  are practically the same as far as

the mean interferences are concerned, the only difference being that the fits to lower grades of accuracy have wider tolerances. Mean interferences are practically the same in the case of fits *Sh* and

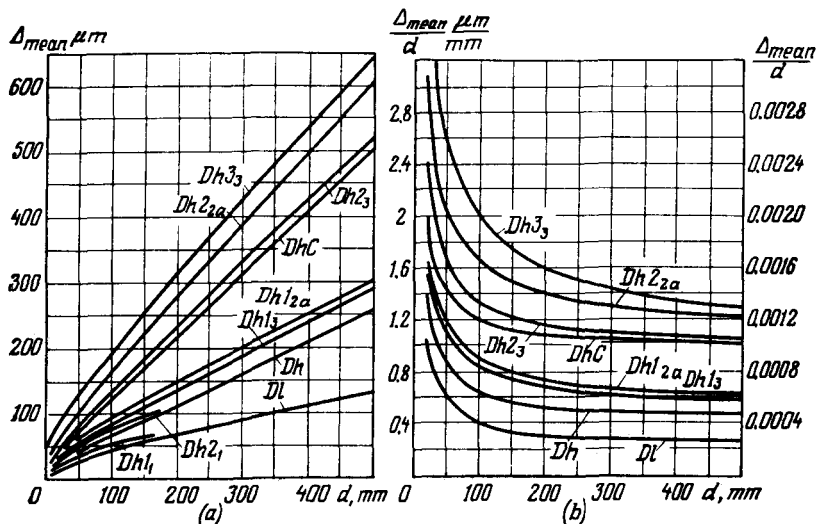


Fig. 16. Mean interference  $\Delta_{mean}$  and relative interference  $\Delta_{mean}/d$  as a function of connection diameter  $d$  for different fits

*Dh2<sub>3</sub>*. The greatest (and almost identical) mean interferences are in the case of fits *Dh2<sub>2a</sub>* and *Dh3<sub>3</sub>*.

The relationship between the mean interference and diameter is approximately expressed by the formula

$$\Delta_{mean} \mu m \approx \psi (D \text{ mm} + 60) \tag{2.1}$$

The proportionality factor  $\psi$  for various fits is as follows

Fits . . . . .	<i>Dl</i>	<i>Dhl<sub>1</sub></i>	<i>Dh</i>	<i>Dh2<sub>1</sub></i>	<i>Dh1<sub>3</sub></i>	<i>Dh1<sub>2a</sub></i>	<i>Sh</i>	<i>Dh2<sub>3</sub></i>	<i>Dh2<sub>2a</sub></i>	<i>Dh3<sub>3</sub></i>
$\psi$ . . . . .	0.23	0.28	0.46	0.44	0.5	0.54	0.95	0.98	1.13	1.16

### 2.2. Strength of Press-Fitted Connections

The axial holding power of a press-fitted connection is

$$P_{ax} = kFf \text{ kgf} \tag{2.2}$$

The torsional holding power

$$M_{tors} = 0.001kFf \frac{d}{2} \text{ kgf} \cdot \text{m} \tag{2.3}$$

where  $k$  = unit pressure on the surface of joint,  $\text{kgf}/\text{mm}^2$   
 $F = \pi dl = \text{joint surface area, mm}^2$

$f$  = coefficient of friction between mating surfaces (for steel and cast iron, on the average,  $f = 0.1-0.15$ )

$d, l$  = diameter and length of the surface of joint, mm

The unit pressure on the surface of joint is found from Lamé's equation

$$k = \frac{\Delta}{d} \cdot \frac{1}{\frac{c_1 - \mu_1}{E_1} + \frac{c_2 + \mu_2}{E_2}} \text{ kgf/mm}^2 \quad (2.4)$$

where  $\frac{\Delta}{d}$  = relative diametral interference ( $\frac{\Delta}{d} = \frac{\Delta \mu \text{m}}{1000 d \text{ mm}}$ )  
 $E_1, E_2$  and  $\mu_1, \mu_2$  = elastic moduli (in kgf/mm<sup>2</sup>) and Poisson's ratios of the materials of the male and female parts, respectively

$c_1$  and  $c_2$  = coefficients expressed as

$$c_1 = \frac{\left(\frac{d_1}{d}\right)^2}{1 - \left(\frac{d_1}{d}\right)^2} \quad (2.5)$$

$$c_2 = \frac{1 + \left(\frac{d}{d_2}\right)^2}{1 - \left(\frac{d}{d_2}\right)^2} \quad (2.6)$$

where  $d_1$  and  $d_2$  are the inner diameter of the male part and the outer diameter of the female part, respectively.

Let us designate  $\frac{d_1}{d} = a_1$  and  $\frac{d}{d_2} = a_2$ . The quantities  $a_1$  and  $a_2$  may be called the relative wall thickness of the male and female parts, respectively. When  $a_1 = a_2 = 1$  the thicknesses of the male and female parts equal zero. Values  $a_1 = a_2 = 0$  correspond to the case of massive male and female parts.

Coefficients  $c_1$  and  $c_2$  may be expressed in a general form as follows (Fig. 17):

$$c = c_1 = c_2 = \frac{1 + a^2}{1 - a^2}$$

Equation (2.4) shows that unit pressure  $k$  and, consequently, the joint strength are proportional to the relative diametral interference  $\Delta/d$ , increasing with the increase of Young's moduli of the materials and decreasing with the increase of  $c_1$  and  $c_2$ , i.e., with the enhancement of the wall thickness factor  $a$ .

The compressive stress in the male part is maximum on its internal surface and is expressed as

$$\sigma_1 = \frac{2k}{1-a_1^2} = \frac{\Delta}{d} \cdot \frac{2}{1-a_1^2} \cdot \frac{1}{\frac{c_1-\mu_1}{E_1} + \frac{c_2+\mu_2}{E_2}} \quad (2.7)$$

The maximum permissible unit pressure determined by the bearing strength of the material is

$$k = \sigma_{bear} \quad (2.8)$$

where  $\sigma_{bear}$  is the ultimate bearing strength of the material.

The reduction in the internal diameter of the male part

$$\Delta_1 \approx \frac{\sigma_1}{E_1} d_1 \quad (2.9)$$

The tensile stress in the female part is maximum on its internal surface and is expressed as

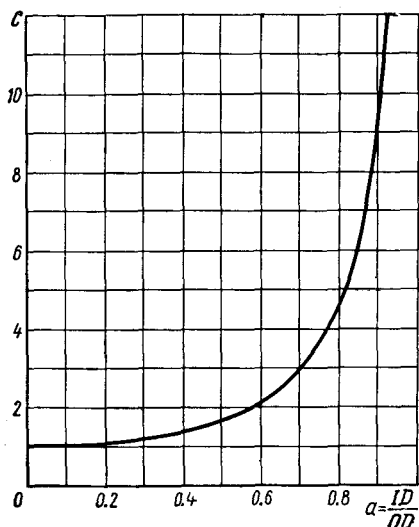
$$\begin{aligned} \sigma_2 &= \frac{2k}{1-a_2^2} = \frac{\Delta}{d} \cdot \frac{2}{1-a_2^2} \times \\ &\times \frac{1}{\frac{c_1-\mu_1}{E_1} + \frac{c_2+\mu_2}{E_2}} \quad (2.10) \end{aligned}$$

The increase in the external diameter of the female part

$$\Delta_2 \approx \frac{\sigma_2}{E_2} d \quad (2.11)$$

Equations (2.4), (2.7) and (2.10) enable some general conclusions to be drawn.

Fig. 17. Coefficient  $c$  as a function of wall thickness factor  $a$



male parts are made of the same material ( $E_1 = E_2 = E$ ;  $\mu_1 = \mu_2 = \mu$ ). Then Eqs. (2.4), (2.7) and (2.10) become

$$k = \frac{\Delta}{d} \cdot \frac{E}{c_1+c_2} \text{ kgf/mm}^2 \quad (2.12)$$

$$\sigma_1 = \frac{\Delta}{d} \cdot \frac{2}{1-a_1^2} \cdot \frac{E}{c_1+c_2} \text{ kgf/mm}^2 \quad (2.13)$$

$$\sigma_2 = \frac{\Delta}{d} \cdot \frac{2}{1-a_2^2} \cdot \frac{E}{c_1+c_2} \text{ kgf/mm}^2 \quad (2.14)$$

Figure 18a shows as a function of  $a_1$  and  $a_2$  the relative pressure  $k_0 = \frac{1}{c_1+c_2}$  which is the value of pressure  $k$  when  $\Delta E/d = 1$ .



The pressure (and consequently the strength of the joint) is maximum when  $a_1 = a_2 = 0$  (both the male and female parts are massive) and decreases with the increase of  $a_1$  and  $a_2$  (i.e., with the decrease of the wall thickness of both the male and female parts), tending to zero when  $a_1 = a_2 = 1$ .

The reduction of the pressure with the decrease of the wall thickness of the male and female parts can be compensated for by increasing the diameter and length of the surface of joint. If, as is usual,

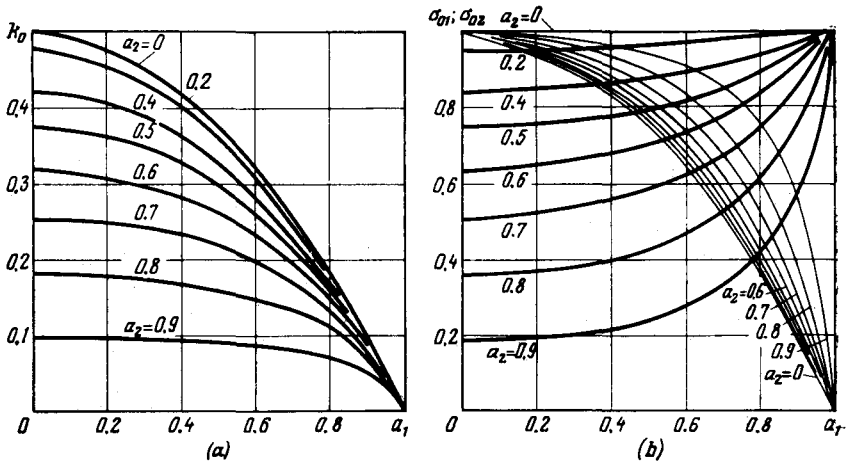


Fig. 18. Effect of wall thickness factors  $a_1$  and  $a_2$  on values of  $k_0$ ,  $\sigma_{01}$  and  $\sigma_{02}$

the length of connection is proportional to its diameter, i.e.,  $l = nd$  ( $n =$  coefficient of proportionality), then, according to Eqs. (2.2) and (2.3),  $P_{ax} = kfn d^2$  and  $M_{tors} = kfn \frac{d^3}{2}$ .

Hence, the resistance of a joint to an axial shift is proportional to the square of its diameter, and its resistance to torsion, to the cube of the diameter.

From Eqs. (2.13) and (2.14) the relative stresses  $\sigma_{01}$  and  $\sigma_{02}$  (the stresses with  $\Delta E/d = 1$ ) are

$$\sigma_{01} = \frac{2k_0}{1-a_1^2} \quad \text{and} \quad \sigma_{02} = \frac{2k_0}{1-a_2^2}$$

These relationships are diagrammed in Fig. 18b. From the graph the following conclusions can be drawn:

stresses  $\sigma_{01}$  in the male part (heavy lines) are maximum ( $\sigma_{01} = 1$ ) with a massive female part ( $a_2 = 0$ ); they decrease as the wall thickness of the female part is reduced ( $a_2 \rightarrow 1$ ) and increase as the wall thickness of the male part is reduced ( $a_1 \rightarrow 1$ );

stresses  $\sigma_{02}$  in the female part (light lines) are maximum ( $\sigma_{02} = 1$ ) with a massive male part ( $a_1 = 0$ ); they decrease as the wall thickness of the male part is reduced ( $a_1 \rightarrow 1$ ) and increase as the wall thickness of the female part is reduced ( $a_2 \rightarrow 1$ ).

Assuming that the male part is a shaft, and the female part, a hub, the following rules can be formulated:

to increase the strength of the shaft it is necessary to increase the thickness of its walls and decrease the wall thickness of the hub (massive shaft and thin-walled hub). This rule is applied when the hub strength is of no concern;

to increase the hub strength it is necessary to increase the thickness of its walls and to decrease the wall thickness of the shaft (massive hub and thin-walled shaft). The rule is applied when the shaft is of sufficient strength.

When the male and female components of a joint are made from dissimilar materials, the above relationships are affected by the rigidity of the materials. If one of the parts (female or male) is made from a material having a smaller elastic modulus ( $E'$ ) than the other one ( $E''$ ), then the unit pressure and the stresses in the parts fall approximately in proportion to the ratio  $E'/E''$  (to a greater degree in the part made from the material of the greater elastic modulus).

The best relationship between the wall thicknesses of the hub and shaft should be established in each particular case by individual calculations.

### (a) Coefficient of Friction

The strength of press-fitted connections is directly proportional to the coefficient of friction between the mating surfaces [see Eqs. (2.2) and (2.3)].

The coefficient of friction depends on the pressure on the contacting surfaces, the magnitude and profile of surface microirregularities, the material and state of the mating surfaces (presence of oil) and also on the assembly technique (connection with the aid of a press, with heating or cooling the parts).

The coefficient of friction rises with an increase in the surface roughness and lowers with a rise in the unit pressure. It is higher when the assembly is done with heating or cooling as compared with a press-fitting. The coefficient can substantially be enhanced by electroplating.

Depending on the above factors the coefficient of friction ranges from 0.08 to 0.3, and sometimes may be even higher. Obviously no accuracy in calculations can be expected with such an extensive  $f$  value scatter. The primary value of the calculation is that it enables one to determine the influence of the geometry and rigidity of the connection elements on the joint strength and outline rational ways to improve it.

In practice lower coefficients of friction ( $f = 0.1-0.15$ ) are generally adopted, including possible increase in the coefficient above these values in the safety factor.

### (b) Effect of Surface Finish

An adequate surface finish of the mating components is an essential condition for the strength of pressed connections.

The measured hole and shaft diameters include the height of microirregularities which are flattened in the course of press-fitting.

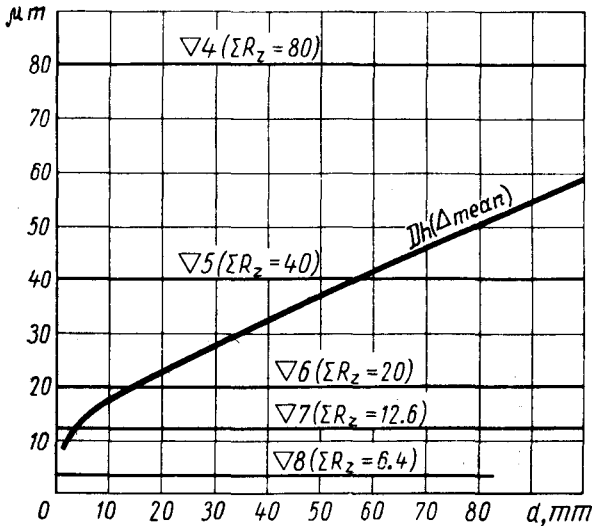


Fig. 19. Mean interferences with Dh grade fit (heavy line) and roughness heights for various classes of surface finish as a function of connection diameter  $d$

If the height of surface microirregularities is commensurate with the interference of mating parts, the actual interference in the pressed connection will then be appreciably smaller.

Shown in Fig. 19 are the mean values of interferences in the case of a heavy drive fit ( $Dh$ ) for different shaft diameters, and the total roughness height  $\sum R_z$  of the shaft and the hole when machined to the 4th-8th class of surface finish. From the graph it is clear that small-diameter connections (less than 30-40 mm) must not be machined worse than to the 6th class because the total roughness height in this case becomes close to the interference value. Hence, in such connections the interference will either be substantially reduced or disappear altogether after the microirregularities are flattened.

Connections with diameters of the order of 50 mm and more, as well as connections with greater interferences, may be machined somewhat rougher. In practice the surfaces of the mating parts in medium-size press-fitted connections are machined to the 8th-10th and 7th-9th classes of surface finish (for shafts and holes, respectively).

Microirregularities have a certain positive effect on the strength of the connection as they act like spurs enhancing the bond between the contacting surfaces. Experiments show that machining better than to the 11th class of surface finish impairs the joint strength because of the reduced coefficient of friction between the contacting surfaces.

Design Eqs. (2.4), (2.7) and (2.10) include the actual interference value. Therefore, when designing pressed connections the assigned nominal interference  $\Delta_{nom}$  should be reduced by the amount of the expected flattening of microirregularities

$$\Delta^t = 2\varphi (R_{z1} + R_{z2}) \quad (2.15)$$

where  $R_{z1}$  and  $R_{z2}$  = roughness height of the shaft and hole, respectively,  $\mu\text{m}$   
 $\varphi$  = flattening coefficient

The amount of the flattening of the microirregularities depends on the interference in the joint, the height of the irregularities, their shape and profile, the density of distribution of the irregularities, the hardness and strength of the material of the mating parts, and the hardness relationship between the surfaces of the female and male parts.

The amount of flattening is largely dependent on assembly conditions. When assembling in a press, the surface irregularities are successively sheared off in the course of longitudinal movement and are flattened much more than in the case of assembly procedures whereby the parts are heated or cooled (i.e., when the surface irregularities are reduced radially).

The actual amount of flattening, determining the operational strength of the connection, depends on the magnitude and type of the load acting upon the connection and also on the number of assembly-dismantling procedures. It is established only after a certain period of operation.

The height of the surface microirregularities decreases with each assembly-dismantling procedure and settles at a definite level after three or four such procedures.

Naturally, it is impossible to duly account for all these factors. Therefore, as a first approximation in calculations it is assumed that the flattening of surface microirregularities averages 0.5-0.6 of the original mean roughness height. The effect of the subsequent

operation of the joint is accounted for by a safety factor which for pressed connections is taken at 2-4.

Assuming  $\varphi = 0.5$ , we find  $\Delta' = R_{z1} + R_{z2}$  and introducing the value  $\Delta_{nom} - \Delta'$  into Eq. (2.3), obtain

$$k = \frac{\Delta_{nom} - (R_{z1} + R_{z2})}{1000d} \cdot \frac{1}{\frac{c_1 - \mu_1}{E_1} + \frac{c_2 + \mu_2}{E_2}} \text{ kgf/mm}^2 \quad (2.16)$$

When the required nominal interference is to be found, the amount of the microirregularity flattening should be added to the calculated interference magnitude

$$\Delta_{nom} = \Delta_{calc} + R_{z1} + R_{z2} \quad (2.17)$$

Then this nominal interference value is used as a reference for selecting the corresponding fit from the standard.

For the 6th-11th classes of surface finish  $R_z$  has the following values:

Class of surface finish . . .	6	7	8	9	10	11
$R_z$ , $\mu\text{m}$ . . . . .	10	6.3	3.2	1.6	0.8	0.4

Corrections for the flattening of microirregularities are substantial when dealing with small-diameter connections. For instance, when  $d = 30$  mm the average interference for a heavy drive fit ( $Dh$ ) is 33  $\mu\text{m}$ . If the mating surfaces are machined to the 8th class of surface finish the correction  $R_{z1} + R_{z2} = 6.4$   $\mu\text{m}$  amounts to approximately 20% of the nominal interference. For a joint with  $d = 150$  mm (interference 110  $\mu\text{m}$ ) the correction will amount to approximately 6%.

### (c) Effect of Thermal Deformations

For connections undergoing heating during operation, the influence of temperature upon the fit must be considered. If the female part is made from a material having a higher coefficient of linear expansion, or is heated in operation more intensively than the male part, the original (cold) interference in the joint will then be reduced during heating.

Conversely, if the male part is made from a material having a higher coefficient of linear expansion, or is heated in operation more intensively than the female part, the original interference will be enhanced during heating.

Whenever heating is involved, Eqs. (2.4), (2.7) and (2.10) must include the temperature interference (with its sign)

$$\Delta_t = 1000d (\alpha_1 \Delta t_1 - \alpha_2 \Delta t_2) \mu\text{m} \quad (2.18)$$

where  $\alpha_1$  and  $\alpha_2$  = linear expansion coefficients of the male and female parts, respectively

$\Delta t_1$  and  $\Delta t_2$  = temperature increments in the heating of the male and female parts, respectively

Equation (2.15) will then take the following form

$$k = \frac{1}{1000d} \cdot \frac{\Delta_{nom} - (R_{z1} + R_{z2}) + (\alpha_1 \Delta t_1 - \alpha_2 \Delta t_2) 1000d}{\frac{c_1 - \mu_1}{E_1} + \frac{c_2 + \mu_2}{E_2}} \text{ kgf/mm}^2 \quad (2.19)$$

According to Eq. (2.19), the original relative interference necessary to keep the assigned pressure  $k$  during heating is

$$\frac{\Delta_{nom}}{1000d} = k \left( \frac{c_1 - \mu_1}{E_1} + \frac{c_2 + \mu_2}{E_2} \right) + \frac{R_{z1} + R_{z2}}{1000d} + \alpha_2 t_2 - \alpha_1 t_1 \quad (2.20)$$

When fitting components onto high-speed rotors the hub centrifugal expansion should be taken account of and compensated for by increasing the original interference.

### 2.3. Selection of Fits

As a general rule, large-interference fits should be avoided, particularly with low-grade accuracies ( $Dh3_3$ ,  $Dh2_3$ ,  $Dh2_{2a}$ ). Because of the wide tolerance range in these classes of fits, there may occur, in the case of unfavourable tolerance combinations, interferences detrimental to the strength of the joint.

When large interferences are necessary it is advisable to use the shrink fit ( $Sh$ ) to the second grade of accuracy.

Large-interference fits are used for thin-walled housings, housings made of light metals, housings expanding during heating and hubs of high-speed rotors.

Particular care must be exercised when selecting fits for thin-walled bushes (e.g., plain bearing bushes). In the press-fitting process the bush bore decreases, thus necessitating additional hole reaming operations after pressing-in (or the hole is made initially oversize by the contraction value).

With large interferences plastic deformation may occur, the bush contracts and the joint strength sharply falls. In practice it is often observed that the fit becomes loose due to the bush expansion during heating, particularly if it is made from a material with a high linear expansion coefficient (e.g., bronze).

Thin-walled bushes are generally assembled by a fit not heavier than  $Dh$ . In most cases it is necessary to prevent bushes from rotation and axial shift.

In each particular case a connection should be designed with due regard for all the factors which influence the operation of the connection.

The work capacity (holding power) of press-fitted connections is calculated proceeding from the minimum interference which may

arise with an unfavourable combination of the hole and shaft sizes (hole made to the *upper* tolerance limit and shaft, to the *lower* tolerance limit).

Stresses arising in female and male parts, as well as the force needed to assemble and dismantle press-fitted connections, are calculated on the basis of the maximum interference (hole made to the *nominal* size, and shaft, to the *upper* tolerance limit).

## 2.4. Calculation Diagrams

On the basis of Eqs. (2.4), (2.7) and (2.10) diagrams are drawn which ease time consuming pressed-connection calculations, allow the influence of pressed-connection parameters on the joint strength to be traced and indicate rational ways of strengthening.

Shown in Fig. 20 is a calculation diagram for male and female parts made from the same material [Eqs. (2.12)-(2.14)].

The lower portion of the diagram presents the values of relative pressure  $k_0 = \frac{1}{c_1 + c_2}$  as a function of  $a_1$  for different magnitudes of  $a_2$ . The top part of the diagram gives relative stresses  $\sigma_0$ , equal for the male and female parts

$$\sigma_{01} = \frac{k_0}{1 - a_1^2}; \quad \sigma_{02} = \frac{k_0}{1 - a_2^2}$$

Absolute values of  $k$ ,  $\sigma_1$  and  $\sigma_2$  are obtained by multiplying the values of  $k_0$ ,  $\sigma_{01}$  and  $\sigma_{02}$  by the factor  $\Delta E/d$ .

Let us now consider the use of the diagram by an example.

Given: a hollow steel shaft with external diameter  $d = 100$  mm and internal diameter  $d_1 = 70$  mm ( $a_1 = 0.7$ ) is pressed into a steel hub with external diameter  $d_2 = 125$  mm ( $a_2 = 0.8$ ) by a shrink fit (*Sh*). The connection length is 100 mm. Both the shaft and hole are machined to the 8th class of surface finish ( $R_{z1} + R_{z2} = 6.4$   $\mu\text{m}$ ). The coefficient of friction  $f = 0.1$ .

Find: pressure  $k$  on the surface of joint, torsional holding power  $M_{tors}$  and maximum stresses  $\sigma_1$  in the shaft and  $\sigma_2$  in the hub.

First determine the  $\Delta E/d$  value. For the *Sh* fit the mean diametral interference when  $d = 100$  mm is 120  $\mu\text{m}$ . Hence, the actual interference is  $120 - 6.4 = 113.6$   $\mu\text{m}$ . Young's Modulus  $E = 21\,000$  kgf/mm<sup>2</sup>. Then

$$\frac{\Delta E}{d} = \frac{113.6 \cdot 21\,000}{1000 \cdot 100} = 24 \text{ kgf/mm}^2$$

From the point  $a_1 = 0.7$  (lower portion of the diagram) draw a horizontal line to intersect curve  $a_2 = 0.8$  (point *a*) and read on the abscissa the value  $k_0 = 0.135$ . The pressure is

$$k = k_0 \frac{\Delta E}{d} = 0.135 \cdot 24 = 3.24 \text{ kgf/mm}^2$$

The torsional holding power [see Eq. (2.3)] is

$$M_{tors} = 0.001 \cdot 3.24 \cdot 0.1 \cdot \pi \cdot 100 \cdot 100 \cdot 50 = 500 \text{ kgf} \cdot \text{m}$$

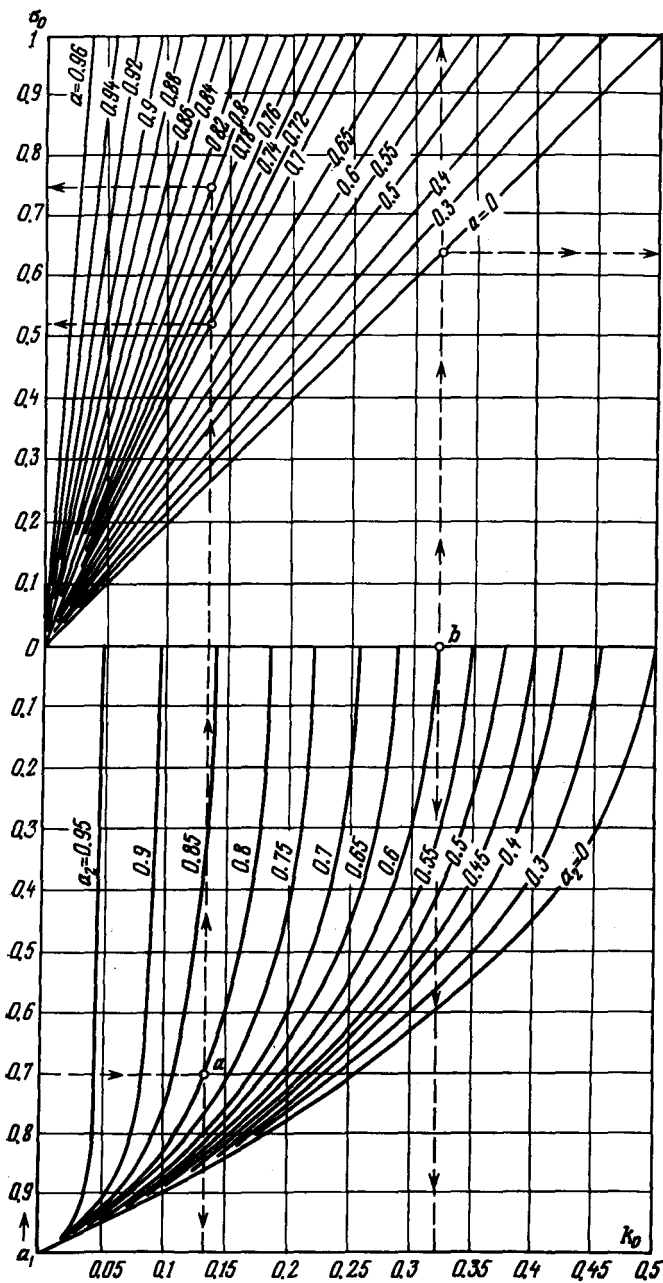


Fig. 20. Diagram for computing press-fitted joints (parts made of the same material)



To determine the stresses draw from point  $a$  a vertical line until it intersects the straight lines  $a = 0.7$  (shaft) and  $a = 0.8$  (hub). Read on the ordinate  $\sigma_{01} = 0.52$  and  $\sigma_{01} = 0.75$ .

Consequently, the stresses in the shaft and hub

$$\sigma_1 = 0.52 \cdot 24 = 12.5 \text{ kgf/mm}^2$$

$$\sigma_2 = 0.75 \cdot 24 = 18 \text{ kgf/mm}^2$$

Let the shaft be solid ( $a_1 = 0$ ) and the external diameter of the hub increased to 165 mm ( $a_2 = 0.6$ ).

Point  $b$  in which the abscissa  $a_1 = 0$  intersects curve  $a_2 = 0.6$  will give  $k_0 = 0.32$ . Hence

$$k = 0.32 \cdot 24 = 7.7 \text{ kgf/mm}^2$$

The torsional holding power will increase by  $\frac{7.7}{3.24} \approx 2.5$  times.

Drawing through point  $b$  a vertical line until it intersects the straight lines  $a = 0$  (shaft) and  $a = 0.6$  (hub), read on the ordinate  $\sigma_{01} = 0.64$  and  $\sigma_{02} = 1$ .

Consequently, the stress in the shaft rises by  $\frac{0.64}{0.52} - 1$  (approximately by 20%), and the stress in the hub, by  $\frac{1}{0.75} - 1$  (approximately by 30%) as compared with the previous case. The rise is rather small, if one takes into account that the strength of the joint increases by 2.5 times.

For a press-fitted connection made up of parts of dissimilar materials, the quantity  $k$ , in accord with Eq. (2.4), is

$$k = \frac{\Delta}{d} \cdot \frac{1}{\frac{c_1 - \mu_1}{E_1} + \frac{c_2 + \mu_2}{E_2}}$$

Transform this equation in the following way

$$k = \frac{\Delta E_2}{d} \cdot \frac{1}{(c_1 - \mu_1) \frac{E_2}{E_1} + c_2 + \mu_2} \quad (2.21)$$

Substituting this value of  $k$  into Eqs. (2.7) and (2.10) gives the following expression:

$$\sigma_1 = \frac{\Delta E_2}{d} \cdot \frac{2}{1 - a_1^2} \cdot \frac{1}{(c_1 - \mu_1) \frac{E_2}{E_1} + c_2 + \mu_2} \quad (2.22)$$

$$\sigma_2 = \frac{\Delta E_2}{d} \cdot \frac{2}{1 - a_2^2} \cdot \frac{1}{(c_1 - \mu_1) \frac{E_2}{E_1} + c_2 + \mu_2} \quad (2.23)$$

Table 4 gives the ratio  $E_2/E_1$  for various material combinations (assumed: for steel  $E = 21\,000$  kgf/mm<sup>2</sup>; for cast iron  $E = 8000$  kgf/mm<sup>2</sup>; for aluminium alloys  $E = 7200$  kgf/mm<sup>2</sup> and for bronzes  $E = 11\,000$  kgf/mm<sup>2</sup>).

Table 4

 **$E_2/E_1$  Ratios for Various Material Combinations in Press-Fitted Connections**

Material of male part	Material of female part			
	steels	cast irons	aluminium alloys	bronzes
Steels	<b>1</b>	<b>0.38</b>	<b>0.33</b>	0.53
Cast irons	2.6	1	0.9	1.38
Aluminium alloys	2.9	1.1	1	1.52
Bronzes	1.9	<b>0.73</b>	<b>0.65</b>	1

The figures in bold type indicate the  $E_2/E_1$  ratios having practical application. These ratios have been employed to plot calculation diagrams (Figs. 21 to 25) on the basis of Eqs. (2.21), (2.22) and (2.23). For plotting these diagrams it has been assumed that  $\mu = 0.15$  for cast iron and  $\mu = 0.3$  for all other materials. In conjunction with the diagram presented in Fig. 20 ( $E_2/E_1 = 1$ ), these diagrams cover all practical cases of pressed connections.

Here are some calculation examples. For greater simplicity the calculations are based on the mean interferences for the given grade of fit. In actual design procedure the extreme interference limits should be used (see pp. 46-47).

**Pressing steel components into cast iron ones** (Fig. 21). A hollow steel column with external diameter  $d = 100$  mm and internal diameter  $d_1 = 70$  mm ( $a_1 = 0.7$ ) is pressed into the hub of a cast iron bed. The external diameter of the hub is  $d_2 = 125$  mm ( $a_2 = 0.8$ ). The fit is  $Dh2_{2a}$  (mean interference  $\Delta = 170$   $\mu\text{m}$ ). The joint surface on the column is machined to the 8th class of surface finish ( $R_{z1} = 3.2$   $\mu\text{m}$ ), and the bore, to the 7th class ( $R_{z2} = 6.3$   $\mu\text{m}$ );  $R_{z1} + R_{z2} = 9.5$   $\mu\text{m}$

$$\frac{\Delta E_2}{d} = \frac{(170 - 9.5) 8000}{1000 \cdot 100} = 12.7 \text{ kgf/mm}^2$$

Using as reference values  $a_1 = 0.7$  and  $a_2 = 0.8$  (point  $a$ ), we find on the diagram that  $k_0 = 0.175$ . Pressure

$$k = 0.75 \cdot 12.07 = 2.2 \text{ kgf/mm}^2$$

Using as reference values  $k_0 = 0.175$ ;  $a_1 = 0.7$  and  $a_2 = 0.8$ , we find that  $\sigma_{01} = 0.69$  and  $\sigma_{02} = 0.98$ .

Stresses

$$\sigma_1 = 0.69 \cdot 12.7 = 8.8 \text{ kgf/mm}^2$$

$$\sigma_2 = 0.98 \cdot 12.7 = 12.4 \text{ kgf/mm}^2$$

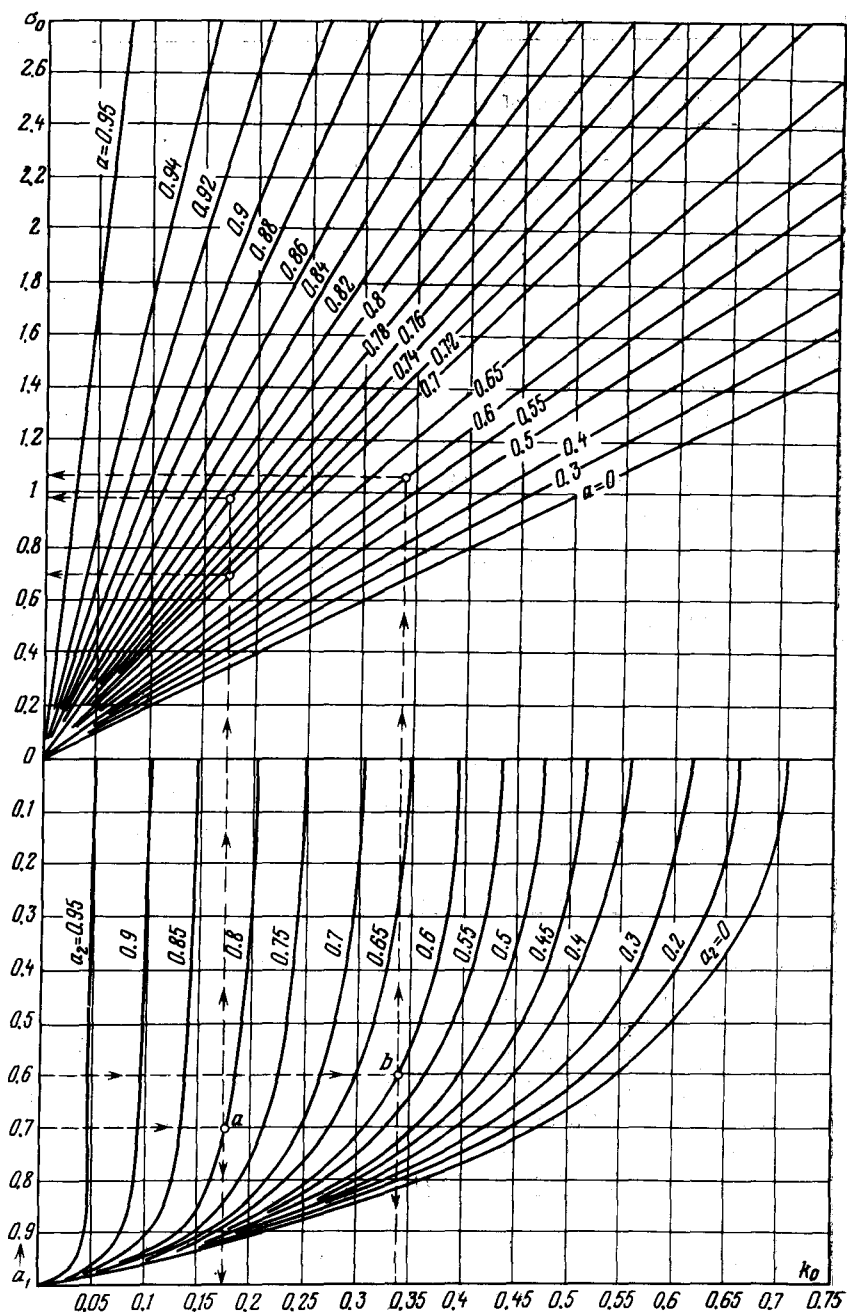


Fig. 21. Diagram for computing press-fitted joints (steel parts pressed in cast-iron parts)

Reduce the internal diameter of the column to 60 mm ( $a_1 = 0.6$ ) and increase the external diameter of the hub to 165 mm ( $a_2 = 0.6$ ). In this case (point *b*)  $k_0 = 0.34$  and  $\sigma_{01} = \sigma_{02} = 1.06$ . Hence,

$$k = 0.34 \cdot 12.7 = 4.3 \text{ kgf/mm}^2$$

$$\sigma_1 = \sigma_2 = 1.06 \cdot 12.7 = 13.5 \text{ kgf/mm}^2$$

The strength of connection is increased by  $\frac{4.3}{2.2} \approx 2$  times, the stresses in the column and hub rise approximately by  $\frac{13.5}{8.8} - 1$  (approximately by 50%) and  $\frac{13.5}{12.4} - 1$  (approximately by 10%), respectively.

**Pressing steel components into those of aluminium alloys** (Fig. 22). A hollow steel shaft with  $d = 100$  mm and  $d_1 = 70$  mm ( $a_1 = 0.7$ ) is press-fitted into the hub of a housing cast in an aluminium alloy. The external hub diameter  $d_2 = 150$  mm ( $a_2 = 0.65$ ). The grade of fit is  $Dh2_{2a}$  ( $\Delta = 170 \mu\text{m}$ ). The class of surface finish of the shaft is the 8th ( $R_{z1} = 3.2 \mu\text{m}$ ) and that of the hole, 7th ( $R_{z2} = 6.3 \mu\text{m}$ );  $R_{z1} + R_{z2} = 9.5 \mu\text{m}$ .

$$\frac{\Delta E_2}{d} = \frac{(170 - 9.5) 7200}{1000 \cdot 100} = 11.5 \text{ kgf/mm}^2$$

On the diagram, for  $a_1 = 0.7$  and  $a_2 = 0.65$  (point *a*) we find that  $k = 0.275$ ;  $\sigma_{01} = 1.09$ ;  $\sigma_{02} = 0.92$ . Hence

$$k = 0.275 \cdot 11.5 = 3.15 \text{ kgf/mm}^2$$

$$\sigma_1 = 1.09 \cdot 11.5 = 12.5 \text{ kgf/mm}^2$$

$$\sigma_2 = 0.92 \cdot 11.5 = 10.6 \text{ kgf/mm}^2$$

Stresses  $\sigma_2$  in the hub exceed the yield limit for cast aluminium alloys in tension ( $\sigma_{02} = 10 \text{ kgf/mm}^2$ ). To reduce the stresses we use the fit grade  $Dh1_{2a}$  obtained with a smaller interference ( $\Delta = 90 \mu\text{m}$ ).

Then

$$\frac{\Delta E_2}{d} = \frac{(90 - 9.5) 7200}{1000 \cdot 100} = 5.8 \text{ kgf/mm}^2$$

The values of  $k$ ,  $\sigma_1$  and  $\sigma_2$  decrease by a factor of  $\frac{5.8}{11.5} \approx 0.5$ . The stress  $\sigma_2$  becomes acceptable:  $\sigma_2 = 0.5 \cdot 10.6 = 5.3 \text{ kgf/mm}^2$ .

Let us now consider the case of pressing a disk of a wrought aluminium alloy onto a hollow steel shaft with external diameter  $d = 100$  mm and internal diameter  $d_1 = 70$  mm ( $a_1 = 0.7$ ). The disk can be regarded as a solid part ( $a_2 = 0$ ). The grade of fit is  $Dh$  ( $\Delta = 65 \mu\text{m}$ ). The class of surface finish of the shaft is the 9th ( $R_{z1} = 1.6 \mu\text{m}$ ), and that of the disk bore, 8th ( $R_{z2} = 3.2 \mu\text{m}$ );  $R_{z1} + R_{z2} = 4.8 \mu\text{m}$

$$\frac{\Delta E_2}{d} = \frac{(65 - 4.8) 7200}{1000 \cdot 100} = 4.3 \text{ kgf/mm}^2$$

From the diagram we find (point *b*) that  $k_0 = 0.465$ ;  $\sigma_{01} = 1.82$ ;  $\sigma_{02} = 0.92$ . Hence

$$k = 0.465 \cdot 4.3 = 2 \text{ kgf/mm}^2$$

$$\sigma_1 = 1.82 \cdot 4.3 = 8 \text{ kgf/mm}^2$$

$$\sigma_2 = 0.92 \cdot 4.3 = 4 \text{ kgf/mm}^2$$

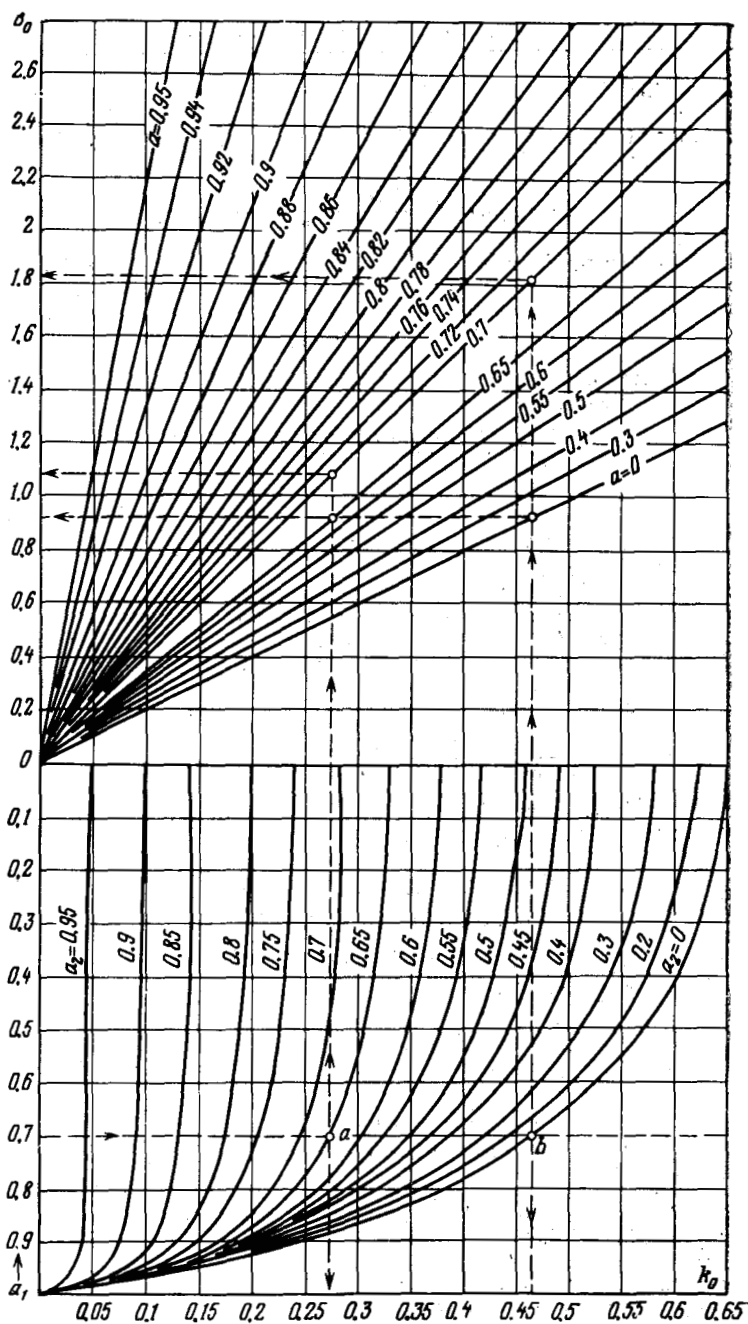


Fig. 22. Diagram for computing press-fitted joints (steel parts pressed in parts of aluminium alloys)

Assume that during operation the disk temperature rises by  $100^{\circ}\text{C}$  (in comparison to the assembly temperature) and the shaft remains cold. As the linear expansion coefficient of an aluminium alloy  $\alpha_2 = 22 \cdot 10^{-6}$ , the disk bore diameter will increase in heating by the value

$$\Delta_t = \alpha_2 t d \cdot 10^3 = \frac{22 \cdot 100 \cdot 100 \cdot 10^3}{10^6} = 220 \mu\text{m}$$

Thus, the original press-fit interference vanishes and instead a clearance amounting to  $220 - (65 - 4.8) = 160 \mu\text{m}$  develops in the joint.

To keep the alignment of the parts a fit of greater interference should be employed, for example, that of the grade  $Dh2_{2a}$  ( $\Delta = 180 \mu\text{m}$ ). In this case during heating of the joint there develops a clearance amounting to  $220 - (180 - 4.8) = 45 \mu\text{m}$  which does not disturb the alignment.

With an interference of  $180 \mu\text{m}$

$$\frac{\Delta E_2}{d} = \frac{(180 - 4.8) 7200}{1000 \cdot 100} = 12.6 \text{ kgf/mm}^2$$

The values of  $k$ ,  $\sigma_1$  and  $\sigma_2$  increase by a factor of  $\frac{12.6}{4.3} \approx 3$ . Stress  $\sigma_2$  in the disk hub (in cold state) becomes  $\sigma_2 = 3 \cdot 4 = 12 \text{ kgf/mm}^2$ , which is acceptable for wrought aluminium alloys.

**Pressing bronze components into steel ones** (Fig. 23). A tin-bronze bush with external diameter  $d = 40 \text{ mm}$  and internal diameter  $d_1 = 35 \text{ mm}$  ( $a_1 = 0.87$ ), is press-fitted into a steel hub with external diameter  $d_2 = 53 \text{ mm}$  ( $a_2 = 0.75$ ). The grade of fit is  $Dh2_{2a}$  ( $\Delta = 80 \mu\text{m}$ ). The joint surface of the bush is machined to the 9th class of surface finish ( $R_{z1} = 1.6 \mu\text{m}$ ) and that of the hub, to the 8th class ( $R_{z2} = 3.2 \mu\text{m}$ );  $R_{z1} + R_{z2} = 4.8 \mu\text{m}$

$$\frac{\Delta E_2}{d} = \frac{(80 - 4.8) 21\,000}{1000 \cdot 40} = 40 \text{ kgf/mm}^2$$

From the diagram we find that when  $a_1 = 0.87$  and  $a_2 = 0.75$  (point *a*),  $k_0 = 0.06$ ;  $\sigma_{01} = 0.5$ ;  $\sigma_{02} = 0.27$ .

Hence

$$k = 0.06 \cdot 40 = 2.4 \text{ kgf/mm}^2$$

$$\sigma_1 = 0.5 \cdot 40 = 20 \text{ kgf/mm}^2$$

$$\sigma_2 = 0.27 \cdot 40 = 10.8 \text{ kgf/mm}^2$$

Stress  $\sigma_1$  in the bush exceeds the yield limit of tin bronze in compression ( $\sigma_{02} = 15 \text{ kgf/mm}^2$ ).

We reduce the internal diameter of the bush to  $d_1 = 30 \text{ mm}$  ( $a_1 = 0.75$ ). On the diagram (point *b*) we find that  $k_0 = 0.1$ ;  $\sigma_{01} = \sigma_{02} = 0.46$ .

Hence

$$k = 0.1 \cdot 40 = 4 \text{ kgf/mm}^2$$

$$\sigma_1 = \sigma_2 = 0.46 \cdot 40 = 18.4 \text{ kgf/mm}^2$$

It is clear that the increase of the bush wall thickness is of little effect; the stresses decrease only by 8% and still exceed the yield limit of the material.

The reduction of the hub wall thickness does not help either. Let  $a_2 = 0.85$  ( $d_2 = 47 \text{ mm}$ ). From the diagram  $\sigma_{01} = 0.35$ , whence  $\sigma_1 = 0.35 \cdot 40 = 14 \text{ kgf/mm}^2$ .

Let us now try to reduce the interference. We take the  $Dh1_{2a}$  grade fit ( $\Delta = 50 \mu\text{m}$ ). Then, the actual interference decreases by a factor of  $\frac{50 - 4.8}{80 - 4.8} = 0.6$ ; the stress in the bush (with the original  $a_1 = 0.87$ ) then becomes acceptable:

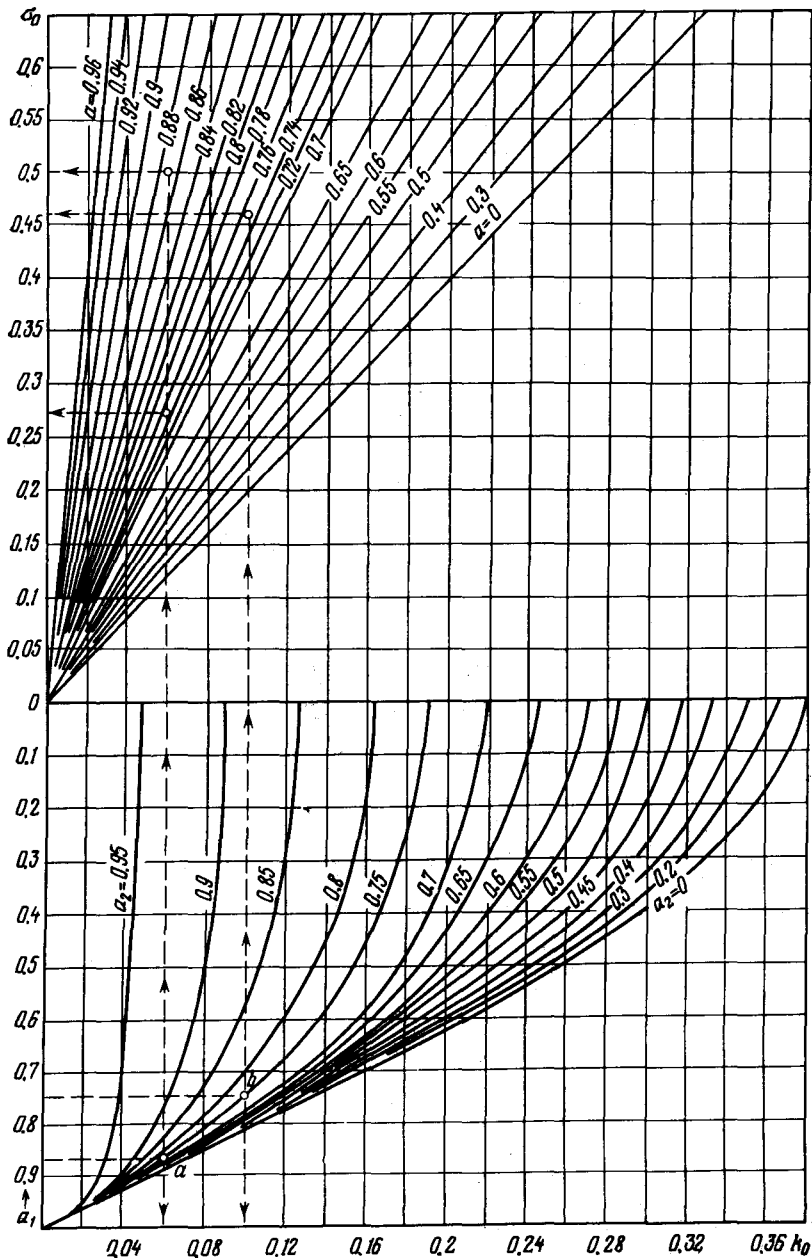


Fig. 23. Diagram for computing press-fitted joints (bronze parts pressed in steel parts)

$\sigma_1 = 0.6 \cdot 20 = 12 \text{ kgf/mm}^2$ , and when  $a_2 = 0.85$  it becomes  $\sigma_1 = 0.6 \cdot 14 = 8.4 \text{ kgf/mm}^2$ .

Now assume that during operation the joint temperature rises by  $100^\circ\text{C}$ . The coefficient of linear expansion of bronze is  $\alpha_1 = 18 \cdot 10^{-6}$ ; that of steel,  $\alpha_2 = 11 \cdot 10^{-6}$ . The temperature interference will then be

$$\Delta_t = 1000 \cdot 100 \cdot 40 (18 - 11) \cdot 10^{-6} = 28 \text{ } \mu\text{m}$$

The interference in the joint  $\Delta = 50 - 4.8 + 28 = 73 \text{ } \mu\text{m}$ .

The unit pressure and stresses are increased by  $\frac{73}{50 - 4.8} = 1.6$  times. For the bush with  $a_1 = 0.87$  the stress becomes  $\sigma_1 = 1.6 \cdot 12 = 19 \text{ kgf/mm}^2$  and still exceeds the yield limit of the material.

Now we take the  $Dh$  grade fit ( $\Delta = 40 \text{ } \mu\text{m}$ ). In contrast to the previous case, the actual interference decreases by a factor of  $\frac{40 - 4.8}{73} = 0.49$  and the stresses in the bush reach an acceptable level:  $\sigma_1 = 0.49 \cdot 19 = 9.3 \text{ kgf/mm}^2$ .

**Pressing bronze components into those of cast iron** (Fig. 24). A bronze bush having the same parameters as in the previous example ( $d = 40 \text{ mm}$ ,  $a_1 = 0.87$ ) is pressed into a cast-iron hub ( $a_2 = 0.75$ ) by the  $Dh2_{2a}$  grade fit ( $\Delta = 80 \text{ } \mu\text{m}$ ). The surface finish is the same as previously ( $R_{z1} + R_{z2} = 4.8 \text{ } \mu\text{m}$ )

$$\frac{\Delta E_2}{d} = \frac{(80 - 4.8) 8000}{40} = 15 \text{ kgf/mm}^2$$

On the diagram we find that for  $a_1 = 0.87$  and  $a_2 = 0.75$  (point  $a$ ),  $k_0 = 0.108$ ;  $\sigma_{01} = 0.91$  and  $\sigma_{02} = 0.5$ .

Hence

$$k = 0.11 \cdot 15 = 1.65 \text{ kgf/mm}^2$$

$$\sigma_1 = 0.91 \cdot 15 = 13.6 \text{ kgf/mm}^2$$

$$\sigma_2 = 0.5 \cdot 15 = 7.5 \text{ kgf/mm}^2$$

Owing to the lower modulus of elasticity of cast iron the stresses in this case are fairly lower than those encountered when pressing the bush into a steel component (the previous example). Nevertheless the stress in the bush is close to the yield limit of bronze. Let the grade of fit be  $Dh1_{2a}$  ( $\Delta = 50 \text{ } \mu\text{m}$ ). The actual interference then decreases by a factor of  $\frac{50 - 4.8}{80 - 4.8} = 0.6$  and the stress in the bush becomes  $\sigma_1 = 0.6 \cdot 13.6 = 8.2 \text{ kgf/mm}^2$ .

Let the joint temperature rise in operation by  $100^\circ\text{C}$ . In the joint there develops a temperature interference equal as previously to  $28 \text{ } \mu\text{m}$  (the coefficient of linear expansion of cast iron is approximately the same as that of steel). According to the previous example, the stress in the bush will increase by 1.6 times and become  $\sigma_1 = 1.6 \cdot 8.2 = 13 \text{ kgf/mm}^2$  (in comparison with  $\sigma_1 = 19 \text{ kgf/mm}^2$  when heating a steel hub). However, in this case too it is recommended that the interference be reduced further. Now we use the  $Dh$  grade of fit. Then, according to the previous conditions, the stress will drop by a factor of 0.49 and become  $\sigma_1 = 0.49 \cdot 13 = 6.4 \text{ kgf/mm}^2$  (in comparison with  $\sigma_1 = 9.3 \text{ kgf/mm}^2$  for a steel hub).

Now consider the case of a solid cast iron part ( $a_2 = 0$ ). Assume that the bush parameters remain as before ( $a_1 = 0.87$ ). The grade of fit is  $Dh$  ( $\Delta = 40 \text{ } \mu\text{m}$ ). On the diagram (point  $b$ ) we find that  $k_0 = 0.15$ ;  $\sigma_{01} = 1.25$  and  $\sigma_{02} = 0.3$ .

$$\frac{\Delta E_2}{d} = \frac{(40 - 4.8) 8000}{1000 \cdot 40} = 7 \text{ kgf/mm}^2$$



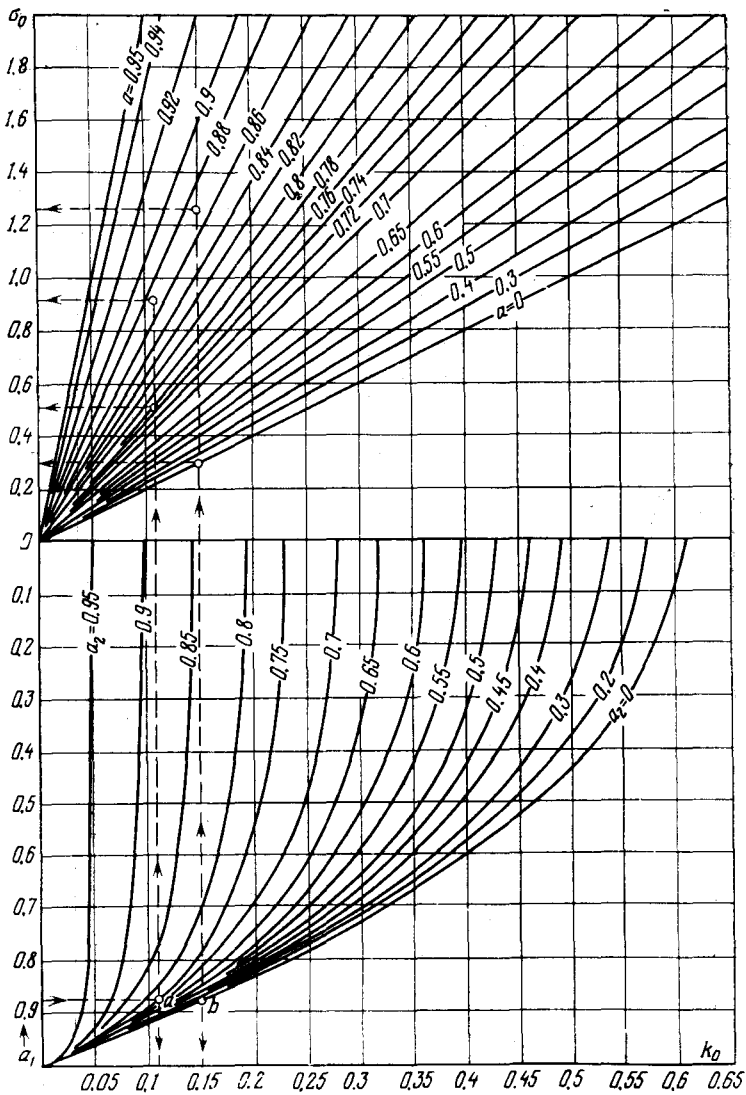


Fig. 24. Diagram for computing press-fitted joints (bronze parts pressed in cast-iron parts)

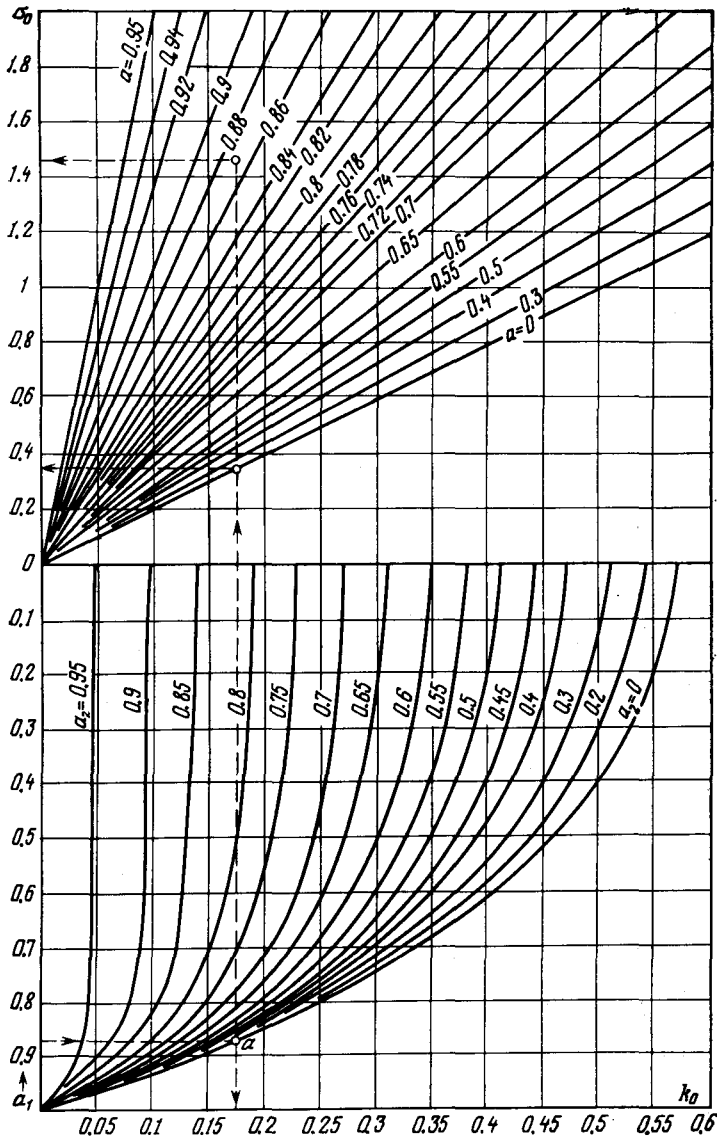


Fig. 25. Diagram for computing press-fitted joints (bronze parts pressed in parts of aluminium alloys)

Hence

$$k = 0.15 \cdot 7 = 1.05 \text{ kgf/mm}^2$$

$$\sigma_1 = 1.25 \cdot 7 = 8.7 \text{ kgf/mm}^2$$

$$\sigma_2 = 0.3 \cdot 7 = 2.1 \text{ kgf/mm}^2$$

Assume that the bush temperature rises by  $60^\circ\text{C}$  during the start-up and that the housing temperature remains constant. In the joint there develops a temperature interference

$$\Delta_t = 1000 \cdot 18 \cdot 10^{-6} \cdot 60 \cdot 40 = 43 \text{ } \mu\text{m}$$

The actual interference thus becomes  $40 - 4.8 + 43 \approx 78 \text{ } \mu\text{m}$ , and the stresses increase by a factor of  $\frac{78}{40 - 4.8} = 2.2$ . Consequently, the stresses in the bush  $\sigma_1 = 2.2 \cdot 8.7 \approx 19 \text{ kgf/mm}^2$ , i.e., they exceed the yield limit of the material. Obviously, the original interference corresponding to the  $Dh$  grade fit in this case is excessive.

Let us use the  $Dl$  grade fit ( $\Delta = 25 \text{ } \mu\text{m}$ ). The actual interference in heating will then become  $25 - 4.8 + 43 = 63 \text{ } \mu\text{m}$  and the stresses will decrease by a factor of  $\frac{63}{78} = 0.8$ . The stresses in the hot bush will be  $0.8 \cdot 19 \approx 15 \text{ kgf/mm}^2$ , which is more or less acceptable. Under such circumstances the bush must be prevented from rotation.

**Pressing bronze components into those of aluminium alloys** (Fig. 25). A bronze bush is press-fitted into a solid housing made from an aluminium alloy ( $a_2 = 0$ ). The bush has the same parameters as above ( $d = 40 \text{ mm}$ ,  $a_1 = 0.87$ ). The grade of fit is  $Dh$  ( $\Delta = 40 \text{ } \mu\text{m}$ ). The surface finish is also the same as above ( $R_{z1} + R_{z2} = 4.8 \text{ } \mu\text{m}$ ). From the diagram we find that when  $a_1 = 0.87$  and  $a_2 = 0$  (point  $a$ ),  $k_0 = 0.175$ ;  $\sigma_{01} = 1.45$  and  $\sigma_{02} = 0.35$

$$\frac{\Delta E_2}{d} = \frac{(40 - 4.8) 7200}{1000 \cdot 40} = 6.4 \text{ kgf/mm}^2$$

Hence

$$k = 0.175 \cdot 6.4 = 1.1 \text{ kgf/mm}^2$$

$$\sigma_1 = 1.45 \cdot 6.4 = 9.3 \text{ kgf/mm}^2$$

$$\sigma_2 = 0.35 \cdot 6.4 = 2.2 \text{ kgf/mm}^2$$

Assume that the joint temperature rises in operation by  $100^\circ\text{C}$ . The diameter of the bush will increase by  $1000 \cdot 18 \cdot 10^{-6} \cdot 100 \cdot 40 = 72 \text{ } \mu\text{m}$ . The diameter of the bore (with the linear expansion coefficient of the aluminium alloy being  $\alpha_2 = 22 \cdot 10^{-6}$ ) will expand by  $1000 \cdot 22 \cdot 10^{-6} \cdot 100 \cdot 40 = 88 \text{ } \mu\text{m}$ . Accordingly, the original interference will decrease by  $88 - 72 = 16 \text{ } \mu\text{m}$  and become  $40 - 4.8 - 16 \approx 19 \text{ } \mu\text{m}$ . The bush must be prevented from rotation.

## 2.5. Probability Calculations for Press-Fitted Connections

The methods for calculating press-fitted connections by the extreme tolerance limits of shafts and holes do not take account of the regularities of the size dispersion and frequency of size distribution. The probability for the manufacture of shafts and holes of extreme sizes is generally very small. And the probability of such extremes being assembled is even less.

In many cases size distribution can be represented by a Gaussian (normal distribution) curve plotted in size vs. size occurrence frequency system of coordinates (Fig. 26). The equation of the curve (with the origin of coordinates on the axis of symmetry) is

$$y = \frac{1}{\sigma \sqrt{2\pi}} e^{-\frac{x^2}{2\sigma^2}}$$

where  $\sigma$  = standard deviation of size  
 $e = 2.718 =$  Napierian base

Ordinates  $y$  indicate the probability of occurrence of each given size. The area under the curve is numerically equal to unity (100% of the parts). The maximum ordinate is

$$y_{\max} = \frac{1}{\sigma \sqrt{2\pi}} \approx \frac{0.4}{\sigma}$$

The branches of the curve asymptotically approach the abscissa axis. The curve has two inflexion points at distances  $+\sigma$  and  $-\sigma$  from the symmetry axis.

The ordinates of these points are

$$y_{\sigma} = \frac{y_{\max}}{\sqrt{e}} \approx 0.6y_{\max} \approx \frac{0.24}{\sigma}$$

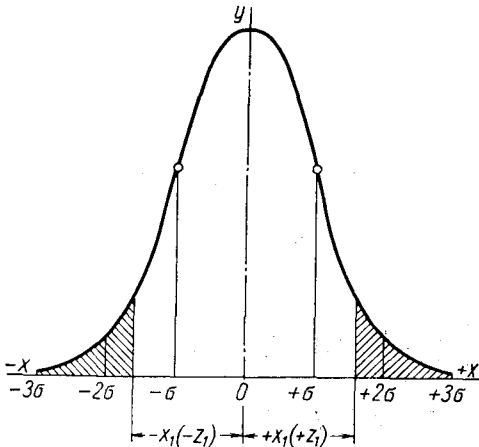


Fig. 26. Gaussian (normal distribution) curve

in the interval  $\pm 1.5\sigma$ ; 95%, in the interval  $\pm 2\sigma$ ; and 99.73%, in the interval  $\pm 3\sigma$ . For practical purposes the curve is confined to the  $\pm 3\sigma$  limits. Then the  $\pm 3\sigma$  interval can be considered to be equal to the margin tolerance  $\delta$ , i.e.,  $\delta = 6\sigma$ , and the curve used for computing the probability of occurrence of sizes within the limits of this margin tolerance.

The percentage of parts falling upon the extreme points of the curve at distances  $\pm x_1$  from the origin is expressed by the ratio  $v$  of the shaded areas to the total area under the curve, taken at 100%. According to the equation of the Gaussian curve

$$v = 1 - \frac{1}{\sigma \sqrt{2\pi}} \int_{+x_1}^{-x_1} e^{-\frac{x^2}{2\sigma^2}} dx$$

Introducing  $z = \frac{x}{\sigma}$ , we have

$$v = 1 - \frac{1}{\sqrt{2\pi}} \int_{+z_1}^{-z_1} e^{-\frac{z^2}{2}} dz$$

The integral function of this expression is given in tabular form in manuals on the theory of chances.

The Table below gives the values of  $v$  (second column) as a function of  $Z$  which presents the ratio of the sum of line-segments  $2z_1$  to the basis  $6\sigma$  of the curve ( $Z = \frac{z_1}{3\sigma}$ ).

$z$	$v$	$v^2$	Risk, %
0.9	0.0069	0.000048	0.0048
0.8	0.0164	0.00027	0.027
0.7	0.0357	0.00127	0.127
0.6	0.0719	0.00517	0.517
0.5	0.1336	0.01783	1.78

The probability of occurrence of combinations of parts with dimensions, corresponding to the given  $Z$  values is equal, in accord with the theory of chances, to  $v$  squared. The value of  $v^2$  expressed in per cent shows the risk percentage, i.e., the probability of occurrence of combinations within limits exceeding  $Z$  (Fig. 27).

With  $Z > 0.5$  the risk percentage is negligible. Thus, when  $Z = 0.7$ , for every 1000 connections approximately one is a risk, and when  $Z = 0.6$ , approximately five connections have parameters exceeding the given limits.

Consequently, there is very little risk in narrowing the margin tolerance to  $Z\delta$  and introducing in place of the extreme nominal deviations  $\Delta_{\min}$  and  $\Delta_{\max}$  probable deviations

$$\Delta'_{\min} = \Delta_{\min} + \frac{\delta(1-Z)}{2}$$

and

$$\Delta'_{\max} = \Delta_{\max} - \frac{\delta(1-Z)}{2}$$

where  $Z$  is a value ranging from 0.9 to 0.5, depending on the adopted risk percentage.

Let us carry out a comparative numerical computation of a press-fitted connection by both conventional and probability methods. Assume a connection comprising a solid steel shaft, 80 mm in diameter, and a steel sleeve with an external diameter of 120 mm. The connection length  $l = 80$  mm. The grade of fit  $A/Dh$ . The shaft and hole are machined to the 8th class of surface finish ( $R_z = 3.2 \mu\text{m}$ ). Hole tolerance:  $+30 \mu\text{m}$ ; shaft tolerance: lower limit  $+45 \mu\text{m}$ , upper limit  $+65 \mu\text{m}$ . Coefficient of friction  $f = 0.1$ .

Nominal interferences: maximum  $65 - 0 = 65 \mu\text{m}$ , minimum  $45 - 30 = 15 \mu\text{m}$ . With a microirregularity flattening coefficient of 0.5, the flattening amounts

to 6.4  $\mu\text{m}$ . The actual maximum interference is, thus,  $65 - 6.4 = 58.6 \mu\text{m}$ , and the minimum,  $15 - 6.4 = 8.6 \mu\text{m}$ .

For the probability computation assume that  $Z = 0.6$  (risk percentage is 0.517). The value  $\frac{1-Z}{2}$  equals 0.2. Probable deviations of dimensions: hole —

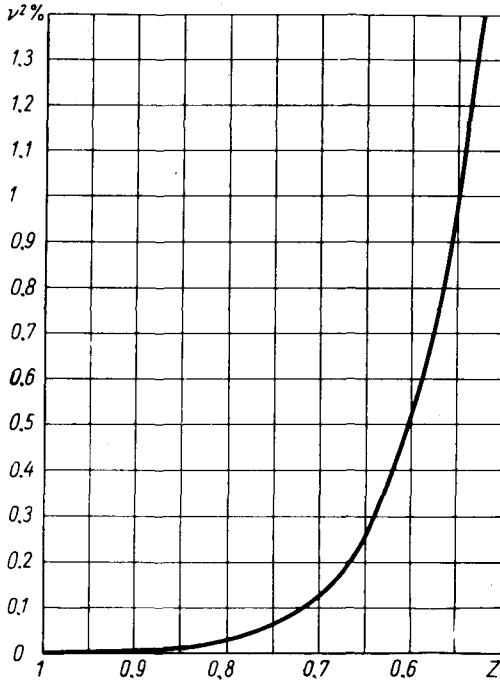


Fig. 27. Risk percentage as a function of  $Z$

minimum  $0 + 30 \cdot 0.2 = 6 \mu\text{m}$ , maximum  $30 - 30 \cdot 0.2 = 24 \mu\text{m}$ , shaft—maximum  $65 - 20 \cdot 0.2 = 61 \mu\text{m}$ , minimum  $45 + 20 \cdot 0.2 = 49 \mu\text{m}$ . Probable interferences: maximum  $61 - 6 = 55 \mu\text{m}$ , minimum  $49 - 24 = 25 \mu\text{m}$ . Accounting for the microirregularity flattening the maximum interference is  $55 - 6.4 = 48.6 \mu\text{m}$ , and the minimum interference,  $25 - 6.4 = 18.6 \mu\text{m}$  (Table 5).

As seen from Table 5 the probability computation gives more favourable characteristics which at the same time are closer to the actual parameters of completed connections.

The normal distribution law is valid wherever a large number of occurrences is involved, and, hence, for mass production and with controlled operations at that. Substantial deviations from this law occur in individual and small-lot production, attributable in the first instance to the small number of occurrences and, secondly, to certain specific features of the machining process. With individual production the operator involuntarily keeps to the lower hole toler-

Table 5

## Calculation Results for a Pressed Connection

Characteristics	Computation by	
	nominal values	probable values
Maximum interference, $\mu\text{m}$	58.6	48.6
Minimum interference, $\mu\text{m}$	8.6	18.6
Press-fitting force (with maximum interference), kgf	8500	7200
Holding power (with minimum interference):		
axial, $P_{ax}$ , kgf	1250	2750
$M_{tors}$ , kgf·m	50	110
Stresses (with maximum interference):		
in shaft, $\sigma_1$ , kgf/mm <sup>2</sup>	8.6	7.1
in hub, $\sigma_2$ , kgf/mm <sup>2</sup>	15.3	12.7

ance limit and the upper limit for the shaft, orienting to the NO-GO side of gauges. Because of this the holes are made, on the average, closer to the minimum (nominal) size, while the shaft dimensions show a tendency toward the maximum (upper) limit of tolerance. The grouping centres on the distribution curves are thereby shifted (Fig. 28) and the probability of obtaining maximum interferences is thus increased.

An asymmetry of size distribution also periodically occurs in mass production with controlled operations. As the cutting tools wear down, hole dimensions approach the minimum, and shaft dimensions, the maximum. The periodicity of this phenomenon depends on operation ad-

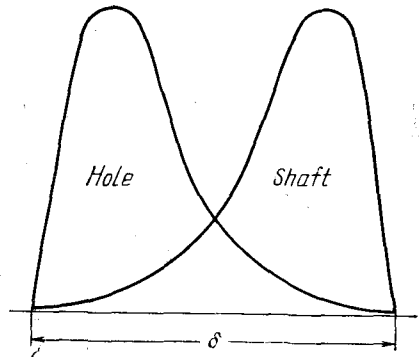


Fig. 28. Distribution curves with displaced grouping centre

justment frequency and is absent only with automatic readjustment. To establish any regularities of the dispersion changes in a general form is difficult.

However it is still necessary to note that any probability computation gives average figures of the expected size distribution over a long time interval and for large batches of products. The possibility

of a temporary crowding of low-probability size combinations is not excluded, as a result of which comparatively large batches of defective connections will appear, although the mean level of risk related to very large batches will still remain within the computed limits.

All this restricts the practical value of the probability computation technique.

When designing press-fitted connections it is better to keep within narrow boundaries such an interference as will ensure good working capacity of the connection without inducing high stresses in the mating components. With the existing systems of press fits, which are noted for their large deviation scatter, it is difficult to achieve. The selective assembly method is undesirable as it complicates production. The general rule is to employ fits to the highest grades of accuracy, in particular, those to the first grade of accuracy. However, this class of fits only covers a limited range of interferences. Therefore it seems advisable to develop a single class of press fits with lower margin tolerances that would encompass the entire range of interferences necessary for the industry.

## 2.6. Press-Fitting with Heating or Cooling of Parts

The press-fitting force may reach substantial values, especially with great interferences and large surfaces of joint. This force progressively increases as the part being press-fitted is forced deeper into the hole, reaching its maximum at the end of the procedure. The maximum press-fitting force may be determined from Eq. (2.2).

Let us find the force necessary to press a solid steel shaft ( $a_1 = 0$ ) with diameter  $d = 100$  mm into a cast-iron hub 150 mm long and having external diameter  $d_2 = 165$  mm ( $a_2 = 0.6$ ) by the  $Dh1_{2a}$  grade fit ( $\Delta = 90$   $\mu\text{m}$ ).

On the diagram shown in Fig. 21 we find that for  $a_1 = 0$  and  $a_2 = 0.6$ ,  $k_0 = 0.39$ . The unit pressure

$$k = k_0 \frac{\Delta E_2}{d} = 0.39 \frac{90 \cdot 8000}{1000 \cdot 100} = 2.8 \text{ kgf/mm}^2$$

The maximum press-fitting force is

$$P = k f F = 2.8 \cdot 0.1 \pi \cdot 100 \cdot 150 = 13\,000 \text{ kgf}$$

The press-fitting procedure can be facilitated by heating the female part or cooling the male part, or else by practising both of these at once. When press-fitting parts into large housing structures only the male component is cooled.

The heating temperature for the female part to have zero interference

$$t - t_0 = \frac{\Delta}{d} \cdot \frac{1}{\alpha_2 \cdot 1000} \quad (2.24)$$



where  $t$  and  $t_0$  = heating temperature and workshop temperature, respectively

$\frac{\Delta}{d}$  = relative interference in the joint

$\alpha_2$  = linear expansion coefficient of the female part material

$d$  = diameter of the joint, mm

Similarly, when cooling the male component

$$t' + t_0 = \frac{\Delta}{d} \cdot \frac{1}{\alpha_1 \cdot 1000} \quad (2.25)$$

where  $t'$  is the cooling temperature.

It should be remembered that at subzero temperatures the linear expansion coefficient  $\alpha'$  decreases (see *Fundamentals of Machine Design*, Vol. 1, Fig. 257).

Assume that in Eq. (2.1)  $\Delta_{mean} \approx \psi D$  and that  $t_0 = 20^\circ\text{C}$ . Then, from Eqs. (2.24) and (2.25) one can find temperatures  $t$  (heating) and  $t'$  (cooling) required to obtain zero interference when assembling joints by different fits. For cast-iron and steel components ( $\alpha \approx 10^{-6}$ ) these temperatures are as follows:

Fits . . . .	$Dh1_1$	$Dh$	$Dh2_1$	$Dh1_3$	$Dh1_{2a}$	$Sh$	$Dh2_3$	$Dh2_{2a}$	$Dh3_3$
$t, ^\circ\text{C}$ . . . .	43	60	65	68	105	108	122	124	
$t', ^\circ\text{C}$ . . . .	-8	-30	-36	-40	-86	-90	-105	-110	

Generally the cooling procedure is effected by using dry ice (evaporates at  $-80^\circ\text{C}$ ); or, for more intensive cooling, liquid nitrogen ( $-196^\circ\text{C}$ ) and oxygen ( $-183^\circ\text{C}$ ).

It must be borne in mind that heated components rapidly cool as they are being delivered from the furnace to the press. Furthermore, during the press-fitting operation the temperature of the heated hub quickly lowers due to its contact with the cold shaft. Therefore, due corrections must be introduced to compensate for the decrease of temperature during handling and press-fitting. In practice this implies that the components to be press-fitted must be overheated by  $30$ - $50^\circ\text{C}$  as compared with the calculated temperature.

The cooling temperature should also allow for the heating effect.

## 2.7. Pressed Connections with Electrodeposited Coatings

The strength of press-fitted connections (axial and torsional holding power) can significantly be increased by electroplating the contacting surfaces. Figure 29 shows the results of comparative tests of pressed connections assembled by the  $A/Dh$  grade fit. The electrodeposited layer on the contacting surfaces was  $0.01$ - $0.02$  mm thick. Two assembly procedures were used: one by means of a hydraulic press and the other with cooling the shaft in liquid nitrogen. In the latter case the radial clearance between the mating surfaces was  $0.05$  mm.

A connection without coating assembled in a hydraulic press (without shaft cooling) was used as a reference specimen, its axial holding power  $P_0$  being taken as the unit of comparison.

From the diagram it is seen that electroplating sharply (by 2-4.5 times) enhances the connection strength, and that the assembly with cooling the shaft assures a much higher connection strength than

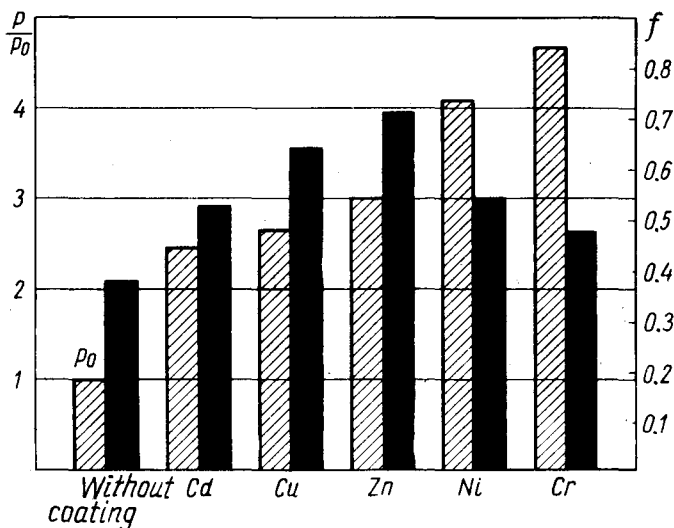


Fig. 29. Relative strength of pressed connections with deposited coatings. Blackened columns indicate assembly with shaft cooling, while hatched columns are for assembly in a press. The strength of a pressed connection without coating and assembled in a press is taken as unity (after G. A. Bobrovnikov)

the press-fitting assembly. For uncoated connections assembled with cooling the joint strength is doubled, and for connections with soft coatings (Cd, Cu, Zn), improved by 20-30% in comparison with the assembly in a press.

The strength of connections with hard coatings (Ni, Cr) and assembled with cooling is worse than that of the same connections assembled in a press.

The greater strength of connections with electroplated coatings is probably due to the occurrence of strong molecular bonds at the joint surfaces. The prolonged dwell under the high pressure existing on the contacting surfaces causes a diffusion process whereby the atoms of the base and coating metals mutually penetrate each other, thus forming some intermediate structure. In other words, a "cold welding" process seems to occur. As for the rather high (approaching unity) values of the coefficient of friction (see the right-hand ordinate of the diagram in Fig. 29), this can readily be explained. The friction coefficient concept in its classical mechanical interpretation in these conditions is no longer valid: the value of the friction coefficient here shows the shear resistance

of the intermediate layer associated with the base and plated metals and not, as is usual, the resistance to the displacement of one surface relative to another.

The lower strength of connections assembled with the aid of a press is attributed to the fact that the ridges of surface microirregularities are flattened and/or cut away. During the assembly with cooling the ridges remain intact and after heating penetrate the valleys in the mating surface, thus adding to the connection strength.

Joints with soft electroplating are disassembled without damage to the surfaces, but when disassembling connections with hard coatings, scores, cracks and deep tears in the base metal are observed, sometimes over considerable areas of the contracting surfaces, due to which reassembly is difficult or even becomes impossible.

The situation is aggravated by the fact that hard electroplating lowers the fatigue strength of the joint.

Due to all these reasons preference should be given to soft coatings.

The application of soft coatings in conjunction with the assembly with cooling allows the connection strength to be improved 3-4 times as compared with that of the press-fitted connections without coatings. Thus, it becomes possible, while maintaining the given joint strength, to employ smaller interferences, reducing, in this way, the tensile stresses in the female part and compressive stresses in the male part. In addition, the electrodeposited coatings protect the fitted surfaces against corrosion and eliminate the "welding" of surfaces subjected to cyclic loads.

The strength of pressed connections can seemingly be improved by metallization and thermodiffusion saturation (e.g., by thermodiffusion zinc plating) of fitting surfaces.

Still further strengthening of pressed connections can probably be attained by depositing dissimilar coatings upon the joint surfaces, for instance, a zinc coating on one surface and a copper one on the other. From the atomic diffusion of the two metals some intermediate structures can be expected in the contact zone, possessing higher strength than homogeneous platings (e.g., brass-type alloys when zinc and copper deposits are combined).

## 2.8. Design of Pressed Connections

The specific feature of pressed connections is that their joint surfaces are already prestressed by interference forces prior to the application of working loads, subjecting the female part to a biaxial tension which is unfavourable from the strength viewpoint. When adding the prestresses to the working stresses, their resultant may exceed the yield limit of the material and cause connection failure.

Moreover, formal calculations of press-fitted joints, based on the assumption of constant cross-sections throughout the entire part length where the end conditions can be ignored does not express true stress values. In practice the strength of a joint strongly depends on the shape of the female and male parts. Uneven rigidity of parts (stepped shafts, hubs with disks, etc.) causes an unequal distribution

of contact pressures and stresses over the connection's length. Sharp stress gradients arise at the joint edges.

Formal calculation, even with high safety margins does not always assure a reliable connection. The more so if one takes into account that the magnitude and distribution of working stresses throughout the part cross-section and their relationships with prestresses remain mostly uncertain, especially in joints subjected to cyclic stresses. Therefore, regardless of computation results all constructive measures to strengthen pressed connections must be taken.

In order to enhance the strength and reliability of pressed connections it is advisable to:

enlarge the diameter and increase length of connections so that unit pressure upon contacting surfaces is reduced;

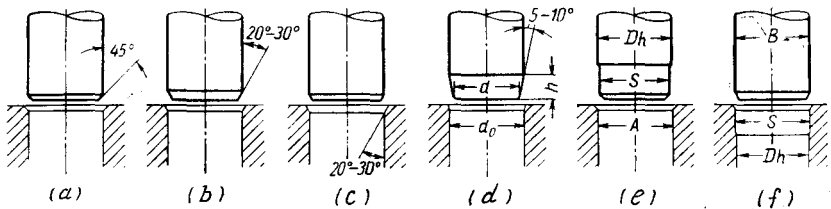


Fig. 30. Lead-in chamfers and recesses in pressed connections

select interference values within narrow margins, making use of more accurate fits;

avoid sharp changes in cross-sections of the connected parts over their contact areas (areas close to these parts), thus preventing abrupt stress relations;

improve contact surfaces by appropriate heat treatment (e.g., low temper hardening, induction hardening, etc.) or strengthen them by mechanical hardening (shot blasting, rolling of shafts, rolling out or burnishing of holes);

use assembly technique in which the female part is heated or the male part is cooled;

electroplate contacting surfaces, using soft metals (Zn, Cu, Cd).

The reliability of pressed connections depends greatly on correct assembly.

To facilitate the press-fitting procedure leading chamfers should be provided on the shaft and in the hole. The chamfers should be made at  $45^\circ$  (Fig. 30a) or, better, at  $20-30^\circ$  (Fig. 30b, c). If great interferences are expected, the shaft must have more gradual chamfers of  $5-10^\circ$  (Fig. 30d). The chamfer leading diameter  $d$  is made 0.1-0.2 mm less than the hole diameter  $d_0$ .

Occasionally the shaft or the hole is designed with leading cylindrical collars having an aligning fit, e.g., a slide fit (Fig. 30e, f).

The location of the aligning collar in the hole (Fig. 30f) necessitates the employment of the basic shaft system.

It is very important to prevent seizure and distortion of the joined parts, which impede the press-fitting process or may even spoil the connection altogether.

Bush-type thin-walled components are guided when being press-fitted by means of a centring mandrel (Fig. 31a). Figure 31b shows

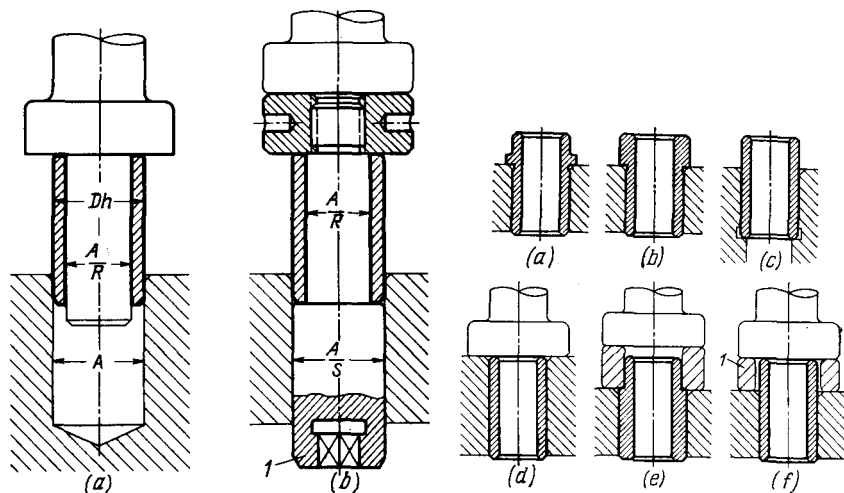


Fig. 31. Methods for press-fitting thin-walled bushes

Fig. 32. Methods for axial fixing of parts when press-fitting

a method of press-fitting used for through holes. A bush is mounted upon a screwed-on mandrel with a pilot shank *1*, introduced into the hole with a slide fit. After the press-fitting is over, the mandrel is screwed off.

Axial position of the part is fixed by pressing the part home to a stop shoulder (Fig. 32a, b), a hole step (Fig. 32c), flush with the hole edge (Fig. 32d), or until the hole edge is flush with a shoulder on the part (Fig. 32e). Plain parts can be fixed in any position by means of distance rings *1* placed under the press plunger (Fig. 32f).

A typical error made when designing pressed connections is the insufficient length of the joint collar. The connection with a short collar quickly fails due to the crushing of the contact surfaces under the effect of working loads. Examples of wrong and correctly designed pressed connections are illustrated in Fig. 33.

For general purposes and rough determination of the minimum length of pressed connections the following formula may be used:

$$l_{\min} = 4d^{2/3} \quad (2.26)$$

where  $l_{\min}$  = length of the press-fitted portion (less chamfers), mm  
 $d$  = connection diameter, mm

A graph based on Eq. (2.26) is plotted in Fig. 34.

If the connection is subjected to high bending or shearing loads, especially alternating ones, or if it is necessary to assure a precise

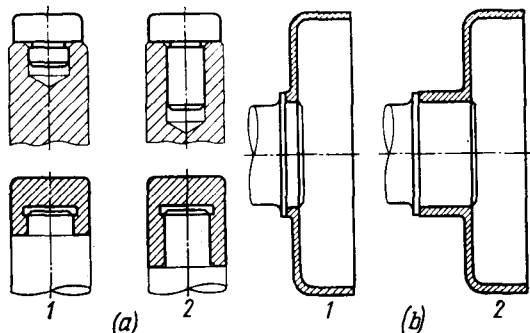


Fig. 33. Pressed connections:

(a) connecting rod end; (b) press-fitting cup-shaped component on shaft; 1 — wrong; 2 — correct

positioning and sound anchoring of the press-fitted component (e.g., bed columns), the length of the press-fitted portion is considerably increased ( $l = 1.5-2d$ ).

Avoid, whenever possible, press-fitting in blind holes, because the latter are more difficult to machine and hamper dismantling.

Should the fitting in blind holes be unavoidable, it is necessary to assure free exit of air during the press-fitting process. Compression of air when pressing, accompanied by increase of its specific volume, can break the female part, particularly when it is thin-walled or made of a less strong material (e.g., light alloys). Air is vented via holes (Fig. 35a, c) or grooves (Fig. 35b).

Never press-fit components through two sections with holes of the same diameter (Fig. 36a): while passing the component through the first section (the upper in the Figure) a misalignment frequently occurs, that impedes the introduction of the male part into the second section. In addition, scores may form on the surfaces of the mating parts.

Under such circumstances each section should have holes of different diameters (Fig. 36b). The axial dimensions of the connection must be so designed that the part enters the second section first to a depth  $m = 2-3$  mm (Fig. 36c), thus obtaining a definite direction, and only after that enters the first section.

It would be wrong to force a bush into a casing as illustrated in Fig. 36d. Here, in order to reduce the amount of precision machining,

the bore has two short joint collars. The error is that both collars have the same diameter. Besides, the distortion of the bush on the fitting areas is inevitable.

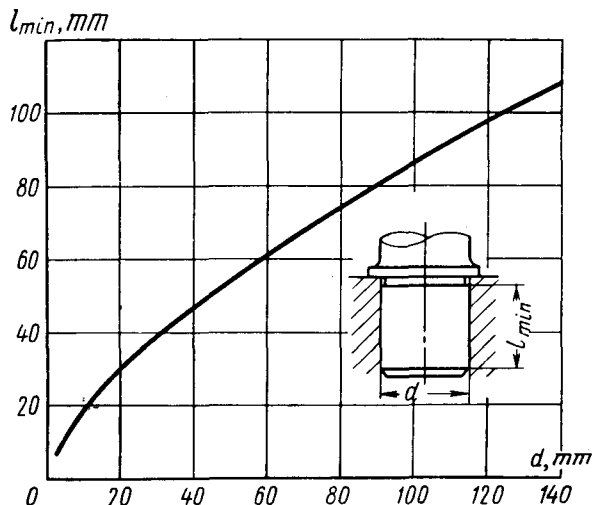


Fig. 34. Minimum length  $l_{min}$  of pressed connections as a function of joint diameter  $d$

If strict linearity of the hole walls is important, the bush then must be reamed after the assembly, or fitted over its complete length (Fig. 36e) or, at least, over a major portion of its length (Fig. 36f).

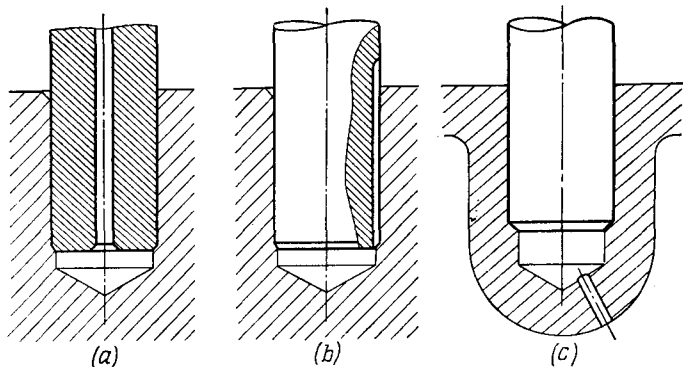


Fig. 35. Air evacuation when press-fitting parts in blind holes

Female components must be given ample rigidity to avoid their deformation during the forcing procedure.

In the case shown in Fig. 36g the upper eye will deflect, thereby making impossible the press-fitting into the lower eye. If for some

design considerations the hole walls cannot be made thick enough, then it is absolutely necessary to employ some stiffening device during the press-fitting procedure. The simplest device is a horse-shoe-shaped spacer *1* inserted in-between the eyes.

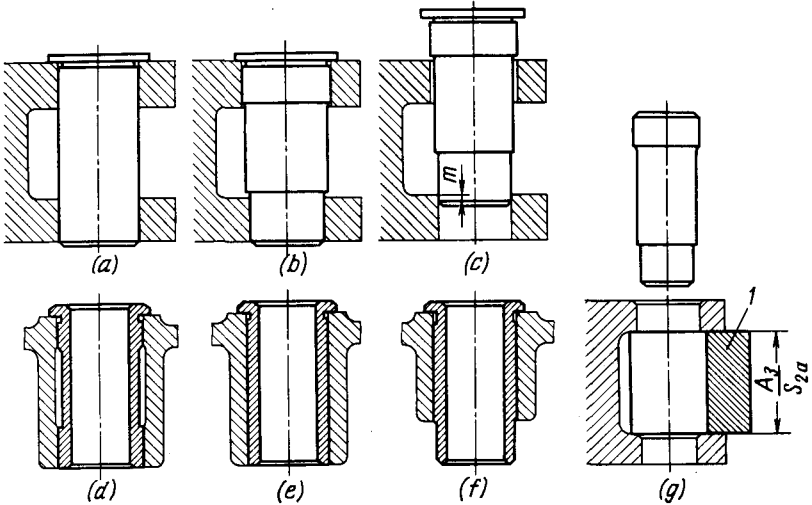


Fig. 36. Press-fitted connections

The employment of such a spacer must be thought of beforehand by designing the distance between the eyes to suit one common spacer which can be used for a series of parts.

The female and male parts should be of uniform rigidity in the radial direction. Local weakenings, cut-outs, etc., should be avoided.

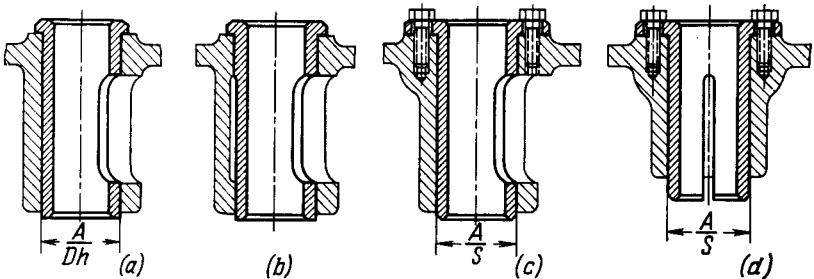


Fig. 37. Press-fitting a bush

In the case depicted in Fig. 37a press-fitting is impeded by the unavoidable deflection of the bush toward the cut-out. Furthermore, at the cut-out area the bush will be given additional deflection due to the unilateral radial interference. The situation can be improved



slightly if the bush is press-fitted into two sections located in the non-cut-out areas of the hub (Fig. 37b). In this case it is better to assemble the bush by a location fit and fasten it in position with bolts (Fig. 37c).

Press-fitting is inapplicable when the female or male part has through-cuts extending to the end face (Fig. 37d). If cut-outs cannot be eliminated the only reasonable way is to employ a location fit.

Occasionally it is necessary to position press-fitted parts at a certain angular attitude. Such, for example, is the case when press-fitting a keyed shaft into its hub. The alignment of the key with its slot is assured if the leading end of the shaft (Fig. 38a) has a location or free fit over length  $l$  which exceeds the distance  $h$  of the key from the shaft end face. The key is first introduced into the keyslot and after that the shaft is press-fitted.

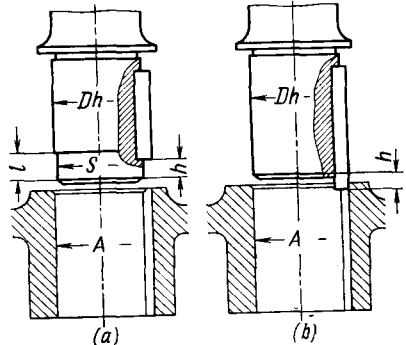


Fig. 38. Fitting a keyed shaft in a hub

Another method: the key protrudes out from the shaft to a distance  $h$  which is sufficient to assure the shaft location in the keyslot before the press-fitting procedure begins (Fig. 38b).

The best practice is to assemble the connection with previously heated hub or cooled shaft in order to obtain a clearance in the

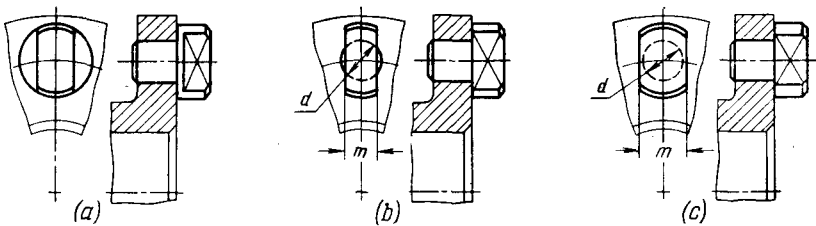


Fig. 39. Press-fitting cams in a disk

connection. The angular location of the shaft in the hole will then present no difficulties.

Lobed cams with given edge setting angles (Fig. 39) should be pressed in place by means of a guiding adapter having radial cut-outs for the cam lobes, which is located from the central hole in the disk. The possibility of applying such an adapter must be considered in designing.

Figure 39a shows an incorrect design: large shank at the cam root prevents the cam passing through cut-outs in the adapter. In alternative, presented in Fig. 39b, the shank size is reduced but the distance  $m$  between the cam edges is less than the fitting diameter  $d$ , therefore, the cut-outs in the adapter must have formed contours. In the correctly designed version, Fig. 39c ( $m > d$ ) a simple adapter can ensure a correct cam orientation.

### (a) Pressing-Out

When designing a pressed connections the possibility of its disassembly must be considered. Parts to be pressed out must have surfaces (preferably flat) which can rest during the pressing-out upon solid plates or bushes.

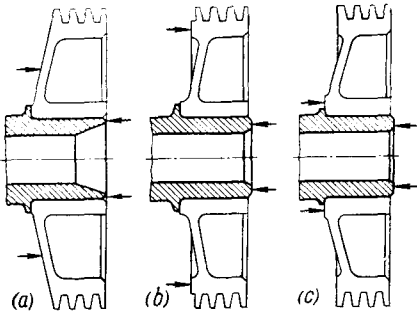


Fig. 40. Pressing-out conditions

can rest during the pressing-out upon solid plates or bushes.

A poor design is illustrated in Fig. 40a. Here, the pulley press-fitted upon the hollow shaft has to rest during the pressing-out procedure on its conically-shaped portion, which complicates the shape of the bearing plate intended to receive the pulley during

the pressing-out. The sharp edges of the shaft are unsuitable for resting against the end face of the press ram.

In the design shown in Fig. 40b the pulley has a bearing cylindrical web; the shaft end face is made flat. However, in the course of pressing-out excessive stresses may arise in the pulley disk, particularly if it has a large diameter.

Therefore it is better to position bearing surfaces close to the hub (Fig. 40c).

The pressing-out force reaches its peak value (rather high) at the initial moment, when the friction of rest is being overcome. After this the pressing-out force decreases because the friction of rest concedes to that of motion, while the length of the press-fitted section continuously decreases as the female part moves off the shaft.

Over the last few years hydraulic systems are used in which pressurized oil, whose pressure exceeds the contact pressure (of the order of up to several hundred atmospheres) is admitted into an annular recess in the joint surface through a hole in the shaft (Fig. 41a) or in the hub (Fig. 41b). The pressure of oil produces elastic radial deformation of the parts to be pressed out. At the same time the

presence of oil minimizes friction during pressing-out. Moreover, the layer of oil, penetrating into a circular slot in-between the parts

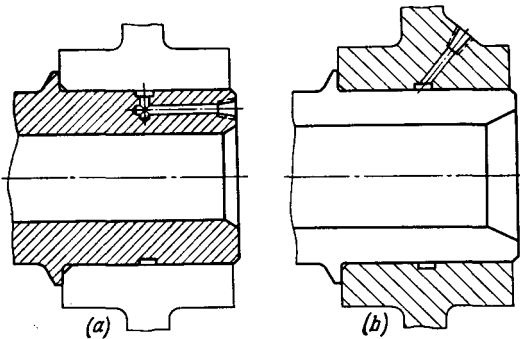


Fig. 41. Pressing-out hydraulically

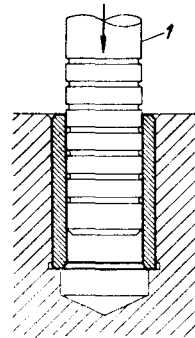


Fig. 42. Pressing-out a bush hydraulically

due to capillary forces, acts as a wedge, which greatly facilitates the pressing-out.

When pressing-out conical joints hydraulically, no mechanical force is required to force the female part off the shaft.

Figure 42 shows how a bush can be pressed-out hydraulically from a blind hole. The bush space is filled up with oil and the bush forced out by a sharp blow on plunger 1.

## 2.9. Conical Fits

Alongside cylindrical press fits extensive use is made of conical press fits (Fig. 43). Tapers  $K$  usually range from 1 : 50 to 1 : 100.

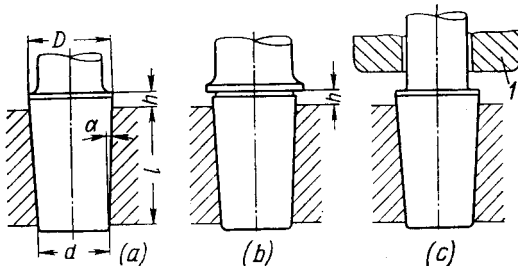


Fig. 43. Conical pressed connections

The required connection interference is obtained by applying a definite force when press-fitting the shaft in place. The force is rigorously controlled since the slow taper easily causes excessive radial interferences.

The press-fitting force may be determined from the relation

$$P = Fk (\sin \alpha + f)$$

where  $F$  = joint surface area,  $\text{mm}^2$

$k$  = unit pressure on the contacting surfaces,  $\text{kgf}/\text{mm}^2$

$\alpha$  = cone generatrix angle (Fig. 43a)

$f$  = coefficient of friction between the mating surfaces

As the magnitude of  $\sin \alpha$  is very small in comparison with  $f$ , it can be omitted. Then

$$P = Fkf$$

As the values of  $D$  and  $d$  are rather close, the joint surface area (i.e., the curved surface of the truncated cone) will be

$$F \approx \pi D l$$

Finally

$$P \approx \pi D l k f \quad (2.27)$$

Another method is forcing the male component into the female one to a definite depth  $h$  (Fig. 43b), counting from the moment the mating surfaces come into close contact. The amount of  $h$  (axial interference) can be found from the relation

$$h = 10^{-3} \frac{\Delta + 2\varphi(R_{z1} + R_{z2})}{2 \tan \alpha} = 10^{-3} \frac{\Delta + 2\varphi(R_{z1} + R_{z2})}{K} \text{ mm} \quad (2.28)$$

where  $K = 2 \tan \alpha = \text{taper}$

$\Delta$  = required diametral interference in the joint,  $\mu\text{m}$

$R_{z1}$  and  $R_{z2}$  = mean roughness height of the shaft and bore, respectively

$\varphi$  = flattening coefficient of microirregularities

( $\varphi \approx 0.5$ )

Let us find the magnitude of  $h$  for a pressed connection when  $D = 50$  mm and  $K = 1 : 50$ .

Assume that  $R_{z1} = 6.3 \mu\text{m}$  (7th class of surface finish) and  $R_{z2} = 10 \mu\text{m}$  (6th class of surface finish). Let the interference be  $37 \mu\text{m}$ , which corresponds to the mean interference in the case of the  $Dh$  grade fit for a diameter of 50 mm.

From Eq. (2.28)

$$h = 10^{-3} \frac{37 + 16.3}{0.02} = 2.6 \text{ mm}$$

The  $h$  value is held either to the difference between the positions of marks on the shaft prior to and after the press-fitting or by pressing the shaft until it rests against a stop shoulder positioned at distance  $h$  from the hole edge (see Fig. 43b). The latter method requires a selective assembly of parts, for inevitable inaccuracies in the joint diameters cause substantial deviations in the dimension  $h$  due to the slow taper.

Often press-fitting is effected by a calibrated blow, i.e., by dropping a weight  $I$  (Fig. 43c) from a certain height. The mass of the weight and the dropping height are found experimentally or calculated by a design subsidence value  $h$  obtained when press-fitting a reference shaft into a reference hole by a blow.

A still better fitting method is that with a preliminary heating of the female part or cooling of the male part, because in this case the male part is introduced into the female one either without any or with a very slight effort. After the female part has cooled (or the male part has warmed) a tight interference fit occurs in the joint. The magnitude of interference (and, for a known interference, the required heating temperature) may be found from Eqs. (2.18) to (2.20).

## 2.10. Serrated Connections

In some instances, to improve the torsional holding power of pressed connections, the shafts are serrated, i.e., given longitudinal grooves having a triangular cross-section (Fig. 44). The external diameter of serrations is made 0.05-0.2 mm greater than the hole diameter. During press-fitting the sharp ridges of the serrations cut into the material of the female part, thus ensuring a strong connection between the shaft and the part.

Generally serrations are produced by cold rolling. The shaft surface must have a hardness of not below 35-40 Rc and the hole surface 10-15 units lower than that.

Serrations are formed either throughout the entire length of the joint surface (Fig. 44a) or (which is more preferable) over a limited section on the side furthest from the press-fitting direction (Fig. 44b).

The latter technique ensures more accurate alignment. Serrated connections allow lower interferences to be used (we mean the interferences on plain sections) than in conventional pressed joints. Small-diameter rods ( $d < 15$  mm) are often introduced into drilled holes without any interference, relying on the strength of connection between serrations and the bore.

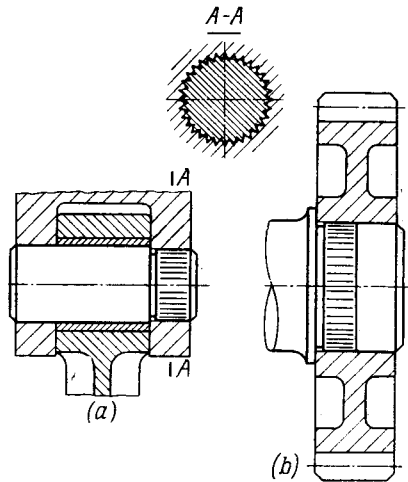


Fig. 44. Serrated connections

Serration is only practicable for permanent connections, since the repeated installation of serrated shafts weakens the connection because the first assembly destroys the hole surface.

### 2.11. Glued Connections

In many cases press-fitted connections can successfully be replaced by glued connections whose strength is comparable with that of the former.

The axial holding power of pressed and glued connections  $P = kFf$  and  $P_{gl} = F\tau$ , respectively, and their torsional holding power,  $M = kFf\frac{d}{2}$  and  $M_{gl} = F\tau\frac{d}{2}$ , where  $k$  is the pressure on the joint surfaces and  $\tau$ , the shear strength of the glue layer.

Equating  $P = P_{gl}$  and  $M = M_{gl}$ , gives a general equistrength relationship

$$k = \frac{\tau}{f}$$

which defines the unit pressure  $k$  in pressed connections equivalent (in terms of strength) to glued joints. For epoxy base glues  $\tau = 2-3 \text{ kgf/mm}^2$ . Calculating by the lower limit, we have  $k = \frac{2}{f}$ . With  $f = 0.15$ ,  $k = 13.5 \text{ kgf/mm}^2$ . This value of  $k$  corresponds to moderate interference fits of grades  $Dh1_1$ ,  $Dh2_1$  and  $Dh$ .

The advantage of glued connections is that they do not cause stresses in the connected parts. They exclude the need for pressing, or heating, or cooling and considerably facilitate the assembly procedure. For thermosetting glues, however, they must be held at a temperature of  $150^\circ\text{C}$  for approximately 2 hours.

Glued connections are assembled by slide or transition fits. In pressing-out the glue film is destroyed. For the repeated assembly it is necessary to wash off the traces of the old film with a solvent and then apply a fresh layer of glue.

Glued connections remain stable at temperatures up to  $200^\circ\text{C}$ , which limits their field of application. Under the effect of cyclic loads, even in cold connections there may develop local seats of increased heat liberation which destroy the glue film.

# Centring Connections

Cylindrical surfaces are generally centred by slide ( $S$ ) of transition [push ( $P$ ), wringing ( $W$ ) and tight ( $T$ )] fits. Occasionally easy side ( $Se$ ) fits are also employed.

Figure 45 shows the mean values of clearances and interferences for various grades of fits as a function of the centring surface diameter.

With slide fits the clearance in the joint is zero only under extreme conditions when the female and male surfaces are made to the nominal size. In the majority of cases the connections have some clearance reaching significant values for the low accuracy classes. Consequently, slide fits cannot ensure accurate centring.

Clearances can also occur with the push fits ( $P$ ). The wringing fits ( $W$ ) are without clearance and should be used when accurate alignment is necessary. Tight fits ( $T$ ) are obtained with insignificant interferences in the connection.

Tight and wringing fits ensure accurate alignment without complicating assembly and disassembly if the centring surfaces have short lengths (e.g., collar flanges). Parts with long centring surfaces (hubs) are better assembled by slide and push fits, if the requirements as to high alignment accuracy are not imperative and there is no danger of the joint surfaces being damaged under the action of loads.

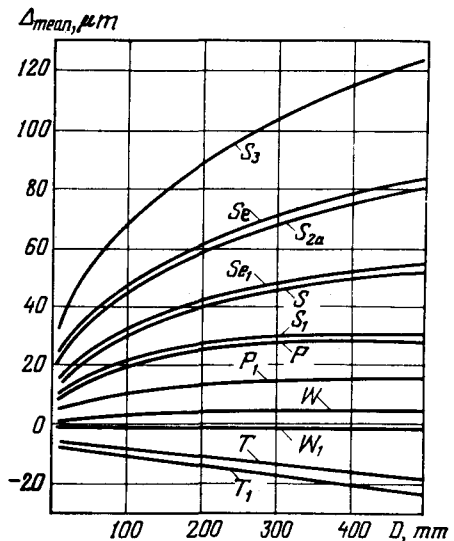


Fig. 45. Mean clearances and interferences  $\Delta_{mean}$  for different fits as a function of centring surface diameter  $D$

Average clearance values depend not only upon the grade of fit, but on the grade of accuracy as well. The easy slide fit to the 1st grade of accuracy ( $Se_1$ ) is practically equivalent to the slide fit ( $S$ ) to the second grade of accuracy (disregarding the narrower margin tolerance); the  $S_1$  fit is equivalent to the  $P$  fit, and the  $Se$  fit, to the  $S_{2a}$  fit.

When nominating fits due consideration must be given to the temperature conditions in which the joint is expected to operate. The original (cold) fit may sharply change during heating, particularly when the female and male components are made of materials with different linear expansion coefficients. In such conditions heat calculations are obligatory.

If during heating the female component expands more than the male part, tighter fits should be nominated ( $P$ ,  $W$  and  $T$ ), and if the male part expands more, free fits ( $S$ ,  $Se$  and even  $R$ ) should be preferred.

Let the diameter of the centring surface be  $D = 200$  mm. The female part is made of a light alloy ( $\alpha_1 = 24 \cdot 10^{-6}$ ), and the male part, of steel ( $\alpha_2 = 11 \cdot 10^{-6}$ ). The working temperature of the connection is  $100^\circ\text{C}$ . The connection is assembled by the  $S_{2a}$  grade of fit (diametral clearance  $\Delta = 0$  to  $0.12$  mm). After heating the clearance becomes

$$\Delta_t = \Delta + 200(\alpha_1 - \alpha_2) 100 = (0 \text{ to } 0.12) + 200 \cdot 13 \cdot 10^{-6} = (0.26 \text{ to } 0.38) \text{ mm}$$

Obviously, the centring accuracy is disturbed. A tight fit will somewhat improve the situation. The maximum clearance with this grade of fit amounts to  $0.056$  mm, and the maximum interference,  $0.064$  mm. Consequently, after heating the resultant clearance in the joint will range from  $0.26 - 0.064 = 0.196$  mm to  $0.26 + 0.056 = 0.316$  mm.

With larger radial dimensions of the connection and higher working temperatures the original fit often alters to such a degree that it is impossible to centre the cylindrical surfaces, and a temperature-independent centring must be used (see *Fundamentals of Machine Design*, Vol. 1, Section 7.3, p. 472).

### 3.1. Design Rules

To enhance the alignment accuracy and reduce the effects of temperature-induced deformations, it is undoubtedly better to centre parts from the smallest possible diameter. Ways of reducing the centring diameters are illustrated in Figs. 46 and 47.

The screwed bracket (Fig. 46*d-f*) is an example. When the centring is accomplished from a large diameter (Fig. 46*d*) equal to, say,  $200$  mm, the maximum clearance with the  $S_{2a}$  grade of fit will be  $0.12$  mm, but when centring from the minimum diameter (Fig. 46*f*) this clearance decreases to  $0.037$  mm, i.e., approximately thrice. The centring is sharply improved and becomes practically temperature-independent.



When centring franged parts a sufficiently long centring shoulder should be provided, allowing for the leading chamfers in the hole

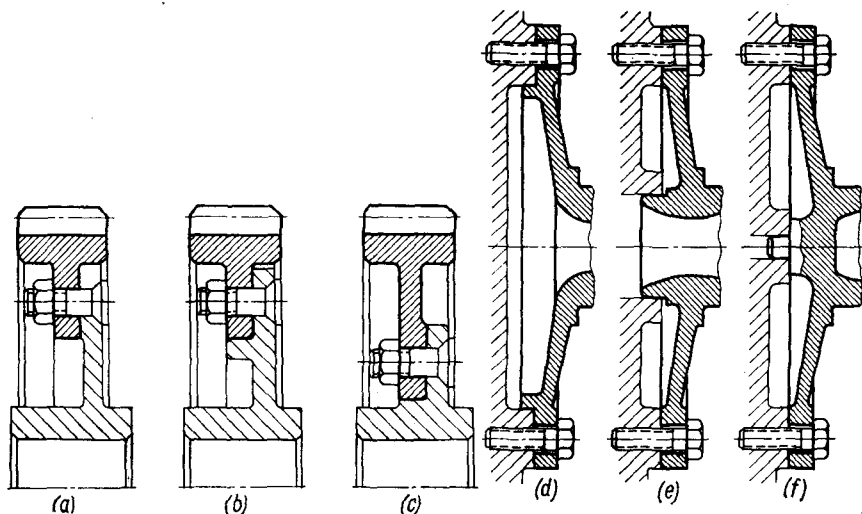


Fig. 46. Reduction of centring diameter  
(a-c) gear rim; (d-f) bolted bracket

and on the male part, as well as gaskets, that considerably decrease the actual length of the centring surfaces.

Shoulder height  $H$  is chosen so as to ensure positive centring from section  $h$  (Fig. 48)

$$H = h + 2c + \Delta H + 2\Delta c + s$$

where  $c$  = length of the leading chamfers with the most unfavourable combination of manufacturing deviations

$s$  = gasket thickness (in compressed state)

$\Delta c$  = plus deviation of the leading chamfer dimensions from the nominal

$\Delta H$  = minus deviation of the centring shoulder height from the nominal

The dimensions of the centring section  $h$  and chamfers (in the hole and on the male part) for mass produced connections may be taken as follows:

Diameter of centring surface, mm	up to 100	100-200	200-300	300-500	over 500
$h$ , mm	3-4	4-5	5-6	6-7	7-8
Chamfers	0.5-45°	0.8-45°	1-45°	1.5-45°	2-45°

The shoulder height  $H$  is practically determined from the relation  $H \approx 0.5 \sqrt{D}$ , where  $D$  is the centring surface diameter (provided that ordinary 0.1-0.2 mm thick gaskets are used).

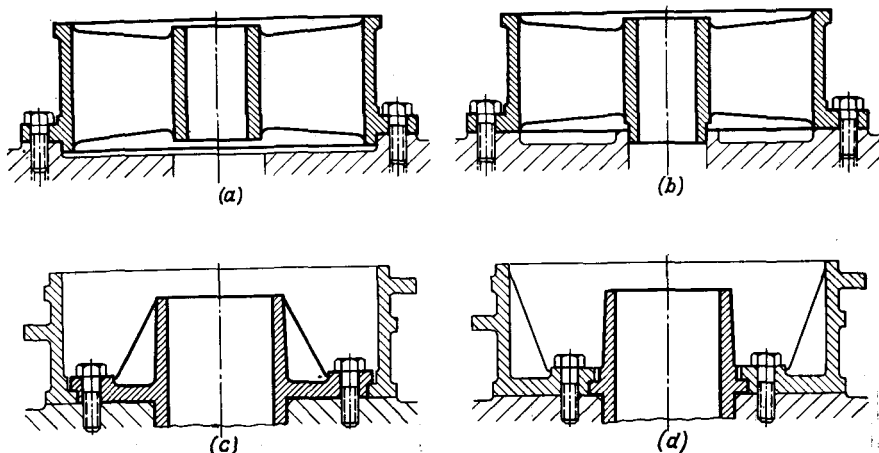


Fig. 47. Reduction of centring diameter in connections of housing-type components

In housing-type components (Fig. 49) the centring surfaces should be made in the form of holes which can readily be machined on boring machines (Fig. 49d, e). The observance of this rule is particularly important when the centring is accomplished from co-axial surfaces positioned on different sides of the housing (Fig. 49f, g). The design illustrated in Fig. 49f is extremely poor as the centring shoulders on such a housing have to be machined in different tool settings and proper alignment can be assured only with the aid of special attachments. In the correctly designed version presented in Fig. 49g the centring surfaces of the housing can be through-machined in a single tool setting, thus ensuring good alignment.

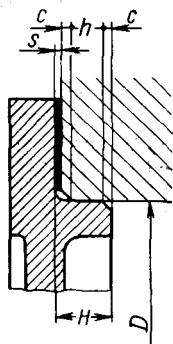


Fig. 48. Determination of centring shoulder height

Simultaneous centring from two surfaces (Fig. 50a) must be avoided whenever possible: the centring must be accomplished from one surface only, leaving a positive clearance  $s$  on the other surface (Fig. 50b, c).

In the flange unit shown in Fig. 50d the centring of splined flange 1 from the shaft is not only superfluous (the centring being effected

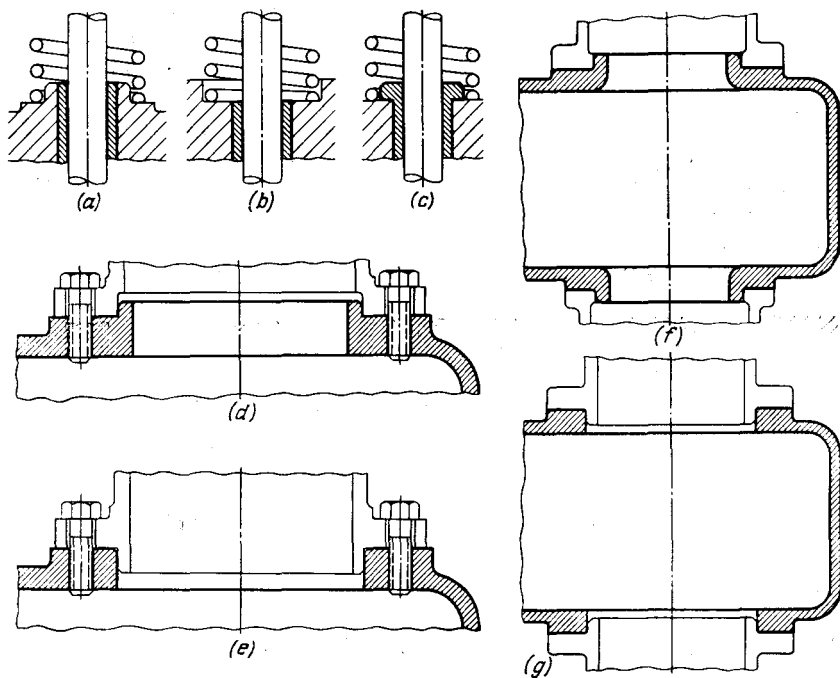


Fig. 49. Positions of centring shoulders  
 (a), (d) and (f) wrong; (b), (c), (e) and (g) correct

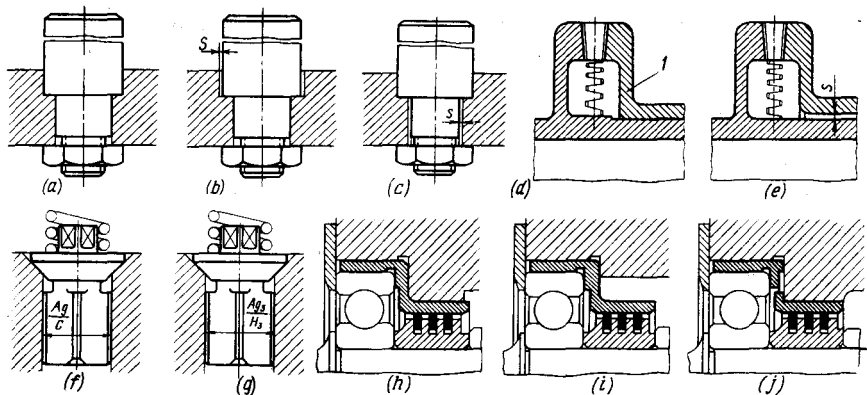


Fig. 50. Elimination of double centring

by the splines themselves) but harmful since it hinders the correct clearance-free fitting of the splines. In the correctly designed version pictured in Fig. 50e clearance  $s$  is provided between the components.

The next Fig. 50f shows an incorrect valve design with a guide shank. The small clearance between the shank and the bore prevents the accurate seating of the valve cone. In a better alternative (Fig. 50g) a greater clearance is given.

Figure 50h presents a wrongly designed assembly of a ball bearing inside a sleeve with two centring surfaces serving simultaneously

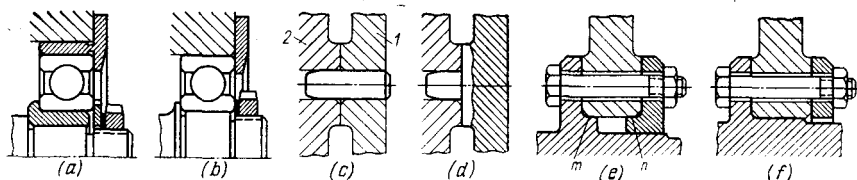


Fig. 51. Reducing the number of centring surfaces

as a sealing bush with split spring rings. Correct alternatives are illustrated in Fig. 50i, j.

In units consisting of several concentrically arranged components the number of centring surfaces should be reduced to the minimum, since the accuracy of the unit as a whole is considerably impaired by the cumulative error introduced by each centring surface, which is the greater, the larger the number of the surfaces.

In the design shown in Fig. 51a, an antifriction bearing is mounted in two intermediate bushes. Apart from the clearances between the rolling bodies and races, there are four centring surfaces. Reducing the number of the centring surfaces down to two (Fig. 51b) improves centring accuracy approximately twice.

When centring from a cylindrical pin (Fig. 51c) pressed in member 1 and fitted by a slide fit in the hole of member 2, the centring errors from the two surfaces are summed. In units requiring accurate centring it is necessary either to machine the centring surface of the pin concentrically to the precision surfaces on the part to be centred, after the pin is pressed in, or the centring pin must be made directly on the part in question (Fig. 51d).

Figure 51e depicts the case of an irrational centring from two surfaces: surface  $m$  on the shaft, and surface  $n$  on a detachable disk. The centring from the surface  $n$  is either fictitious (if the disk is fitted on the centring part with a clearance) or disturbs the centring from the surface  $m$  (if the disk is fitted on the shaft with an interference). It is better to centre the part from the shaft, the disk being freely mounted (Fig. 51f).

As a rule, cylindrical surfaces must be centred from a full circumference. Small recesses, however, hardly affect the alignment accuracy. In some instances, when necessary for the design, parts may

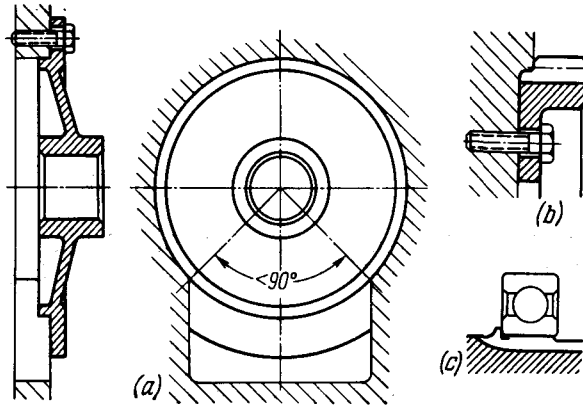


Fig. 52. Centring from incomplete cylindrical surfaces

be centred from incomplete circumferences, if the centring arc is not less than  $270^\circ$  (Fig. 52) and the part being centred has ample rigidity in the radial direction. In practice they often implement

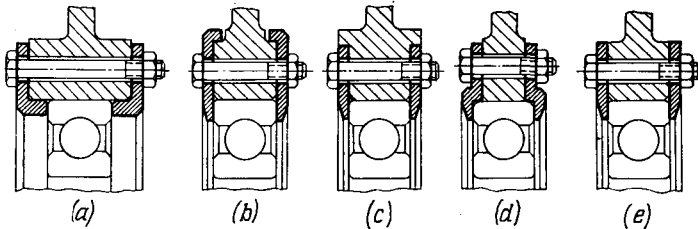


Fig. 53. Elimination of superfluous centring  
(a-d) incorrect designs; (e) correct design

centring from teeth (Fig. 52b), splines (Fig. 52c) or even from individual lugs, when the latter are at least three in number and are spaced symmetrically over a circumference.

A common mistake of young designers is to introduce centring where for operation it is superfluous and can be dispensed with. For instance, for the intermediate mounting of an antifriction bearing the centring of the lateral cheeks (Fig. 53a-d) is actually not necessary. Here it is sufficient to fix the cheeks in radial direction by means of fastening bolts (Fig. 53e), this considerably simplifying the manufacture.

# Screwed Connections

The principal requirement for correct functioning of screwed connections is that the threads must be free from bending and shearing stresses.

A bolt loosely mounted in the holes of the clamped parts and subjected to the action of transverse forces (Fig. 54*a*) deforms. With a full elimination of clearance at bolt sections near the joint more shear stresses arise. Furthermore, the bolt is subjected to tension due to which it elongates under the displacement of the pulled part. All these stresses are added to the tensile stresses induced in the bolt during the preliminary tightening. As a result, in the bolt body

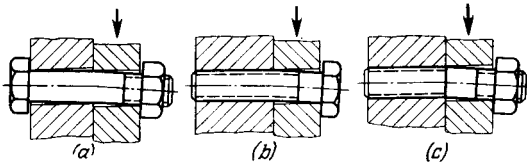


Fig. 54. Flexure of threaded parts

a complex state of stress occurs, produced by the simultaneous action of bending, shearing and tension forces, and the bolt's strength abruptly drops.

A screwed-in bolt has still worse working conditions (Fig. 54*b*) when in its critical section (close to the joint plane) a thread is cut, appearing as a very strong stress concentrator. Most unfavourable is the case of the bending of a stud screwed home in a hole (Fig. 54*c*). Here high tensile stresses arise in the critical section, comprising the prestresses and stresses produced as the stud is tightened against the hole bottom. As in the previous case, here the stress concentration occurs in the section where the thread comes to the critical section plane.

Also unfavourable are the working conditions for the material of the threaded holes of tightened components. The transverse forces, acting at the joint, wedge out the threads of the screwed hole, producing higher local bearing stresses which in time weaken the thread and loosen the fit of the screwed stem, particularly under alternating loads.

The problem of strengthening tightened connections consists in the elimination of the complex stressed state in the fastening elements and assure conditions in which these elements would operate only in tension when under the influence of preliminary tightening

and working forces. Transverse acting forces must be taken up by additional shear load-carrying elements.

Let us consider the case of a cantilevered rod, screwed in a housing (Fig. 55a). Design 1 is obviously unsatisfactory, because the maximum bending moment from the transverse force  $P$  is in the weakened threaded portion. High stresses at the imbedment point inherent in the cantilever make the rod bend and crushes the threads in the hole and on the rod.

Provision of a shoulder in the tightening area (version 2) helps little, since the shoulder thrust face is nearly parallel to the direction of bending displacement and the deformation is resisted only by the friction forces arising at the thrust face when tightening.

In more correct designs 3 and 4 the rod has a cylindrical or tapered section which closely fits the housing hole and efficiently impedes transverse strains and rod displacement. Since it is rather difficult to assure strict alignment of the threaded and plain sections, the screwed end must have clearance.

The best are designs 5 and 6 which have a cylindrical or tapered fitting section in the housing. In this case the threads are completely relieved from bending and take up only the tightening tension.

Figure 55b illustrates various methods of fixing a cast stand loaded with a transverse force to a housing. Version 7 is absolutely incorrect: the fastening stud is subjected to bending from the transverse force. Version 8 is hardly better: here the stand is aligned by the plain stud portion. In the improved version 9 the stud has a centring cylinder which closely fits into the holes of the housing and stand. In design 10 shearing forces are taken up by check pins and in design 11 by the stand centring shoulder.

Illustrated in Fig. 55c are various methods of taking up shearing stresses in a counterbalance unit joint loaded with a centrifugal force, and in Fig. 55d, in a flanged connection transmitting a torque. Designs 12 and 17 are wrong, and the rest to a more or less degree provide correct operating conditions for bolts.

Bending of bolts is often the result of their incorrect positioning relative to the acting loads (Fig. 55e). The bracket in design 22 has two errors: lack of an element taking up the shear stresses and the bending of the bolt stems due to the off-centre application of the axial load. Under the action of force  $P$  the bracket tends to turn about point  $A$ . With the relationships presented in the Figure, the

force acting upon each bolt is  $N = \frac{Pl}{2b} = 1.7P$ . The bolt is subjected

to bending by a moment  $M = \frac{Nd}{2}$ , where  $d$  is the diameter of the bolt head.

With the flange turned through  $90^\circ$  (version 23) the load upon the bolt becomes practically central (owing to the extension of arm  $b$ ).

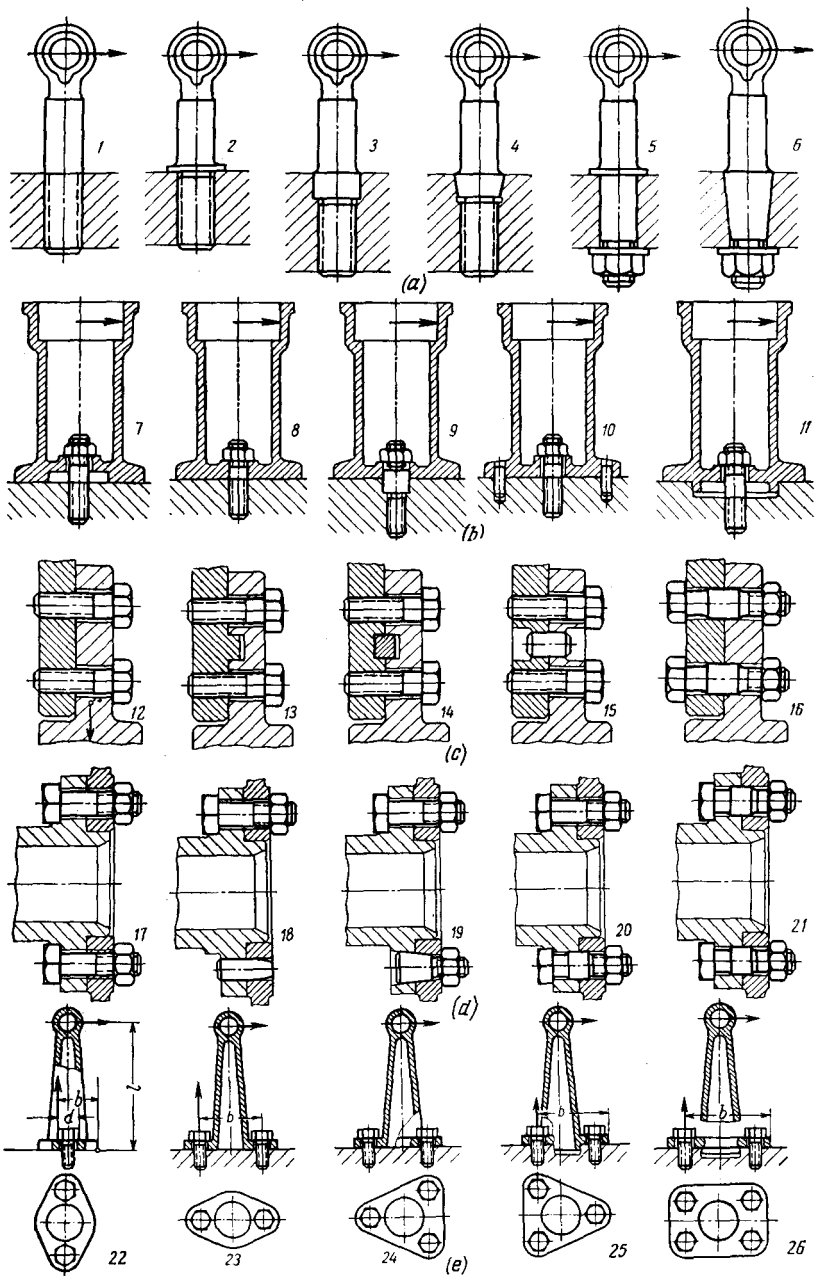


Fig. 55. Relieving threaded parts from flexure and shear



Since in the given case only one bolt is active (the right-hand bolt is relieved), the force applied to the bolt still remains rather great ( $N = 1.7P$ ).

The introduction of a triangular flange (design 24) in no way enhances the joint strength, as the added bolts do not take part in the work. In the rational alternative 25 two bolts are active. The force acting upon each of the bolts is thus reduced to  $N = P$ . The bolt

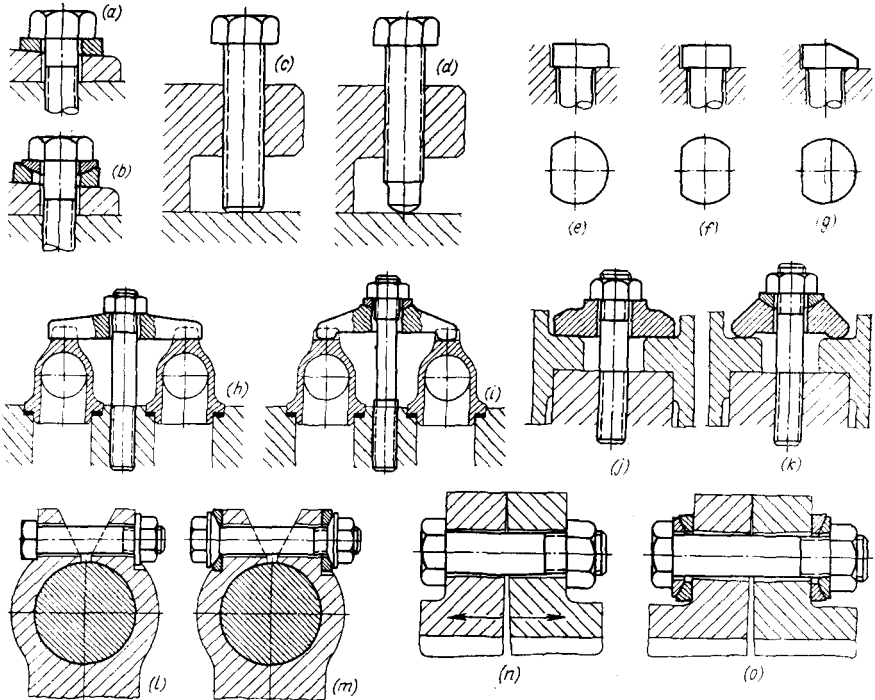


Fig. 56. Eliminating flexure of threaded parts

shearing is forestalled by means of the bracket centring shoulder. In design 26 (the square-shaped flange) the base area is enlarged and, as a result, the bolt load is reduced to  $N = 0.7P$ .

Fastening elements are often bent due to the distortion of the support surfaces, which causes an off-centre load application (Fig. 56). Should the supporting surface be angled, then tapered washers (design *a*) or, better, spherical washers (design *b*) are obligatory. To prevent off-centre loads the flat end faces of pressing, lifting and other screws (design *c*) must be changed to spherical ones (design *d*).

Off-centre flexure may also arise with an unsymmetrical shape of bolt heads, for example, a bolt head having a flat preventing its

rotation when tightening (version *e*). The flexure here can be eliminated by machining flats on two sides (alternative *f*) or by decreasing the head rigidity in the area opposite to the flat (version *g*).

Self-alignment of fastening elements is a radical means to avoid flexure. In design *h* (clamping down adjacent angles of hydraulic communication system with the aid of a crossbar) distortion of the crossbar is inevitable, also inevitable are bending of the bolt and non-uniform tightening of the angles. These defects are eliminated in version *i* by providing a self-aligning crossbar.

Wrong *j* and correct *k* alternatives of clamping the flanges of adjacent cylinders to the crankcase are shown in Fig. 56.

Flexure may also arise as a result of elastic strains emerging in the tightened parts. When tightening clamp-type connection *l* the ends of the clamps distort and the load becomes eccentric. In design *m* the flexure of the clamping bolt is prevented by the introduction of spherically shaped washers.

In all connections where the bolts are displaced from the plane of acting forces flexure is inevitable (e.g., in flanged connections *n* loaded by the internal pressure). Self-aligning bolts *o* are recommended for heavily loaded critical connections.

#### 4.1. Longitudinal and Transverse Location of Parts in Screwed Connections

Screwed connections do not ensure accurate mutual location of the clamped parts.

Generally, fastening bolts and studs are introduced into their holes with some clearance whose amount is dependent on the number and spacing, as well as accuracy of centre-to-centre distances, of holes, and on the average varies from 0.5 to 1 mm. If such a clearance is absent, the assembly becomes impossible due to certain mismatching of mated holes in the parts to be coupled and the displacement of holes one relative to another in each part, a fact inevitable in practice.

To ensure accurate mutual location of parts it is necessary to introduce certain locating elements. The methods of such a location are illustrated by an assembly example of a bearing cover to a housing (Fig. 57). Often the location is accomplished from longitudinal shoulders (Fig. 57*a-c*) machined in the cover or the housing, which are tightly fitted in corresponding slots.

The design alternative with a locating lug (Fig. 57*d*) is not suitable because it requires a close contact over four surfaces at once. The location with fitted-in prismatic keys (Fig. 57*e*) is also not recommended.

The cylindrical shape of the centring shoulder (Fig. 57*f*) facilitates accurate manufacture of the shoulder and its housing seat and ensures longitudinal and transverse cover location. The cover, however, is not prevented from turning about the line of joint.

The design seems to be more advantageous for single bearings; for series-arranged bearings it is better to employ longitudinal shoulders and slots machined in a single tool setting.

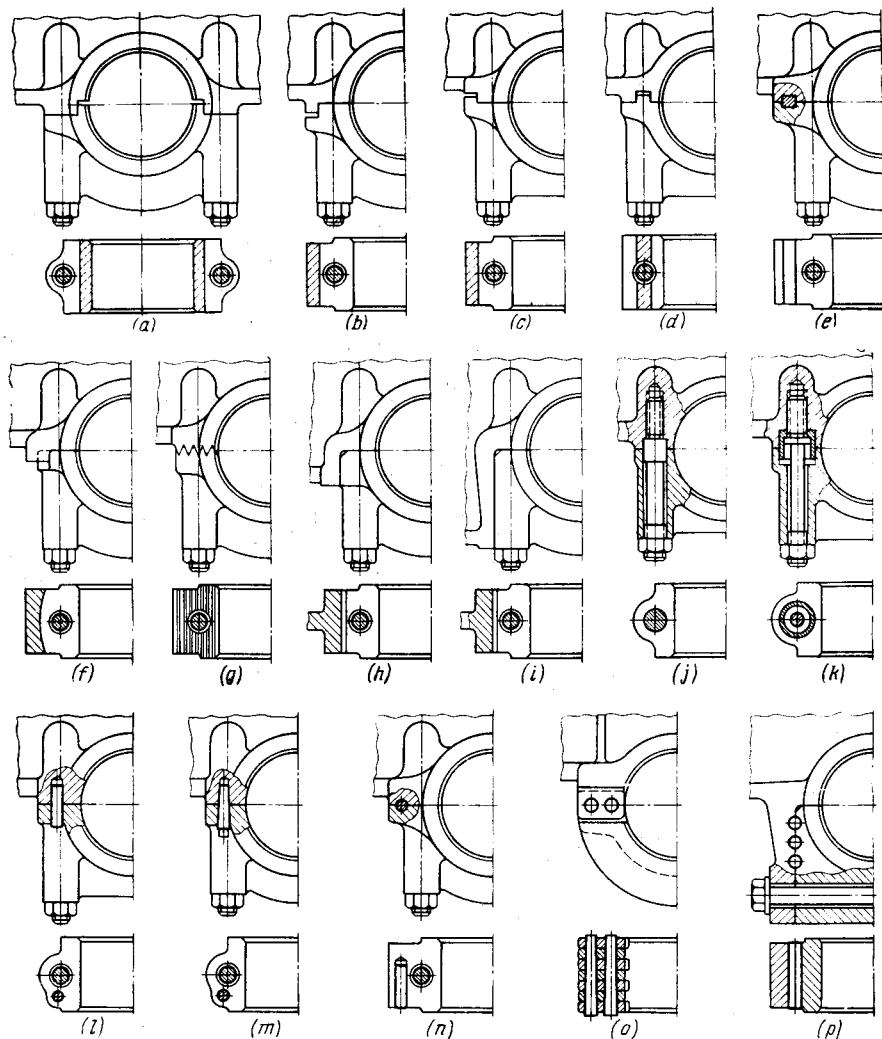


Fig. 57. Methods of fixing bearing caps to housings

Occasionally the cover is located by means of endwise splines having a triangular section (Fig. 57g) and produced by outside broaching. This method is technically possible (provided the necessary equipment is available) and enables a sturdy joint to be obtained.

Higher robustness is assured by mounting the covers in lengthwise housing recesses (Fig. 57*h, i*).

The methods illustrated in Fig. 57*a-i* ensure a transverse location of the cover. If the bearing has to take up axial loads, a lengthwise location is necessary to assure the matching of the cap and housing end faces. Such a location is accomplished by means of cylindrical collars on studs (Fig. 57*j*), insert-type cups (Fig. 57*k*) or dowel pins (Fig. 57*l*).

Detachable taper locating pins (Fig. 57*m*) ensure a more accurate location, but are much more difficult to produce and assemble. Moreover, they have to be prevented from falling out. Location by means of lengthwise dowel pins (Fig. 57*n*) is practicable only when the bearing end face can be directly drilled and reamed. This method cannot provide for the taking up of longitudinal loads.

The design in Fig. 57*o* shows a unique method of fastening the cover with the aid of taper pins press-fitted into a row of lugs milled in the housing and cover. Lengthwise location is effected by fitting closely the lugs of the cover (or a pair of lugs) inside the receiving slots of the housing.

Still another method is the location by means of lengthwise pins (Fig. 57*p*) introduced into the holes machined in the vertical joint surfaces between the cover and housing. The system is tightened transversely by bolts. If it is impossible to drill or ream directly in the bearing end face, broached triangular-section splines must replace the pins.

## 4.2. Centring in Screwed Connections

Screwed connections of conventional accuracy do not ensure precise centring due to the practically unavoidable run-out of the thread pitch diameter, as well as thread clearances. Exceptions from this rule, however, are encountered occasionally when dealing with precision centring threads—mostly large trapezoidal threads produced by milling and grinding.

With the usual manufacturing accuracy the centring from the threads is not permitted (Fig. 58*a-g*). If threads must be used, then additional centring surfaces should be introduced. Most often the problem is solved by using plain cylindrical collars. Threads in this case should be made loose so that the centring is unobstructed. The position of such centring collars relative to the threads depends on the actual operating conditions of the joint. From technological viewpoint it is wise to make the diameter of such a centring collar slightly smaller than the thread minor diameter, locating the collar behind the thread (Fig. 58*h*). This allows precision through-machining of the centring bore. The loading scheme of the connection must also be considered. Should the force act as shown in Fig. 58*i* then

the correct position of the centring collar is before the thread, even though it incumbers slightly the machining of the bore.

Screwed joints of conventional accuracy also fail to assure true perpendicularity of the screwed component's end face relative to the

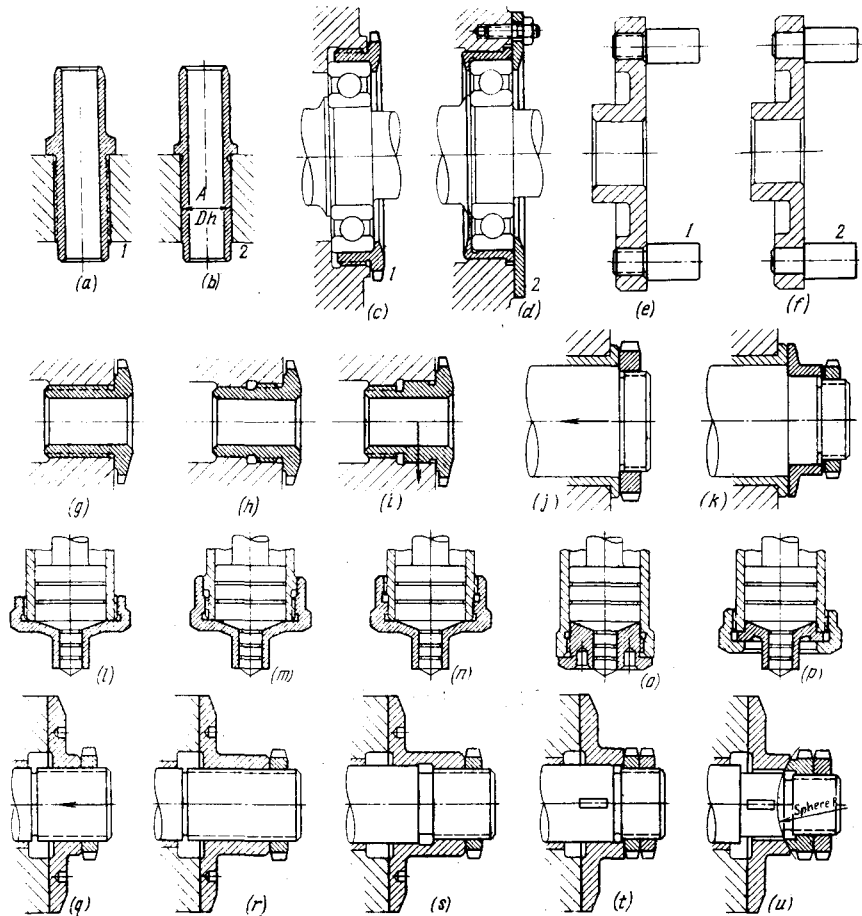


Fig. 58. Centring in screwed connections  
1 — wrong; 2 — correct

thread effective diameter. For this reason the nut end face cannot be used as a bearing surface taking up axial forces in frictional units (Fig. 58j). In this case the inevitable misalignment of the nut end face relative to the shaft axis causes a unilateral force application and increases the wear of the bearing shoulder. The correct design is illustrated in Fig. 58k.

A plunger assembly with a rod sliding in the bore of a screwed-on detachable cover (Fig. 58*l*) does not ensure axial alignment of the holes in the cylinder and cover. An aligning collar tailored beyond the thread boundaries (Fig. 58*m*) rectifies but partially the displacement of the cover.

An aligning collar located nearby the cylinder end face (Fig. 58*n*) ensures alignment only if the cylinder outside centring surface is made exactly concentric with the hole. Still better is the design with a female thread (Fig. 58*o*); here the collar is centred directly from the cylinder walls. The most reliable way of effecting the alignment is by means of a cylindrical shoulder with the cover clamped down by a captive nut (Fig. 58*p*).

Figure 58*q-u* shows units enabling a continuous adjustment of the axial position of the shaft mounted in a bearing and loaded with a force of constant direction. The alternative in which a thrust plate is screwed on (Fig. 58*q*) is unsatisfactory due to the plate distortion which causes wear on one side of the plate bearing face. An increase of the threaded portion (Fig. 58*r*) only worsens the situation. A satisfactory solution is the introduction of a cylindrical centring collar (Fig. 58*s*) which eliminates the distortion of the plate end face, if it is machined strictly perpendicular to the centring cylindrical surface and the thread clearance is large enough not to interfere with the plate placement on that surface. A still more reliable mounting of the plate is illustrated in Fig. 58*t* where the plate is fitted upon a plain centring collar and its axial position is adjusted by means of a nut and a locknut. A still better design is presented in Fig. 58*u* in which the plate can align itself on the spherical surface of the nut.

### 4.3. Design Rules

Screw threads in heavily loaded connections must always be tightened, otherwise they will quickly fail, particularly under cyclic and dynamic loads, owing to the crippling, work hardening and, sometimes, welding of the threads.

The design of a valve in which the valve plate is screwed into the valve stem (Fig. 59*a*) is poor, as under the action of forces and bending moments, when the drive cam runs against the plate, the threaded connection works loose. Moreover, the free thread does not accurately locate the plate relative to the stem. Lengthening the threaded portion (Fig. 59*b*) only partially eliminates this disadvantage. It is better to tighten the screwed connection by a locknut (Fig. 59*c*). The turnbuckles shown in Fig. 59*d, e* are similar examples.

Screwed connections of the usual accuracies are not seal-proof. When applying screw threads to vessels containing gases or liquids under pressure, preliminary measures must be taken against leakage through the threads. Fitting gasket washers under nuts (Fig. 60*a*)

is insufficient because liquid penetrates along the threads. In such cases one should use cap nuts (Fig. 60b) or install below the nuts bushes having inserts made of some elastic material (rubber, plastic), which will assure the sealing of the joint over the plain cylindrical part on the bolt (Fig. 60c).

Studs the ends of which penetrate into the internal cavity containing the liquid must not be used (Fig. 60d). However, interference-

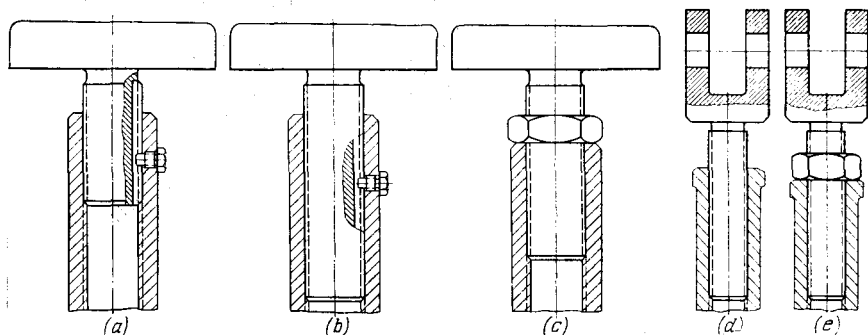


Fig. 59. Tightening of screwed connections

fitted studs used with sealing compounds assure hermetic sealing but this method is not recommended as there is no guarantee that the replacement studs changed during repairs will continue to seal

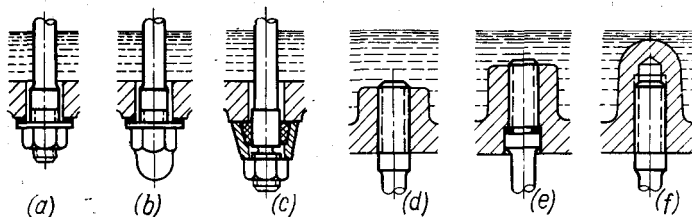


Fig. 60. Sealing of screwed connections

correctly. Tightening studs onto sealing gaskets (Fig. 60e) complicates the design and is not fully reliable. The best way to prevent leakage is to fit the studs in blind bosses (Fig. 60f).

Through-holes for studs (ref. No. 1, Fig. 61) and bolts are permitted in spaces where the liquid is present in the form of droplets, splashes or films covering the walls. In oil baths the fastening studs must be blind-mounted (2).

Plugs in oil-containing cavities must have sealing gaskets (Fig. 62a). Tapered threads (Fig. 62b) have self-sealing properties, particularly when screwed into housings made of plastic metals.

Parts, for which an accurate angular position is essential, should not be screwed in. When positioning a threaded angular pipe connection (Fig. 63a), its accurate location can be ensured either by scraping the end face surface of the bearing shoulder or by selecting a gasket of a suitable thickness. These measures complicate assembly.

In later reassemblies the correct position of the connection will inevitably be disturbed. The most advisable solution in this case is to mount the connection on a flange (Fig. 63b).

Figure 63c-f shows various bracket designs for a handrail. When

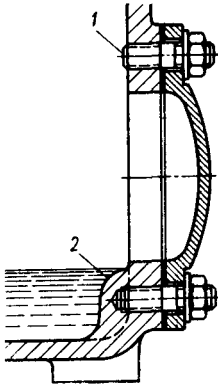


Fig. 61. Installation of fasteners in oil-containing cavities

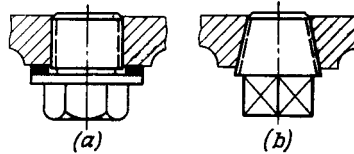


Fig. 62. Plugs

using a threaded connection it is practically impossible to put the bracket at its required angular attitude (Fig. 63c). It is better to fasten the bracket with a cylindrical stem (Fig. 63d), tightening the nut after the handrail is introduced into the bracket head. The

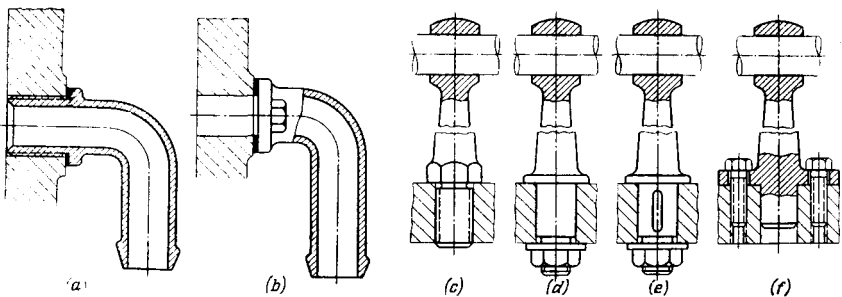


Fig. 63. Angular location of threaded parts

angular position of the bracket can also be set with a key (Fig. 63e), or by means of a flange (Fig. 63f). Readjustment in the first case is accomplished at the expense of the clearances between the key and its seat, and in the latter case, at the expense of the clearances between the bolts and their holes in the flange.



Power tightening should always be made possible for threaded connections. In the poor designs shown in Fig. 64*a, c* friction forces produced during tightening on the bearing flange surfaces, being applied over a large radius, sharply increase the tightening torque, thus making power-tightening impossible. In the correctly designed

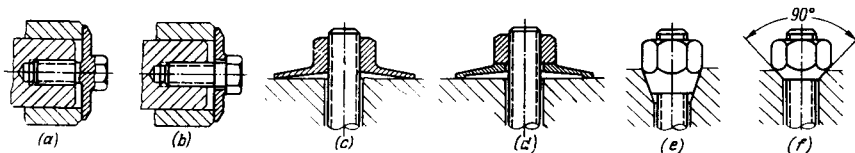


Fig. 64. Reduction of tightening torque

versions (Fig. 64*b, d*) the friction forces act at the minimum distance from the bolt axis, this distance being equal to the average radius of the bearing surface of the bolt head.

In joints where tightening is effected over gently tapered surfaces (Fig. 64*e*) power-tightening is impossible because of the impeding

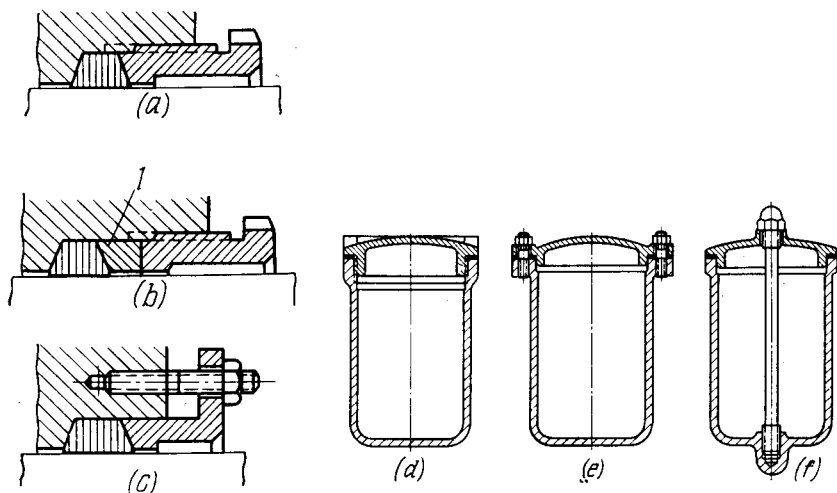


Fig. 65. Tightening over soft gaskets

effect of frictional forces on the tapered surfaces and also due to the compression of the stem threads by those of the nut over the tapered area. Cone angles not exceeding  $90^\circ$  (Fig. 64*f*) are recommended.

Tightening on soft materials (packings, gaskets, etc.) should be avoided.

For instance, tightening of a packing gland nut (Fig. 65*a*) causes twisting and collects the packing on the nut end face. This can be

avoided by installing an intermediate metallic ring 1 (Fig. 65b) or by replacing the nut with a flanged bush (Fig. 65c).

Figure 65 further illustrates an incorrect (Fig. 65d) and correct (Fig. 65e, f) examples of a cover with a sealing gasket.

In general, screwed joints with large diameter threads should be avoided (Fig. 66a) and bolted and studded connections used instead (Fig. 66b).

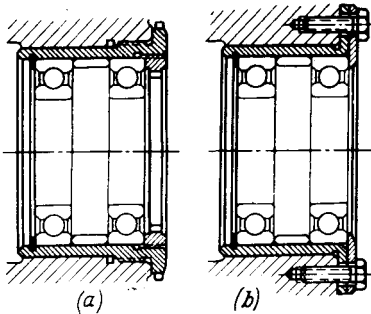


Fig. 66. Replacing threaded connection by bolted joint

Large diameter threads are difficult to produce, particularly in big housings. Threaded holes for fastening elements are more economic, even with a large number of holes. Furthermore, small-sized fasteners are more convenient in assembly and allow commercially produced fasteners to be employed.

It is strongly recommended that large diameter threads in components made of ductile and plastic materials (light and zinc alloys, stainless steels) be avoided. Ductility and low antifriction properties of these materials cause tearing of threads thus hampering tightening.

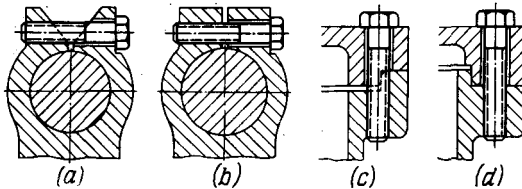


Fig. 67. Threaded hole designs  
(a) and (c) wrong; (b) and (d) correct

Threaded holes with skew (Fig. 67a) or stepped (Fig. 67c) edges are unacceptable under any circumstances, since it is extremely difficult to screw a fastener into such a hole. They can tap such holes only having left beforehand a flat area on the hole end face which will be removed after tapping.

#### 4.4. Reinforcement of Fastening Joints

Fastening bolts and studs should be positioned at the rigidity nodes of the assembled parts so that the fastening force is spread over as large an area as possible.

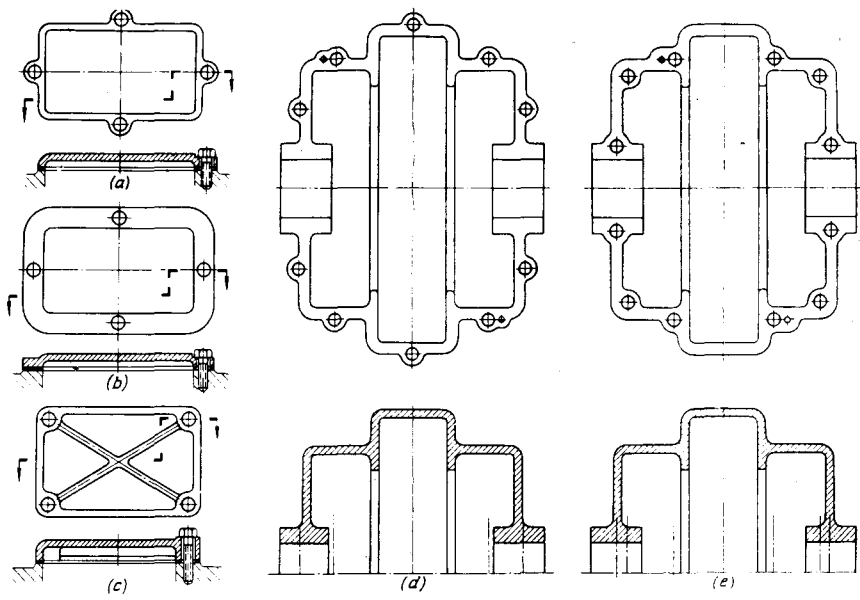


Fig. 68. Positions of fastening bolts

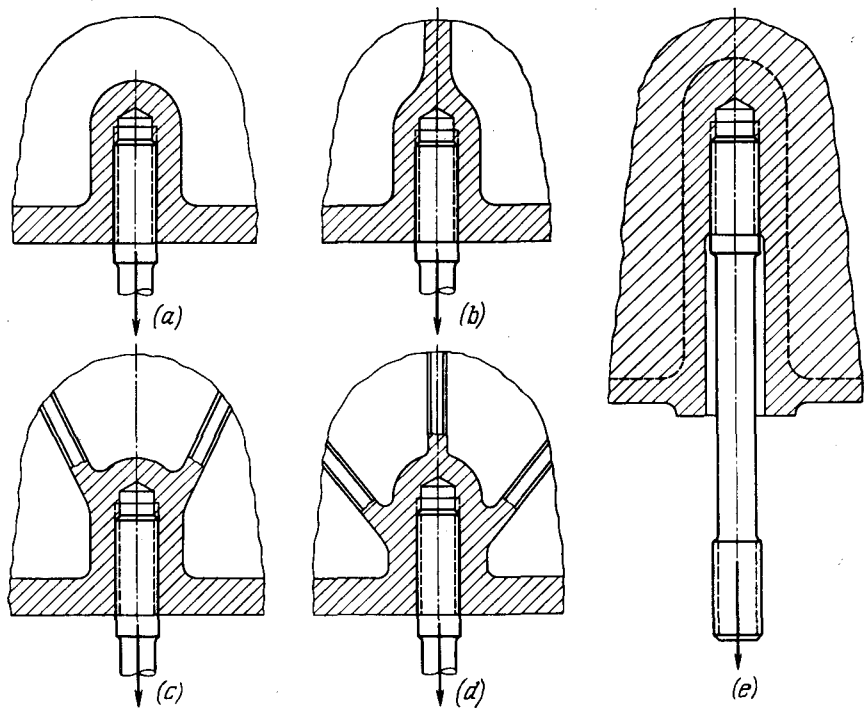


Fig. 69. Methods of reinforcing fastening units

The spacing of the lid fastening bolts shown in Fig. 68a is wrong as the bolts are arranged in bosses positioned in areas weakly connected with the part body. Somewhat better is the design in Fig. 68b where the lid has a stiffening edge improving the force distribution over the tightening area. In the correctly designed version (Fig. 68c) the bolts are spaced at the rigidity nodes at the corners. The rigidity

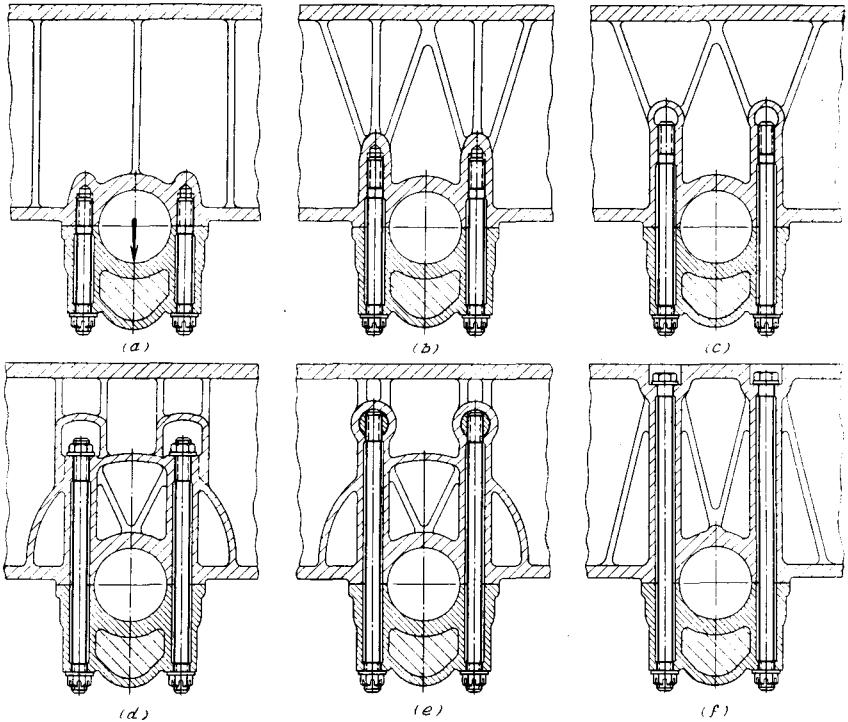


Fig. 70. Fastening a bearing cap to crankcase

of the lid as a whole is further enhanced by diagonal stiffening ribs, tying up the fastening points with the part body.

Figure 68d shows badly positioned bolts in an intricately shaped flange. The correctly designed version is pictured in Fig. 68e where the bolts are positioned at the rigidity nodal points within the part's external contour, which enhances clamping rigidity and improves the outer appearance.

The bosses in cast parts intended for receiving screwed ends of bolts and studs (Fig. 69) must be reinforced with ribs oriented preferably in line with the bolt axis (Fig. 69b-d). Load-carrying studs and bolts (Fig. 69e), particularly when the clamped parts are made from low-tensile alloys, should be screwed deeper into the parts

so that the maximum cross-sectional area of the wall is engaged in the work. Furthermore, longer studs under cyclic loads are stronger and ensure a more reliable fastening.

Figure 70 shows the subsequent stages of strengthening a crankcase and bearing cap assembly loaded in tension. The weakest design is that with the short studs (Fig. 70a). Here is a further defect, namely, the crankcase strengthening ribs are offset relative to the stud axes and do not share the load. In improved versions (Fig. 70b, c) the studs are positioned deep into the case body and the bosses reinforced with ribs. In the design illustrated in Fig. 70d the stud ends are tightened with nuts, relieving the case thread from load; the crankcase cross-section, which works in tension, is reinforced with an arch-shaped strengthening collar.

Studs can be relieved from bending (in one plane) by installing their screwed ends in cylindrical swivelling inserts (Fig. 70e).

The most advisable design (Fig. 70f) has the stud ends outside. The tensioning of the material inherent in the previously illustrated versions is practically eliminated and the load is taken up by the entire crankcase cross-section.

# Flanged Connections

When designing flanged connections it is necessary to ensure strength and rigidity with the minimum weight, as well as the rigidity of the sections connecting the flanges to the walls of the part.

Illustrated in Fig. 71 are typical flange designs for turned steel cylindrical parts (a sleeve held to a housing), approximately in the order of increasing rigidity.

The design in Fig. 71*a* is unsatisfactory: the flange connection to the walls is too thin and inadequately rigid. The principal flange strengthening methods are: introducing fillets (Fig. 71*b, c*) and tapers (Fig. 71*d-f*) in the areas where the flanges are connected to the walls. When large fillets and tapers are used, nut bearing surfaces are machine faced (Fig. 71*c, e, f*) so that the fastening studs may be brought closer to the walls.

The weight of flanges is reduced by holes machined between the fastening studs (Fig. 72*a*), by removing superfluous material off the periphery (Fig. 72*b, c*) and surface (Fig. 72*d, e*), and by face recesses (Fig. 72*f, g*) and radial recesses (Fig. 72*h*).

Typical designs of cast flanges are pictured in Fig. 73. The rigidity of flanges is improved by ribbing (Fig. 73*b*), by making local bosses in the fastening hole areas (Fig. 73*c*), by making the flanges higher (Fig. 73*d-f*). To eliminate excessive solidness high flanges are undercut. Flanges with through undercuts (Fig. 73*d*) have the disadvantage that the flange is subjected to bending when tightening fastening studs. This shortcoming is eliminated in the design having bosses around the fastening holes (Fig. 73*e, f*).

Flanges can be reinforced with a continuous peripheral rib (Fig. 73*g*) linked by transverse ribs to the walls of the part. Occasionally a flange is made in the form of two flanges interconnected by bosses of the fastening holes (Fig. 73*h*).

Rigidity is significantly enhanced by locating fastening studs in recesses, which have semi-circular cross-sections (Fig. 73*i-k*). Still further improvement can be attained by increasing the height of fastening stud bosses (Fig. 73*l, m*).

In the designs depicted in Fig. 73*n-p* the stud-receiving bosses are made in the form of columns; the nut-bearing surfaces are slightly

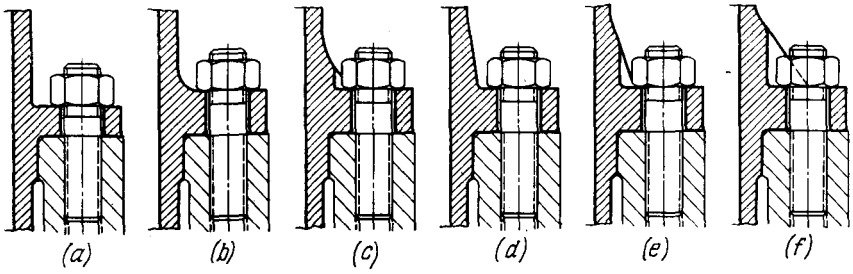


Fig. 71. Flanges on lathe-turned cylindrical parts

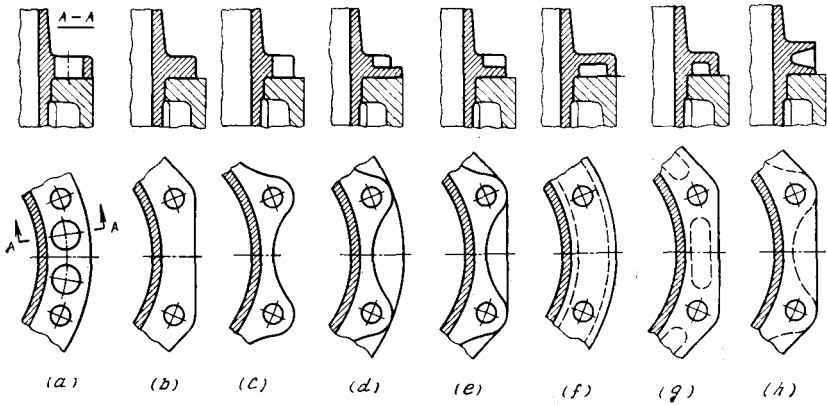


Fig. 72. Methods of reducing the weight of flanges

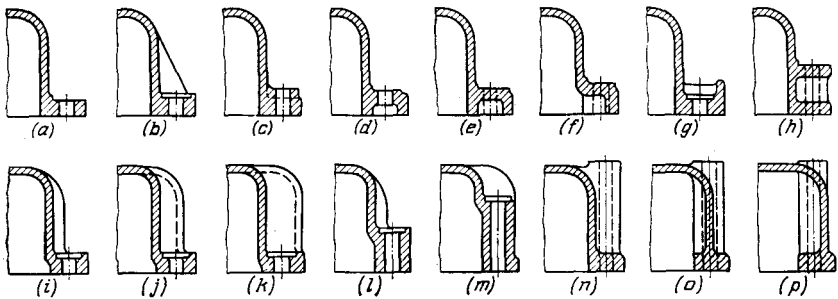


Fig. 73. Flanges on cast parts

raised above the top horizontal wall of the part. This enables column end faces to be through-machined and facilitates nuts tightening. The highest strength and rigidity are possessed by the design pictured in Fig. 73*p* in which the vertical wall of the part is matched with the column extreme points.

Figure 74 shows flange designs of conical and spherical castings. With small (in respect to flange diameter) cone sizes the flange is connected to the part walls by means of a tulip-shaped mouth

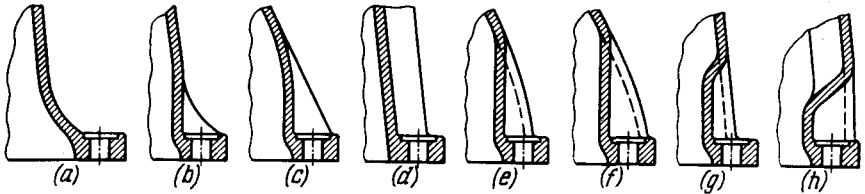


Fig. 74. Flanges on conical and spherical parts

(Fig. 74*a*), thus ensuring a streamlined transition of the force flow from the part walls to the flange. In cones of large diameter sizes the joint between the flange and the part walls is reinforced with ribs (Fig. 74*b-d*) or by positioning fastening holes in recesses (Fig. 74*e, f*).

With small slope angles the recess walls are extended excessively. In these cases they are given a semi-closed arched form (Fig. 74*g*).

To obtain the greatest rigidity and strength the walls are positioned at the flange periphery and the recesses ceiling linked with the walls by internal ribs (Fig. 74*h*).

The sizes of the vaulted recesses in height and cross-section must permit easy assembly of fastening parts. With insufficient height (i.e., when the

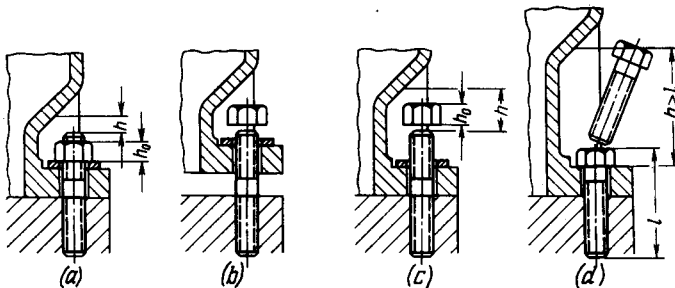


Fig. 75. Mounting fasteners in recesses

clearance  $h$  between the recess ceiling and stud end face is less than nut height  $h_0$ , Fig. 75*a*), the unit can be assembled only by raising the part (Fig. 75*b*) and placing all the nuts on the studs ends, a procedure seriously hampering the assembly. The correct version ( $h > h_0$ ) is pictured in Fig. 75*c*. When using bolts (Fig. 75*d*) the recess height must be greater than the bolt length.



To reduce the weight of low flat flanges the latter are often shaped (in plan), making them narrower in width at the areas between fastening bosses (Fig. 76*a-c, g-i*). In the extreme limit the flange actually vanishes so that only bosses remain which are cast directly onto the part walls (Fig. 76*d, j*). These methods must be used very carefully

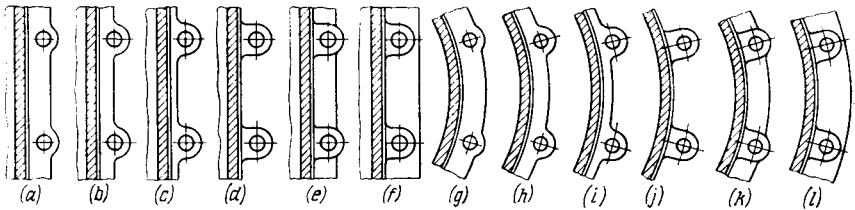


Fig. 76. Reducing the weight of cast flanges

since the flange rigidity and strength is lowered and the connection between the bosses and part walls weakened. When reducing the flange width to trespass beyond the fastening holes centre line is not recommended (Fig. 76*b, h*). It is useful to strengthen the connection between bosses and part walls with local ribs. More preferable are solid flanges (Fig. 76*f, l*) ensuring higher rigidity and better fastening stability.

### 5.1. Alignment of Flanges

Cylindrical flanges are usually aligned by a shoulder and a recess which are machined on the flanges and fit to one another (Fig. 77*a, b*). In the joints fastened with screwed-in bolts or studs the above-said

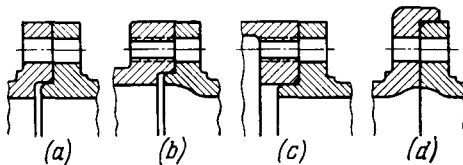


Fig. 77. Centring of cylindrical flanges

recess is substituted by the minimum internal flange diameter of one of the flanges (Fig. 77*c*). Alignment can also be accomplished on an external flange rim (Fig. 77*d*).

The aligning shoulder must be at least 3-4 mm distant from the extreme points of fastening holes (Fig. 78*a*), otherwise thin rags (*m*) or sharp-pointed burrs (*n*) will form which easily break in service and impair the shape of sealing gaskets.

In exceptional cases, in order to obtain smaller sizes, the aligning step can be provided at the area where fastening holes are located (Fig. 78*b-d*). This method is practicable only for bolted connections; cutting threads in stepped holes and screwing-in fastening elements into such holes offer formidable difficulties. Stepped holes are machined on assembly which complicates manufacturing. The designer should not position the centre-aligning step behind the axial

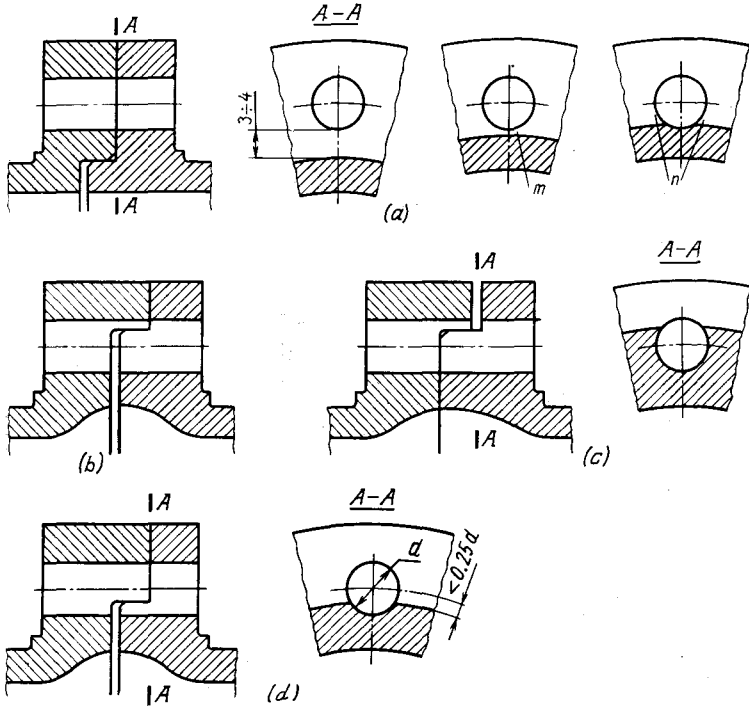


Fig. 78. Centring of flanges

line of fastening holes (Fig. 78*b, c*) as this would inevitably lead to the formation of sharp rags and burrs. Furthermore, such connections bend as the fastening bolts are being tightened. As obvious from Fig. 78*c* a gap formed in the joint accumulates dirt. An acceptable interval at which the centre-aligning step may be positioned is  $0.25$  hole diameter from the holes axial line (Fig. 78*d*).

To attain close contact between the joint surfaces it is necessary to preclude the corners of aligning surfaces from touching each other. This can be achieved by providing a chamfer that clears the fillet radius where the aligning shoulder meets the flange (Fig. 79*a*), or it can also be accomplished by radial, face or diagonal undercuts (Fig. 79*b-d*).

The height  $H$  (see Fig. 79*a*) of centre-aligning steps can be taken for conventional joints at  $0.5 \sqrt{D}$  ( $D$  — centring diameter).

A usual mistake made when designing flanged connections is that the aligning recess weakens the flange (Fig. 80a, region 1).

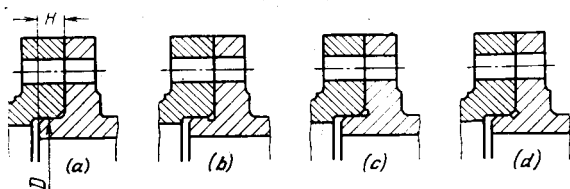


Fig. 79. Centring shoulder designs

The defect can be cured by making the flange thicker (Fig. 80b) or (if sizes and casting technology permit) by reducing the diameter of the centring surface (Fig. 80c).

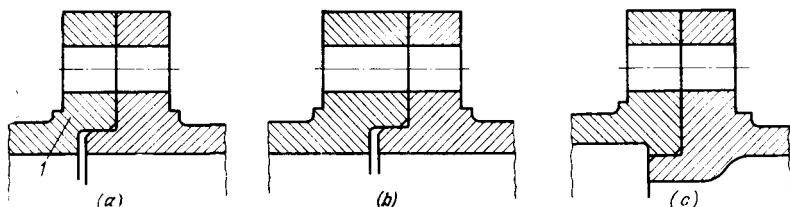


Fig. 80. Strengthening of flanges

Flanges other than round are made flat, and positioned by fitted pins. Non-critical detachable parts (covers, casings, etc.) are held in place by fastening elements alone.

## 5.2. Machining the End Faces of Fastening Holes

When designing flanged connections the designer must anticipate and specify in the drawing the methods by which the bearing surfaces under nuts and fastening bolt heads will be machined.

Cylindrical flanges may most simply be lathe-turned (Fig. 81a). However, with cast components the lathe-turning adversely affects the strength as it removes the hard surface crust and undercuts the flange in the black surface transition region. It is also inadvisable to lathe-turn flanges with jutting bosses (Fig. 81b, c) as the tool receives multiple repeated impacts from the bosses and quickly becomes blunt making it difficult to obtain high standards of accuracy and surface finish.

It is more reasonable to machine bosses by milling cutters (Fig. 81d) or core drills, centre-guided by previously made pilot holes (Fig. 81e). The most productive process is machining with a combination tool that is a core drill combined with a twist drill (Fig. 81f). In view of the inevitable dimensional inaccuracies encountered in

moulding practice, the core drill diameter  $D$  is made larger than the nominal boss diameter  $D_0$  (on average  $D = 1.2D_0$ ). This must be allowed for when specifying joint dimensions.

When spot facing sunk bearing surfaces (Fig. 81g) the flange contour should be 3-4 mm distant from the extreme points of the machin-

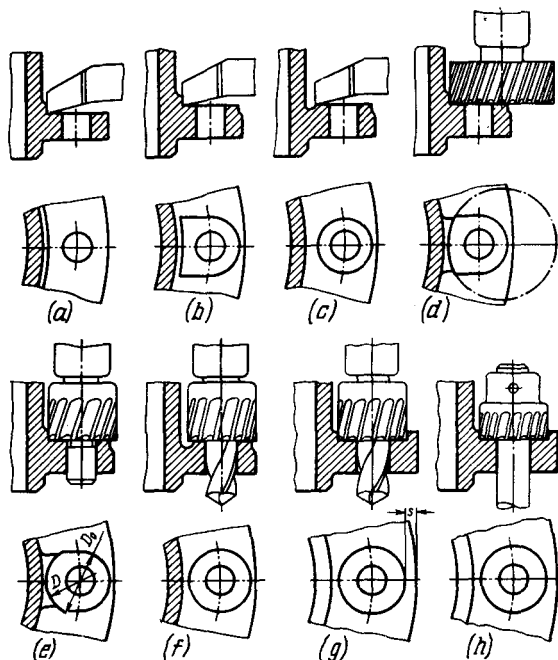


Fig. 81. Machining methods for nut and bolt head bearing surfaces

ed surfaces. Otherwise the possibility of forming the easily broken rags and burrs occurs.

If a core drill cannot be used directly on the work surface then inversed core drilling is practised, where the core drill is mounted upon an arbor passed through a previously drilled hole (Fig. 81h). Machining efficiency is sharply reduced with this method, so that the latter is applicable in the event of holes not less than 10-12 mm in diameter.

The end faces of holes in half-closed recesses are machined by milling (Fig. 82a) or inversed core drilling (Fig. 82b). The height and radius  $R$  of recesses, taken in cross-section, must be consistent with the dimensions of cutting tools.

The modern highly accurate casting techniques (shell mould casting, chill casting, pressure die casting, investment casting, etc.) obviate, in certain cases, machining of support surfaces. However, for critical, heavy-loaded structures

machining is obligatory with the assurance that the bearing surfaces are strictly perpendicular to the hole axis, thus avoiding fastening bolt distortion and flexure.

Table 6 gives the moulded flange design relationships for the conventional range of bolt diameters ( $d = 8-20$  mm).

The machining allowance  $t$  depends on the size and grade of accuracy of the casting. On drawings which depict cast components

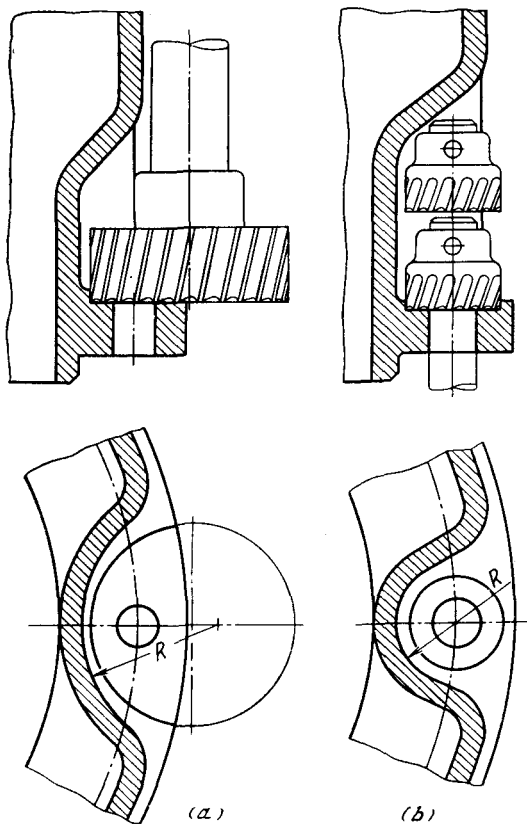


Fig. 82. Machining bearing surfaces in recesses

the value of  $t$  is generally omitted, which, nevertheless, in no way implies that the designer may neglect this value when calculating the dimensions of parts.

The minimum distance  $s$  between the machined and the nearest black surfaces is established proceeding from the accuracy standards of casting, dimensions of parts and distances of surfaces from the

Table 6

Relationships of Cast Flange Elements

	Flange elements	Material	
		grey CI, light alloys bronze	steel, high-tensile CI
	Minimum flange height $h$	$1.5d$	$1.2d$
	Minimum dimensions of machined surfaces ( $a, R, D/2$ )	$1.2d$	$1.2d$
	Minimum bolt axis distance $b$ from machined wall	$1.3d$	$1.2d$
	Minimum bolt axis distance $A$ from flange end face	$1.7d$	$1.5d$

black and machined datum points. With respect to the small- and medium-sized components (200-500 mm) obtained by conventional sand casting  $s = 3-5$  mm; these values can be reduced by 30-50% by applying higher-accuracy casting methods.

### 5.3. Diameter and Spacing of Bolts

The proper choice of the diameter and spacing of bolts depends on many factors, the most important of which are the operational conditions, material of parts and rigidity of structures. The requirements are quite different for connections subjected to small static loads and connections undergoing high cyclic and dynamic loads, working under pressure and where complete sealing is necessary.

For the simplest cases (flange-coupled connections, loaded with moderate forces, free of internal pressure and elevated temperatures), the following approximations can be recommended.

The diameter of bolts fastening cylindrical flanges

$$d = 6 + (0.015 \text{ to } 0.018) D$$

where  $D$  is the mean flange diameter.

The thickness of the flanges:

for components made of grey cast iron and light alloys

$$h = 6 + (0.022 \text{ to } 0.025) D$$

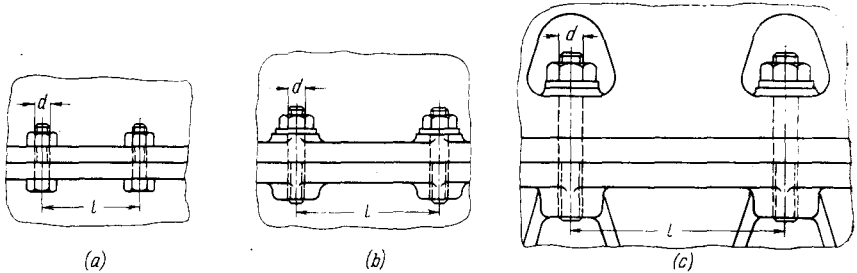


Fig. 83. Bolt spacing for flanges of different rigidity

for components made of steel or high-strength cast iron

$$h = 4 + (0.022 \text{ to } 0.025) D$$

The pitch of bolts

$$l = ad$$

For small-sized non-rigid flanges (Fig. 83a)  $a = 6-8$ ; for moderately rigid flanges (Fig. 83b)  $a = 8-10$ ; for flanges of higher rigidity fastened with large bolts (Fig. 83c)  $a = 10-12$ .

The parameters of joints subjected to cyclic loads and operating at elevated temperatures are obtained by calculation (see Chapter 1).

#### 5.4. Three-Flange Joints

When designing housing-type components it is often necessary to connect three flanges in one unit. Let us take, as an example, a unit comprising an intermediate partition (membrane) installed between the joint faces of two housings (Fig. 84).

The simplest method is tightening the membrane between the flanges of the housings (Fig. 84a-e), the alignment being accomplished from internal or external shoulders. The installation accuracy is the highest in Fig. 84b, c and e (the alignment is effected from one cylindrical surface).

The design presented in Fig. 84e is less strong than the others. To

avoid interference the flange is usually assembled with an axial clearance of 0.1-0.2 mm, owing to which proper membrane tightening cannot be assured.

Should it be necessary to preserve integrity of mechanisms during dismantling, then it is better to secure the membrane on one of the housings (Fig. 84*f-i*). After the housings are separated from each

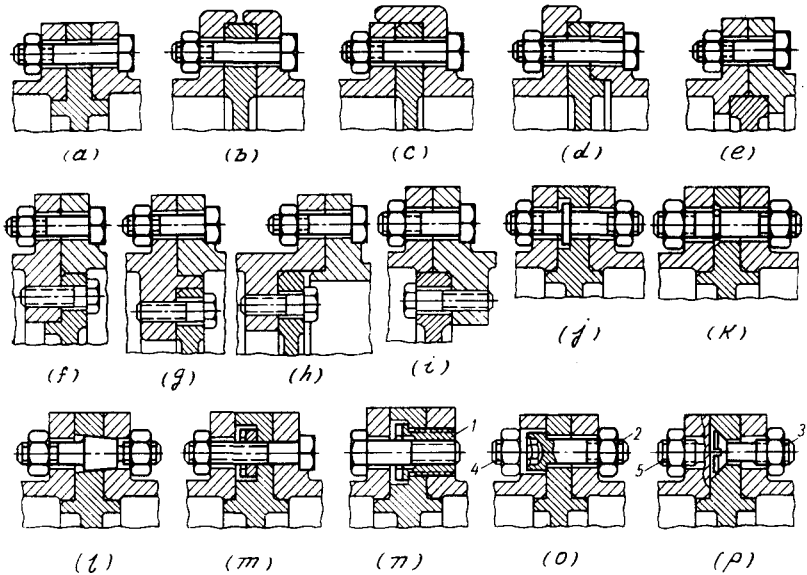


Fig. 84. Three-flange connections

other the membrane remains secured on one of the housings, carrying all the members mounted on it. Designs differ in alignment methods. In terms of accuracy the most preferable versions are those shown in Fig. 84*h, i*.

Independent mounting of the membrane can also be implemented by holding (pinching) the flange with various forms of pinch bolts (Fig. 84*j-p*), which may be shouldered (Fig. 84*j*), with stop rings (Fig. 84*k*), tapers (Fig. 84*l*) and nuts (Fig. 84*m*).

Occasionally the membrane is secured with the aid of tapped bushes 1 (Fig. 84*n*), into which the fastening bolts of the other housing are screwed, or the membrane can be held to the housing with independent bolts 2, 3 (Fig. 84*o, p*) spaced between bolts 4, 5, which hold the housings together. The heads of type 2 bolts are lodged in the housing flange apertures, while those of type 3 are sunk in the membrane.



### 5.5. Conical Flange Joints

For butt-jointing pipelines, cylindrical sections and loaded connections use is made of quick-acting split clamps which tighten upon outer conical flange surfaces (Fig. 85). Parts may be connected at any angle in the joint plane. When angles must be fixed or when the connection transmits torque fitted pins are used.

Joined parts are aligned with the aid of cylindrical shoulders (Fig. 85a). Sometimes the joint is made plain (Fig. 85b) relying

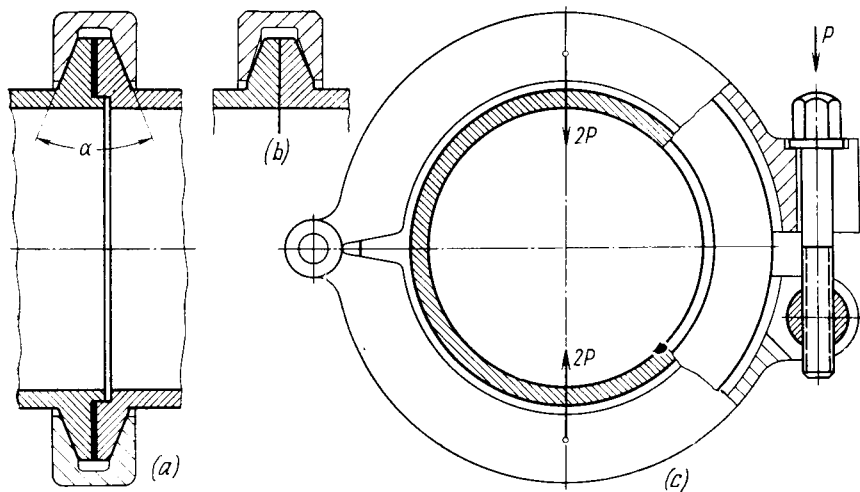


Fig. 85. Conical flange connection

upon the alignment given by the clamp's conical surfaces. The latter method is preferred when the parts to be joined cannot be brought together axially and must be manoeuvred in the joint plane.

Conical flange joints ensure a good strong joint with a relatively moderate tightening force being applied to the joint. Assuming the simplest transfer of the tightening force  $P$  to two points (as in Fig. 85c, a rigid clamp), then the axial tightening force will be

$$P_{ax} = \frac{2P}{\tan \alpha/2}$$

where  $\alpha$  is the cone angle. For the usual  $\alpha$  values varying from 20 to 30°,  $P_{ax} = (8 \text{ to } 10) P$ .

The cone angle  $\alpha'$  on the clamp collars is made 1-2° less than that of the clamping flanges (Fig. 86a) so that the tightening force is applied closer to the collar base with the aim of increasing joint rigidity and sealing reliability. Similar results are obtained if the clamp walls are made flat (Fig. 86b).

Pictured in Fig. 86c-e are conical flange connections with sealing gaskets.

Figure 86f-h illustrates various designs of thin-walled tube conical flange connections.

In certain cases inverted conical flange connections are employed. The inverted conical flanges of the connected parts have through slots (Fig. 87a). During assembly the projecting lug of one flange enters the slot in the other, thereby forming between the flanges a conical cavity into which is placed the central tightening collar (Fig. 87b).

The binding clamp of a taper flange joint must open fully so that it may be installed on the flanges from the side and axially and

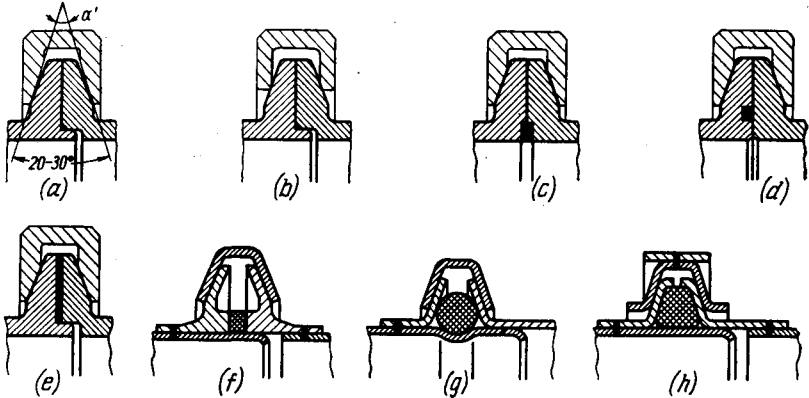


Fig. 86. Conical flange connections

assure uniform circumferential flange tightening, i.e., be compliant radially. The clamp must be quick-acting.

The clamp comprising two halves fastened together by bolts (Fig. 88a) is not quick-acting. A more practicable design has its

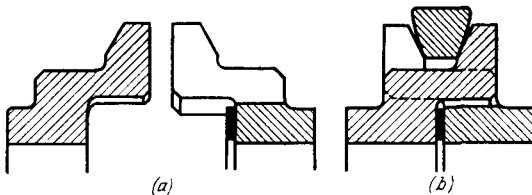


Fig. 87. Inverted conical flange connection

halves linked with a pin and tightened by one bolt (Fig. 88b, c).

In the quick-action lock with a swing bolt (Fig. 88d) radial slits are provided in the hoop walls to enhance the compliance of the system. A circlip-type lock is applied to fasten light joints (Fig. 88e).

In a load-carrying structure furnished with a quick-action lock (Fig. 88f) the coupling bolt extends through a cylindrical nut 1

mounted in a half-open cup; the bolt end terminates in articulated joint 2. As the bolt is being unscrewed, the nut leaves the cup and the bolt can be freely swung away by rotating it about the joint axis.

In the design pictured in Fig. 88g the two halves are tightened together by means of a swing lever with pressure screw 3. In the

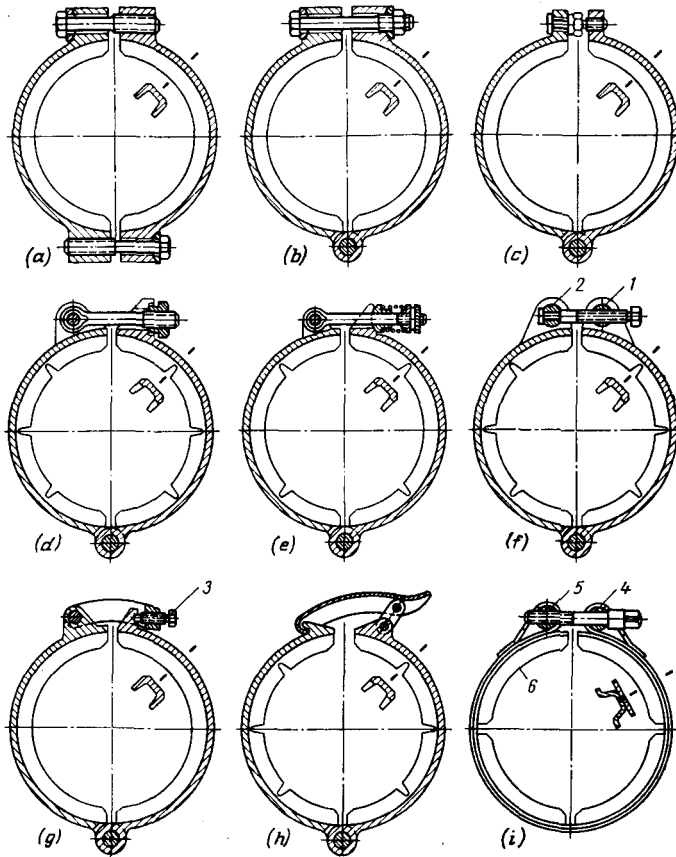


Fig. 88. Collar clamps

version presented in Fig. 88h use is made of a swing-type three-link mechanism ("frog"). In the latter case an elastic packing must be inserted between the flanges, which would compensate for the rigidity inherent in such a mechanism in the locked position.

Figure 88i illustrates an elastic clamp made of a steel ribbon with welded-on channel-sectioned segments 6. The coupling bolt extends through pin 4 of the articulated joint and is screwed into the cylindrical nut 5.

---

# General Principles which Should Be Followed when Designing Units and Parts

## 6.1. Unification of Design Elements

When designing one should repeatedly use elements for all parts of the design which in the assembly process reveal average rated parameters and allow the parts' list to be reduced to its minimum.

Subject to unification in the first instance are fitted connections (their nominal sizes, type of fits and classes of accuracy), threads (diameter, pitch and classes of accuracy), splined and keyed connections, fasteners, specifications, etc. It is also advisable to reduce the number of material grades, unify surface finish classes, finishing operations and electroplating techniques, welding methods, forms of welded seams, etc.

Figure 89*a-c* illustrates the arrangement of a typical engineering unit (a shaft carrying some elements and mounted in a bronze bush). In the design presented in Fig. 89*a* the choice of fitting diameters is badly thought over. The basic fitting size (diameter of the shaft bearing journal), taken from standard specifications ( $\phi$  50), is correctly chosen, but from this point mistakes occur. Wishing to economize on the consumption of scarce bronze, the designer used a bush wall thickness of 3.5 mm, thus obtaining a non-standard size for the external diameter of the bush ( $\phi$  57) and, moreover, while striving to enhance the shaft strength at the fitted connection, he reduced the shaft diameter relative to the journal diameter by 3.5 mm on each side, thus obtaining again a non-standard diameter ( $\phi$  43), which, in turn, meant choosing an M42 screw thread size for the clamping nut.

In the arrangement in Fig. 89*b*, which is based on standard dimensions, the external diameter of the bush is 60 mm and the diameter of the fitted connections 40 mm. Hence, the clamping nut thread size is M37. However, standardization of the dimensions in this case has lowered somewhat the shaft strength and also increased the weight of the bronze bush. The most rational version depicted in Fig. 89*c* has its shaft journal diameter equal to 55 mm, bush O.D. 60 mm and the fitted connection diameter 45 mm.

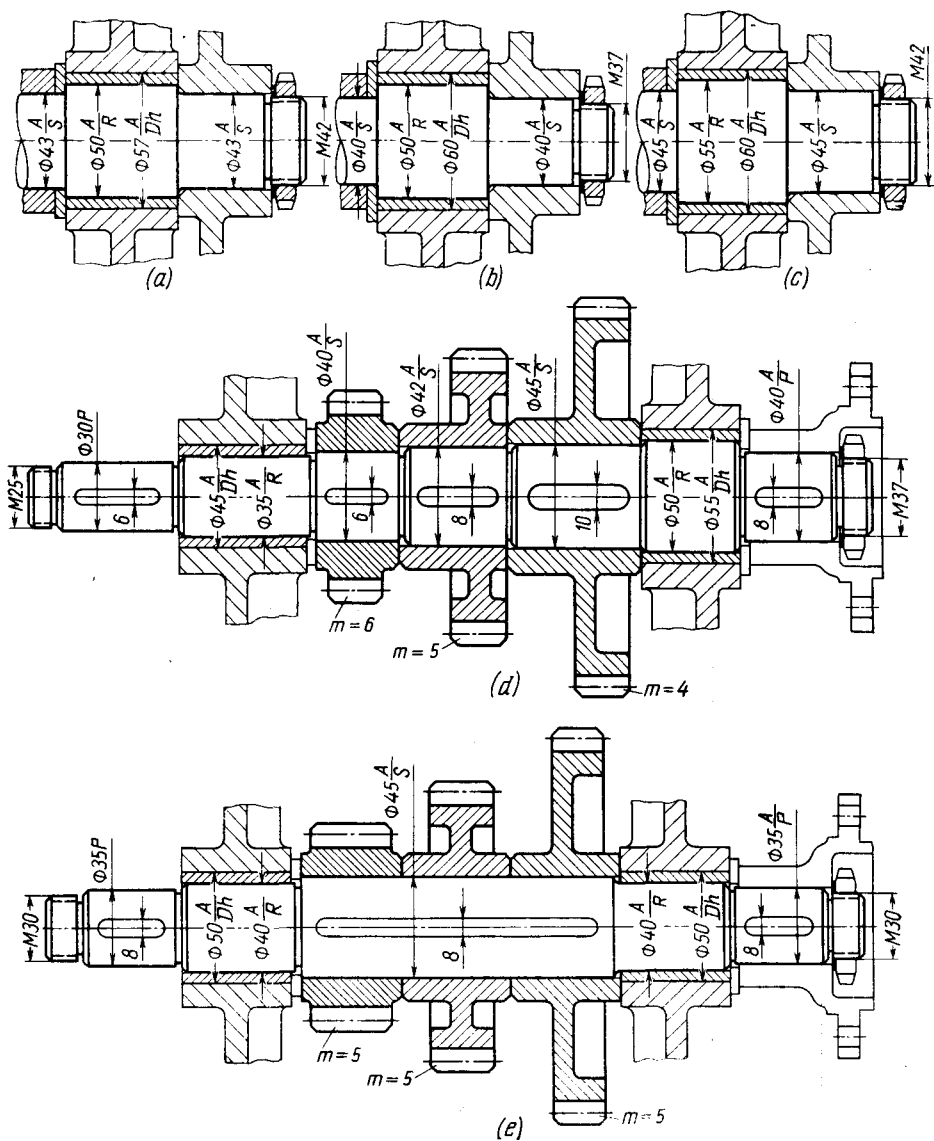


Fig. 89. Unification of design elements

Table 7

Comparative Table of the Back Gearing Dimensions

Design element	Design parameter according to Fig. 89d	Qty	Design parameter according to Fig. 89e	Qty	Design element	Design parameter according to Fig. 89d	Qty	Design parameter according to Fig. 89e	Qty		
Diameters and fits	30P	1			Threads	M25	1	M30	2		
	35A/R	1				M37	1				
	40A/S	1	35P	2	Keys <i>b</i> , mm	6	1	8	1		
	40A/P	1				40A/R	2			8	3
	42A/S	1				45A/S	2			10	1
	45A/S	1	50A/Dh	2	Tooth module, <i>m</i>	4	1	5	1		
	45A/Dh	1				5	1				
	50A/R	1				6	1				
	55A/Dh	1				Total	18		7		

Naturally, other solutions are possible, but under any circumstances it is important for the diameters to be standard. Another example is given in Fig. 89*d, e* (back gear).

The design in Fig. 89*d* has significant irregularities in the sizes of fitting diameters, threads, keys and tooth modules. In the rational version shown in Fig. 89*e* the number of fitting dimensions has been reduced and the keys and tooth modules unified. The necessary tooth strength for the small gears is obtained by the increased face width. The unification results are presented in Table 7. All-in-all the number of machine elements is cut down from 18 to 7 items.

To illustrate the unification of wrench sizes, let us consider a unit for adjusting a reduction valve (Fig. 90). In the design shown in Fig. 90*a* three wrench sizes (1-3) are used, whereas the unified design in Fig. 90*b* uses only a single wrench size (4).

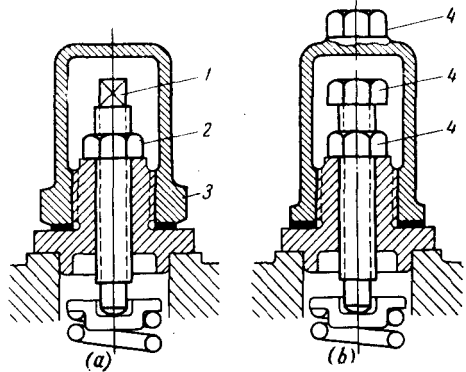


Fig. 90. Unification of wrench sizes

## 6.2. Unification of Parts

Individually designed parts must be unified as much as possible. This is particularly important for labour-consuming parts and those in general use (gears, clutches, chain links, etc.).

Figure 91*a* shows a conveyer chain composed of links of two types. The rational design (Fig. 91*b*) has unified links. The tightening clamp illustrated in Fig. 91*c* consists of two labour-consuming components. Connection by an intermediate link (Fig. 91*d*) enables the clamp to be made of two similar halves. Figure 91*e, f* shows the unification of pressed steel components in the unit of a built-up pulley, while Fig. 91*g, h* shows unification embodied in the design of a cylindrical pressed reservoir.

Often unification is only attained as a result of purposeful, original, constructional working out of the design.

In an angle drive presented in Fig. 92*a* the required gear ratio is ensured with the aid of two different shafts having different bevel gears. To position the lower gears within preset spaces, one of the gears is displaced relative to the other and the tooth face width of the driving gear 1 made longer. As a result, the design contains five gears (numbered 1 to 5) and two shafts (numbered 6 and 7).

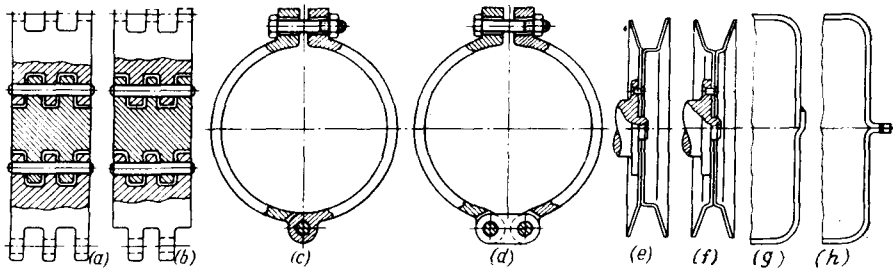


Fig. 91. Unification of parts

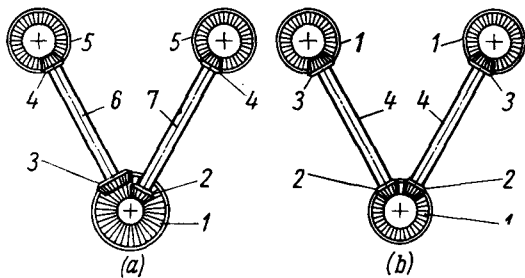


Fig. 92. Unification of parts in angle drive unit

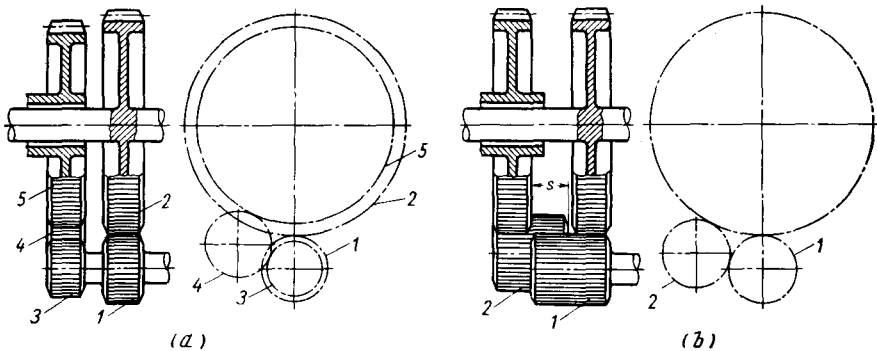


Fig. 93. Unification of parts in coaxial reduction gear unit



In the alternative, Fig. 92*b*, the diameter of lower gears 2 is decreased so that they can be driven by the one gear 1. To keep the gear ratio the same the diameter of upper gears 3 is increased. As a result of the conversion the required number of gears is reduced to three (1 to 3) and of the shafts, to one (4).

Now, let us examine a reduction gear unit with two concentric shafts running at the same speed in opposite directions (Fig. 93*a*). The unit driving shaft carries two gears, one of which (1) engages with gear 2 of the reduction unit, while the other (3) meshes via idler 4 with gear 5. The total number of gear units is four (1-3, 2, 4, 5). The large number of components and complexity of the design are caused by the necessity to avoid fouling between gears 3 and 5, which means reducing the diameter of gear 3 and, accordingly, that of gear 5 (in order to retain the same gear ratio).

In the unique solution (Fig. 93*b*) the design is simplified as follows: gear 1 of the drive shaft meshes on one side with the reduction unit right-hand pinion and on the other side, with gear 2 of the drive. The number of gears is thus cut down to two and the pinions and gear wheels of the unit are identical pairs. To realize this design it is sufficient to separate the gear wheels by a distance  $s$  sufficient to engage the pinions.

### 6.3. Principle of Unitization

It is advisable to design units as self-contained assemblies, which are individually assembled, adjusted, run-in, tested and finally installed as completely ready-to-operate units upon a machine. Such successive unitization allows parallel and independent assembly of machine units, facilitates mounting, prompts prototype testing and eases the employment on new machines of finished units which were checked during manufacture. Furthermore, unitization simplifies repair as worn out units can be directly replaced by new ones. Sometimes unitization may complicate the design, but in the long run, it always gives large savings in the total machine manufacturing costs, reliability and convenience in use.

Some examples of the unitization of small assemblies are presented in Fig. 94. In the design illustrated in Fig. 94*a* the reduction valve is mounted directly in the housing body. When the valve is assembled in a separate bush the design becomes unitized (Fig. 94*b*).

The end face seal depicted in Fig. 94*c* is unsatisfactory because during dismantling the sealing disk 1 is forced by the spring to leave the ways and slots which prevent its rotation, and the unit disintegrates. Equally unsuitable is the seal assembly. The introduction of locking ring 2 unitizes the construction (Fig. 94*d*).

Another example of unitization is offered in Fig. 94*e-g* where the unit of a distributing slide valve is shown progressively improved.

The construction given in Fig. 94*e* is grossly wrong: an accurate hole intended to receive the valve was made directly in the frame casting. At the spot where the valve is located (i.e., in the concentration of material) there may occur pits and voids which make valve sealing impossible. Moreover, as the hole wears out during use it can only be repaired by introducing bushes.

The first step to an improved design is to mount the valve in an intermediate bush (Fig. 94*f*) made of a high-grade material with a

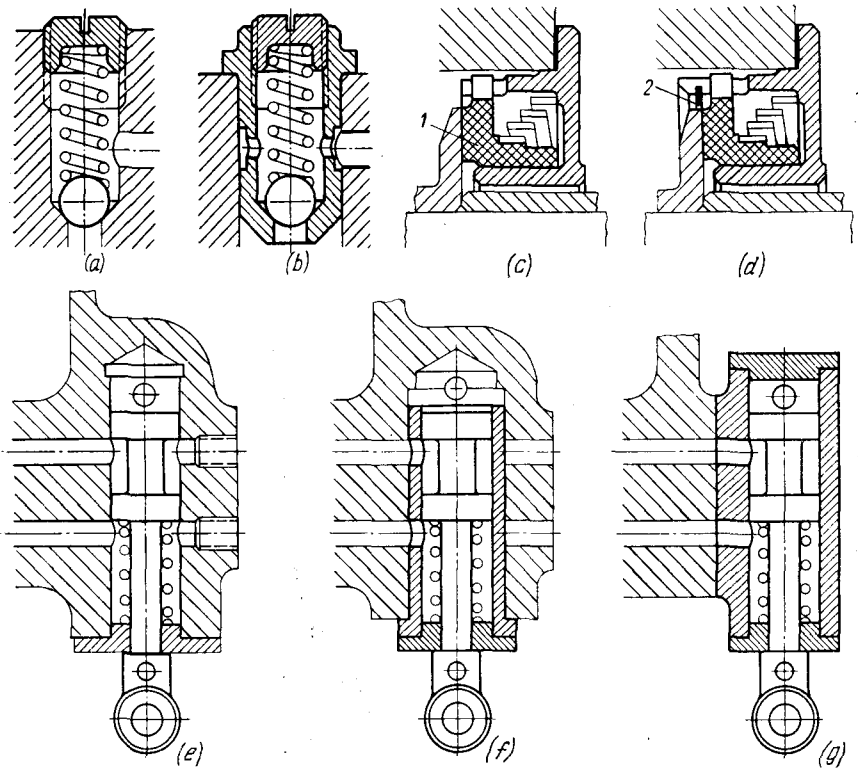


Fig. 94. Examples of unitization

good wear resistance. In the most rationally designed version (Fig. 94*g*) the component has been fully unitized. Here the unit is made separately; it is assembled, ground-in, verified for geometry and attached to the frame on a milled surface.

Shown in Fig. 95*a* is a worm reducer which is coupled directly with the machine driving shaft. The worm wheel shaft is mounted in supports installed in different housings. To maintain support alignment when machining is difficult. The assembly procedure is

very ambiguous as it is necessary to fit the worm wheel first onto the main shaft, install the reducer housing and then assemble the worm by screwing it into the worm wheel teeth. To verify the cor-

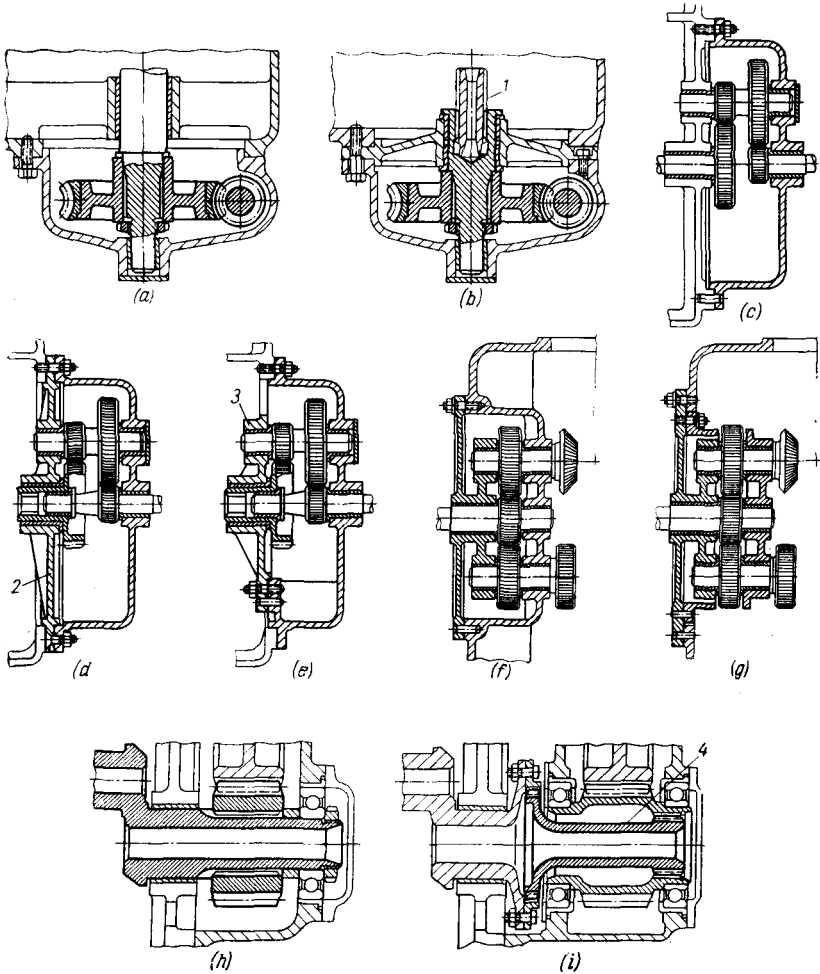


Fig. 95. Unitization of gear transmissions

rectness of engagement and align the worm wheel under these circumstances is very difficult.

In the unitized construction (Fig. 95*b*) the worm wheel shaft is mounted in two supports, one of which is accommodated inside the housing and the other in the housing cover. Both supports can be machined together, thus obtaining good alignment. The shaft end

is coupled with the driving shaft by the splined adapter *1*. Hence, the reducer assembly is considerably simplified.

The gearing mounted in a frame (Fig. 95c), in addition to the drawbacks inherent in the non-unitized constructions, presents difficulty in introducing the idle gear shaft into the support housing. As soon as the housing is removed from frame, it loses both supports and falls to pieces. To verify the correctness of meshing and alignment of the shaft and supports is impossible.

In unitized constructions the gear supports are mounted in diaphragm *2* (Fig. 95d), or in bracket *3* (Fig. 95e) screwed by its feet to the gearing casing. With the latter design it is easy to inspect the mechanism during assembly.

Figure 95f, g shows the unitization of a gear drive mounted on a frame; Fig. 95h, i, a reduction unit driven from an engine crankshaft. In the unitized version (Fig. 95i) the reduction unit is mounted in a separate housing; the shaft torque is transmitted by means of adapter *4*.

#### 6.4. Elimination of Adjustments

Fitting and adjustment of units and parts when in position must be eliminated. Adjustments, particularly when accompanied by machining or fitting operations, lower assembly productivity and deprives the construction of interchangeability.

An example of fitting in situ is shown in Fig. 96a, b. The gear is placed in position on the shaft so that it meshes with its mating gear. This done, the position is fixed by a self-piercing screw (Fig. 96a) or by a taper pin (Fig. 96b), which requires drilling and reaming in situ. Chips inevitably fall into the unit. After the machining it is necessary to dismantle the unit, flush it and then reassemble. Marking during assembly with a subsequent transfer to machine tools further complicates assembly.

A better engineering method is to lock the gears in position by ring-shaped stop washers which are placed into grooves previously machined on the shaft (Fig. 96c).

If a bearing has been installed in a housing by the "in situ" technique (Fig. 96d), its originally correct position will be disturbed every time the bearing is dismantled, thus necessitating readjustment. Fixing the bearing by dowel pins (Fig. 96e) entails machining on assembly. The correct solution is displayed in Fig. 96f, where the bearing is aligned against the bore in the housing, this bore being machined to the required accuracy, which ensures correct functioning of the unit.

If a straight machine way is mounted on a bed as illustrated in Fig. 96g, then its position must be verified on assembly and holes drilled to suit fastening bolts. In this case the way will not be guaranteed against offset within the clearance values existing between

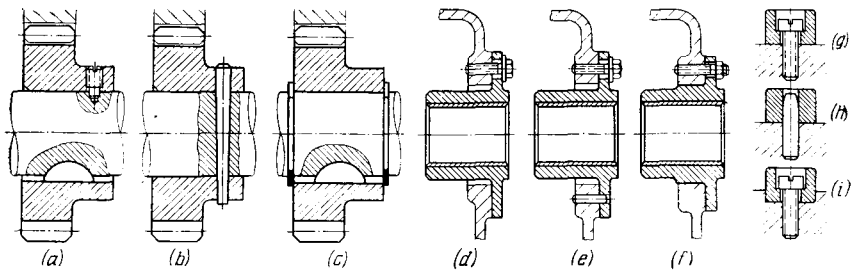


Fig. 96. Elimination of adjustments

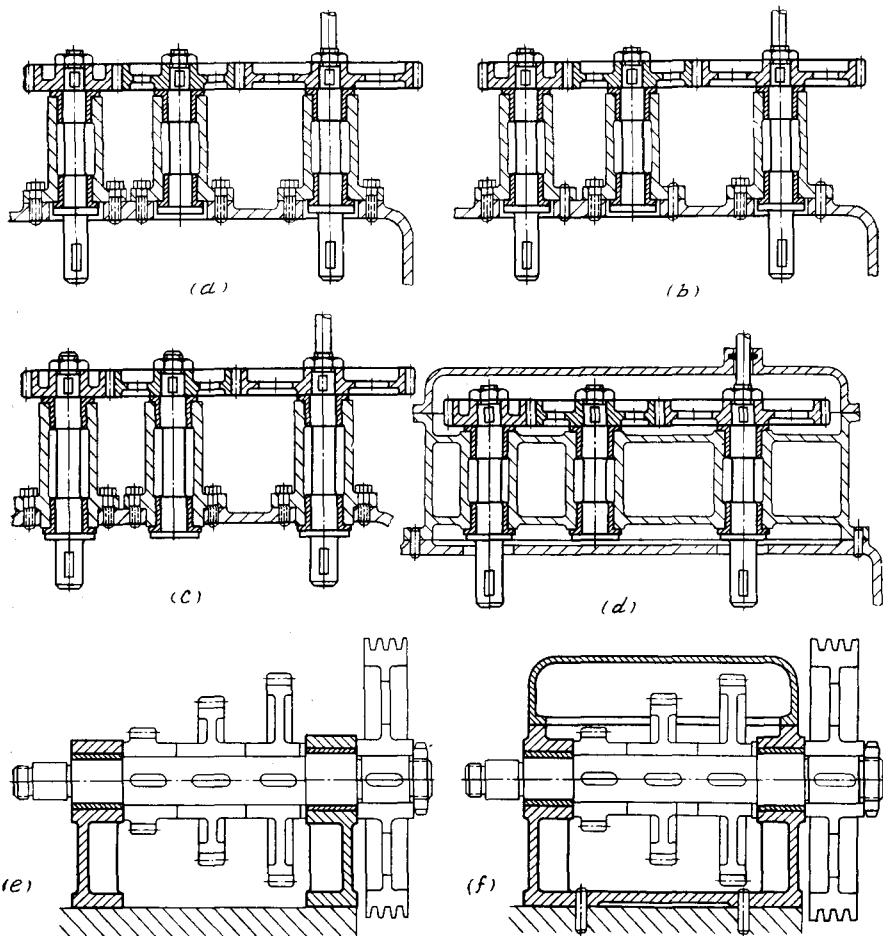


Fig. 97. Elimination of adjustments when assembling units

the bolts and their holes. Fixing by dowel pins (Fig. 96*h*) means drilling and reaming holes in the way and bed. In the rational design (Fig. 96*i*) the way is mounted in groove machined in the bed.

The gear drive illustrated in Fig. 97*a* is unsatisfactory. The gear supports are bolted to the housing. The fitter is compelled to adjust the support position so as to assure correct gear meshing. Dismantling will inevitably disturb the arrangement, thereby necessitating readjustment on assembly. The supports can be fixed in position by dowel pins (Fig. 97*b*), but this will involve additional job operations in assembly.

In the correct design (Fig. 97*c*) the gear studs have been aligned against holes whose spacing relative to each other has been maintained within close tolerances during machining of the housing. In the best version (Fig. 97*d*) all the gears are enclosed inside a common housing, which brings about full unitization and advantageous operating conditions.

Figure 97*e* gives a wrong, and Fig. 97*f*, a correctly designed version of a back gearing with a V-belt drive.

### 6.5. Rationalization of Power Schemes

The perfection of a structure, its weight, size and, to a significant degree, its capability of work are dependent on the rationality of its power scheme. A power scheme is rational if all acting forces are mutually equalized over as short a section as possible with the help of elements loaded mostly in tension, compression or torsion (but not flexure).

As an example let us examine a screw-type conveyer (Fig. 98*a*) driven from an electric motor via a worm-type reduction unit 1 and chain transmission 2. The conveyer housing, which is several metres long, is made of steel sheet and rests upon four tubular legs. The main error consists in the fact that the housing is loaded with the drive force (the direction of force is shown by an arrow), which bends and deforms the non-rigid housing, mounted on unsteady supports. Owing to a small internal clearance between the conveyer screw and housing the screw edges scrape the inner walls. The intensified friction increases the driving torque which, in turn, increases the bending force still more and, consequently, the friction and finally the screw jams in the housing.

The defect can partially be eliminated by changing screw rotation with a corresponding change in screw helix. The driving side of the chain drive is now the lower side of the chain drive and the torque moment acting upon the housing is substantially reduced. Alternatively, it is possible to move the reducer into the symmetrical plane of the entire assembly, redistribute the legs, strengthen the housing and mount it upon a stiff foundation. Nevertheless, all

these measures fail to eliminate the principal defect, namely, the presence of external forces in the system.

A radical solution is presented in Fig. 98*b*. Here the screw is driven from a flange-mounted electric motor via a reduction unit installed coaxially on the housing end face. The drive torque and reactance

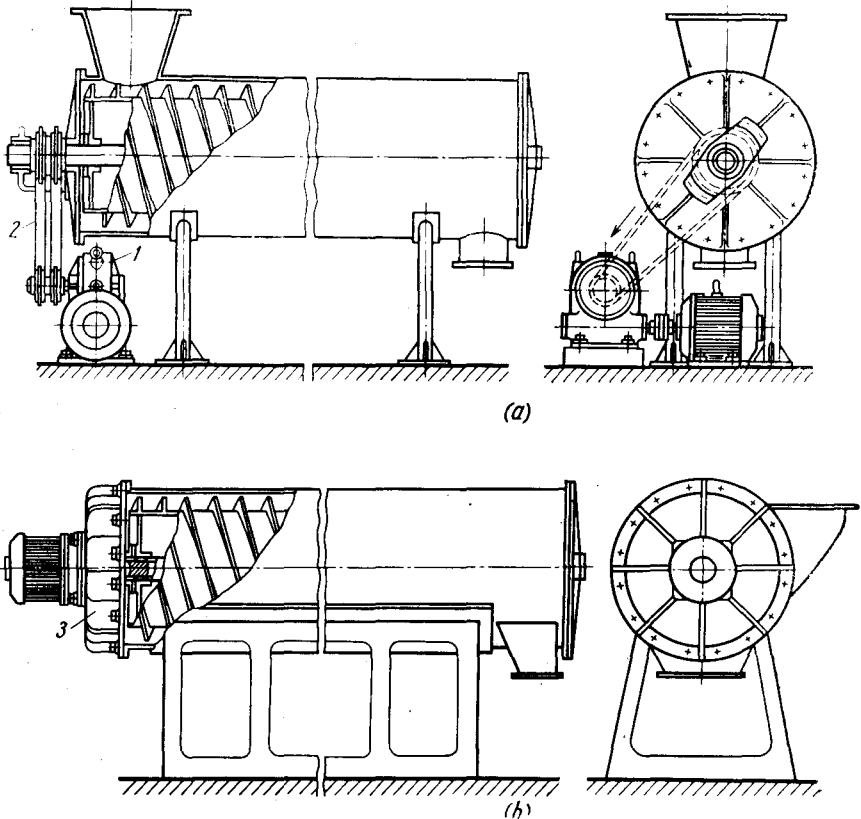


Fig. 98. Improvement of power scheme of screw-type conveyor

torque on the housing quench each other at the connection joint. The housing is absolutely free from the action of external forces and deformation is eliminated.

In the drive of a suspended conveyer (Fig. 99*a*) comprising a reduction unit 1, bevel gearing 2 and spur gears 3, which impart motion to the driving sprocket 4 of a chain drive, the load-carrying elements are irrationally arranged. Indeed, the support units of the drive, the fastening bolts and foundations are all loaded with drive forces and a large number of elements are in flexure. The drive units are

separated; they are installed on individual bases and are not fixed one relative to the other. Such a design only ensures satisfactory functioning after the mechanisms have been carefully aligned.

Furthermore, the cast iron gears are not protected from fouling and can only be periodically lubricated by packed grease. The

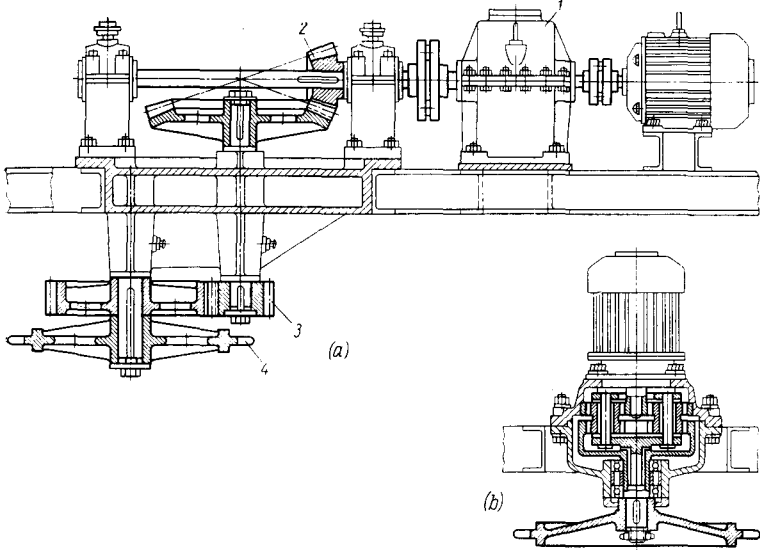


Fig. 99. Improvement of power scheme of suspension-type conveyer drive

supports of the horizontal and vertical shafts are also lubricated periodically.

The entire unit is excessively large, explained by the isolation of units and also by the employment of a low-strength material (cast iron) for manufacture of the most critical components (gears).

In fact, the design is typical of old design practice.

In the modern unitized enclosed construction with a rational power arrangement (Fig. 99b) the drive is from a flange-mounted electric motor, installed vertically, which obviates the necessity for the angular transmission. The required gear ratio is obtained in one coaxially mounted reduction unit. The employment of gears made of a high-grade and appropriately heat-treated steel in conjunction with the application of a centralized oiling system, sharply reduces overall sizes. The drive forces are absorbed in one casing. The casing and base are loaded only by the force of the final driving sprocket. These changes result in tremendous savings in the weight and size of the installation, simplicity of manufacture, convenience in mounting and attendance, reliability and a long service life.



## 6.6. Compensators

For multistation machine systems having mechanical drives the design of couplings which transmit torque is of extreme importance. Such a coupling must compensate for lengthwise displacements,

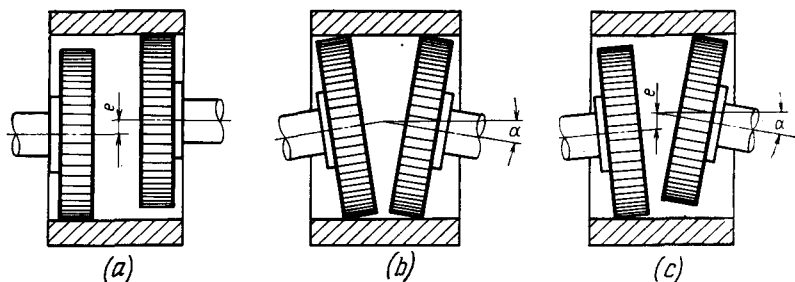


Fig. 100. Misalignments in coaxial connections

parallel misalignment  $e$  and conical misalignment  $\alpha$  of the units being connected (Fig. 100).

For this purpose involute splined connections are most commonly employed (Fig. 101). The advantages of involute teeth, are as follows:

due to the thickening of the tooth towards the root (particularly with positive correction) the tooth possesses increased strength and stress concentration at the root is not great;

involute teeth, both external and internal (with a sufficiently large rim diameter), can be machined to close tolerances on conventional gear cutting machines.

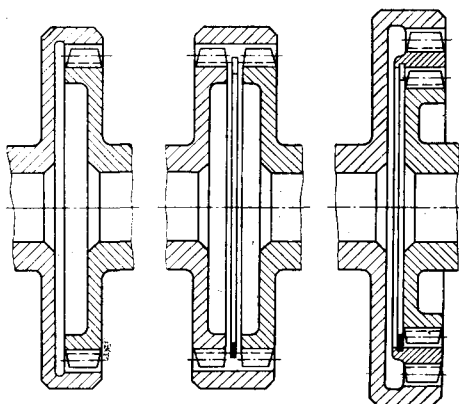


Fig. 101. Compensators with involute teeth

External involute teeth can be given high surface hardness by heat and chemical-heat treatments, followed by finish machining on conventional gear-grinders.

The operating conditions for teeth in compensating connections are much more harder than for the centring splined connections. The enhance their compensation ability such connections are made with an increased circular clearance  $s = (0.05 \text{ to } 0.07) m$ , where  $m$  is the tooth module. In the case of a misalignment the forces are con-

centrated at the tooth extreme edges lying in a plane perpendicular to the misalignment. As a result the linear contact over the tooth face changes to point contact, thus sharply increasing local bearing stresses. Since each tooth passes through the zone of loading twice per revolution, the load upon the teeth will be cyclic, regardless of torque behaviour.

The working capacity of the connection can materially be intensified by enhancing surface hardness of teeth. To eliminate work hardening and promote removal of heat, produced during tooth impacts and warpage, ample lubrication is obligatory. The most effective

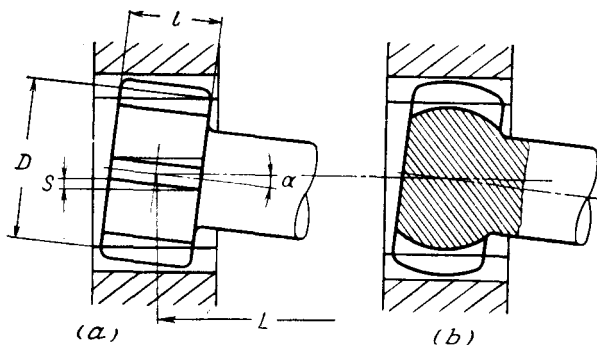


Fig. 102. Determination of maximum conical misalignment in a compensator

method of obtaining an efficient connection is to increase the gear rim diameter since this offers certain advantages in manufacture, namely, the internal teeth can be gear-cut in place of using expensive broaches.

The amount of misalignment admissible in a coupling is limited, first of all, by the tooth edge contact in a plane perpendicular to the misalignment direction (Fig. 102a). The teeth positioned in the misalignment plane have much displacement freedom as the clearance in the radial direction with a standard pressure angle ( $20^\circ$ ) is approximately three times greater than the circular clearance.

The maximum possible misalignment angle  $\alpha$  may be determined from the relation

$$\tan \alpha = \frac{s}{l}$$

where  $s$  = circular clearance in teeth

$l$  = tooth face width

The maximum displacement of the compensator's extreme points

$$S = L \tan \alpha \frac{Ls}{l} \quad (6-1)$$

where  $L$  is the compensator length.

Compensation can be improved by decreasing the tooth face width, obtained without weakening the tooth by increasing the gear rim diameter.

The circumferential force acting upon the splined rim

$$P = \frac{2M_{tqe}}{D} \quad (6.2)$$

where  $M_{tqe}$  = torque transmitted  
 $D$  = mean diameter of the splined rim

For small displacements the tooth strength is determined from the bearing stress on the spline faces

$$\sigma_{bear} = \frac{P}{lzh} = \frac{P}{lzm} \quad (6.3)$$

where  $l$  = spline width  
 $z$  = number of splines  
 $h = am$  = working spline height, proportional to the spline tooth module  
 $a$  = constant  
 Since  $z = D/m$ , then

$$\sigma_{bear} = \frac{P}{Dla} = \frac{2M_{tqe}}{D^2la}$$

whence

$$l = \frac{2M_{tqe}}{D^2\sigma_{bear}} = \frac{\text{const}}{D^2} \quad (6.4)$$

The spline length  $l$  [Eq. (6.4)] and maximum possible displacement  $S$  of the compensator's extreme points [Eq. (6.1)] as a function of diameter  $D$  are shown graphically in Fig. 103 ( $s$  and  $l$  when  $D = D_0$  are assumed to be equal to unity).

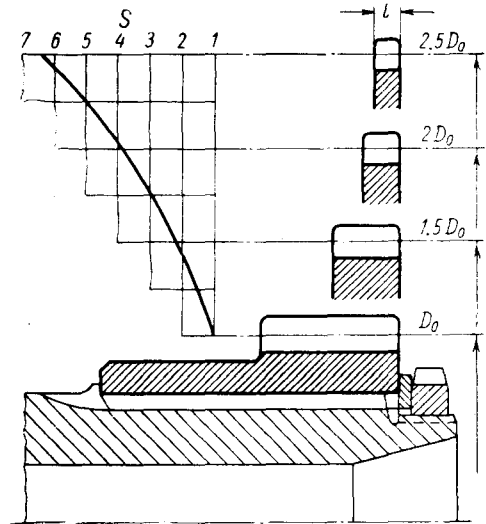


Fig. 103. Spline length  $l$  and maximum displacement  $S$  vs. spline diameter

To decrease the load upon the tooth edges and increase the permissible misalignment angle, it is good practice to give a barrel-like shape to the teeth. The tooth end face edges should be rounded along the entire tooth contour. For large conical misalignments the tooth faces and roots should be made spherical (see Fig. 102b).

Illustrated in Fig. 104 is an intermediate compensating bush which permits large free displacements and in its general scheme resembles a cardan joint. The bush has incomplete internal tooth rims; the toothed portions of both rims are at right angles. The disks with external teeth have complete gear rims, which ensures correct assembly at any angular attitude of the flange relative to the intermediate part.

Some of the design alternatives of compensating connections are presented in Fig. 105. Connection by means of splines cut directly on drive shafts (Fig. 105a) is unreasonable, because the compensation ability of such a joint is rather low and it is determined only by the amount of spline displacement in the gap between spline edges. Increasing the drive shaft shank length (Fig. 105b) only worsens the position since the splined shank owing to inevitable manufacturing inaccuracies and assembly is apt to runout proportional to the distance at which the end is spaced from the drive shaft supports.

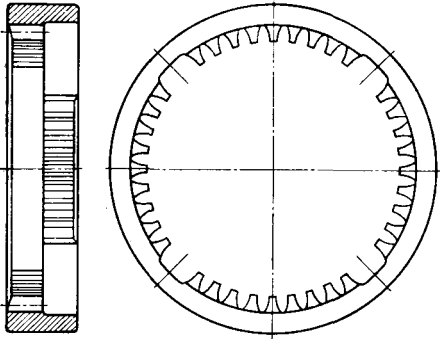


Fig. 104. Cardan-type compensator

If a splined reducing bush is freely mounted upon the splines of shafts and acts as an adapter (Fig. 105c), then the compensating ability, determined by the total clearance in the splines will be twice that of the design given in Fig. 105a.

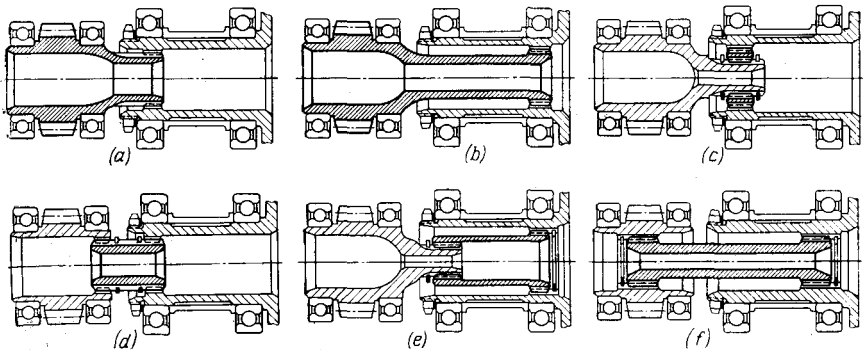


Fig. 105. Transmission of torque through a compensator

The best construction has the driving ends of the splined bush spaced apart longitudinally (Fig. 105d). Compensation in this instance is improved due to the displacement of the bush itself. Still better is the case when a longer bush is used (Fig. 105e). However, this alternative is more difficult to produce because of the different splined rims on the bush ends.

The best design has a long splined shaft, a torsion bar (Fig. 105f), having high compensation characteristics.

### 6.7. Torsion Bars

Torsion bars (torsion bar springs) not only compensate for misalignments, they also damp torque-induced vibrations, thus contributing to quieter and smoother operation. This advantage is particularly important in machines operating under pulsating torsional loads (piston-operated machines).

Thanks to their small radial dimensions, torsion bars can readily

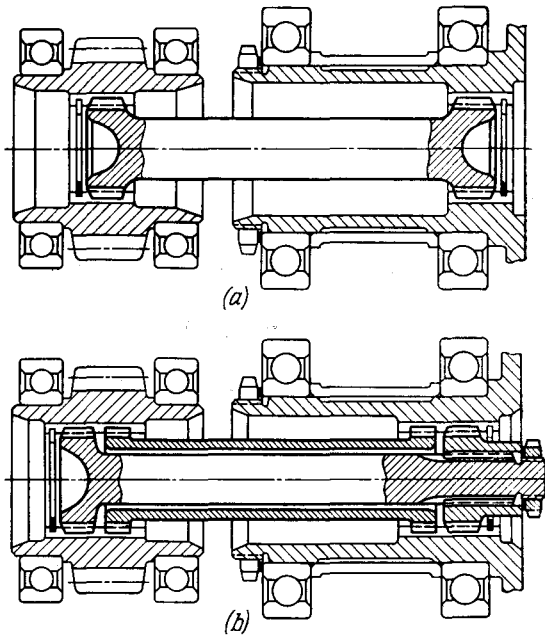


Fig. 106. Torque transmission by means of torsion bars

be included in shaft interiors, thereby adding to the compactness of design (Fig. 106a).

To avoid the breakage of torsion bars by overloading, provision is occasionally made of a torque limiter. The latter is generally made in the form of a splined bush mounted concentrically with the torsion bar (Fig. 106b). The side clearance in the torque limiter splines exceeds that of the torsion bar splines so that the limiter takes up the load as soon as a certain angle of torsion is reached.

General-purpose torsion bars are made of silicon spring steels, grades 60C2A, 70C3A or 60C2XA, which, when subjected to appropriate heat treatment (hardening plus moderate tempering), possess a fatigue limit  $\tau_0 = 65-70 \text{ kgf/mm}^2$  under pulsating torsional loads and  $\tau_{-1} = 30-35 \text{ kgf/mm}^2$  under symmetrical alternating torsional loads.

For stressed structures, as well as for structures operating under elevated temperatures, use is made of silicon-nickel, silicon-tungsten and silicon-vanadium steel grades 60C2H2A, 65C2BA and 60C2XΦA, for which  $\tau_0 = 80-90 \text{ kgf/mm}^2$  and  $\tau_{-1} = 40-50 \text{ kgf/mm}^2$ .

The elastic torsion of torsion bars can be enhanced by increasing the design stress level. For pulsating cycles  $\tau = 30-40 \text{ kgf/mm}^2$  is generally adopted, which corresponds (in terms of fatigue limits) to a safety margin of the order of 1.5-2. In structures designed for a limited service life the admissible stresses can be increased to 80-100  $\text{kgf/mm}^2$ .

The fatigue strength of torsion bars can materially be improved by means of plastic strain hardening. For instance, torsion bars intended for operation under alternate cyclic loading, are hardened by shot blasting, while torsion bars, designed for pulsating loads are hardened through prestraining (i.e., applying a static moment of the same direction as the operating one, the stress level being 20-40% in excess of the material yield point). The shot blast technique and prestraining procedures enable torsion bar service life to be approximately doubled. The best results are obtained by means of strain hardening (shot blasting with prestrain) which further increases service life by 20-30%.

Torsion bar splines are strengthened by rolling in the axial direction with rolls profiled to suit the spline tooth space. Involute splines are strengthened by rolling against a hardened sizing gear.

The torsional stress in a torsion bar

$$\tau = \frac{M_{tqe}}{W_{tors}} \text{ kgf/mm}^2 \quad (6.5)$$

where

$M_{tqe}$  = transmitted torque  
 $W_{tors} = 0.2d^3 (1-a^4)$  = torsion resisting moment of the torsion bar section

$a = d_0/d$  = ratio between the I.D. and O.D. of the bar section (for solid torsion bars

$a = 0$ )

The torsion bar twist angle is

$$\varphi = \frac{M_{tqe}l}{GI_{tors}} [\text{rad}] = \frac{360^\circ}{2\pi} \cdot \frac{M_{tqe}l}{GI_{tors}} [\text{deg}] = 57.3 \frac{M_{tqe}l}{GI_{tors}} [\text{deg}] \quad (6.6)$$

where

$G$  = modulus of torsional shear (for steels  $G = 8000 \text{ kgf/mm}^2$ )

$l$  = acting torsion bar length, mm

$I_{tors} = 0.1d^4 (1 - a^4)$  = polar moment of inertia of the torsion bar section

The twist angle expressed as a function of stress  $\tau$

$$\varphi = \frac{\tau}{G} \cdot \frac{2}{d} l [\text{rad}] = 57.3 \frac{\tau}{G} \cdot \frac{2}{d} l [\text{deg}] \quad (6.7)$$

Let a solid torsion bar transmit power  $N = 100 \text{ hp}$  at a speed  $n = 2000 \text{ rpm}$ . The acting torsion bar length  $l = 200 \text{ mm}$ .

The torque

$$M_{tqe} = \frac{75N}{\omega} = \frac{75 \cdot 100}{0.1047n} = \frac{75 \cdot 100}{210} = 36 \text{ kgf} \cdot \text{m} = 36 \cdot 10^3 \text{ kgf} \cdot \text{mm}$$

Assume that the design stress  $\tau = 40 \text{ kgf/mm}^2$ . According to Eq. (6.5), the diameter of the torsion bar will be

$$d = \sqrt[3]{5} \sqrt[3]{\frac{M_{tqe}}{\tau}} = 1.7 \sqrt[3]{\frac{36 \cdot 10^3}{40}} \approx 17 \text{ mm}$$

The twist angle

$$\varphi = \frac{\tau}{G} \cdot \frac{2}{d} l = \frac{40}{8000} \cdot \frac{2}{17} \cdot 200 = 0.118 \text{ rad} = 57.3 \cdot 0.118 \text{ deg} = 6^\circ 45'$$

Assume that the torsion bar drives a gear with pitch circle diameter  $D_0 = 200 \text{ mm}$ . The elastic displacement of the gear rim under load at the pitch circle radius  $R_0 = 100 \text{ mm}$  is  $f = R_0 \varphi$  [rad] =  $100 \cdot 0.118 \approx 12 \text{ mm}$ . Such a result can hardly be obtained with other absorbing elements (e.g., an elastic clutch with coiled springs placed between the drive shaft and gear rim).

Some typical torsion bar design alternatives are shown in Fig. 107. For transmitting low torques the simplified design version 1 with

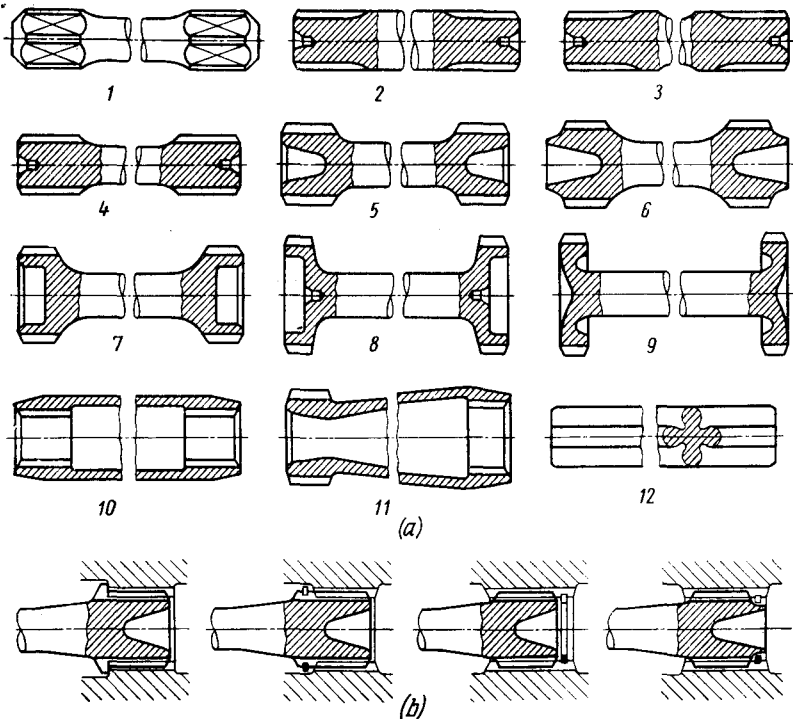


Fig. 107. Torsion bars

squared shanks is used. Much more sturdy are torsion bars which have involute splines (design examples 2 to 10). Version 2 is unacceptable because of the different strength properties offered by the

stem and splines. Versions 3 to 6 are better designs due to the increased spline diameter. The larger the spline diameter (designs 7, 8 and 9), the smaller the spline load and the better the torsion bar compensator. For a given compensation value the increase of diameter enables spline clearance to be decreased, thus improving spline working conditions and prolonging service life.

To reduce weight, torsion bars are generally made tubular (designs 10 and 11). Cross-shaped torsion bars (12) have better elasticity.

Lengthwise fixing of torsion bars is most frequently accomplished with ring-shaped stop washers (Fig. 107b).

### 6.8. Floating Cross-Sliding Couplings

If considerable misalignment is involved it is good practice to employ compensating floating cross-sliding couplings (Oldham's couplings). A typical example of the kind is illustrated in Fig. 108a. Each of the two connecting flanges has two jaws milled on its face, which enter into slots in the intermediate plate 1. The flanges can

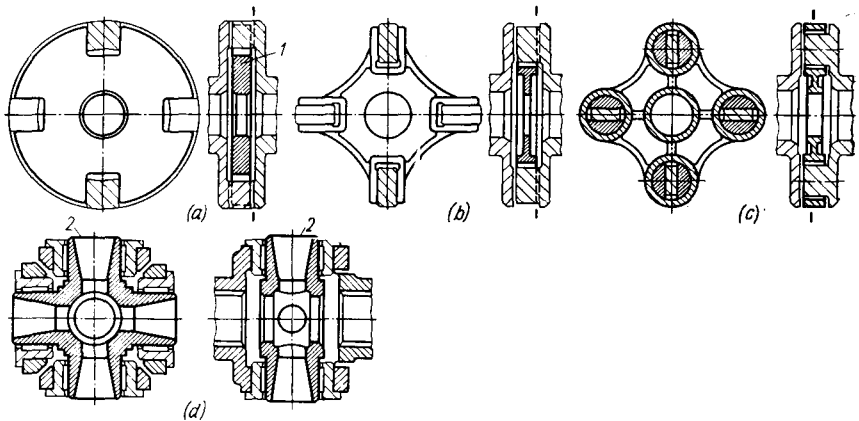


Fig. 108. Floating cross-sliding couplings

freely move in the plate slots one relative to the other in any radial direction. The plate continuously moves in the plane, normal to the shafts axes and slides on the side faces of the jaws. For this reason the plate is made of some antifriction material (cast iron, bronze or, for light loads, from plastics) or, at least, is provided with antifriction shims.

The joint loadability can be increased if the drive elements are made of hardened steel and if an abundant flow of lubricant is brought to the rubbing surfaces. The floating element can be made in the form of a star-shaped steel plate with hardened working surfaces (Fig. 108b), or manufactured as a set of selfaligning cylindrical



insert pieces (Fig. 108c), which ensure uniform load distribution on the working surfaces.

The compensator, designed to transmit huge torques (Fig. 108d) is a combination of a floating cross-sliding coupling and a cardan joint. The principal component is the crosspiece 2 mounted on needle bearings in the yokes of the driving and driven shafts. The misalignment of the shafts is compensated for by the displacement of the yokes along the trunnions, and angular displacements, by the yokes turning about the trunnion axes; the axial inaccuracies of the shafts are rectified by shifting the shafts along the yoke splines during assembly.

### 6.9. Elimination and Reduction of Bending

Whenever the design permits, bending must be changed to other more preferable kinds of loading—tension, compression or shear. Rod, bar or other similar structures, whose elements work mainly in tension or compression, are preferred.

If bending stress is unavoidable, then the moment arm of the bending force must be decreased and the resisting moment of critical sections increased. This is especially important for cantilevered loads which are most unfavourable from the standpoint of strength and rigidity.

Some practical suggestions aimed at eliminating or, at least, reducing bending stresses are presented in Fig. 109. The arms of an angular lever (Fig. 109a) are subjected to bending from the forces applied at the extreme points. As obvious from Fig. 109b, the rib introduced between the lever ends eliminates bending completely.

If a roller unit is secured to the frame in a way illustrated in Fig. 109c, the fastening lug will be subjected to bending. The design with stiffening ribs (Fig. 109d) is somewhat better. However, the best way is to mount the roller under the frame wall, which in this instance is subjected to compression (Fig. 109e).

In the unit of a roller tappet (Fig. 109f) the stem acts like a cantilever; the forces acting upon the roller bend the tappet, causing also increased guideway support reactions. Finally, the slot in the tappet stem is loaded by a moment which tends to rotate the tappet about its axis.

The operating conditions are improved by mounting the roller centrally (Fig. 109g).

The design of the roller tappet drive unit (Fig. 109h) is bad, since the cantilevered tappet guide sleeve is bent excessively by the drive cam. Fastening the sleeve end in the frame eliminates bending (Fig. 109i).

The successive improvements to the welded joint of a lug and pipe is illustrated in Fig. 109j-l. The design in Fig. 109j is irrational: the lug overhang is excessive and the whole joint is subjected to bending.

the weld length is insufficient, owing to which high tensile stresses occur in the weld top points.

In the strengthened design depicted in Fig. 109k the lug is oriented along the force action line and is subjected to tension. The weld is in

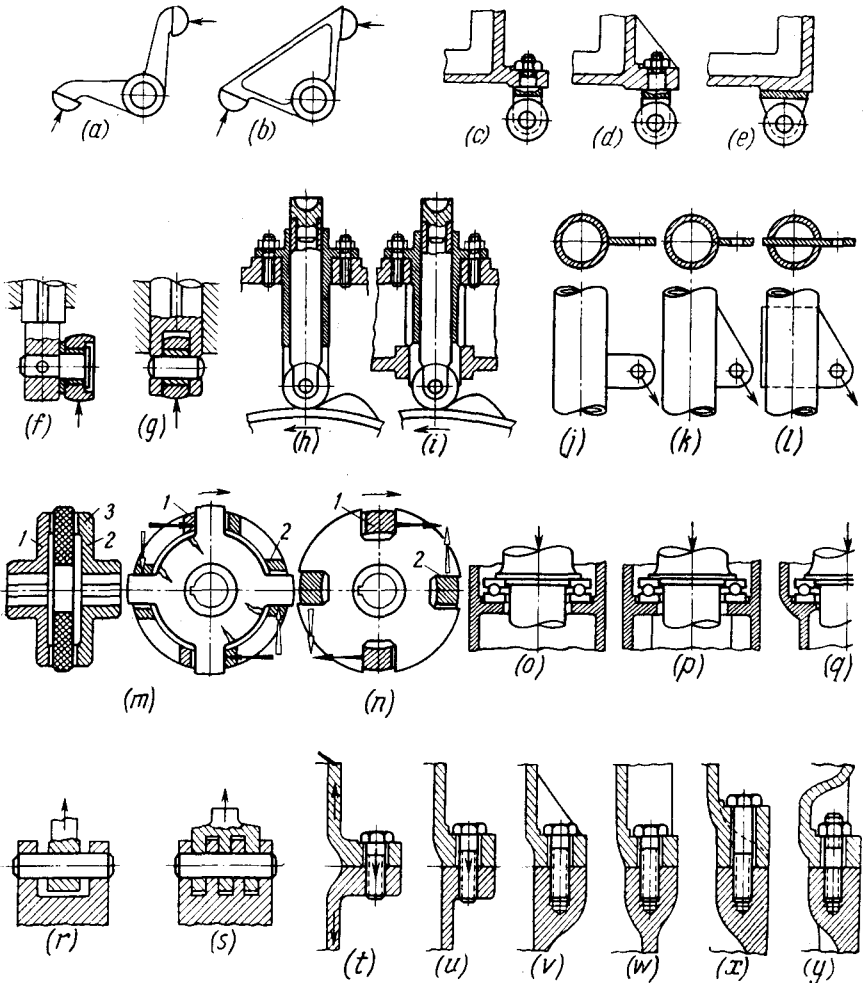


Fig. 109. Elimination of bending

made longer and is now mostly in shear. In the still sturdier design (Fig. 109l) the lug is cut into the pipe.

Pictured in Fig. 109m, n is a cross-sliding coupling comprising drive plate 1 and driven plate 2 interlinked with a plastic floating plate 3.

In the version given in Fig. 109*m* the radial lugs of the intermediate plate are located in parts inside the slots between the drive jaws and inside the slots of the driven plate. The driving forces (indicated by black arrows) and reactive forces on the driven plate (indicated by clear arrows) tend to bend the lugs of the intermediate plate.

In the inversed scheme (Fig. 109*n*) the lugs are changed to slots into which the jaws of the driving and driven plates enter in pairs. The design has a more favourable force distribution. Furthermore, the sections between slots are subjected mainly to compression and the cylindrical portion, to tension, from the resulting drive and reactive forces.

In the step ball bearing (Fig. 109*o*) the circular flange undergoes severe bending from the working load. In the improved version (Fig. 109*p*) the flange is ribbed for rigidity. In the best alternative (Fig. 109*q*) the force is transferred directly onto the housing walls which in this case work in compression.

In the connecting rod yoke joint (Fig. 109*r*) the pin and yokes are subjected to bending.

In the design shown in Fig. 109*s* the pin is passed through a comb of spurs, thus eliminating bending for shear across several planes.

Figure 109*t-y* depicts some methods by which a flanged connection loaded in tension can successively be improved. The design in Fig. 109*t* is poor due to the excessive fastening bolt overhang from the walls of the mating parts. Bending at the joint face can be reduced by decreasing the bolt overhang to its minimum permitted by the bolt head sizes and their facing requirements (Fig. 109*u*). Still greater sturdiness can be achieved by introducing stiffening ribs (Fig. 109*v, w*) and bringing the wall surfaces closer to the bolts axes (Fig. 109*x, y*).

A source of bending stresses, which often escapes the designer's attention in practice, is also the curvilinear shape of parts subjected to tension or compression.

For example, let us consider curvilinearly profiled ribs (Fig. 110*a*). Elongation bends the ribs which is accompanied by high tensile stresses along the rib edges. Straightening the profile (Fig. 110*b*) and particularly positioning the ribs along the acting force line (Fig. 110*c*) lessen these internal stresses.

Tensile or compressive forces applied to parts with eyes (Fig. 110*d*) bend and deform the walls. The defect can be rectified by designing streamlined transitions (Fig. 110*e*). The eyes can be strengthened with stiffening ribs (Fig. 110*f*) or webs (Fig. 110*g*).

A lifting hook (Fig. 110*h*) undergoes bending from the moment  $Pl$  ( $l$  = arm of force  $P$  due to the lifted load relative to the neutral axis of the critical section  $A$ ). In a two-horn hook (Fig. 110*i*) the bending moments on both sides of the hook will equalize each other; hence, the hook stem is in tension. The bending moment acting

in the critical section  $B$  decreases to  $Pl'/2$  ( $l' =$  arm of force). With the relations like those in the Figure, the bending moment will drop by  $2l/l' \approx 5$  times as compared with the original design.

In the case of tensile-compressive loading the bending is often caused by an off-centre load application.

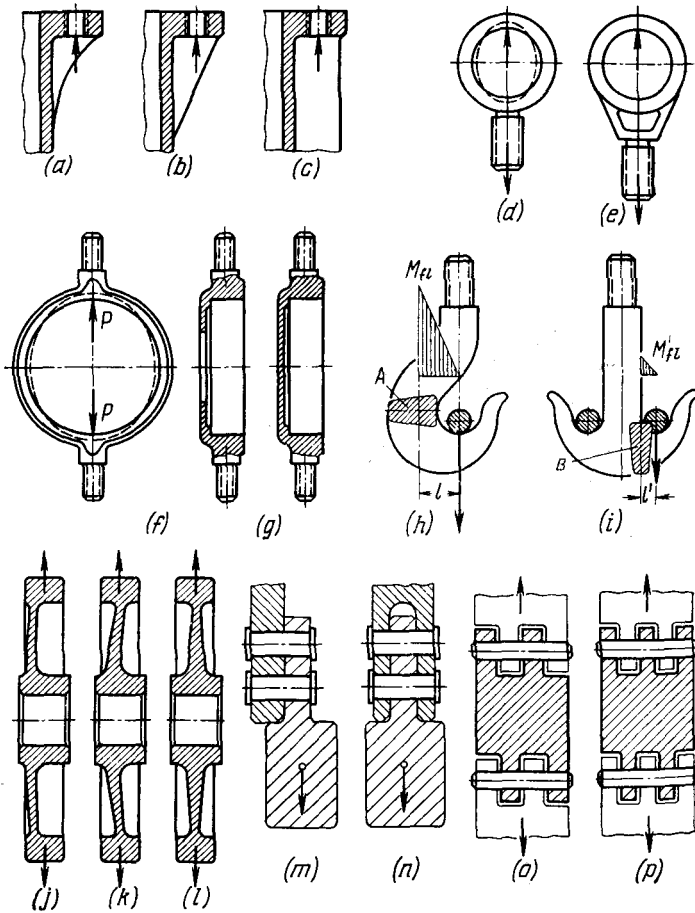


Fig. 110. Elimination of bending

In a high-speed rotor with a disk displaced from the axis of symmetry of the rim (Fig. 110j) the centrifugal forces tensioning the rim, cause spatial bending of the disk. In the design with a conical disk (Fig. 110k) which connects on the symmetry axis of the rim the bending will be notably less. The best design has a central disk (Fig. 110l) which works in tension.

If a counterweight is secured to a crank web as shown in Fig. 110m, the web will be subjected to bending due to the off-centre position of the counterweight and the rivets will also work partially in bending. In the designs shown in Fig. 110n the bending has been eliminated by securing the counterweight in a fork. The rivets now work primarily in shear and the number of shear planes double that of the previous designs.

If conveyer chain links are joined as in Fig. 110o, they will bend when the chain is tensed because of the asymmetrical arrangement of the eyes. Positioning the eyes symmetrically eliminates the defect (Fig. 110p).

Bending may also be caused by local form irregularities in parts at the spots to which forces are applied. Figure 111 illustrates bolt

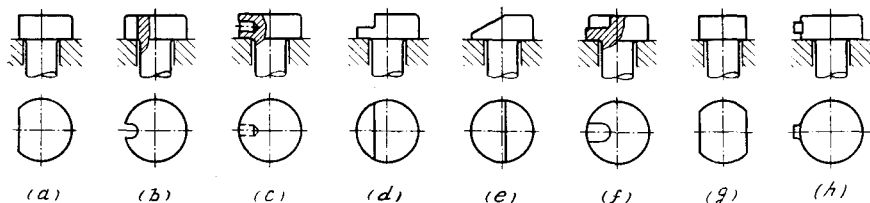


Fig. 111. Elimination of off-centre force application

heads. The asymmetry of the bearing surfaces of the bolt heads (Fig. 111a, b) and their non-uniform rigidity (Fig. 111c, f) cause the bolt stems to bend when in tension. Eliminating the asymmetry assures central force application (Fig. 111g, h).

The successive improvement in a connecting rod and piston unit is illustrated in Fig. 112. In the version shown in Fig. 112a the piston crown, bosses and pin are subjected to bending under the gas pressure. The bending is sharply reduced if the bosses are fixed to the crown with ribs (Fig. 112b) or solid webs (Fig. 112c). The rigidity and strength of the crown are enhanced by shaping it as a concave sphere (Fig. 112c).

Tapering the connecting rod small end (Fig. 112d) minimizes the area of non-supported surface of the crown and will simultaneously decrease the bending of the wrist pin. Furthermore, this lowers the gas pressure specific load on the operating surfaces of wrist pin.

Finally, the piston crown and wrist pin can be completely relieved from bending if the underneath side of the crown rests directly against the connecting rod small end (Fig. 112e) or upon the pin through a cut-out in the connecting rod end (Fig. 112f).

Figure 113a, b shows irrational designs of a suspended frame bracket loaded by a tensile force. Due to the curvilinear shape bending stresses occur in the frame rods. Bending can partially be reduced

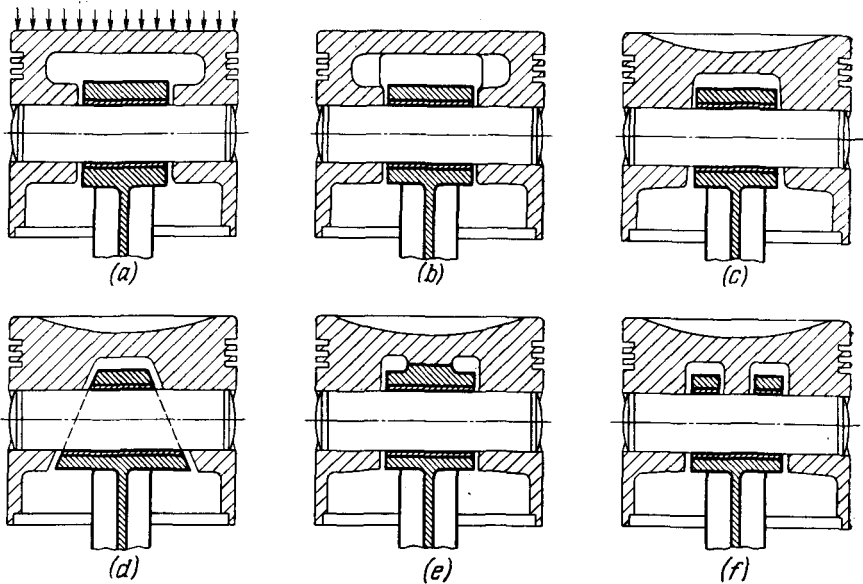


Fig. 112. Elimination of bending in connecting-rod-to-piston joint

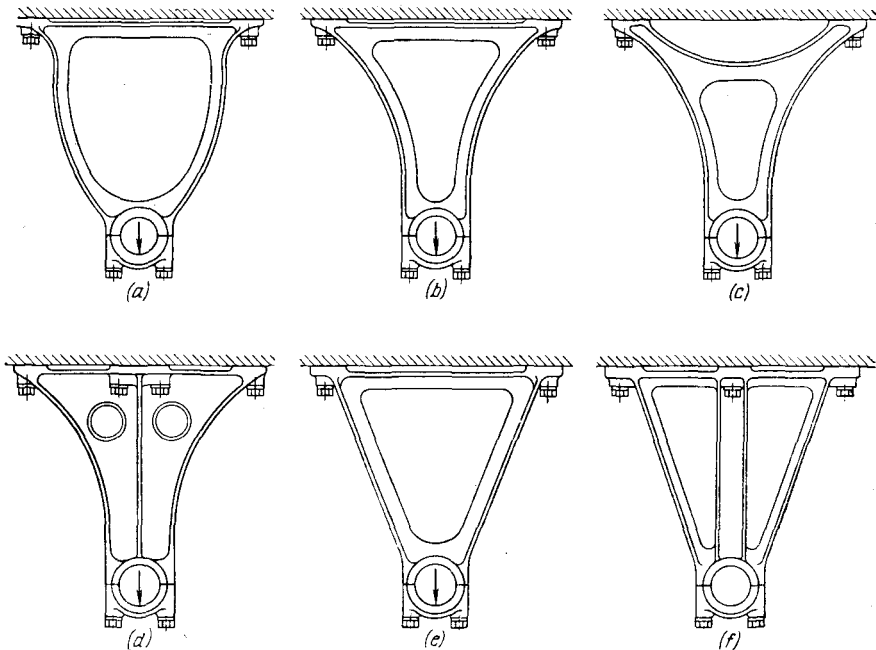


Fig. 113. Elimination of bending in suspended frame bracket

by introducing a stiffening web (Fig. 113c) or it may be completely eliminated by introducing a solid web between the rods (Fig. 113d). The last design, however, loses the weight advantage.

If for some reasons the frame-like structure is preserved, it is better to employ straight rods (Fig. 113e). In this case the system will be similar to a truss frame. Bending (of a secondary order) will occur only as a result of the positive imbedment of the rods in the joint (in ideal girder structures the bending of rods is prevented by articulated joints). In the most preferable design (Fig. 113f) the load is taken up by the reinforcing central rod subjected to tension. The side rods enhance the stability of the system in the transverse direction.

### 6.10. Elimination of Deformation Due to Tightening

When structural parts are tightened, appropriate measures must be taken to avoid their deformation. Fastening with studs and bolts in a "hanged-up" state (Fig. 114a) entails deflection of the walls and overstresses the material. Studs and bolts passing through hollow

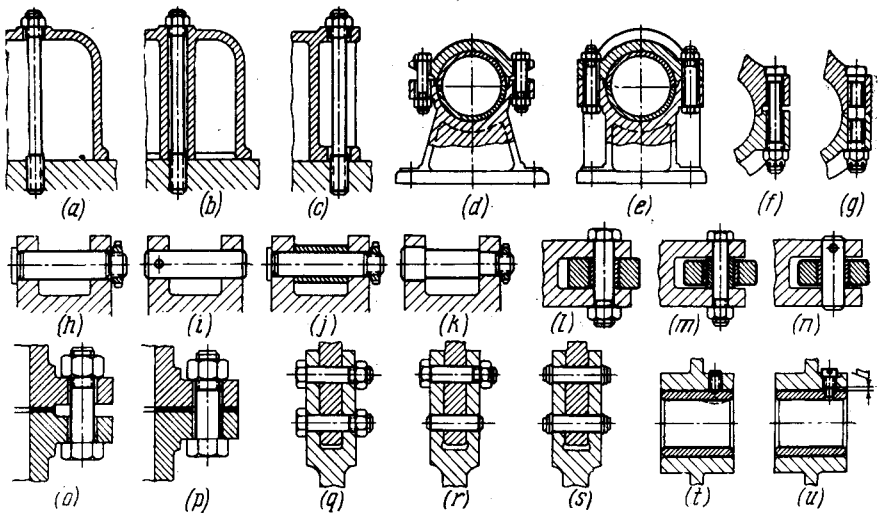


Fig. 114. Elimination of deformation during tightening

components must be enclosed in rigid columns (Fig. 114b). Occasionally reinforcing the assembled walls with ribs will suffice (Fig. 114c), provided they are close to the fastening element.

The bearing cap design shown in Fig. 114d is wrong as the bolts during tightening will deform the cap and badly affect the true cylindrical form of the bearing. Moreover, bending stresses will

occur in the bolts. In the design presented in Fig. 114e the cap is relieved from the tightening forces.

Figure 114f shows an incorrect and Fig. 114g, a correct fastening of a connecting rod cap.

If a pin is fastened as in Fig. 114h, the end eye lugs will be subjected to bending. Fastening the pin to one lug with a dowel (Fig. 114i) alleviates the system from internal stresses, but deprives it of rigidity. Reinforcing the eye lugs with a spacer bush (Fig. 114j) makes it necessary to accurately keep to the spacer length and lug span width, thus complicating the manufacture. It is more correct to tighten the pin in one lug (Fig. 114k), leaving the other end of the pin free for self-centring.

Mounting a roller in a yoke (Fig. 114 l) brings the fork lugs towards each other as the bolt is being tightened and the roller loses its mobility. The introduction of a spacer bush (Fig. 114m) improves the situation but complicates manufacture. For the most correct alternative (Fig. 114n) the pin is fixed in one lug only. The necessary end play enabling the roller to rotate freely is ensured by longitudinal clearance between the roller and lugs.

Figure 114o illustrates a wrong and Fig. 114p, a correct tightening of flanges.

Fastening of a connecting rod in a yoke (Fig. 114q) requires accurate machining or exact fitting of the mating surfaces on both parts. Otherwise, either the yoke will be spread out by the rod, or the yoke will be bent as the bolts are tightened. In an improved design (Fig. 114r) the lower bolt is changed for a dowel pin working in shear. The eyes are bent (if clearance is present in the joint) only as a result of tightening the upper bolt, which, however, in this case will induce less stresses than in the version shown in Fig. 114q. In the design pictured in Fig. 114s the parts are fastened by means of dowel pins and are free of bending stresses. Yet, the joint lacks the capability of being tightened.

In terms of averaged indices of strength and rigidity the best alternative seems to be that in Fig. 114r.

Figure 114t depicts a badly fixed bearing bush. The locking screw is driven to stop against the bush, thus deforming it (shown by dashed line). In a correct design version (Fig. 114u) the screw head rests against the bearing body, with a clearance  $h$  being left between the thread and the bush.

An example of an erroneous tightening of a thrust washer juxtaposed onto a plain bearing end face is given in Fig. 115a. The shaft shoulder is insufficiently high; in the course of tightening the washer is deformed by force  $P$ . To preserve the washer flatness the shoulder height must be increased and the diameter of the nut, decreased (Fig. 115b), or the washer must be given a stiff collar (Fig. 115c).

The defect of the gear fitted on aligning tapers (Fig. 115d) is that



the tapers are positioned under the teeth which deform as the assembly is tightened (shown by dashed line). In the correct design (Fig. 115e) the tapers are brought beyond the gear rim boundaries.

The design of a sealing unit with split spring rings (Fig. 115f) is bad. During tightening the housing crests are deformed and the

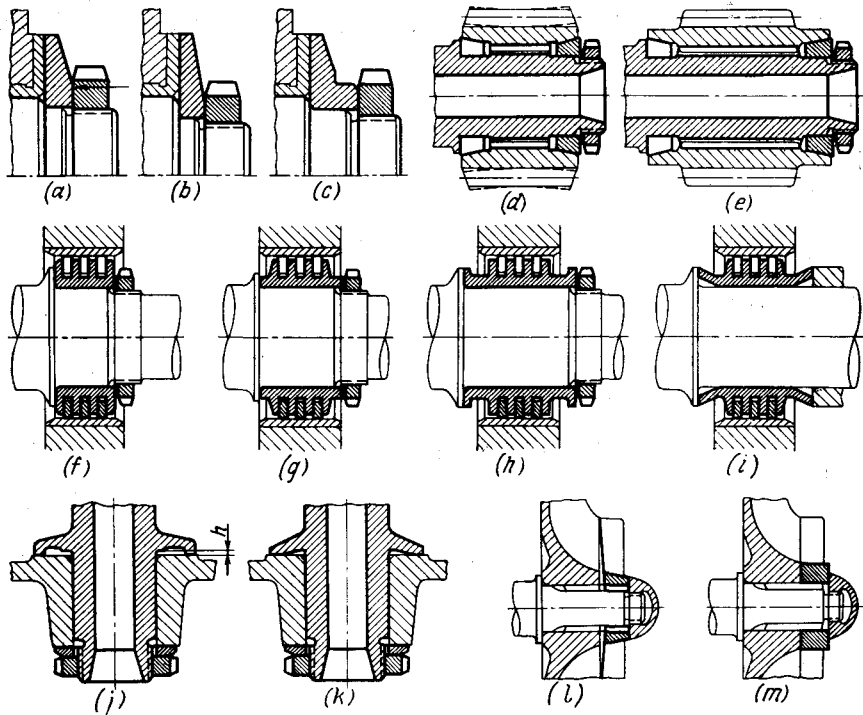


Fig. 115. Elimination of deformation during tightening

rings lose their mobility. Correct designs, free of rings seizure, are illustrated in Fig. 115g-i.

Occasionally a limited deformation is introduced in order to enhance the rigidity and stability of assembly. For example, when securing a column in a pedestal (Fig. 115j) a clearance  $h$  is left between the column flange and bearing surface. This clearance is taken up in the process of tightening. The amount of such a clearance is chosen either through calculations or experimentally so as to keep the stresses in the flange within safe limits.

Similar results can be obtained by making the flange bearing surface slightly tapered (Fig. 115k).

Sketched in Fig. 115l is an assembly of a guide-vane unit and an impeller of a centrifugal pump. The vane ends are machined to a taper and they intimately close the impeller blades in tightening (Fig. 115m), thereby precluding blade vibration when running.

### 6.11. Design Compactness

Compactness is a feature of a rationally designed component. Efficient utilization of space enables the overall size and weight to be decreased and the strength-to-weight ratio, increased.

Axial dimensions may often be reduced by spreading the structure in the radial direction. In the unit of a mechanical face seal as shown

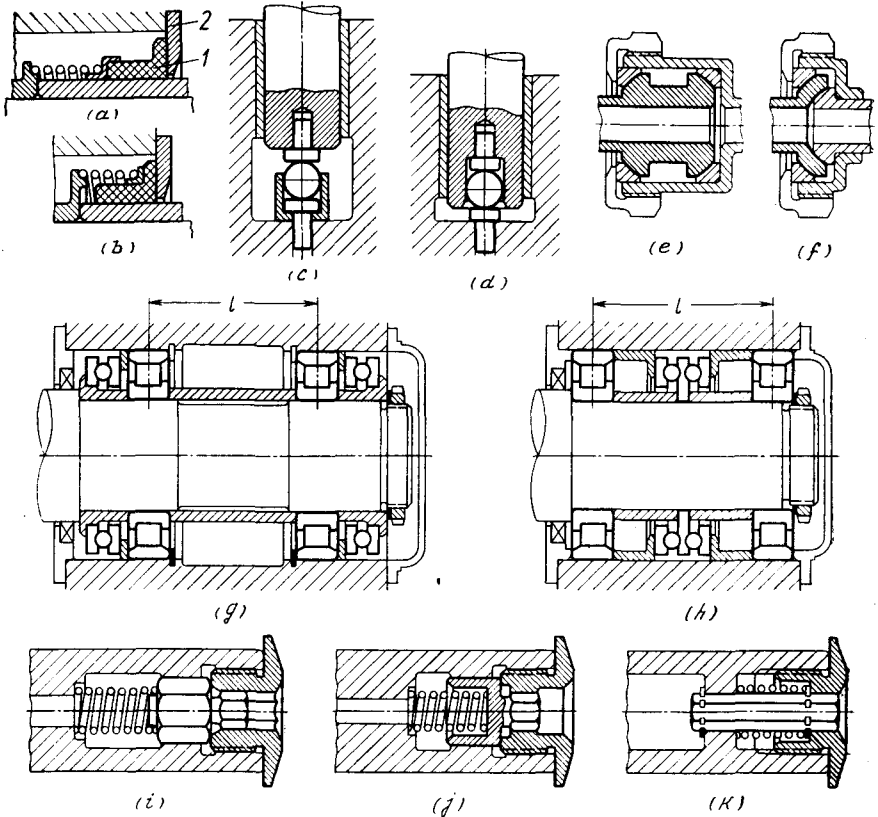


Fig. 116. Reduction of overall dimensions

in Fig. 116a bush 1 is forced by the spring to the sealing disk 2; now, if the spring is installed over the bush (Fig. 116b) the entire system becomes more compact without any adverse effect to the parameters determining the efficiency of the unit.

An example of dimensional reduction through structural incorporation of elements into parts is shown in Fig. 116c, d which pictures a step ball bearing unit.

In the spherical connection of a pipe unit (Fig. 116e) considerable reduction in dimensions is achieved by changing one of the external spherical surfaces to an internal spherical surface (Fig. 116f).

In the unit of a shaft end mounting loaded with alternating radial and axial forces (Fig. 116g) the axial load is taken up by two single-row thrust bearings. The design is cumbersome. The shaft fixing in the lengthwise direction is not accurate: the thrust bearings spaced at a fair distance from each other must be installed with an axial clearance which compensates for temperature deformations; also axial backlash is unavoidable in this system.

In the design presented in Fig. 116h the axial load is taken up by a double-row thrust bearing installed between radial supports. The overall dimensions are decreased and the axial play minimized. Preserving the same dimensions as in Fig. 116h, one may increase the radial spacing of the supports 1.5 times, thus beneficially influencing the shaft stability.

Figure 116i-k illustrates the design and operational improvement of a unit intended to lock an internal nut mounted on a shaft end. In the original design (Fig. 116i) the nut is locked with a spring-loaded stopper provided with two hexagons, the larger one of which slides in the shaft hexagonal hole and the other smaller one enters the hexagonal bore of the nut. Unscrewing the nut should be preceded by sinking the stopper as this will bring the smaller hexagon out of engagement with the nut. The axial size of the unit is unreasonably large. The nut internal hexagon is brought to the nut end face so that a poorly experienced fitter may try to unscrew the nut without having released the stopper beforehand. As the stopper is not fixed lengthwise it will drop out of the shaft hole during unscrewing.

Now, if the spring is mounted inside the stopper hexagon (Fig. 116j) the nut internal hexagon becomes shorter, thus preventing the nut unscrewing without preliminary release of the stopper.

In the most rational alternative (Fig. 116k) the stopper is made of a hexagonal bar. Hexagonal holes in the shaft and nut are machined by the same broach, whereas in the previous examples two different broaches were needed. Mounting the spring outside the stopper allows plan dimensions of the unit to be reduced 1.5 times as compared with the original design. Here the stopper is fixed axially by means of a circlip and does not drop out of the hole after unscrewing the nut. The nut cannot be unscrewed unless the stopper is released.

Figure 117a illustrates a bevel gear unit in which the gear is installed conventionally in a cantilevered mode. An improved design shown in Fig. 117b has two supports: one end of the driving gear shaft is installed in the casing wall and the other, in detachable cover *I* with a port provided in the area where the gears mesh. In this alternative the size of the gears is decreased and their stability improved.

The axial size can be reduced to half that of the original construc-

tion if the gear is moved to the other side of the driving shaft (Fig. 117c).

Apart from the excessive overall dimensions, the bevel gear reducer sketched in Fig. 117d is inefficient in that its gears are mounted in various housing components and accurate engagement is therefore difficult to obtain. The accuracy of engagement can only be verified by blacking in.

In the improved design (Fig. 117e) the housing volume is utilized in the most efficient way as the bearings of the major bevel gear are incorporated into the housing contour. One of the bearings of the minor gear is also located inside the housing. Further decrease of the overall dimensions has been reached through changing the gear key-type shanks to internal splines. All the bearings are housed inside a single component, this being very beneficial from the viewpoint of the accuracy of the bevel gears positioning. The design is unitized: after the cover is removed, the gear unit remains in place and is easily accessible for inspection and adjustment.

Figure 118 shows how the axial dimensions of a gear reduction unit can be reduced. In the original design (Fig. 118a) end gear 1 is cantilever-mounted in diaphragm 2. The drive gear is mounted in two bearings, one of which is installed in cover 3 and the other, in the end gear recess. This latter bearing is arranged in a cantilevered way in relation to the main bearings. The intermediate gears shaft is supported at one end in diaphragm 2 and at the other, in cover 3. The axial dimensions of the system are unreasonably large. The supports of the driving and intermediate shafts are located in different components. The bearing surfaces of the drive pinion cannot be machined together, this imposing higher demands for the alignment of the end gear shaft bearing surfaces. The assembly procedure of the unit is extremely complicated. As the diaphragm is fitted together with the cover the ends of the driving and intermediate gears shafts, which have previously been fixed each in its support, hang; the fitters are thus compelled to blindly place them into the second supports. In the improved version (Fig. 118b) the shafts supports are positioned within the shaped diaphragm 4 and tightened against cover 5. Owing to this feature the entire system becomes unitized. Now all the fitting surfaces can be machined in one setting with the diaphragm being screwed to the cover. The reduction gear unit can be assembled and checked as an individual unit. Any part of the unit is readily accessible for inspection during the assembly procedure. Axial dimensions are reduced by half as compared with the original design. This is achieved by the following measures (apart from the introduction of the detachable diaphragm):

the rim of the end gear drive splines (which in the previous design is machined on a separate fitted part) is made integral with the end gear as extension of the teeth;

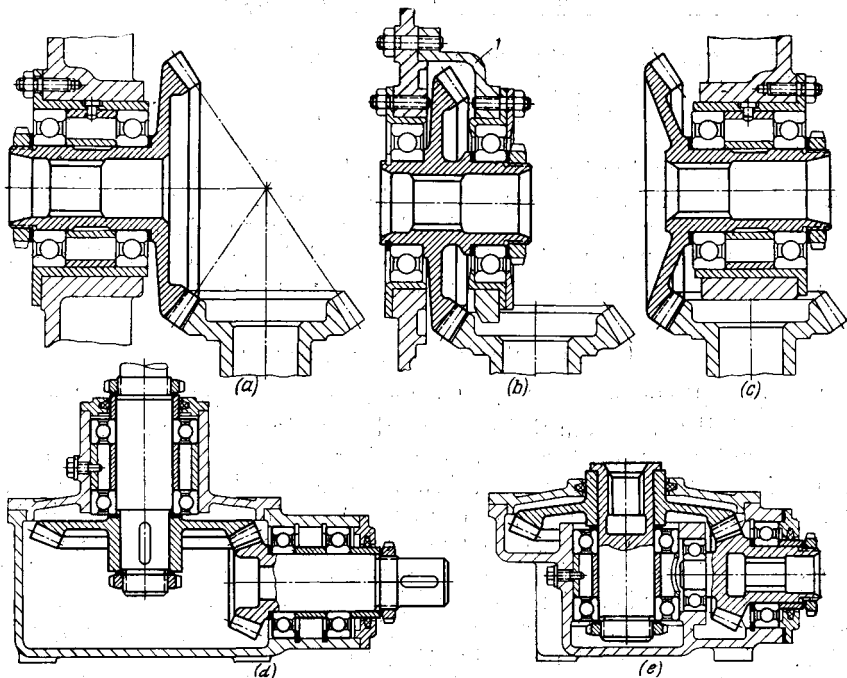


Fig. 117. Reduction of overall dimensions of bevel gear drives

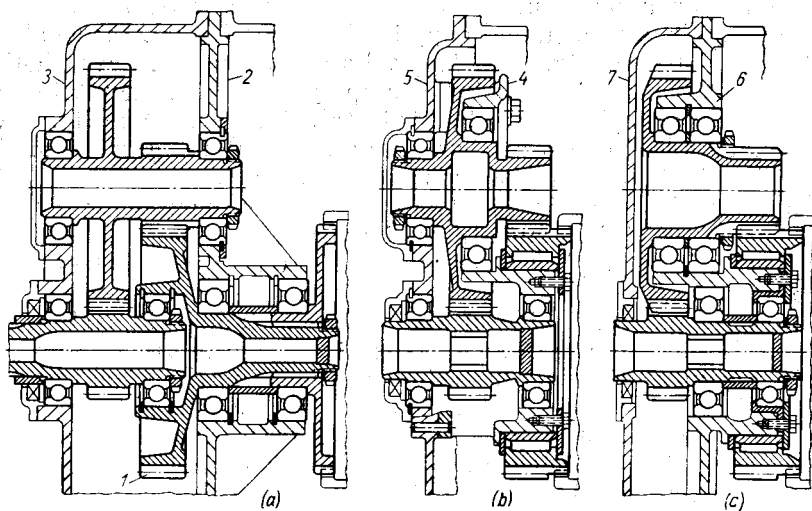


Fig. 118. Reduction of overall dimensions of gear drive

the end gear is mounted on a needle bearing installed upon a cylindrical flange of the diaphragm;

all the external splines of the input shaft are replaced by internal ones.

In the alternative illustrated in Fig. 118c the gearing is mounted on a single component, namely, on diaphragm 6. Cover 7 is non-bearing and is connected to the reduction gear mechanism only by the seal which encompasses the tip of the driving shaft. In this case manufacture and assembly are still more simplified.

## 6.12. Combining Design Functions

The overall size and weight of a structure can sometimes be decreased materially by combining several functions in one component.

In a paired radial-thrust ball bearing intended to take up axial loads in both directions (Fig. 119a), the actual load is taken up by one of the bearings (at a given moment), while the other is idle.

In the single-row double-thrust ball bearing (Fig. 119b) the balls are encased in races which have deep grooves; for assembly convenience the outer ring is split. When subjected to load the balls are forced against one side of the groove, leaving, accordingly, the opposite side. With a changed load direction the opposite groove is loaded. Such bearings of the same load capacity have half the axial length of the paired bearings. Furthermore, by encasing outer split races inside a common ring (Fig. 119c) the assembly becomes a unitized component.

Another example, similar to the above, is a helical ball drive (the system is very commonly applied in power drives). In the alternative depicted in Fig. 119d two balls are arranged in each helix, consequently, the axial load is taken up by one half of the total number of balls only. If only one ball is installed in each helix (Fig. 119e) the axial load will then be shared by all the balls (regardless of the load direction), thus the load capacity is doubled.

In the rod journal joint of a two-part crank the connection is clamped with a bolt (Fig. 119f). In the improved version (Fig. 119g) the connection is accomplished by using the shank of the left-hand part of the crank.

In the flexible mounting of a gear rim on its hub (Fig. 119h) the alternating torque is transmitted from the gear rim via a number of springs mounted (in order to avoid distortion) on cylindrical inserts 1 resting in specially provided nests in projections 2, 3 of the rim and hub. Here one half of the springs damp the torque-induced vibrations in one direction, and the other half, in the opposite direction.

In the improved alternative (Fig. 119i) the projections of the rim and hub are superimposed (in plan view); hub projections 4 are introduced into recess in the rim projections 5. Owing to such an

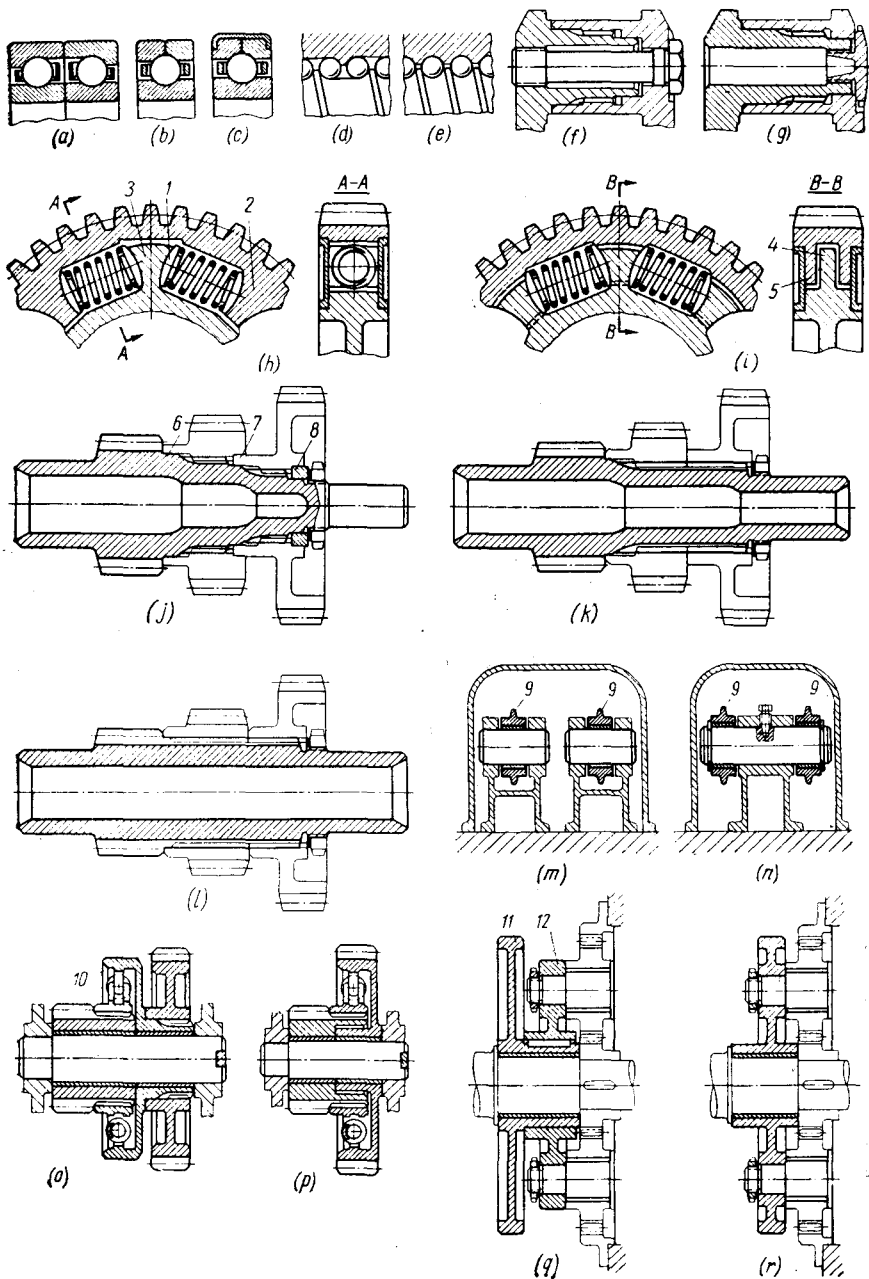


Fig. 119. Combining design functions

arrangement all the springs take up torque-induced vibrations in both directions simultaneously. The unit is capable of transmitting doubled torque or damping vibrations whose amplitude is twice that of the previous system.

When mounting gears as shown in Fig. 119j, each gear is secured in place on its own splines. The small spline lengths encountered in the system forces the introduction of aligning elements, the cylindrical collars 6, 7 and 8. In the design shown in Fig. 119k the gears are slipped onto one common spline. The result: special tools<sup>9</sup> list (broaches, hobs) is cut down by half; the assembly is simplified; the shaft strength, enhanced; the shaft right-hand journal diameter and the length of splines, increased, which enables the additional alignment of gears to be obviated.

In the most perfect alternative (Fig. 119l) the gears are held on an extension of the pinion gear's teeth. The only special tool required is a broach for machining the splined holes.

In the unit of a valve drive mechanism (Fig. 119m) rockers 9 are mounted each on a stud of their own. In the better version (Fig. 119n) both rockers are cantilever-mounted on a common pin.

Figure 119o gives an example of gears mounted with intermediate spring coupling 10. In the alternative shown in Fig. 119p damping springs are arranged in the gear wheel of the drive. As a result the weight and axial dimensions are reduced and rigidity improved.

In the planetary drive unit of a cam plate 11 (Fig. 119q) the satellites are mounted on an individual, in fact, superfluous part 12. In the improved design (Fig. 119r) the satellites are mounted directly on the plate. As a result, the unit becomes lighter and more compact and manufacture is eased.

### 6.13. Equistrength

Some ways in which machine components can be imparted uniform strength are illustrated in Fig. 120.

When a simply supported shaft is loaded with a transverse bending force (Fig. 120a), a body of equal bending resistance with the same maximum stresses in all sections will have the profile of a cubic parabola (shown in the Figure by a thin line). The design in this case is not equistrong: the equal-resistance parabola is twice (on the shaft tapered section and beyond the cylindrical lug) outside the actual part contour. These sections are weak in comparison with the remaining ones.

In a correctly designed version (Fig. 120b) the parabola is contained within the part contour. The through hole provided in the part hardly affects the strength, but considerably reduces the weight of the part.



Under complex loading conditions (Fig. 120c-f) the shaft undergoes bending from the force of the tooth drive and in the section between the teeth and splines which transmit the driving force the shaft is subjected to the action of operating torque  $M$ .

In the design shown in Fig. 120c the shaft section is designed to meet maximum flexural and torsional stresses across  $AA$ , without

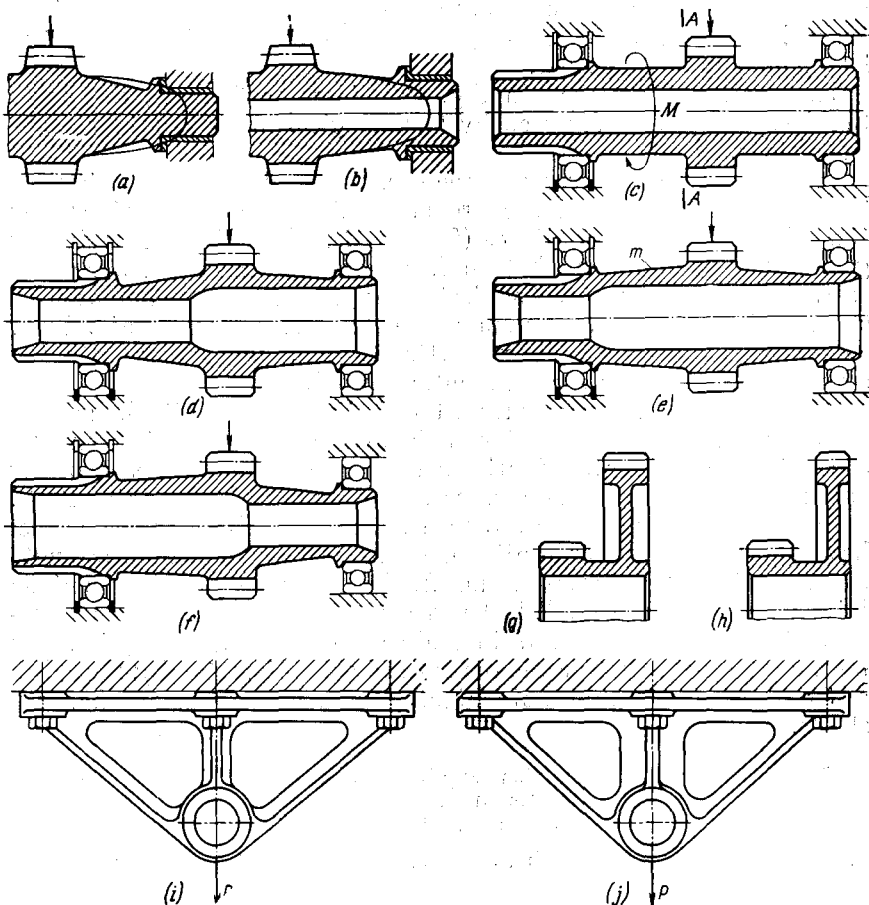


Fig. 120. Imparting equal strength properties to parts

considering the drop of the bending moment towards the supports. Also neglected is the fact that the shaft right-hand end is subjected to bending alone, whereas the left-hand end undergoes bending and torsion. Hence, the latter is loaded more severely.

In the equal-strength design (Fig. 120d) the shaft is made tapered, thus meeting accordingly the bending moment variation along the

axis. The equal strength of the left-hand (heavily loaded) and right-hand (lightly loaded) sides of the shaft is achieved by stepping the internal bore.

Equal strength can also be achieved by increasing the outer dimensions of the tapered portion  $m$  (Fig. 120e), or by decreasing the diameter of the right-hand ball bearing (Fig. 120f). Here the internal hole is again stepped but on the opposite side to the previous examples, accompanied also by an increase in the diameter of the left-hand support bearing.

The designs illustrated in Fig. 120d-f are equivalent, therefore, the design choice is dictated by technological and operational considerations.

In a cluster gear (Fig. 120g) the gear teeth offer uneven resistance to bending and crushing. The circumferential force on the minor gear rim will under any conditions (i.e., with multiplying and reducing gear ratios) be less than that on the major gear rim by a factor equal to their diametral ratio. The design can be made more balanced in strength if the width of the major gear teeth is decreased (Fig. 120h) even though not strictly in proportion to the acting forces (with due regard for the higher circumferential speed).

In a bar bracket loaded with a tensile force (Fig. 120i) the middle bar carrying the greater portion of the load is overloaded in comparison with the lateral, slightly loaded bars. The system becomes equally strong if the middle bar cross-section is increased (Fig. 120j).

For units to have equal strength means that all their parts must have equal stresses (for similar materials) or possess equal strength (for materials of different strength). The design version of a splined joint illustrated in Fig. 121a has a non-uniform strength on two counts: the strength of shafts in plain sections (diameter  $d$ ) is much more better than that across the splined part (diameter  $d_0$ ); the splined bush has a considerably higher resistance to torsion than the shafts.

The equal-strength condition requires that both the bush and the shafts have equal resisting moments in torsion:  $0.2D^3(1 - a^4) = 0.2a^3$ , where  $a = d/D$ . For the relationships in the Figure ( $a = 0.68$ ) the strength of the bush is  $\frac{1 - a^4}{a^3} = 2.5$  times greater than that of the shafts.

In a rational design (Fig. 121b) the diameter of the shafts is reduced in comparison with the internal diameter of the splined joint and the external diameter of the bush ( $D'$ ) is reduced to the technologically acceptable minimum value.

In the connection of a screw propeller blade (aluminium alloy) with a steel hub (Fig. 121c) the predominant stress is that of tension produced from the centrifugal force as the propeller rotates. The design has unequal strength. The thread profile both at the blade

root and in the hub is the same although the permissible stresses in bending and shear for aluminium alloy are lower than those for steel.

In the design shown in Fig. 121*d* the height (in the axial direction) of the blade threads is made higher than that of the bush so as to render them equally strong. The bush is given a shape offering equal resistance to tension. The bush cross-section progressively increases

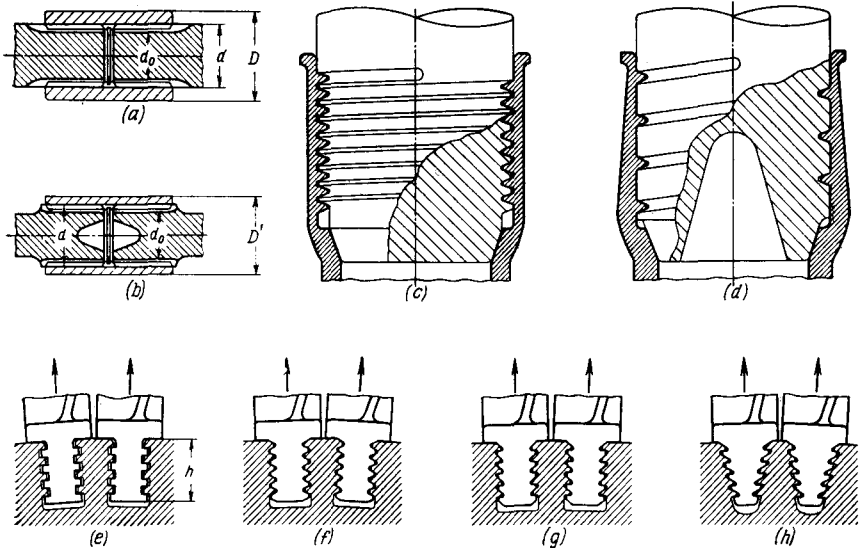


Fig. 121. Imparting equal strength properties to units

downward coping accordingly with the rising tension forces transmitted to the bush by the blade threads. A relieving recess is made in the blade.

The square-profiled toothed-slot fastening of turbine blades in the rotor (Fig. 121*e*) is irrational for two reasons. First, the blade root is uniform in thickness and therefore is not equally strong. The full centrifugal force is taken up by the cross-section lying nearest to the blade root platform and this section is overloaded as compared with the other sections in which the acting force progressively decreases towards the root tip. The picture is opposite in the rotor webs, where the most severely loaded section lies close to the root tip, while the above-lying sections are loaded to a lesser degree.

Secondly, because of the square-shaped teeth the material of the root is not utilized to its best. The total section working in shear and flexure is approximately equal to one half of the root section (over height  $h$ ).

The entire root height can share the load if the teeth are made triangular (Fig. 121f) or trapezoidal (Fig. 121g). In this case the tooth shear strength improves approximately twice and the flexural strength, 4 times. Trapezoidal teeth have an additional advantageous feature, namely, lower bearing stress on the teeth working faces.

In the most rational version (Fig. 121h) the root is wedge-shaped, thus coping with progressively decreasing forces acting upon the root. Such a shape increases the critical sections of the blade root and rotor webs about 1.5 times, with a corresponding increase in the joint strength.

#### 6.14. Uniform Loading of Supports

When designing units with antifriction bearings, the latter should advisably be made of equal durability.

Let us consider an example of a gearing (Fig. 122a). The drive load  $P_1$  on the pinion exceeds load  $P_2$  on the gear, by a factor of  $D_2/D_1 \approx 2.5$

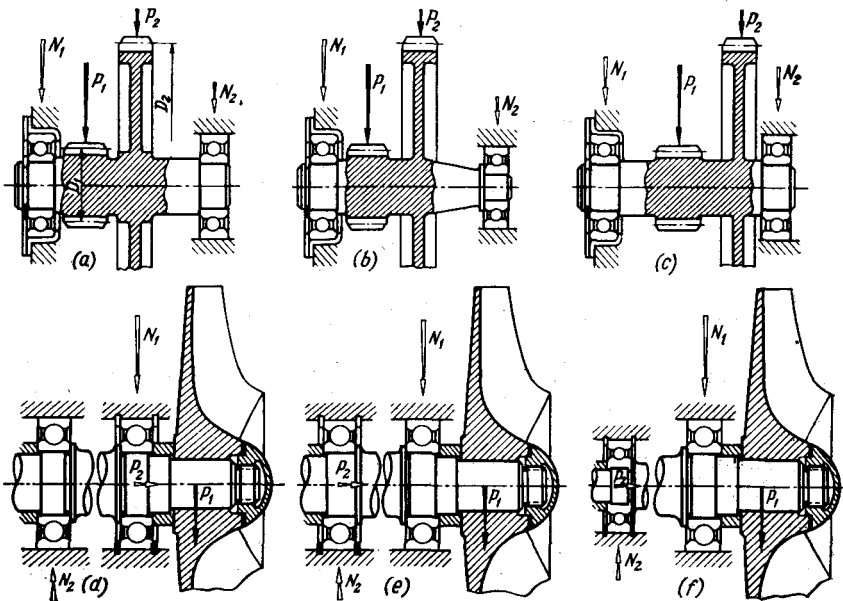


Fig. 122. Imparting equal durability to supports

$\approx 4$ . With the supports spaced as in the Figure, the left-hand bearing is loaded with force  $N_1$  which is 2.5 times greater than force  $N_2$  acting upon the right-hand bearing. The supports can be made of equal durability if on the shaft right-hand end is mounted a smaller bearing (Fig. 122b) whose load capacity is 2.5 times less than that

of the left-hand bearing. If in the interests of unification it is still preferable for both bearings to have the same size, then the position of the supports relative to the acting forces should be altered so that the load on both bearings is the same (Fig. 122c).

In a cantilevered impeller unit of a centrifugal compressor (Fig. 122d) the shaft is acted upon by radial force  $P_1$  (resulting from impeller imbalance) and axial force  $P_2$  (from the operating fluid). The design is inefficient. The front (nearest to the impeller) bearing is loaded by a large radial force  $N_1$  and axial force  $P_2$ , while the rear bearing is loaded by a very small radial force  $N_2$ . In the version shown in Fig. 122e the axial force is taken up by the rear bearing, this resulting in more uniformly distributed bearing loads. The alternative illustrated in Fig. 122f has its shaft mounted in different bearings whose capacities are consistent with the acting loads.

### 6.15. Self-Alignment Principle

In sliding mechanical connections, where distortions and deflections are possible, preliminary thought should be given to free self-alignment so that the connection works correctly with all assembly and manufacturing inaccuracies.

The most simple example is a toe bearing. If the bearing plate is rigidly mounted in the housing (Fig. 123a) the toe edges will work over the plate due to which distortions are inevitable in the system. In the design shown in Fig. 123b the plate is placed on a spherical support, which assures intimate contact along the entire friction surface, thus increasing loading capacity and durability.

The self-alignment principle is extensively used when designing shaft supports subjected to bending and distortion. Self-alignment is particularly important for plain bearings with great length-to-diameter ratios. If the mounting is rigid (Fig. 123c) the shaft's bending and distortion causes higher edge pressures thus sharply worsening bearing operating conditions. To enable self-alignment the bearings are installed on spherical supports (Fig. 123d).

In radial ball bearings (Fig. 123e) shaft flexure distorts the bearing and unilaterally loads the balls by a value which may exceed the designed load. The defect can be eliminated by placing the bearing into a spherical ring (Fig. 123f) or by applying double-row spherical bearings (Fig. 123g).

It should be noted that double-row spherical bearings have lower load capacities than the single-row radial bearings (due to the outer race shape which is unfavourable to contact strength) and cannot withstand large axial forces. For this reason when designing units intended to receive higher axial loads it is better to employ single-row bearings on spherical supports or double-row self-aligning bearings with barrel-shaped rollers.

Another example — a two-stage air compressor piston (Fig. 123*h*). Piston 1 slides in a low-pressure cylinder, while the rod slides in a high-pressure cylinder (air passages are not shown in the Figure). The defect of the system is that the piston and rod are made as one. This means that accurate alignment of working surfaces is necessary,

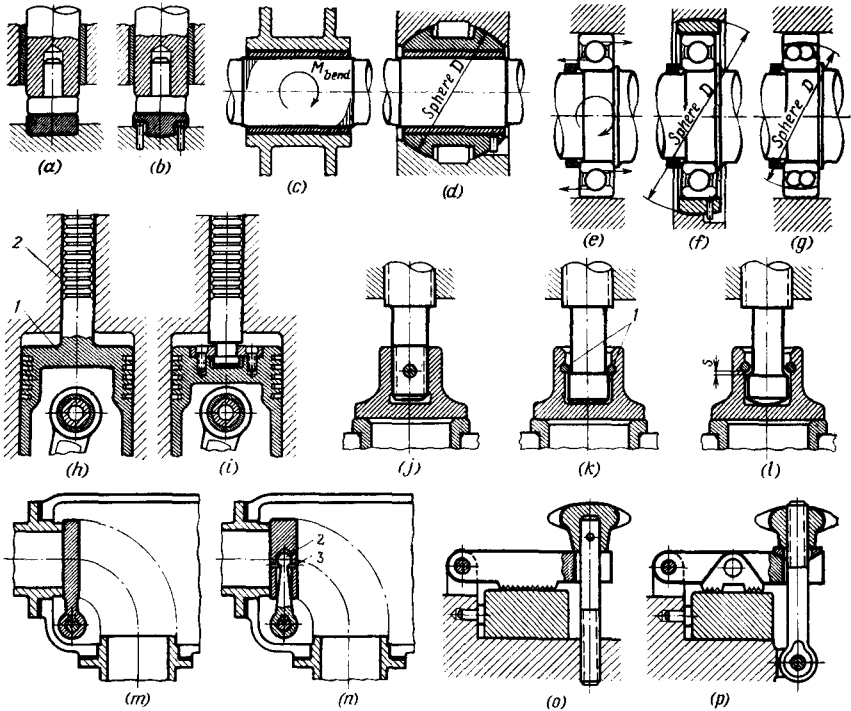


Fig. 123. Imparting self-alignment properties

i.e., those of the piston and rod on one hand and bores of the high- and low-pressure cylinders on the other. Since the clearance between the rod and high-pressure cylinder walls is much less than that between the piston and low-pressure cylinder walls, transverse drive forces are taken up mostly by the rod, which causes its excessive wear.

In the advisable design (Fig. 123*i*) the rod can deflect and move about the piston axis as it is separated from the piston. The drive forces are taken up by the piston, and the rod is relieved of transverse loads. Thus, rigorous alignment of the bores of the low- and high-pressure cylinders is now not necessary.

The plate valve design (Fig. 123*j*) in which the plate is positively fixed to the stem end fails to assure leak-tight valve-to-seat contact

because of the inevitable non-perpendicularity of the seating surface in respect to the stem axis. Another mistake is that during closure the plate rotates together with the stem relative to the seat. The latter error is eliminated in the design in Fig. 123*k* where the plate is fixed to the stem end by means of two transverse pins 1. As the valve is being closed, the stem rotates relative to the plate, however, a tight valve seating is still not achieved.

In the correctly designed version (Fig. 123*l*) the stem end is made spherical, owing to which the plate can freely self-align and seat tightly regardless of the manufacturing inaccuracies. The free self-alignment is due to clearance  $s$  between the transverse pins and the stem end shoulder.

A flap which alternately closes two pipes, square to each other (Fig. 123*m*) cannot closely seat, especially as the pipes have soft gaskets which can appreciably alter pipe positions during reassemblies. In the correct design (Fig. 123*n*) the flap is mounted on a spherical pivot 2. Moreover, it is locked endwise with transverse pins 3 and prevented from rotation about the stem axis by placing the pins in shallow holes in the stem.

In the clamp illustrated in Fig. 123*o* the clamping effort is taken, in fact, by one point of the rifled surface. Hence, the fastening bolt thread is subjected to bending.

The design version in Fig. 123*p* is free from distortions in all its links. The articulated bolt also adds to the convenience in operation.

Sketched in Fig. 124 is a wedge-type gate shutting off coaxial pipes. When the gate is rigidly fastened to the driving rod (Fig. 124*a*) it cannot be simultaneously pressed tightly against both seats; the gate self-alignment is only possible with clearances in the system and flexible deformation of the rod.

A somewhat better design is shown in Fig. 124*b*, in which the gate can freely move relative to the rod thanks to a cylindrical hinge. Here any inaccuracy in the rod position relative to the seat will in no way impair the functioning of the system. However, manufacturing inaccuracies between the gate and seat tapered surfaces, axial misalignments and pipe distortions, pipe angular displacements in the plane normal to the axis, etc., are not considered.

Figure 124*c* shows a gate composed of two halves coupled to each other and to the driving rod by a cylindrical pin. To preclude spontaneous opening of the halves with the gate up, distance springs are incorporated between the halves. The problem has been solved but partially, because the gate halves can self-align in the plane of rotation about the axis only and not in the plane running normally to the pipe axis. This drawback is eliminated by making the pin-receiving holes in the rod and eyes oval-shaped. Then (Fig. 124*d*) self-alignment is ensured in any direction (within the clearance between the pin and hole walls).

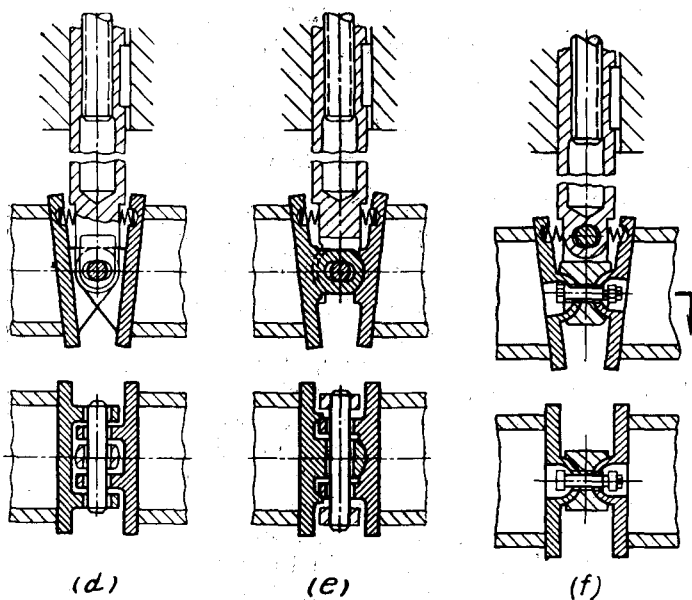
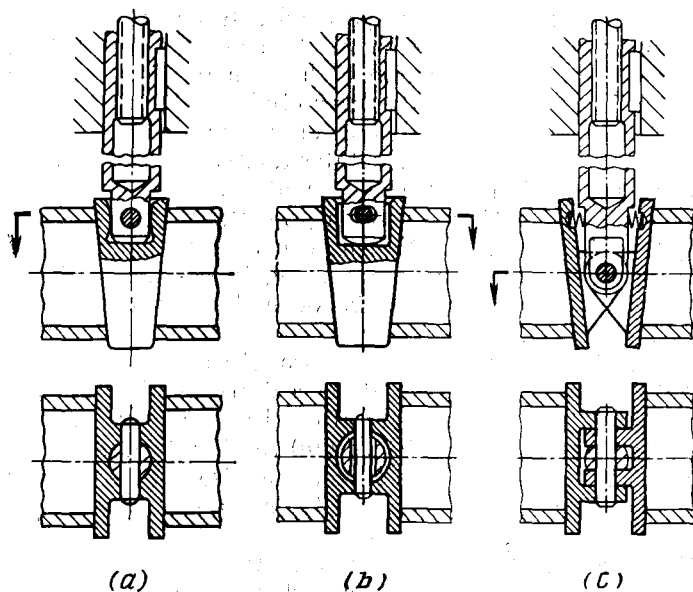
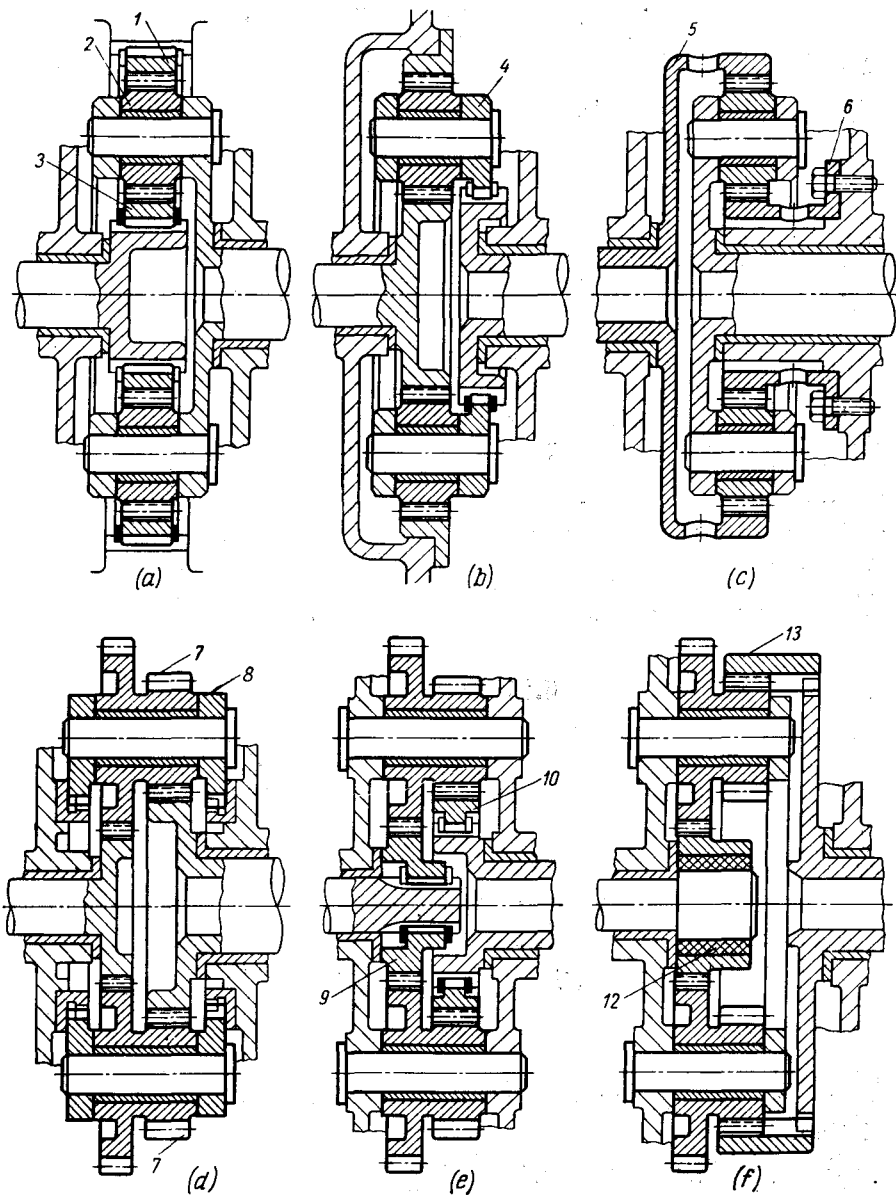


Fig. 124. Imparting self-alignment properties to sluice valve gate





**Fig. 125. Levelling out loads on gear teeth**  
 (a-c) planetary gearings; (d-f) multitrain gearings

Most correct designs are those in Fig. 124*e, f*. In the first case the eye halves are spherical and the pin which links the mechanism parts in the free state is mounted in the rod yoke. In the second case the gate halves are fixed by semi-spherical hinges at the rod head.

The self-alignment principle is utilized to equalize gear tooth loads in planetary and multiple gearings.

In the planetary gear drive (Fig. 125*a*) crown gear 1 is freely mounted on satellites 2 and prevented from rotation by a splined connection with the gearing casing. Gear 3 is also freely mounted on the splines of the driving shaft. Both these gears are free to shift (within splined connection clearances) in radial directions, thus the loads upon the satellites are balanced.

In the design shown in Fig. 125*b* self-alignment is accomplished by fitting satellite holder 4 freely on the splines of the final shaft, while in the version in Fig. 125*c* the object is achieved by imparting elasticity to the rims of gears 5 and 6.

Self-alignment in multiple gearings can be ensured by installing intermediate gear 7 (Fig. 125*d*) in cage 8 locked against rotation by casing splines; by fitting the driving gear 9 (Fig. 125*e*) and driven gear 10 on free splines; by coupling driving gear 11 with the driving shaft by means of a flexible bush 12 made of elastomer, and driven gear 13 with the final shaft, by means of splines (Fig. 125*f*).

## 6.16. Cambering

Any linear or flat contacting surface operating under load should be cambered outwards to assure central load application and eliminate excessive edge pressures caused from assembly and manufactur-

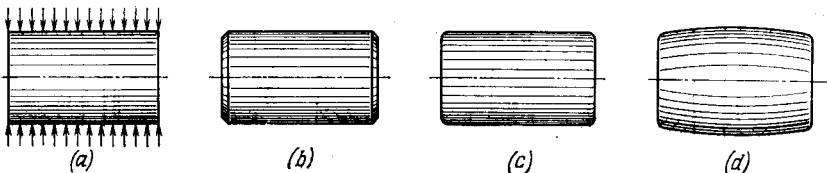


Fig. 126. Ensuring uniform contact over roll length

ing inaccuracies. The method known as cambering is extensively applied to parts working under heavy loads, rolling and sliding friction.

Figure 126 shows the application of this principle to an antifriction bearing roller. If the roller has sharp edges (Fig. 126*a*) excessive edge pressures are inevitable. Chamfering the edges (Fig. 126*b*) does not rectify the situation. The only difference is that the edge pressure is applied to dulled edges. Things are slightly better in Fig. 126*c* where the sharp edges are radiused.

In the cambered design (Fig. 126*d*) the roller has a slight barrel shape. The roller profile is either found by calculation or determined experimentally so that the load is uniformly distributed throughout the entire contact length. The difference between the maximum

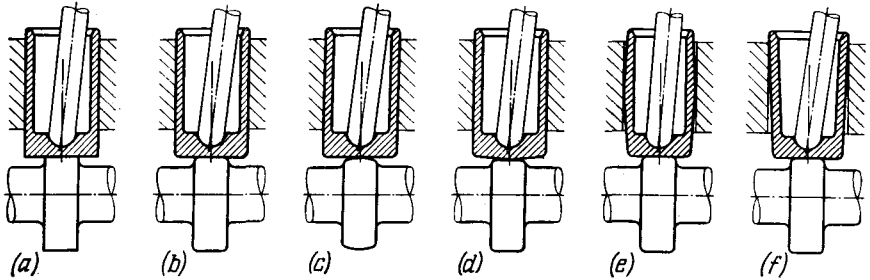


Fig. 127. Ensuring self-alignment of tappet drive unit

and minimum diameters of the roller is generally some hundredths of a millimetre.

Figure 127*a* shows an example of a cam-actuated drive of a cylindrical tappet. Sharp edges on the contact surfaces (Fig. 127*a*) are inadmissible. It is necessary, at least, to round off the end faces (Fig. 127*b*). In Fig. 127*c* the cam is cambered. It is technologically simpler to camber the working surface of the tappet (Fig. 127*d*).

In Fig. 127*e* it is the guide surface of the tappet that is cambered. With off-centre loads the tappet will self-align within certain limits, maintaining a more or less uniform contact over the working surfaces. Another way to ensure self-alignment is to make the tappet guide surface slightly tapered (Fig. 127*f*).

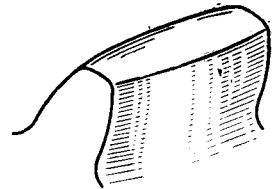


Fig. 128. Barrel-shaped tooth

Recently cambering has been rather extensively applied to gear teeth, so that excessive edge pressures in the event distortions are avoided. The teeth of a pair of gears (or one gear only) are given a barrel-like shape (Fig. 128). Such a shape is produced (provided the tooth hardness is not in excess of 40-45 Rc) by shaving on a machine tool with an oscillating table. When hard teeth are ground by dished grinding wheels (i.e., by the basic rack method) such a surface can be obtained by periodically moving the work to the grinding wheel or by oscillating the table in the feed plane.

To avoid intricate profile processing methods when cambering flat and cylindrical surfaces a method of preliminary elastic deformation is used. The technique is illustrated in Fig. 129*a-d*, where the plate of a tappet is given a slightly spherical shape. During finishing the tappet stem is clamped in

a cylindrical arbor, which causes the plate to camber inwards and assume the shape exaggeratedly illustrated in Fig. 129*b*. The working surface is then ground flat (Fig. 129*c*) and after the tappet is detached from the arbor, the plate

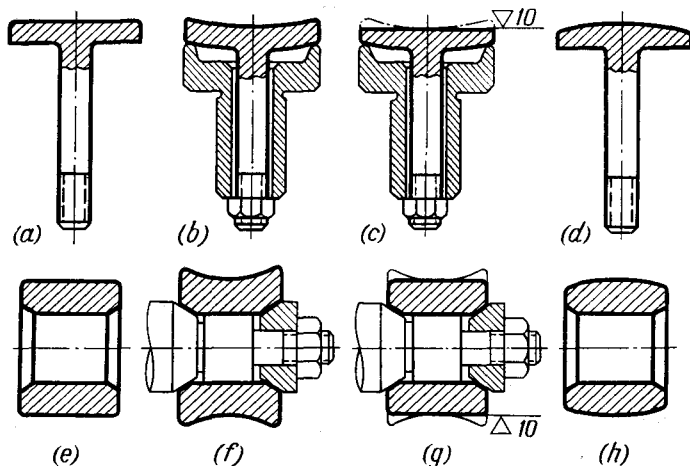


Fig. 129. Cambering procedures

straightens and assumes a slightly outward-cambered shape (Fig. 129*d*). The amount of convexity is controlled by the arbor tightening force.

A similar cambering technique as applied to a roller is pictured in Fig. 129*e-h*.

Another method is based on the application of a strictly controlled load to the finished part, which induces therein residual deformations of the required level.

### 6.17. Effect of Elasticity upon Load Distribution

Elastic deformations substantially influence load distribution and the magnitude and distribution of stresses in the body of the part. The directions of elastic deformations in the part must be precisely known and used to lower the stresses and balance the loads.

As an example Fig. 130*a* presents a splined connection unit of a gear and shaft. The gear disk is displaced relative to the splines. The torque transmitted by the gear is taken up mostly by the part of splined connection positioned at the rigidity node, i.e., in the disk plane. The qualitative picture of the bearing stress distribution over the splines working face is presented by the curve. Obviously, the stresses reach their maximum in the disk plane and are insignificant over most of the spline length. If the splines rim is inverted (Fig. 130*b*), the torque from the shaft end twists the shaft. As a result, the splines on the left of the gear come into close contact with the hub splines over their entire length and also twist the hub. Thus, the torque is transmitted more uniformly throughout the connection. In some measure the system exhibits self-levelling properties:

the greater the torque and, hence, the shaft twist, the more uniform is the load distribution along the splines.

In the press-fitted connection (Fig. 130e) the pressure on the contacting surface is concentrated [predominantly at the rigidity node, i.e., in the plane of the fitted disk. The pressure can be distributed more uniformly by placing the disk centrally and by reinforcing the hub with ribs (Fig. 130d).

Another example of using elasticity to level out force distribution is given by the seating of a column into its pedestal. With the usual design (Fig. 131a) the bulk of the load is applied at the rigidity node, namely, at the transition section where the flange meets the column body.

If the flange support surface is made slightly conical (Fig. 131b), the flange rim will first touch the bearing surface and then, during tightening, will elastically deform and distribute the tightening force more uniformly over the bearing surface. The joint, as a whole, obtains greater rigidity and steadiness.

Figure 131c, d shows a method of strengthening the fastening of a turbine blade in a fir-tree-shaped rotor slot. In the design shown in Fig. 131c the working surfaces of the blade's trapezoidal teeth, taking up centrifugal force  $P$ , in the initial position contact the rotor slots thrust faces. With the centrifugal force applied the blade root extends, while the rotor body deforms to a lesser degree, thanks to its greater rigidity. Due to this the load is taken mainly by the first teeth (see the curve).

In Fig. 131d the blade teeth fit the slots with clearances  $h_1$ ,  $h_2$  and  $h_3$  which increase successively from the root to the blade platform. As the blade extends, the working surfaces of the teeth successively contact the rotor slots thrust faces, thus a more even load distribution among the teeth results and, consequently, the connection becomes stronger.

In practice, when dealing with fir-tree-shaped connections, allowances should be made for thermal deformations due to the non-uniform blade heating in the interblade rotor sections and for the creep of the blade root.

In conventional threaded connections (Fig. 132a) the thread load distribution is uneven. This condition is aggravated by the fact that the elastic deformations of the bolt and nut differ in direction; the bolt elongates by a value  $f_1$  under the action of tightening forces and operating loads and the nut contracts by a value  $f_2$ . As a result, the first threads of the bolt (from the nut bearing surface) under load tighten onto the first threads of the nut (Fig. 132b) and take up most of the load. Both theoretical and experimental data proves that the first thread carries approximately 30% of the total load.

Recently efficient methods have been devised which enable the load to be equalized throughout the thread by correcting the thread

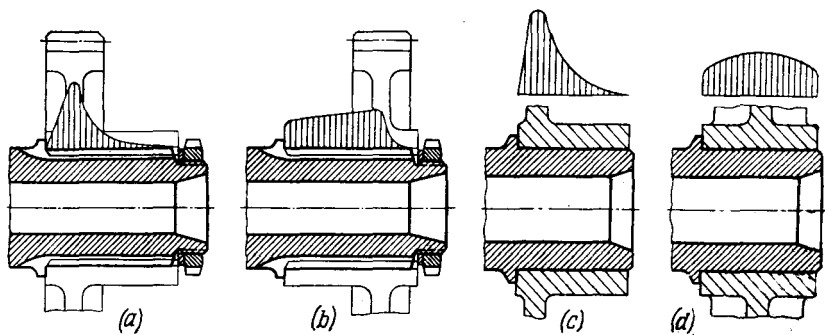


Fig. 130. Effect of elasticity on load distribution

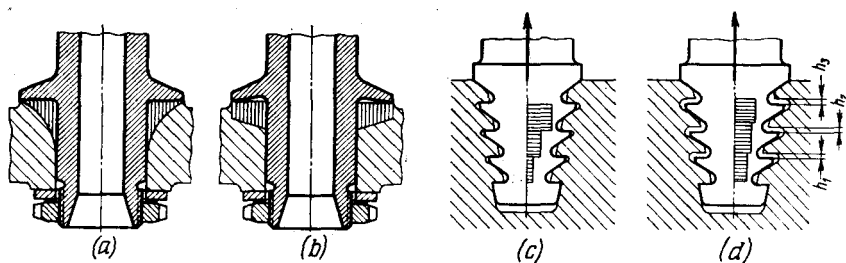


Fig. 131. Effect of elasticity on load distribution

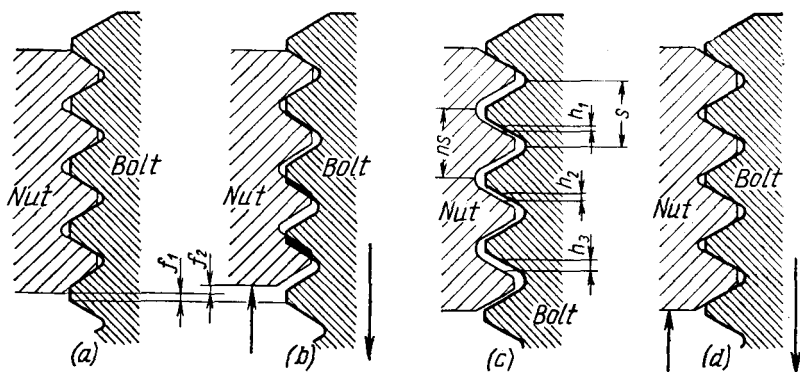


Fig. 132. Distribution of loads in screwed connections

geometry. The simplest of these methods consists in making the nut thread pitch larger than that of the bolt by a factor that depends on the magnitude of the acting force established either by calculations or experimentally. On the average this factor varies from 1.002 to 1.004. In screwed connections with usual pitches (1-2 mm) the difference between the nut and bolt pitches is 3-5  $\mu\text{m}$ . Furthermore, increased radial clearances are provided in such connections in order to ensure self-alignment of the nut relative to the bolt and the bearing surface. In the free state the bolt topmost thread contacts the topmost thread of the nut (Fig. 132c) and progressively increasing axial clearances  $h_1$ ,  $h_2$  and  $h_3$  are formed between the adjacent threads. As soon as a load is applied, the bolt elongates and the nut

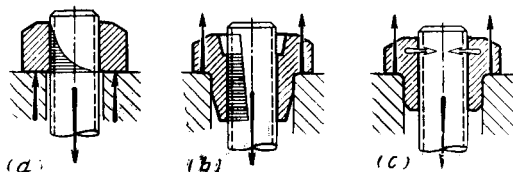


Fig. 133. Nut designs

contracts, thus the bolt threads tighten successively onto the threads of the nut (Fig. 132d). With a correctly chosen pitch difference the load will be taken up by all the threads. Uniform loading can be assured only at a certain design magnitude of the force acting on the joint. But even with forces close to the above the load is distributed more evenly along the threads than with threads of the same pitch.

Another method is based on reversing the direction of the nut deformation. If the threaded section is subjected not to compression (Fig. 133a) but to tension (Fig. 133b), then the first nut threads acted upon by the load shift in the same direction as those of the bolt. As a result, the load is distributed more uniformly over the threads. Such nuts are called tension nuts.

In a semi-tension nut (Fig. 133c) the bearing surface is positioned approximately in the middle of the screwed section whose lower part takes up tensile stresses. To involve into efficient use the upper threads, it is necessary to utilize the effect of elastic deformation of the nut upper portion. The forces acting upon the bearing surface cause a radial deformation of the nut body (in the direction shown by light arrows) and, as a result, squeezing of the upper bolt threads. Today both tension and semi-tension nuts are widely used in critical screwed connections.

The profile of a tension nut with a uniformly distributed load is determined proceeding from the following considerations. Let the length of the threaded nut section be  $h$  (Fig. 134a). For uniform distribution of thread load the tensile force acting upon the nut in any section at a distance  $x$  from the thread start

must be

$$P_{nut} = P \frac{x}{h} \quad (6.8)$$

where  $P$  is the force applied to the bolt.

The tension force acting upon the bolt in the same section

$$P_{bolt} = P - P_{nut} = P \left(1 - \frac{x}{h}\right) \quad (6.9)$$

For deformation compatibility the relative elongation of the nut in any section must be equal to that of the bolt

$$\frac{P_{nut}}{E_{nut}F_{nut}} = \frac{P_{bolt}}{E_{bolt}F_{bolt}} \quad (6.10)$$

where  $F_{nut}$ ,  $F_{bolt}$  and  $E_{nut}$ ,  $E_{bolt}$  are the cross-sectional areas and moduli of elasticity for the materials of the nut and bolt, respectively.

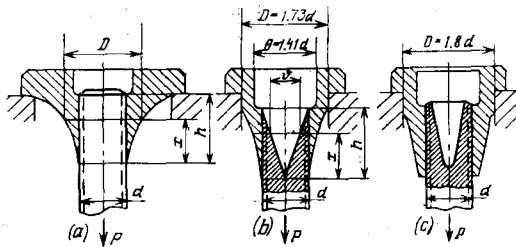


Fig. 134. Determination of tension nut profile

Substituting in Eq. (6.10) the values of  $P_{nut}$  and  $P_{bolt}$  from Eqs. (6.8) and (6.9), we obtain

$$F_{nut} = F_{bolt} \frac{x}{h-x} \cdot \frac{E_{bolt}}{E_{nut}}$$

If the nut and bolt are made of same material ( $E_{nut} = E_{bolt}$ )

$$F_{nut} = F_{bolt} \frac{x}{h-x} \quad (6.11)$$

Substituting in Eq. (6.11) the values  $F_{bolt} = 0.785d^2$  and  $F_{nut} = 0.785 \times (D^2 - d^2)$ , where  $d$  is the bolt diameter and  $D$  running external diameter of the nut, we get

$$D = d \sqrt{\frac{h}{h-x}} \quad (6.12)$$

When  $x = h$ , diameter  $D = \infty$ .

Obviously, this condition can only be approximated. For any finite nut diameter (where the thread plane finishes) the upper threads will be loaded more than the lower ones.

Uniform distribution of thread loads can be achieved by increasing the bolt end compliance. Let a conical recess be made in the bolt stem (Fig. 134b) so that its peak begins in the same plane as the thread. The running diameter  $\phi$  of the recess is

$$\phi = d \frac{x}{h}$$

where  $d$  is the initial recess diameter (assumed to be equal to that of the bolt).



The running cross-sectional area of the bolt is

$$F_{\text{bolt}} = 0.785(d^2 - \theta^2) = 0.785d^2 \left[ 1 - \left( \frac{x}{h} \right)^2 \right]$$

Substituting this relation in Eq. (6.11) gives

$$D = d \sqrt{\frac{(h+x)x}{h^2} + 1} \quad (6.13)$$

When  $x = h$ , diameter  $D = d\sqrt{3} = 1.73d$ .

This nut shape can be realized in practice.

The cross-section of the nut above the threaded portion is determined from the equal strength condition for the nut and bolt in tension

$$F_{\text{nut}}^* = F_{\text{bolt}} \quad (6.14)$$

Let the diameter of the recess in the nut above the threaded portion be  $\theta$ . Then, according to Eq. (6.14)

$$0.785 [(1.73d)^2 - \theta^2] = 0.785d^2$$

whence

$$\theta = d\sqrt{2} = 1.41d$$

Figure 134c shows a design approximation of the theoretical nut and bolt shapes, where the load is uniformly distributed along the threads.

Figure 135 illustrates how a heavily loaded screwed connection (namely, a propeller blade fastening unit) can be rationally redesigned.

The factor of elasticity must necessarily be taken into consideration when designing bearing units. Figure 136a, b shows a paired installation of antifriction bearings. In Fig. 136a the greater part of the load is taken up by the bearing positioned in the rigidity node (housing wall plane). The other bearing mounted at the hub end is lightly loaded because of the hub being compliant. The bearing loads can be evenly distributed (thus contributing to a better load-carrying capacity of the unit as a whole)

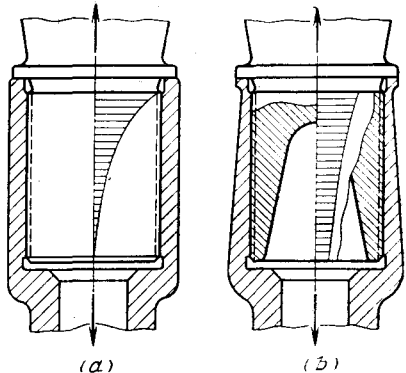


Fig. 135. Reinforcement of propeller blade fastening

if the hub end is stiffened with another web (Fig. 136b).

Another example of elasticity utilization is given in Fig. 136c in which the bearings are installed in a thin-walled steel bush. Thanks to the elasticity of the bush the system can adapt itself to shaft distortions, and resembles a system which has bearings mounted in a spherical support.

Thus, by utilizing elasticity one can obtain optimum distribution of load between bearings. In the bearing unit loaded with radial

force  $P$  and unilateral axial load  $Q$  (Fig. 136d) it is better to distribute the load according to the bearings function: one of the bearings should be loaded with the radial force and the other, with the axial

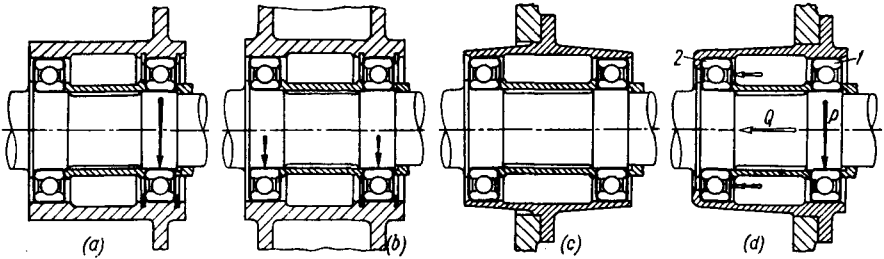


Fig. 136. Effect of housing elasticity on load distribution in paired bearing installation

force. This can be realized by mounting the bearings in an elastic cantilever-type bush. Bearing 1 located in the rigidity node (i.e., in the fastening flange plane), takes the radial load. Bearing 2, mounted at the cantilever end receives axial load only.

### 6.18. Fitting to Several Surfaces

It is good practice to avoid, whenever possible, fitting parts to several surfaces (Fig. 137a, b). As a rule, parts should be fitted to one

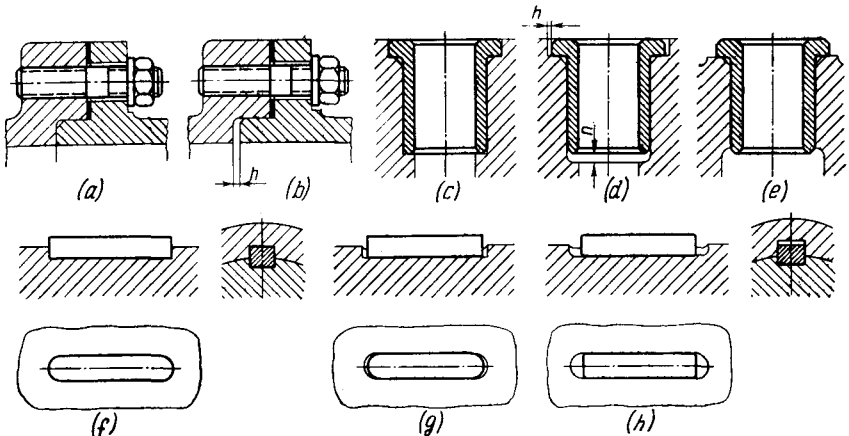


Fig. 137. Matching of surfaces

surface, while for other surfaces clearances  $h$  (Fig. 137b, d) must be provided. These clearances must be sufficient to exclude contact of surfaces under the conditions of any possible inaccuracy of produc-

tion, elastic deformations, thermal expansion of the system or under compression of sealing gaskets.

Rough errors, like those sketched in Fig. 137*a, c*, are only characteristic of inexperienced designers. Still more typical errors include superfluous fitting or alignment, etc. For example, fitting a prismatic loose key throughout the entire contour of the keyway (Fig. 137*f*) will heavily, and, which is still more important, quite unnecessarily complicate the production. It is more reasonable to fit the key to the working edges only, providing clearances on the key end faces, as well as between the key top surface and the keyway bottom (Fig. 137*g, h*).

### 6.19. Tightening Up on Two Surfaces

Occasionally it may be necessary, due to some design features, to tighten a unit of two surfaces. Figure 138 (tightening three flanges) reviews techniques applied under these conditions.

Simultaneous and uniform tightening of all surfaces (Fig. 138*a*) presumes] that the end flange faces should be machined together

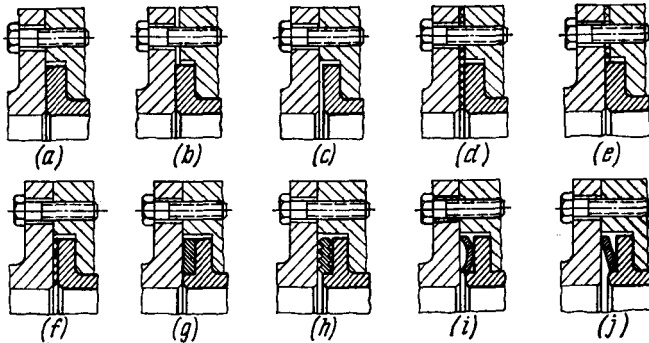


Fig. 138. Tightening against two surfaces. Fastening of intermediate flange

and fitted or have undergone extremely accurate manufacture. If a flange protrudes from its recess (Fig. 138*b*), an interference may occur and the tightened part will bend. On the other hand, if the flange is sunk in its recess (Fig. 138*c*), the flange axial fixing will be lost.

The introduction of elastic gaskets (Fig. 138*d-f*) improves the design and seals the joint if the gasket is sufficiently thick and flexible and overlaps non-flush sealing surfaces.

Whenever the good sealing and accurate axial fixing of a flange are necessary, it is recommended to employ gaskets of some soft metal (red copper, lead, aluminium, etc.) whose thickness exceeds the depth of the recesses where the gaskets are to be fitted. During

tightening the metal gasket plastically deforms (Fig. 138g), seals the joint and fixes the flange. Some space must be provided to enable excessive metal to freely flow out. The bearing stresses arising in the gasket under the action of working axial forces must be below the yield point of the gasket material. Otherwise, accurate axial fixing will be lost.

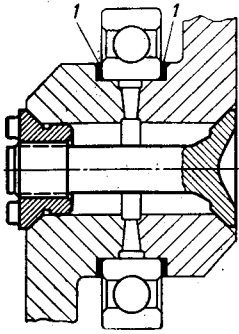


Fig. 139. Tightening against several surfaces. Two-part crank journal

If harder metals (brass, bronze, low-carbon annealed steel) are used for the gaskets, these must be made corrugated or comb-like (Fig. 138h) to assure plastic deformation. Spring gaskets (Fig. 138i, j) are also applied.

Figure 139 shows two-piece crank connected in a main journal by means of triangular-shaped end-face splines, an antifriction bearing being simultaneously clamped between the two parts of the crank. The tightening of the splines and inner bearing race in this case is ensured on the account of the deformation of metallic rings 1 placed on either side of the inner race.

## 6.20. Axial Fixing of Parts

Parts must be fixed axially at one point so that they can freely self-align throughout their length. If, for instance, a pin is fixed by self-tapping screws at both supports (Fig. 140a) then additional stresses are likely to occur as a result of thermal dimensional changes. In the correct design shown in Fig. 140b only one end of the pin is fixed, while the other end is free to move in its support.

In the badly designed herringbone gearing (Fig. 140c) the lower gears are fixed in position twice: by their teeth and stops *m*. To obtain the complete coincidence of fixing positions is impossible. The error can be eliminated by providing clearances *s*, which assures gear self-alignment by their teeth (Fig. 140d).

The gear shaft mounted in plain bearings (Fig. 140e) is fixed in two points spaced far away from each other.

Accurate fixing in this case is impossible because a large clearance must be provided between fixing surfaces in order to avoid seizure of bearing surfaces due to thermal expansion of the housing. Furthermore, due account must be taken of the inevitable inaccuracies of manufacture and assembly due to the required clearances between mounting surfaces.

The design is somewhat improved by bringing the fixing surfaces closer together (Fig. 140f). In the correct designs (Fig. 140g, h) the shaft is fixed over a short distance (in the design presented in Fig.

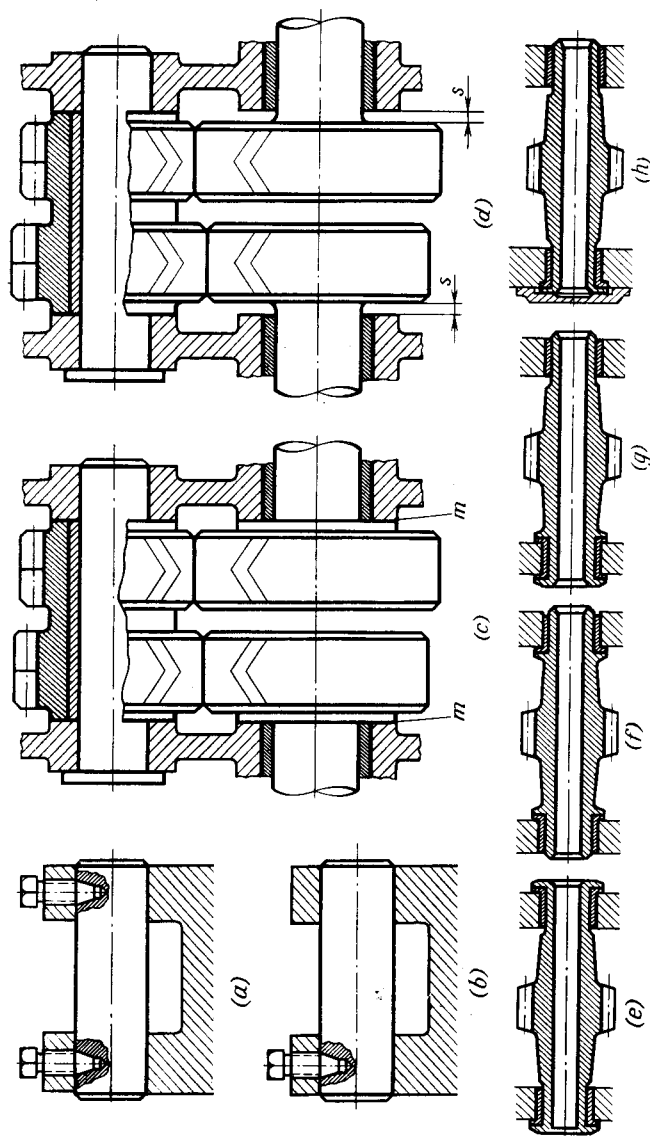


Fig. 140. Axial fixing of parts

140*h* it is fixed practically in one plane); the other end of the shaft is allowed to self-align in its support.

Free areas of parts must be given certain margins for self-alignment and compensation for manufacturing dimensional inaccuracies. Let us consider the case of a shaft installed inside a housing on antifriction bearings. In the design illustrated in Fig. 141*a* the axial dimensions, predetermining the mutual location of the shaft, bearings and housing, are held to the nominal size. In the alternative

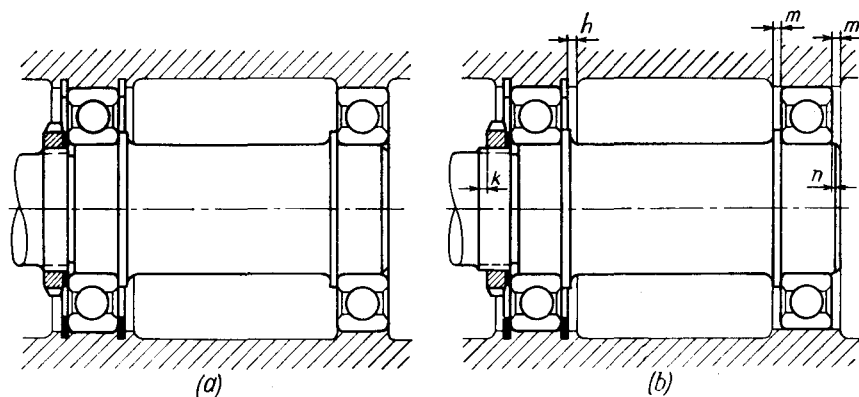


Fig. 141. Introducing margins on fitting surfaces

pictured in Fig. 141*b* the following clearances are provided:  $m$  — on the fitting surface of the housing to suit the floating bearing;  $h$  — on the fitting surface of the housing relative to the fixing stop rings;  $k$  — in the thread for the fastening nut;  $n$  — on the fitting surface of the shaft to suit the floating bearing.

The clearance values are found by calculating the dimensional chains and thermal expansions in the system. The maximum clearances should be provided in the areas of transitions to black cast surfaces where dimensional variations are particularly great (for medium-sized castings of moderate accuracy such clearances are taken at 3-4 mm).

### 6.21. Control of Direction

Parts reciprocating linearly along two guideways should be guided along one way only, the other guide only supporting the part (Fig. 142*b, d*). A simultaneous guiding along two ways (Fig. 142*a, c*) means much more stringent machining requirements to the guides and ways. Any change in temperature conditions may impair orientation and, hence, the part may seize in its guideways.

If the use of two guideways is inevitable, their manufacture must be simplified as much as possible. In a design with two guiding rods (Fig. 143a) the necessity to accurately keep the centre distance between the rod sockets in the driven part and the guiding holes in the

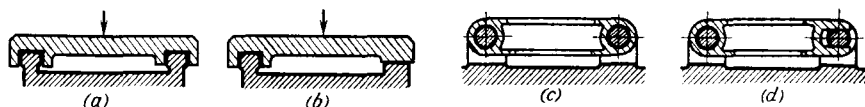


Fig. 142. Guiding of parts  
(a) and (e) wrong; (b) and (d) correct

housing can be eliminated by increasing the diameter of the sockets (Fig. 143b) and fixing the rods in their sockets after aligning them with the guiding holes. Another method consists in machining the

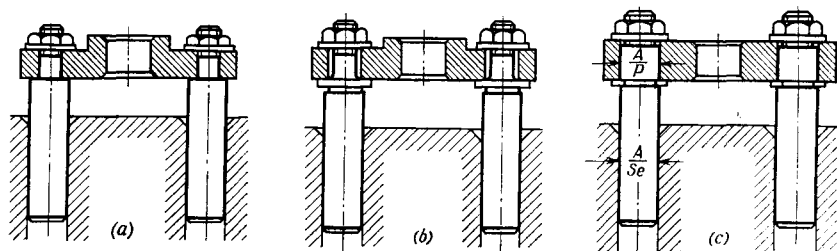


Fig. 143. Ensuring accurate guidance over two surfaces

rod sockets and guiding holes together. In this case the diameters of the guiding holes and the rod sockets must be the same (Fig. 143c). However, different fits for the rods are required, namely a sliding fit in the housing and an interference fit in the rod sockets.

## 6.22. Mounting Surfaces

Generally speaking, any mounting surface for detachable parts should be flat. Fastening on cylindrical surfaces should be avoided (Fig. 144a). The manufacture of such connections is labour consuming. The fitting surface of the detachable component must be machined in a fixture to assure the equality of the diameters of the mounting surfaces on the part and housing and it is rather difficult to uniformly tighten angularly-spaced bolts. The correct design with a flat mounting surface is pictured in Fig. 144b.

Sometimes it may be necessary to fasten parts to surfaces positioned at an angle to one another (Fig. 144c).<sup>†</sup> The connection seems strong and rigid. Its manufacture, however, is difficult as it is

absolutely necessary to keep the angular equality between the fitted part and housing to preclude the deformation of the part during fastening. Fastening bolts must be alternately tightened and each time by small amounts in order to assure the close fitting of the part to both mounting surfaces. Obviously, a design with a plane mounting surface is much more preferable (Fig. 144d).

Flat attachment is of particular importance when air-tight connections have to be obtained. Sealing surfaces must be free of any

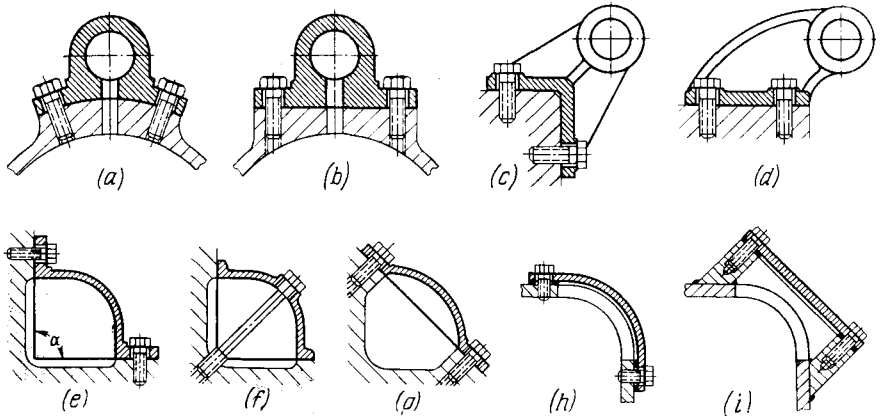


Fig. 144. Clamping on curved surfaces

steps, as well as of outer or inner corners. Fitting to curvilinear surfaces is inadmissible. An example is presented in Fig. 144e, which shows a cover enclosing an angular space in a housing. The design has two defects. First, it is practically impossible to seal off the space end walls forming reentrant angle  $\alpha$ . Secondly, the proper tightening of the cover is made impossible by the fact that screwing up one row of bolts will interfere with screwing up the other row of bolts. The latter of these two defects is eliminated in the design pictured in Fig. 144f where the cover is tightened up by a row of diagonally arranged bolts. This technique is rather common in fastening shields over spaces which do not require sealing, and also when enclosing through tunnels. Should the air-tightness be necessary, the only correct solution will be that illustrated in Fig. 144g where the cover is fitted on a flat surface.

Also erroneous is the design of a cover intended to enclose a hatch in the corner of a welded sheet-steel housing (Fig. 144h), since it is practically impossible to provide close tightening over a curvilinear surface even when using a thick gasket. A correct design sketched in Fig. 144i incorporates a flat frame welded to the hatch and forming a flat fitting surface.



### 6.23. Butt-Jointing on Intersecting Surfaces

Butt-jointing on intersecting surfaces complicates the manufacture and sealing of joints.

An incorrect joint design is pictured in Fig. 145*a*. Here the side cover *I* is mounted upon the joint of the housing and the upper

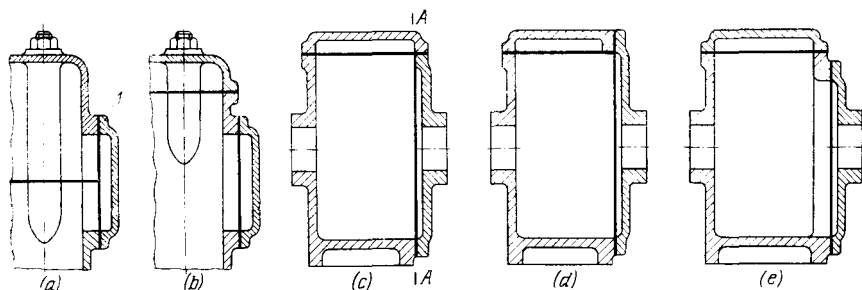


Fig. 145. Fitting on intersecting surfaces

cover, which means that its fitting surface must be machined after the assembly of the housing and the upper cover, and to assure the tightness of the joint, a thick elastic gasket must be used. In

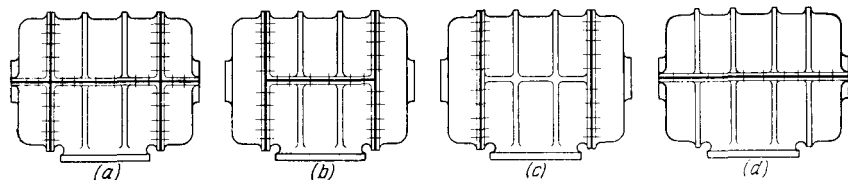


Fig. 146. Methods of fastening split housings

the correct design shown in Fig. 145*b* the housing-to-upper-cover joint is moved beyond the side cover.

A non-technological design is that of a housing made up of two halves joined in vertical plane *AA* (Fig. 145*c*). The upper cover is mounted on the joint of the halves. Still worse is the design in Fig. 145*d* where the cover is joined with the housing halves in two mutually perpendicular planes. In the correct design (Fig. 145*e*) the joint surfaces are separated.

Figure 146*a* shows a rotor machine housing split in the horizontal plane with two end covers also split horizontally, which makes the joint sealing difficult. The slightly improved version in Fig. 146*b* has solid end covers. The best designs have either a housing and covers (Fig. 146*c*) joined in vertical planes (axial assembly), or a housing (Fig. 146*d*) split in the horizontal plane (radial assembly).

### 6.24. Interchangeability of Rapidly Wearing Parts

It is good practice to manufacture any rubbing or rapidly wearing part of a machine component as an easily interchangeable piece. The latter can be made of a material with special properties which are absent in the basic material of the component.

Figure 147a illustrates a T-slot made in the body of a cast-iron bed. To provide for machining convenience, longer service life

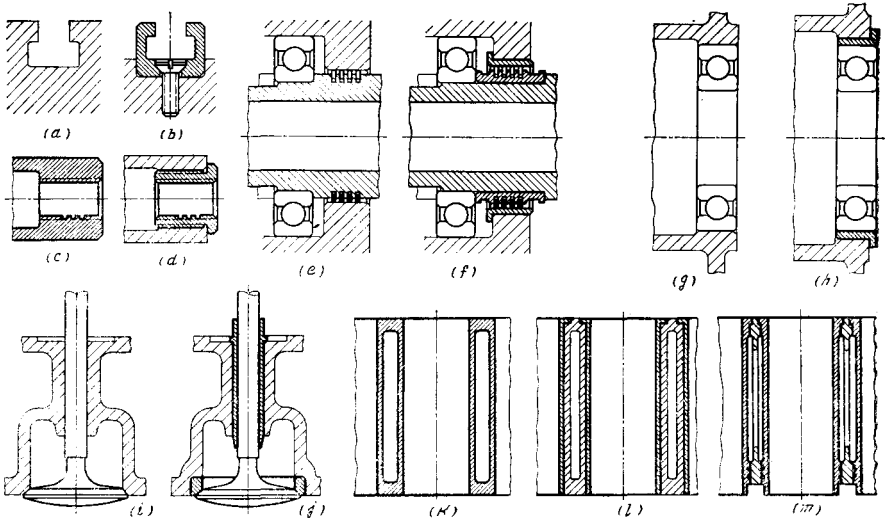


Fig. 147. Introduction of replaceable parts

and changeability it is advantageous to make the T-slot as a separate piece from some durable material and to fasten it to the bed, e.g., in a slot (Fig. 147b).

To ensure reliable operation of the threaded pair in an internally threaded steel rod for a lead screw (Fig. 147c), it is advisable to use a bronze bush (Fig. 147d) which possesses antifriction properties and can easily be changed.

Figure 147e illustrates an erroneously designed seal with split spring rings fitted in shaft grooves, the external cylindrical surfaces of the rings sealing against the housing. When the grooves in the shaft and the hole in the housing get worn, both these expensive components have to be rejected. In the correct design (Fig. 147f) the rings are assembled in a changeable bush and work in a sleeve made from a harder material.

When installing an antifriction bearing in a light-alloy housing (Fig. 147g) the seating surface rapidly crushes during operation. Machining the hole even slightly oversize causes the rejection of

the entire housing unit. In the correct design (Fig. 147h) the bearing is installed in an intermediate bush made from a harder material, which reduces the seat wear and enables defective housings to be rectified.

To install the valve of an internal combustion engine in the manner depicted in Fig. 147i, i.e., directly in a cast iron head, is bad practice. It is better to install the valve in a guide bush made of a harder material (Fig. 147j) and introduce an insert-type seat of a heat-resistant material.

Figure 147k-m shows a water-cooled engine block. If the cylinder working surfaces are machined directly in the cast block (Fig. 147k) the design is bad. To obtain high-quality mirror-finish bores in a large casting is difficult. Furthermore, the cylinder walls may have defects (blisters, voids, pits, etc.) which sometimes are exposed only during finish machining. Clearly, a single defective cylinder means rejection of the whole block. Finally, excessive wear in one of the cylinders during operation means failure of the entire expensive unit.

The correct solution is to use insert liners (Fig. 147l). The best design has wet liners which are directly surrounded by water (Fig. 147m). This system has significant additional advantages: simpler casting techniques, reduced weight and better cooling of the cylinders.

## 6.25. Accuracy of the Alignment of Parts

Parts requiring accurate mutual location are preferably installed in one housing with a minimum number of transitions and fits.

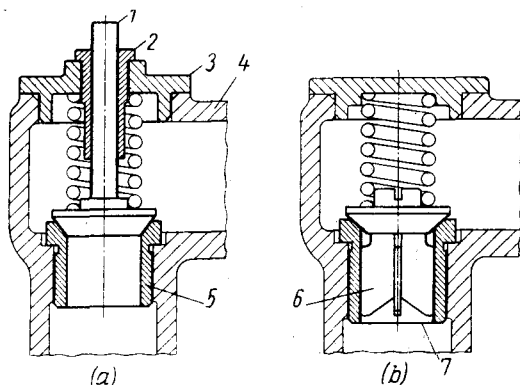


Fig. 148. Reduction valve design

For example, let us take a reduction valve unit (Fig. 148). The most important factor predetermining the reliability of the unit is the fitting of the valve tapered chamfer on the seat. In our exam-

ple it is accomplished with a number of transitional connections, each being the source of inaccuracies, namely:

- running fit between valve stem 1 and guide bush 2;
- press fit between bush 2 and cover 3;
- slide fit between cover 3 and casing 4;
- press fit between valve seat 5 and casing 4.

The design requires accurate alignment of the following elements:

- in the valve—guide surface and bevelled edge of the plate;
- in the bush—bore and seating surface;
- in the cover—hole and centring shoulder;
- in the casing—centring bore for the cover and hole for the seat;
- in the seat—chamfer and seating surface.

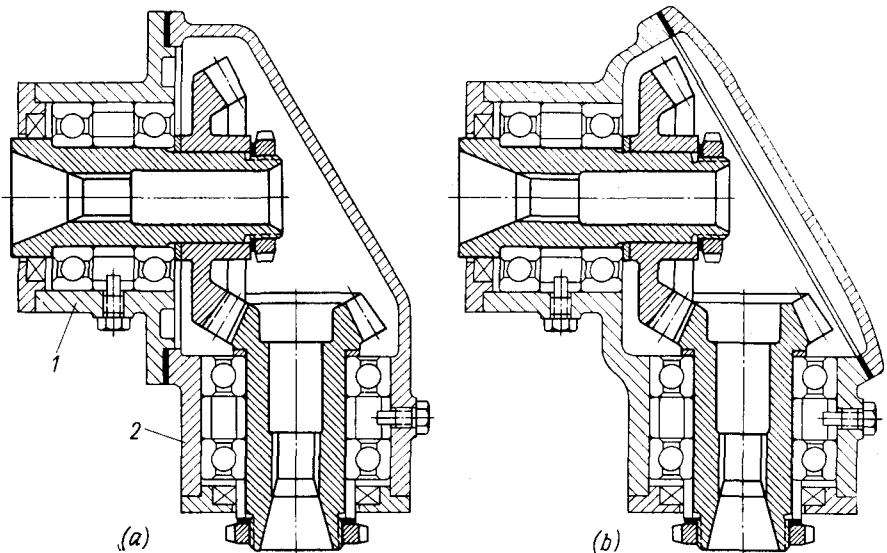


Fig. 149. Angle gear drive

When being ground-in to its seat, the valve is centred in guide bush 2. The seal obtained by the grinding-in procedure is spoilt during reassembly because of the displacement of cover 3 in relation to casing 4.

In the rational design (Fig. 148b) the valve is centred directly on the seat. The accuracy of the valve motion is now dependent on a single joint only, i.e., on the slide fit of guide shank 6 in seat 7 of the valve.

In this case strict alignment of the following elements will assure good functioning of the unit:

- in the valve—guide surface of the shank and chamfer;

in the seat—chamfer and seating surface.

The remaining elements can safely be manufactured to lower standards of accuracy.

In the grinding-in process the valve is centred in its seat and reassembly does not destroy the seal obtained by the grinding-in process. Another example is an angle gear drive. In the design shown in Fig. 149*a* the gears are installed in different housings 1 and 2, which hampers the manufacture. The joint surface of housing 2 must be machined strictly parallel to the pinion axis. Nevertheless, the mounting accuracy is disturbed when the sealing gasket in the joint is tightened. Another defect is the obstructed access to the gears. The axial position of the gears can be adjusted only by blacking-in in several repetitive tests, the gear being detached each time. The adjustment accuracy may be impaired during reassemblies due to a non-uniform tightening of the gasket.

With the gears installed in one housing, their positional accuracy is not disturbed during installation and subsequent reassemblies (Fig. 149*b*). The gears can now be easily inspected during assembly. The gears' engagement adjustment is greatly simplified.

## 6.26. Relief of Precision Mechanisms

Precise moving connections and mechanisms should be relieved from the action of external forces which may cause excessive wear or disturb the correct working of the mechanism. The working surfaces when in use must be protected against extraneous forces and negligent treatment.

Figure 150*a* illustrates a conical plug-type cock with a handle provided directly on the plug shank, which is wrong for the following reasons: the effort exerted in turning the handle is taken up by the cock ground-in surfaces; occasional impacts against the handle may spoil the sealing surfaces. Furthermore, an inexperienced operator may pull the cock handle axially, thus injuring the tightness of the cock. The self-alignment of the plug in the conical seat is hampered by the fact that the shank should simultaneously be centred in the cock cover.

In the design presented in Fig. 150*b* the driving shaft with the handle are mounted in a separate body and spline-connected with the plug. Here the plug is relieved from external forces and can self-align in its seat.

This design has an additional improvement: the axial position of the plug is adjusted by pressure screw 1. At the beginning the screw is loosened, allowing the plug (actuated by a spring) to tightly fit its seat. Then the screw is slightly screwed in, thus slightly lifting the plug. This hardly impairs the tightness, but enables the cock to be turned much easier. As the plug wears down, the adjustment is repeated.

In the design of a flat face slide valve illustrated in Fig. 150c the tightness may easily be spoiled by depressing inadvertently the handle and thus displacing the slide valve away from the surface being sealed. The defect is eliminated if the driving shaft and the valve are separated (Fig. 150d).

In the unit of a distributing cam-operated slide valve (Fig. 150e) the actuating forces from the cam are taken up by accurately ground-in surfaces of the slide valve. During operation these surfaces

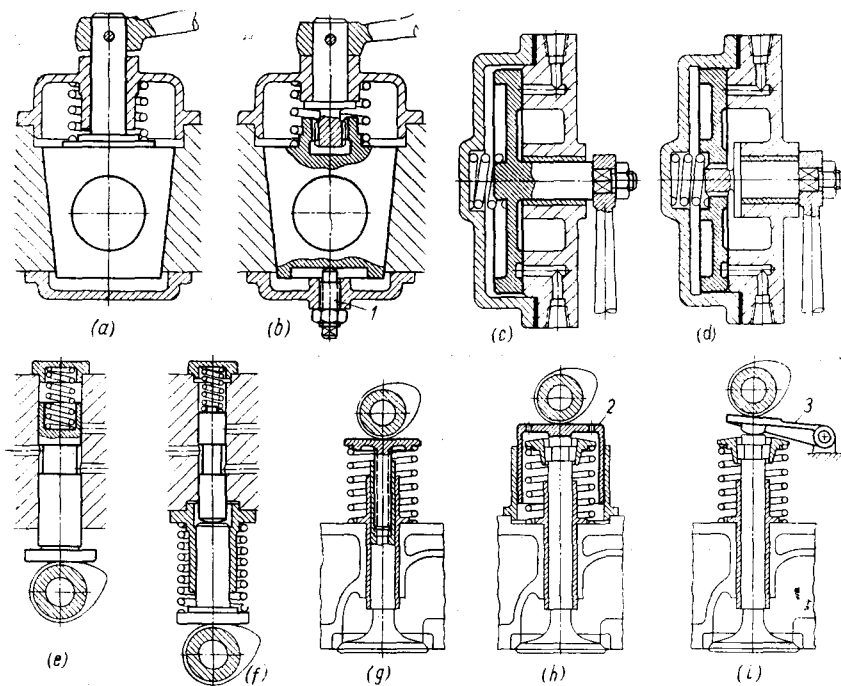


Fig. 150. Relieving mechanisms from extraneous forces

wear down. In the better alternative (Fig. 150f) the drive forces are taken up by an individual tappet, hence the slide valve is relieved from the action of the transverse forces and the wear on the sealing surfaces is reduced to the minimum.

Another example is the drive of an internal combustion engine valve. In the version presented in Fig. 150g the cam acts directly on the plate which is screwed into the hollow valve stem. As the valve opens, the cam runs against the plate and the valve distorts (within the guide clearance); the sealing chamfer of the head leaves its seat and forms a crescent-shaped slit. This is particularly dangerous with exhaust valves because a jet of hot gases gushes through

the slit, causing a one-sided erosion and burning of the valve. When the cam runs off the plate, the valve rests sideways in its seat. Consequently, the wear of the valve sealing chamfer and seat occurs on one side.

In the design shown in Fig. 150*h* the transverse force components are taken up by intermediate sleeve 2, so that the valve is acted upon by an axial, centrally-applied force. The increase in the mass of the reciprocating parts means some limitation to the engine speed. This defect is eliminated in the design depicted in Fig. 150*i* where the valve is driven through intermediate lever 3. Now the valve is practically relieved from the action of transverse forces (not as fully as in Fig. 150*h*).

### 6.27. Coupling Parts Made from Hard and Soft Materials

Frictional units incorporating parts made from hard and soft materials must be designed so that the rubbing surface of the harder and more wear-resistant material overlaps completely the rubbing surface of its mating member made of a softer and less wear-resistant material. Observation of this rule assures a uniform wear of the

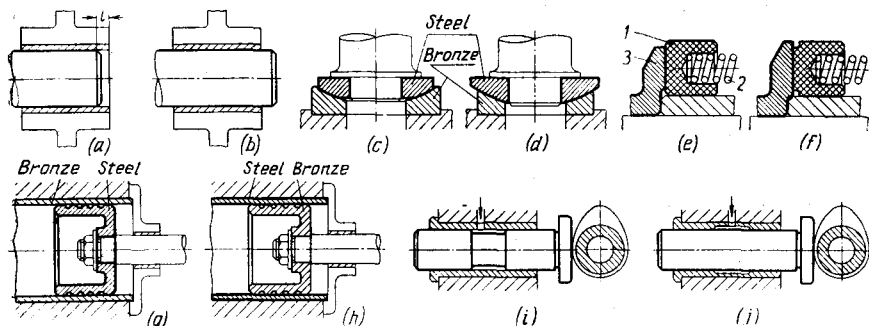


Fig. 151. Combination of parts made from materials of different hardness

softer part. If the soft surface overlaps the harder one, a stepped worn spot appears which impairs the operation of the unit.

Let us now examine this fact through examples. In the end trunnion bearing installed in a bronze bush (Fig. 151*a*) the trunnion end is shorter than the bush. After wear, part  $l$  of the bush will be stepped and hinder the axial self-alignment of the trunnion. It is also incorrect to hold the axial dimensions to the nominal sizes, for manufacturing errors, assembly inaccuracies, as well as thermal deformations in the system may produce a displacement of the trunnion end inward of the bearing with the same result as previ-

ously. In the correctly designed version (Fig. 151b) the trunnion projects beyond the bush for a distance, which allows all possible variations of the longitudinal dimensions to be catered for.

In the self-aligning spherical footstep bearing (Fig. 151c) the rubbing surface diameter of the steel disk is less than that of the bronze support. Eventually the disk will inevitably wear steps in the bronze support, thus obstructing the shaft self-alignment. The correct design is shown in Fig. 151d.

A wrongly designed face-type mechanical seal is pictured in Fig. 151e, in which an immovable textolite bush 1 is pressed by springs 2 against a hardened steel disk 3 rotating together with

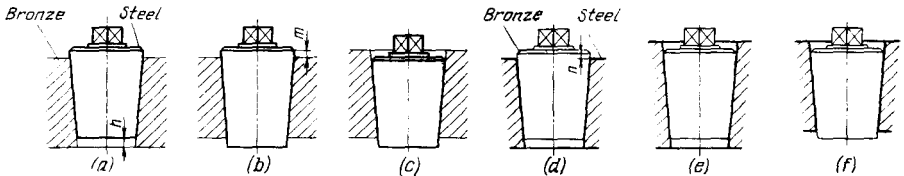


Fig. 152. Design versions of conical stop cocks

the shaft. Here the frictional surface of the steel disk is smaller than that of the textolite bush, thus causing uneven wear. In the correct design (Fig. 151f) the steel disk face overlaps the textolite bush.

Figure 151g, h shows respectively wrong and correct designs of a cylinder-piston unit.

In the tappet unit in which the tappet slides in a bush (Fig. 151i) the oil-distributing recess is provided in the tappet stem. The more reasonable design has the recess machined in the bush (Fig. 151j), thus ensuring equal wear of the stem and bush.

Figure 152a-c illustrates a stop-cock whose conical plug, made of a hard material, is mounted in the body of a soft material. The design in which the plug is shorter than the conical socket in the body (Fig. 152a) is wrong as during the grinding-in process a step is formed at the part *h* of the socket. This step hinders the deepening of the plug into the socket. The same occurs as the socket wears in operation.

In the improved version (Fig. 152b) the plug end extends out of the socket, thus ensuring uniform wear. An insignificant step, however, may appear at part *m* of the plug. The best design is given in Fig. 152c, where the plug top is slightly below the socket surface. Now the wear of the socket and plug in no way hampers the deepening of the plug. The design in operation has a self-grinding-in property.

For the inversed case, i.e., a soft plug and hard body, the afore-said remains valid. The construction in Fig. 152d is incorrect,



because from the grinding-in processes and wear a step is formed at part *n*. This step prevents the plug from going deeper. The defect can be eliminated by lowering the plug below the socket face (Fig. 152e). A still better design is shown in Fig. 152f, where any possibility of step formation is utterly excluded, both on the plug and in the socket.

Thus, we may generalize all cases, including those when the plug and body are of equally hard material, and say that the plug top end must be below the surface and the lower smaller end must protrude beyond the socket.

This statement remains true for fixed connections made of materials which differ in hardness. It would be wrong to fit a soft hub

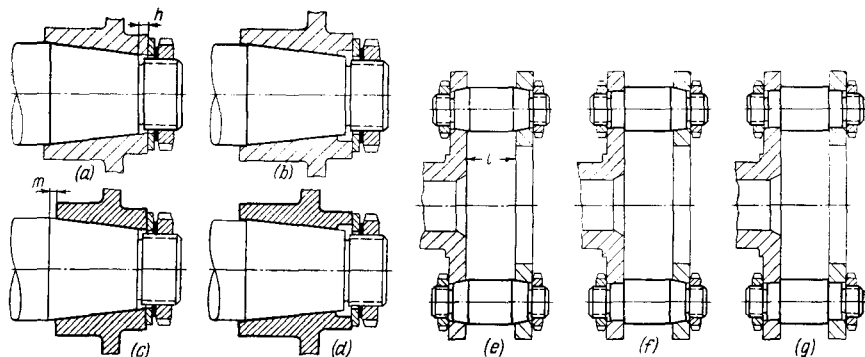


Fig. 153. Tightening of tapered joints

onto a conical portion of a steel shaft (Fig. 153a). Here the hub front face, i.e., the one nearest to the nut, extends beyond the shaft taper. As the hub is ground-in to the taper, and also while the hole loses its true roundness in running, a step is formed at part *h*. This step obstructs the hub assembly on the shaft in the course of repeated tightenings. In a correct version (Fig. 153b) the shaft taper extends beyond the hub, so that changes in the hole size when fitting and because of bearing deformations in no way interfere with the proper tightening. Should the material of the hub be harder than that of the shaft (a fact rare in practice), then the most dangerous case is the one when the hub rear face does not reach the start of the taper (Fig. 153c), because now, in the process of grinding-in and tightening, a step is formed at part *m* of the shaft. In the correct version (Fig. 153d) the hub end overlaps the taper.

Conical fits fail to assure accurate longitudinal fixation. The mutual position of the fitted parts depends to a great extent upon the manufacturing accuracy of the tapers both on the shaft and in the hub, upon the tightening force, number of reassemblies, bearing deformations and wear of the surfaces. For

these reasons conical fits must not be used when accurate axial positions are required.

For example, let us consider the pinion carrier of a planetary drive, whose disk is attached to the casing by means of the satellite shafts. In the design presented in Fig. 153e it is practically impossible to maintain precisely distance  $l$  in respect to all fixture points. Because of the inevitable inaccuracies in the taper diameters and axial distances between them, the lengthwise disk displacements in the course of tightening will differ from shaft to shaft. This displaces, buckles and overstresses the disk. Furthermore, it is difficult to maintain strict centre distances between the tapers. It is also impossible to ensure registration of holes in the connected parts by machining them together (as is often done with cylindrical holes). In fact, the parts cannot be accurately assembled.

The design showing shafts with only one tapered end (Fig. 153f) is better only because the errors are halved.

Such kinds of assemblies should have cylindrical fitting surfaces with the disk tightened up on stops (Fig. 153g). The distances between the fixing steps on the shafts can be held to close tolerances. Registration of the holes' centres in the cover and casing is attained either by machining the holes in a jig or by through machining them together.

## 6.28. Elimination of Local Weak Spots

Local weak spots due to decreased cross-sectional areas and stress concentrators can sharply reduce the strength of components.

Often such a weakening results from a miscalculation of the cross-sectional areas of the part. This mistake often occurs when designing small parts deemed not worth calculations, which allegedly take on loads (except tightening forces). A characteristic example is

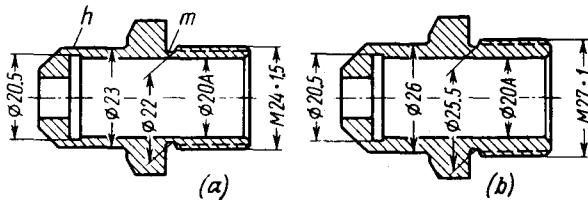


Fig. 154. Elimination of local weak spots. Nipple

illustrated in Fig. 154a. A nipple has a hole  $\phi 20A$ . To enable free retraction of cutting tools the hole bottom has an undercut  $\phi 20.5$ . The threaded nipple portion ( $M24 \cdot 1.5$ ) also has an undercut  $\phi 22$  to clear the thread-cutting tool. For the given dimensions the wall thickness at part  $h$  (over the internal groove) is 1.25 mm, and at part  $m$  (under the external groove) the wall thickness is 1 mm. Clearly, the nipple wall will break even in the case of a weak tightening against the hexagon.

In the improved design (Fig. 154b) the diameter of the part across the internal groove section is increased to  $\phi 26$ ; hence, the minimum

wall thickness is increased to 2.75 mm. A larger thread M27 with a finer pitch ( $s = 1$  mm) is used, which increases the wall thickness at the external groove to 2.75 mm.

Very often a local weak spot can be eliminated by shifting the weakening element into a zone of larger cross-sections. The example given in Fig. 155*a* illustrates this. The bush is sharply weakened by two grooves in the same plane (position *h*), which

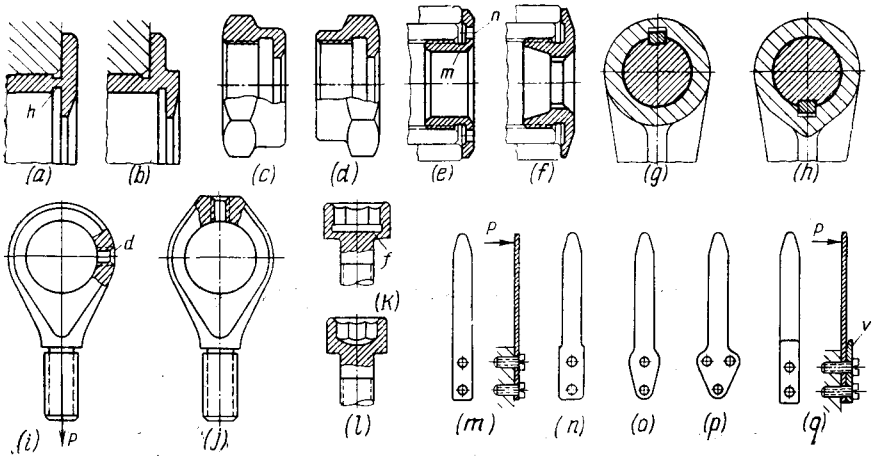


Fig. 155. Elimination of local weak spots

enable a free withdrawal of cutting tools. Moving the internal groove into the flange plane (Fig. 155*b*) strengthens the part.

In the nozzle cap nut (Fig. 155*c*) the undercut should be provided in the hexagon plane (Fig. 155*d*).

The internal nut (Fig. 155*e*) is seriously weakened at the section *m* where a tool retraction groove is provided and at the sections *n* where spanner-receiving holes are drilled. In the improved design (Fig. 155*f*) the holes are replaced by splines and at the weak section the wall thickness is enhanced.

If a lever is secured to a shaft in the way shown in Fig. 155*g*, the hub will be seriously weakened by the keyway. In the better design (Fig. 155*h*) the keyway is moved to the area of increased cross-section, namely, to the transition where the hub joins a longitudinal rib.

An eye bolt loaded with a tension force  $P$  (Fig. 155*i*) is weakened by hole *d* located in the most severely stressed area and intended to receive an oiler. In the strengthened construction (Fig. 155*j*) the hole is arranged in the thickened portion of the eye.

The bolt head with an internal hexagon produced by broaching (Fig. 155*k*) is heavily weakened by a groove at the section *f*, which is intended to clear the broach where the bolt stem turns into the head (this section undergoes bending). Changing the broaching to upsetting (Fig. 155*l*) eliminates the weakness and the bolt acquires additional strength thanks to a more favourable grain orientation.

The strength of the leaf spring fastening unit (Fig. 155*m*) is lowered by the screw-fastening hole at the critical section. The strengthening methods in Fig. 155*n-p* complicate the manufacturing procedure and cause greater waste since the springs are produced by blanking from steel sheet or ribbon.

The strongest and most technological design of the spring made from steel strip and secured by strap *v* is shown in Fig. 155*q*. Now the spring takes up stresses with its unweakened section and is safely protected by the strap at the most critical section.

### 6.29. Strengthening of Deformable Areas

The strength of a part can be substantially enhanced by reinforcing its non-rigid areas which are readily deformed under the action of operating forces.

Let us take, for example, the slot-tang joint unit of shafts illustrated in Fig. 156*a, b*. In the irrational design (Fig. 156*a*) the tang of the driving shaft deforms the forks of the slotted shaft when transmitting torque. This loosens the fit. A press-fitted binding hoop over the fork end (Fig. 156*b*) sharply increases the joint strength and rigidity.

In the universal joint (Fig. 156*c*) the torque is transmitted by a pin press-fitted into the driving shaft knuckle and passing into slots machined into the driven shaft end. In the reinforced construction internal slots are used instead of the forked end in the solid shaft (Fig. 156*d*).

The fork-end connection in Fig. 156*e* is irrational, because the fork opens under the action of tension forces (shown by light arrows). The unit strength will considerably improve, if the forks are additionally tightened on to an auxiliary bush (Fig. 156*f*).

Figure 156*g* shows the fastening section of turbine blades mounted in a T-shaped tenon on the rotor rim. Under the action of centrifugal forces the blades roots move apart (shown by dashes). In the better design (Fig. 156*h*) the roots are provided with spurs *m* entering the annular recesses in the rotor rim, thus preventing the roots from moving apart.

The two-part crank pictured in Fig. 156*i* is coupled in such a way that its crankpin tightens against the flat web face *n*. The elastic

deformations of the unit from the working loads cause conical deformation of the crankpin end, and work hardening and welding of the fitting surfaces.

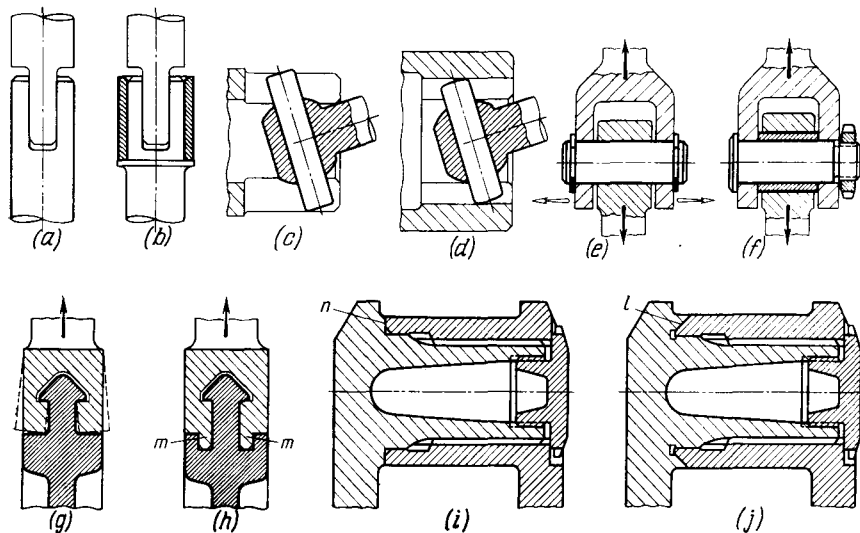


Fig. 156. Reinforcement of units

In the strengthened design (Fig. 156j) the crankpin end is coned and fits into the conical recess  $l$  in the web. The tightness of the fitted collar stops the conical deformation and work hardening.

### 6.30. Composite Constructions

In many cases it is advisable to separate parts, connecting them correctly later by press-fitting, welding, brazing, riveting, etc., or by means of fastening bolts. Such composite designs simplify machining and geometry, save weight and economize on rare or expensive materials.

The separating into different components in many instances saves considerable labour when manufacturing large bed castings. A bed casting with the lower halves of longitudinal shaft bearing housings cast integrally (Fig. 157a) is not correct technologically, as it is necessary to bore the cylindrical holes in the bearing caps and bed simultaneously and maintain strict parallelism of the hole centres, etc. The machining is particularly difficult when the bearings arranged in a line are spaced at substantial distances.

In the design with separate housings (Fig. 157b) machining is much easier, as it only means milling or planing the surfaces to which

the bearing housings are attached. The housings are positioned on the bed by dowel pins.

Another example is the mounting of rollers on the corners of a movable bed (Fig. 158a). To obtain axial alignment of the rollers and

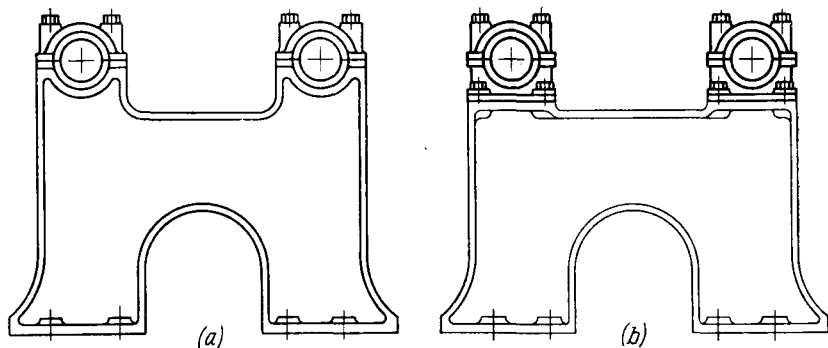


Fig. 157. Bed with bearings

position them in the same horizontal plane is very difficult, especially when the rollers are spaced rather far from each other. The use of separate eye fastenings simplifies the processing (Fig. 158b).

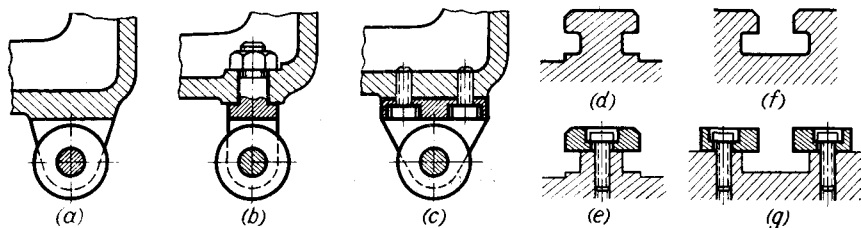


Fig. 158. Simplification of machining of housing-type components through introduction of detachable parts

The best version is given in Fig. 158c. Here the seating surfaces for the roller lugs can be through-milled, which ensures that the rollers are positioned in the same plane. Furthermore, the lugs are more rigid than the eye fastenings and are reliably fixed against rotation relative to the bed.

Easing the machining of slots in beds through the application of detachable parts is illustrated by the examples in Fig. 158d-g.

Figure 159 illustrates how fabrication by welding can simplify machining. The cluster gear (Fig. 159a) is very difficult to produce because of the shaped cavity between the gears. The composite design (Fig. 159b) in which two separate gears are joined by resistance

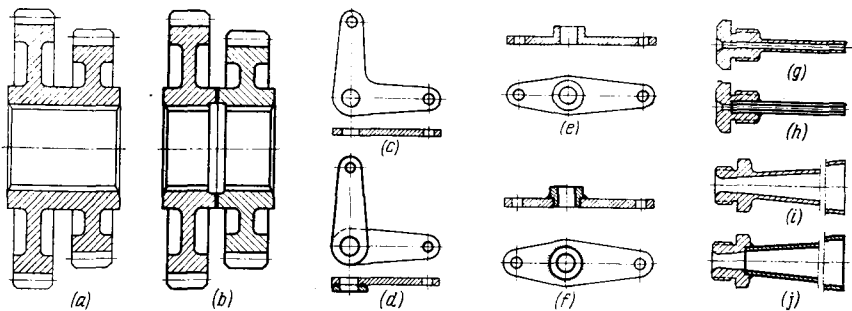


Fig. 159. Simplification of machining through introduction of welded constructions

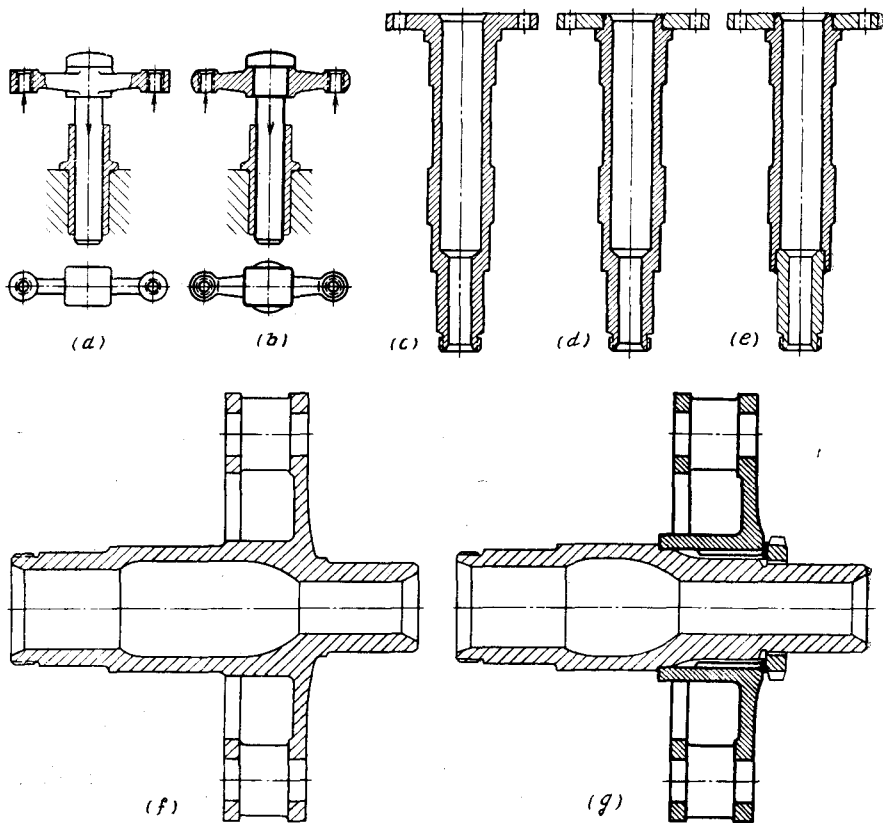


Fig. 160. Composite constructions as substitutes for forgings

welding enables easy machining of the gears of required configuration. The angle lever which is rather difficult to blank (Fig. 159c) can advantageously be changed to a welded design composed of two similar parts of simple shape (Fig. 159d).

Other examples of composite constructions are given in Fig. 159e-j.

Composite constructions are extremely helpful for intricately shaped components. The cross-piece (Fig. 160a) which serves to transmit motion from a cam to two valve tappets can be produced only by stamping in enclosed dies, the latter being economical only in the event of batch production. In piece production it is reasonable to use a built-up component made from two lathe-turned parts press-fitted together (Fig. 160b).

Composite constructions are popular substitutes for forgings when dealing with shafts having large-diameter flanges, etc.

Figure 160c-e shows an example of how a forged flanged shaft is transformed into a welded construction. In Fig. 160d the problem is solved but partially: the shaft here is produced from round rolled stock and involves difficult drilling and boring operations.

In the improved design presented in Fig. 160e the shaft is produced of a seamless pipe; the shaft end is formed by welding a length of a smaller-diameter seamless pipe. Such a construction reduces machining operations to the minimum.

It is very essential to note that the employment of composite constructions as substitutes for forgings is justifiable only under small-batch production conditions. Generally it is more advantageous to produce parts from forgings that approximate as close as possible in configuration, as this results in substantial strength gains, lesser machining, greater productivity and, in the final analysis, less cost.

However, even in batch production it is sometimes more reasonable to resort to composite designs as a means of simplifying forgings. Let us take, for instance, the shaft of a planetary reduction unit with a pinion carrier (Fig. 160f). Clearly, an attempt to forge these units as one will cause quite a lot of difficulties. In the composite design (Fig. 160g) the pinion carrier is made as a separate part and fitted to the shaft on splines. The forging of both parts is very much simplified.

In a number of cases components are made of light alloys, which enables the weight of the unit to be radically decreased.

The cam plate (Fig. 161a) is better made from aluminium alloy, to which a steel cammed rim is attached (Fig. 161b). Other examples are: the axial compressor rotor with a steel drive splined rim (Fig. 161c, d); the brake drum with a steel liner on its frictional surface (Fig. 161e, f).

Composite constructions find wide application as a means of economizing on expensive and scarce materials.



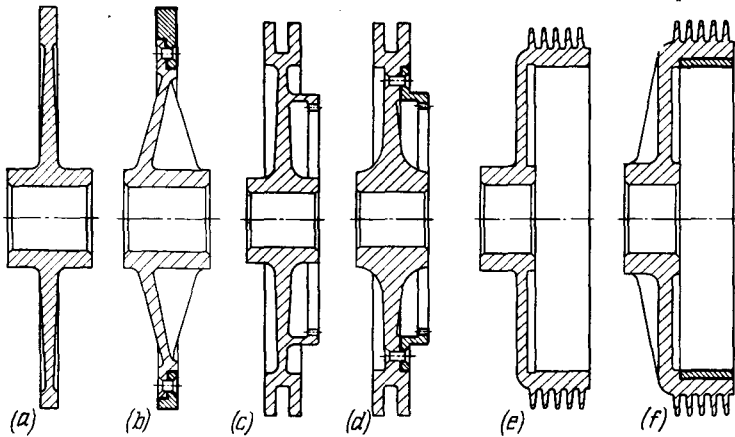


Fig. 161. Composite constructions made of light alloys

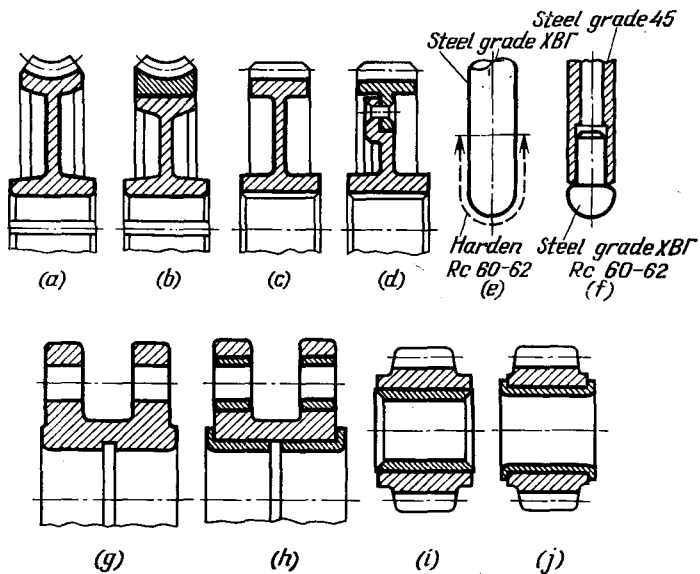


Fig. 162. Composite constructions as a means of saving scarce materials

Worm gear teeth (Fig. 162a) working in sliding friction conditions are normally made of antifriction bronze which is rather expensive. To economize on bronze, bronze hoops are used (Fig. 162a), which are then press-fitted upon carriers made of some cheaper material (e.g., carbon steel, cast iron). Compared to Fig. 162a the amount of bronze in Fig. 162b is reduced to one third.

Clearly, with the gears shown in Fig. 162c only the gear rim need be made of high-grade steel (Fig. 162d).

Figure 162e illustrates a rod made completely of alloy steel, with its spherical end being hardened. The more economical construction in Fig. 162f has only the spherical end made of alloy steel.

Lead bronzes and babbitts surely belong to short-supply materials. Whenever conditions permit, low-lead or even leadless bronzes and babbitts, as well as adequately qualitative substitutes, e.g., antifriction aluminium alloys should be used.

Should the application of difficult-to-obtain non-ferrous alloys be avoided, their consumption must be reduced to the minimum. Let us take, for instance, a housing with many friction surfaces (central bore and lug holes). In the alternative presented in Fig. 162g the housing is made completely of expensive antifriction bronze, but the rationalized version, illustrated in Fig. 162h uses cast iron (or some other abundant material), and bronze bushes for the friction surfaces.

An example of how a material in short supply can be spared in the production of bearing bushes is given in Fig. 162i and j. Here the thick bronze bush (Fig. 162i) is changed to a thin-walled one rolled from strap brass (grade JIC-59-1) and strengthened by rolling and expanding in the seating bore (Fig. 162j).

An effective way of economizing on lead babbitts is by decreasing the thickness of babbitting. These days the thickness is reduced to 0.2-0.3 mm (instead of 1-3 mm practised quite recently). The most economic bearings are those with a double-layer babbitting and consisting, in effect, of a babbitt layer whose thickness varies within several hundredths of a millimetre. The layer is deposited by an electrodeposition technique upon a sublayer of porous bronze. The deposition of babbitt in the pores of the bronze sublayer assures good cohesion between babbitt and bronze and creates in the bronze sublayer a structural interface which is rather similar to lead bronze in terms of antifriction properties.

### 6.31. Shoulders

Shoulders (Fig. 163a-d) serve as positive rests for components in fixed joints or as stops which restrict the axial displacement of parts in movable connections. The most rationally designed shoulders are those that have (owing to their shape) equal resistance to bending (Fig. 163d). Such shoulders possess the least weight and are simple to produce. The non-working surfaces of shoulders are sloped at 45°

so that they can easily be turned by means of a bull-nose lathe tool whose nose angle is  $45^\circ$ .

Shaped shoulders are uneconomical because they are difficult to produce (Fig. 163b).

Shoulders must be kept as low in height as possible: the higher the shoulder, the greater the metal wastes in the form of chips and

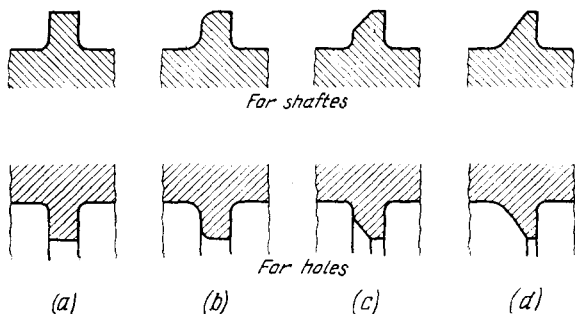


Fig. 163. Shoulder designs

the more difficult the production process. Figure 164 shows how a high shoulder in a gear unit can be eliminated. Shoulder *m* is for holding the gear shaft in the housing and fixing the gear axially (Fig. 164a). It is the latter function which needs such a high shoulder. Now, replacing the shoulder by the washer *n* which works upon a low step of the shaft (Fig. 164b) makes the shaft manufacture easier.

Illustrated in Fig. 165a-o are various techniques enabling one either to make lower shoulders or to eliminate them at all (for fixed joints only).

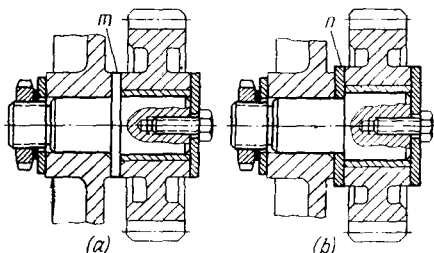


Fig. 164. Reduction of shoulder height

In Fig. 165b-d the fitted part is tightened against an intermediate washer resting against a step or shoulder of reduced height.

Shoulders are often replaced with ring stops having rectangular cross-sections (Fig. 165e). The strength of the unit can further be enhanced by fitting the ring into a cylindrical recess made in the part or in some intermediate member, thus preventing the ring from loosening and leaving the recess (Fig. 165f, g).

A very strong stop is ensured by rings enclosed in a conical recess either in the part or in an intermediate washer (Fig. 165h-j).

Occasionally use is made of half-rings placed into grooves on the shaft and locked either by means of a recess in the part to be tightened up (Fig. 165*k, l*) or by means of an embracing ring (Fig. 165*m*). In the design alternative given in Fig. 165*n* embracing ring 1 is

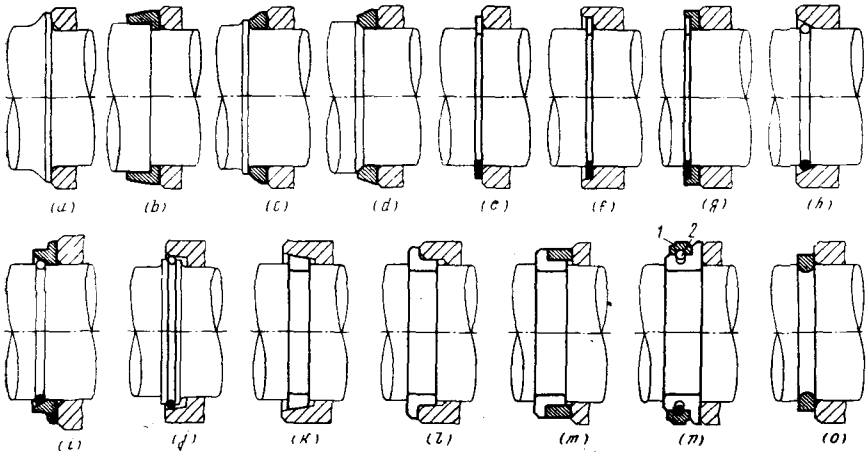


Fig. 165. Reducing the shoulder height and replacing shoulders

fixed on half-rings by locking spring ring 2. The joint is easily disassembled manually by merely shifting the ring axially.

In the version pictured in Fig. 165*o* the shoulder is formed by swaging a plastic metal ring into a groove on the shaft. The process is done on rotary swaging machines; after swaging, the ring is machined together with the shaft.

It should be noted that grooves weaken shafts, and fitting rings into such grooves is not recommended for joints subjected to high cyclic loads. In some cases weakening can be avoided by making the shaft thicker across the section where a groove is needed (Fig. 165*j*).

### 6.32. Chamfers and Fillets

Generally all external corners must be chamfered (Table 8) and all internal corners, filleted (Table 9).

Conventionally the chamfers are made at  $45^\circ$ . The leg  $c$  of a chamfer for usual cylindrical components is obtained from the relationship  $c = 0.1 \sqrt{D}$ , where  $D$  is the diameter of the cylinder. The values obtained with the aid of this relationship are rounded off to standard values:

$$c = 0.2; 0.5; 0.8; 1; 1.2; 1.5; 1.8; 2; 2.5; 3; 3.5; 4; 5$$

Free, non-contacting surfaces are given chamfers within 0.1-0.2 mm. Such chamfers are not indicated in drawings (in contrast to the design chamfers); a note merely says "Remove sharp corners". Often the necessity for removing

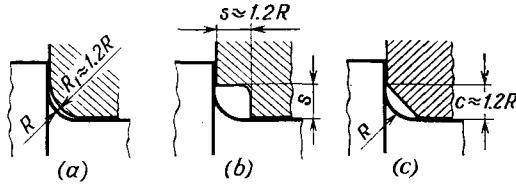


Fig. 166. Overlapping of fillets

sharp corners is indicated in the Technical Specifications pertinent to the part, the chamfer sizes and tolerances being specified.

Figure 166 shows the methods of overlapping fillets. The overlapping is effected by a fillet whose radius is larger than that of the part being encompassed (Fig. 166a), or by a recess (Fig. 166b) or else by a chamfer (Fig. 166c). The latter method is the simplest one.

## Chamfers

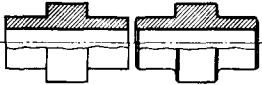
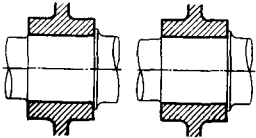
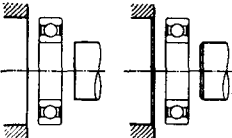
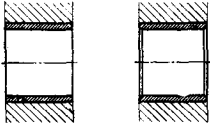
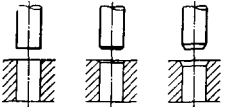
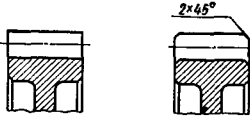
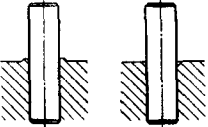
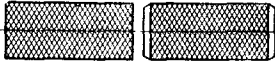
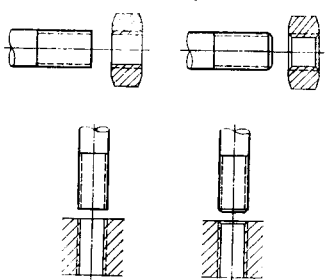
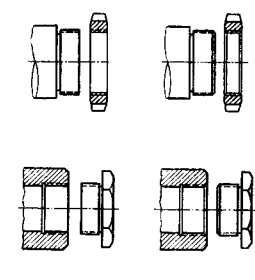
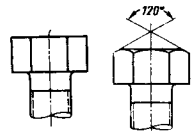
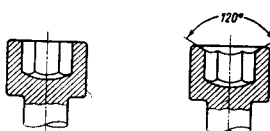
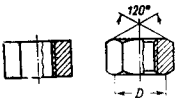
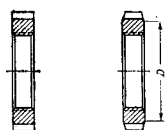
Design		Application	Purpose	Design		Application	Purpose
wrong	correct			wrong	correct		
		All machined parts	To protect hands from injury. To protect precision surfaces from chance damage			Fixed joints	To reduce edge pressures
			To facilitate assembly			Slide bearings and other movable connections	
		Press-fitted connections	To facilitate press-fitting			Gear teeth. Parts working under contact loads	To eliminate load concentration at edges
		Press-fitting into soft-metal parts	To prevent metal from rising around hole edges			Knurled parts	To improve appearance

Table 8 (continued)

Design		Design		Application	Purpose
wrong	correct	wrong	correct		
				<p>Threaded connections</p>	<p>To facilitate screwing of nuts and threaded rods</p>
					<p>To facilitate use of spanners</p>
					<p>To form an annular bearing surface (with diameter <math>D</math>). To prevent point contact on bearing surface</p>

## Fillets

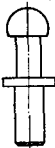
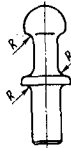
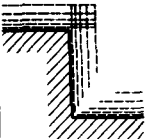


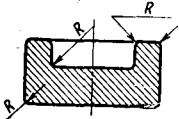


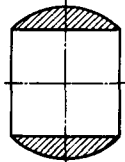
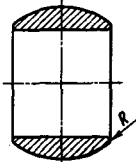

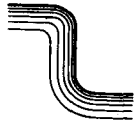
Design		Application	Purpose	Design		Application	Purpose		
wrong	correct			wrong	correct				
		Heat-treated parts	To prevent edges from overheating and decarbonization. To reduce quenching stresses at transitions			Electro-plated parts	To prevent local variations in current density. To ensure uniform deposition of metal		
								Painted, varnished and polymerized parts	To ensure uniform coating. To prolong service life of coatings
				Cast parts	To ensure uniform saturation of surface layer of introduced elements				
									



Table 9 (continued)

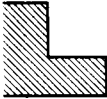
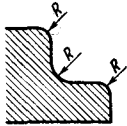
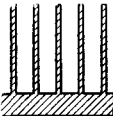
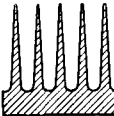
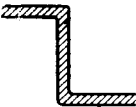
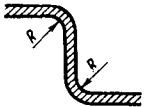
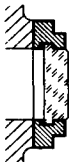

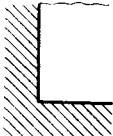
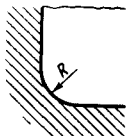

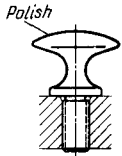
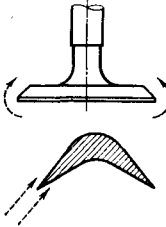
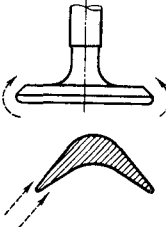
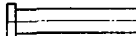
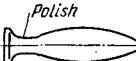
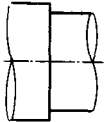
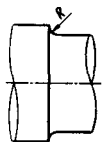
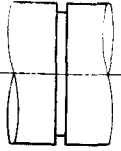
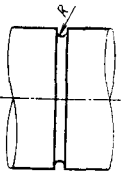
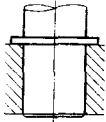
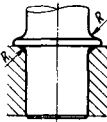
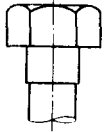
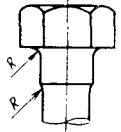
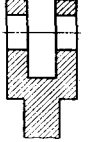
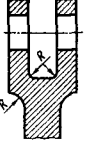
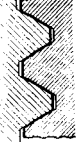
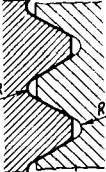
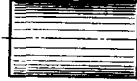

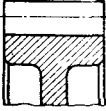
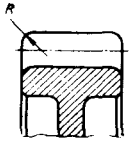
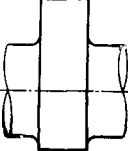
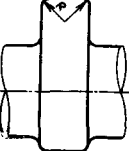
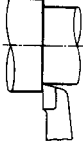
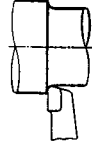
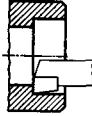
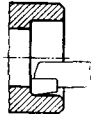
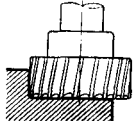
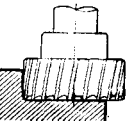
Design		Application	Purpose	Design		Application	Purpose
wrong	correct			wrong	correct		
		Stamped parts	To improve metal flow and fill die reentry angles			Heat-dissipating fins	To improve heat transfer from part body to fins
		Parts stamped from sheets	To improve metal flow. To prevent disruptions at transition areas			Decorative parts	To improve outer appearance. To facilitate polishing
		Reservoirs	To eliminate corrosion at corners. To facilitate flushing			Hand controls	To protect hands from injury and facilitate manipulation. To facilitate polishing
		Parts subject to heat erosion	To prevent edges from overheating and burning				

Table 9 (continued)

Design		Design		Design		Application	Purpose
wrong	correct	wrong	correct	wrong	correct		
						Any loaded part	To increase static and cyclic strength at transitions
							
						Parts subjected to contact loads	To reduce edge pressures
						Machined parts	To enhance durability of cutting edges

# Index

- Accuracy of parts alignment, 179
- Alignment of flanges, 105
- Axial fixing of parts, 172
  
- Bending, elimination and reduction of, 137
- Butt-jointing on intersecting surfaces, 177
  
- Cambering, 161
- Chamfers, 196
- Combining design functions, 150
- Compactness of design, 146
- Compensators, 129
- Composite constructions, 189
- Connection(s),
  - centring, 79
  - conical flange, 113
  - design rules for, 80
  - glued, 78
  - loaded, 12
  - pressed, design of, 67
  - pressed, with electro-deposited coatings, 65
  - press-fitted, 37
  - screwed, centring in, 92
  - serrated, 77
  - strength of, 38
  - three-flange, 111
  - tightened, 7
  - unloaded, 7
- Control of direction, 174
- Coupling of parts of different hardness, 183
- Coupling(s), floating cross-sliding, 136
  
- Design,
  - compactness of, 146
  - of equally strong parts, 152
  - general principles of, 116
  - of pressed connections, 67
  - of screwed connections, 94
  
- Elasticity, effect on load distribution, 164
- Elimination,
  - of adjustments, 124
  - of deformations due to tightening, 143
  - of local weak spots, 186
- Equistrength, 152
  
- Fillets, 196
- Fitting to several surfaces, 170
- Fit(s),
  - conical, 75
  - drive, 37
  - press, 37
  - selection of, 46
  
- Interchangeability of rapidly wearing parts, 178
  
- Methods of controlling preloads, 32
- Mounting surfaces, 175
  
- Press-fitting,
  - with cooling of parts, 64
  - with heating of parts, 64
  
- Rationalization of power schemes, 126
- Relaxation, 25
- Relief of precision mechanisms, 181
  
- Self-alignment, 157
- Shoulders, 194
- Strengthening of deformable areas, 188
  
- Tightening up on two surfaces, 171
- Torsion bars, 133
  
- Unification,
  - of design elements, 116
  - of parts, 119
- Uniform loading of supports, 156
- Unitization, principles of, 121

*TO THE READER*

Mir Publishers welcome your comments on the content, translation, and design of the book.

We would also be pleased to receive any suggestions you care to make about our future publications.

Our address is:

USSR, 129820, Moscow, I-110, GSP, Pervy Rizhsky Pereulok, 2,  
Mir Publishers

*Printed in the Union of Soviet Socialist Republics*

## OTHER BOOKS FOR YOUR LIBRARY

### MECHANISMS IN MODERN ENGINEERING DESIGN.

BY I. ARTOBOLEVSKY

A handbook in six volumes for engineers, designers, and inventors on the mechanisms used in modern engineering design. Each mechanism is represented by a diagram of its working principle, with a concise description, and classified by a scheme proposed and developed by the author.

#### **Vol. I. Lever Mechanisms.**

Illustrates and describes 912 lever mechanism. *Contents.* Elements. Simple lever mechanisms. Jointed lever mechanisms.

#### **Vol. II. Lever Mechanisms (in two parts).**

Illustrates and describes 1376 lever mechanisms.

*Contents.* Link-gear mechanisms. Slider-crank mechanisms.

Lever-cam mechanisms. Gear-lever mechanisms. Lever-ratchet mechanisms. Flexible-link lever mechanisms. Elastic-link lever mechanisms. Wedge-lever mechanisms. Lever-screw mechanisms.

#### **Vol. III. Gear Mechanisms.**

Illustrates and describes 689 toothed, friction and cam mechanisms.

*Contents.* Simple gear mechanisms. Lever-gear mechanisms. Pin-gear mechanisms. Cam-gear mechanisms. Ratchet-gear mechanisms. Worm-gear mechanisms. Complex gear mechanisms.

## MACHINE TOOLS. BY N. CHERNOV

A textbook for technical colleges and apprentice engineers on the standard parts and mechanisms, electrical and hydraulic equipment of machine tools, the equipment of automatic transfer lines, and N/C machine tools.

*Contents.* Introduction to machine tools. Standard parts and mechanisms. Electrical equipment. Hydraulic equipment. Automatic (Numerical) control. Standard lathes. Turret lathes. Backing-off lathes. Multihead machines. Semiautomatic and automatic lathes. Drilling machines. Boring machines. Milling machines. Dividing heads. Principles of tracer milling machines. Thread-cutting machines. Shapers and planers. Broaching machines. Grinders. Lapping machines. Gear-cutting machines. Machine tools built from standard units. Automatic transfer lines. Electrosparking, ultrasonic and other machines. N/C machine tools. Modernization. Installation. Testing, maintenance and repairs of machine tools.

## MACHINE ELEMENTS. BY V. DOBROVOLSKY *et al.*

A textbook for university mechanical engineering faculties. Contains rules, methods and standards for designing the elements on the basis of their working conditions. Acquaints the reader with the design of individual elements, and the various forms of assembly and drive used in modern engineering.

*Contents. Part I.* Fundamentals of designing machine elements. Criteria of operating capacity and calculation of machine elements. Selection of material. Standardization. Production soundness.

*Part II. Joints.* Types of joint. Riveted joints. Welded joints. Joints formed by interference fits. Threaded joints. Cottered fastenings. Keyed, splined and keyless joints.

*Part III. Power transmission.* Types of drive. Friction drives. Belting. Gearing. Helical and hypoid gears. Worm gears. Globoidal gears. Reduction gears. Chain drives. Power screws.

*Part IV. Shafts, bearings and couplings.* Shafts and axles. Sliding-contact bearings. Rolling-contact bearings. Couplings and clutches.

*Part V. Springs and frames.* Springs. Machine frames.

**ENGINEERING TECHNIQUES FOR ANALYZING STRENGTH  
AND RIGIDITY. BY G. GLUSHKOV**

A monograph on the theory of moments developed by the author, and its application to engineering design problems on the strength, rigidity, and stability of beams and columns. The approximate (and occasionally exact) solutions obtained can be employed to analyze loads of all kinds. The method is also applicable to various-non-linear problems.

*Contents.* Fundamentals of the theory of moments. Application of the theory. Fundamentals of the moment-operational techniques.

**FORMULAS FOR DESIGNING COMPLEX FRAMES.**

*BY G. GLUSHKOV I. EGOROV, V. ERMOLOV.*

A collection of formulas for calculating the moments and reactions at supports and joints of complex frames and arches under various loads.

*Contents.* Frames with stepped supports (16 variants). Multispan and multistorey frames (49 variants). Arches (14 variants). Force diagrams and load factors (117 variants).

*Appendices.* Examples of analyses. Formulas for calculating shearing forces, bending moments, and the angles of rotation and sag of simple beams (117 variants).